The Hashemite Kingdom of Jordan Scientific Research Support Fund The Hashemite University

JJEES

Jordan Journal of Earth and Environmental Sciences

Volume (12) Number (1)

Cover photo © J H Powell

JJEES is an International Peer-Reviewed Research Journal

ISSN 1995-6681 jjees.hu.edu.jo March 2021

Jordan Journal of Earth and Environmental Sciences (JJEES)

JJEES is an International Peer-Reviewed Research Journal, Issued by Deanship of Scientific Research, The Hashemite University, in corporation with, the Jordanian Scientific Research Support Fund, the Ministry of Higher Education and Scientific Research.

Submission address:

Manuscripts should be submitted electronically to the following e-mail:

jjees@hu.edu.jo

For more information and previous issues:

www.jjees.hu.edu.jo

Hashemite Kingdom of Jordan

Scientific Research Support Fund

Hashemite University

Jordan Journal of Earth and Environmental Sciences

JJEES

An International Peer-Reviewed Scientific Journal

Financed by the Scientific Research Support Fund

Volume 12 Number (1)

http:// jjees.hu.edu.jo/

ISSN 1995-6681

Cover page photo: Natural rock arch in the Cambrian Umm Ishrin Sandstone Formation (Ram Group); Wadi Ram area, Jordan. Note overturned cross-bedding, lower right.
Photograph, J H Powell.

JJEES

JJEES (2021) 12 (1): 1-12
ISS`N 1995-6681

Jordan Journal of Earth and Environmental Sciences

Mitigating the Effects of Quaternary Ammonium Compounds on Biological Wastewater Treatment Systems during the COVID-19 Pandemic

Malek Hajaya

Tafila Technical University, Civil Engineering Department, Jordan

Received 4 June 2020; Accepted 5 August 2020

Abstract

The global pandemic of COVID-19 has sparked an increase in disinfectants' usage around the world. Among these are quaternary ammonium compounds (QACs), which are found in cleaner formulations that are commonly used in various sanitation applications. QACs' concentrations are projected to increase in the influents of wastewater-treatment plants, where their poor target specificity will, initially, adversely affect the plant performance. This paper provides an insight into the possible mitigation of QACs' effects on the treatment plants by manipulating a group of the plant operational parameters (each individually), to alter the plant operation in order to combat these effects. The study used computer simulations of a benchmark model for a treatment plant that take into consideration reactions taking place in the biological units (Anoxic and Aerobic). It was found that increasing the solids' recycle ratio (up to 4), reducing the influent wastewater (by a fraction no less than 0.8), and increasing the oxygen supply rate to its maximum are effective measures that will alleviate the effects of QACs on the plant performance. Altering the nitrate recycle ratio had no tangible effects. Results presented here should be helpful in maintaining an adequate operation of the plants during the first exposure to increasing QACs' concentration, while the model can provide a framework for assessing wastewater treatment plants' performance upon receiving inhibitory material in their influents.

Keywords: COVID-19, Quaternary ammonium compounds, Inhibition, Mitigation, Modeling.

1. Introduction

In February 2020, the World Health Organization (WHO) officially named the disease caused by the novel corona virus as Corona virus Disease 2019 (COVID-19) (Zu et al., 2020), and in March of the same year, the WHO declared the COVID-19 outbreak a global pandemic (Cucinotta and Vanelli, 2020). The spread of COVID-19 triggered the WHO to publish a multitude of guidelines to ensure the prevention and control of this epidemic (WHO, 2020), which include the disinfection of hard surfaces, as they provide a medium for the transmission of the virus (WHO, 2020; Thomas et al., 2020; Van Doremalen et al., 2020). One of the recommended disinfectants for this purpose are virucidal agents that contain Quaternary Ammonium Compounds (QACs) (EPA, 2020; Marnie and Peters, 2020). QACs represent well-known disinfectants composed of a hydrophobic hydrocarbon chain (one at least) connected to a nitrogen atom (positively charged), and another short-chain alkyl group such as methyl or benzyl groups. They are effective in eliminating the viral infection by targeting the lipid structure of the viral envelope (Cross and Singer, 1994). In general, QACs are extensively used worldwide, where their annual consumption was estimated in 2004 to be half a million ton (Chen et al., 2018). Furthermore, more than one million pounds of QACs are manufactured or imported annually, designating them as "high production volume chemicals" by the EPA and the Organization for Economic Cooperation and Development (Hora et al., 2020). The extensive usage in domestic applications (among many others) has led to the detection of QACs in many Wastewater Treatment Plants' (WWTP) influents, and treated effluents, as well as in surface water, and sediments. Concentrations of QACs were detected to be between 1 and 60 μg/l in effluents and surface water (Ding and Liao, 2001; Ferrer and Furlong, 2001; Martínez-Carballo et al., 2007; Tezel and Pavlostathis 2011; Zhang et al., 2015; Pati and Arnold, 2020), and at concentrations ranging from 0.3 to 3 mg/l in WWTP influents (Conidi et al., 2019). Additionally, QACs were found in samples collected from sewers at concentrations ranging between 4.7 and 7.7 μg/l (Wieck et al., 2018), while sewage sludge was found to contain QACs at concentrations ranging between 0.09 and 191 μg/g of dray weight (Ruan et al., 2014). In the environment, QACs are known to proliferate antibiotic resistance in microbial communities (Pereira and Tagkopoulos, 2019), while being toxic to aquatic and soil organisms (Jardak et al., 2016). Additionally, QACs are known to form a carcinogen known as N-Nitrosodimethylamine (NDMA), when combined with chloramines (Kemper et al., 2010). Chloramines results from chlorine disinfection, in the presence of the ammonia, of the effluents of WWTPs prior to their release into the environment (Mitch and Sedlak, 2004).

QACs inhibit the operation of WWTP by targeting the biologically driven reactions. The WHO clearly states that

* Corresponding author e-mail: mhajaya@ttu.edu.jo

there is no evidence of COVID-19 transmission through wastewater, within the confinement of WWTP (WHO, 2020). However, as an indirect consequence to the global pandemic, WWTPs operation could be negatively affected. As a response to the global COVID-19 pandemic, an expected rise in the usage of QAC-containing disinfectants is projected in various locations to combat the spread of the disease. Accordingly, and in an indirect way, QACs' concentration in WWTP influents will increase to higher levels than reported before.

This, by its turn, will present a challenge to WWTP operators due to the adverse effects of QAC-containing wastewaters on the biological treatment systems in such plants. QACs are highly effective disinfectants, yet they have poor target specificity, attacking the microbial group operating within biological WWTPs. Their inhibitory effect to respiratory enzymes will result in a decreased chemical oxygen demand (COD) and the substrate utilization rates (Zhang et al., 2011; Hajaya and Pavlostathis, 2012). QACs will cause total inhibition of nitrification at concentration of 2 mg/l (Sütterlin et al., 2008; Hajaya and Pavlostathis, 2012), and a QAC concentration greater than 50 mg/l has been reported to inhibit heterotrophic denitrification (Hajaya et al., 2011; Hajaya and Pavlostathis, 2012; Yang et al., 2015).

The fate and effect of QACs in WWTPs will mainly be dictated by three processes: adsorption, inhibition, and biotransformation (Hajaya and Pavlostathis, 2012; Chen et al., 2018). The aforementioned processes represent how WWTPs interact with QACs in their influents under conventional circumstances. However, an expected increase in usage due to the unusual circumstances brought by the global pandemic (Tullo and Bettenhausen, 2020) represents a new challenge for WWTPs, as a great percentage of the compounds will ultimately find way into their influents (Tezel and Pavlostathis, 2011).

Ultimately, WWTPs will cope with the presence of QACs in their influent wastewaters, with the effectiveness of the process reaching pre-QACs exposure levels through microbial acclimation, biodegradation, or adsorption (Ren et al., 2011; Hajaya and Pavlostathis, 2012; Chen et al., 2018), but not before going through an operational period that will drastically affect the plant's nitrogen removal efficiency, resulting in high concentrations of nitrogen in the plant effluents during that period (Hajaya and Pavlostathis, 2012).

Consequently, there should be criteria within the operational parameters available to the operators of WWTPs to allow them to cope with the expected and temporary decline in their performance while treating wastewaters that include higher levels of QACs (Conidi et al., 2019).

The purpose of this work is to provide an insight into the range of operational parameters that can be exploited to mitigate the impact of a sudden increase of QAC concentrations in the influent domestic wastewater of a WWTP, because of their extensive usage to combat the spread of COVID-19 infection. This task will be performed through mathematical simulations of a benchmark WWTP model that takes into account the inhibitory effect of QACs on the various biological processes in the WWTP.

2. Methods

2.1 The Layout of the Benchmark WWTP

The WWTP model mainly adapted the characteristics of the BSM1 benchmark (Alex et al., 2008). Figure 1 shows the plant layout.

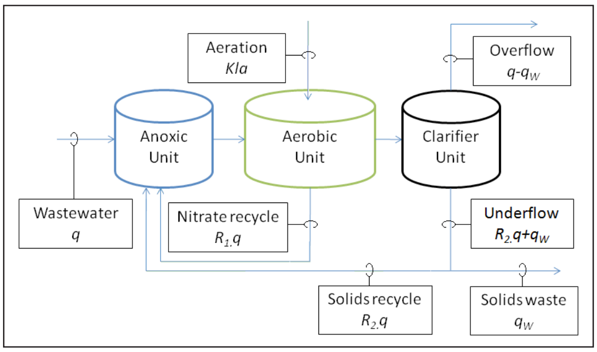

Figure 1. The WWTP layout used in the mathematical model simulations.

Similar to the benchmark, the WWTP is sized for an average domestic wastewater flow rate (q) of 18500m^3/d. The organic load in the wastewater is comprised from 300 mg COD/l of biodegradable organic carbon along with 50 mg N/l of nitrogen. The anoxic and aerobic unit volumes are 2000 m^3 (V_1) and 4000 m^3 (V_2), respectively. Two recycles are found: a nitrate recycle (q_{R1}) with a recycle ratio of 5 (R_1), and a solids' recycle (q_{R2}) with a recycle ratio of 1 (R_2). These ratios dictate the value of the nitrate recycle flow rate ($q_{R1}= R_1 . q$) and the solids' recycle flow rate ($q_{R2}= R_2 . q$) in relation to the flow rate of the wastewater.

Solids' waste flow rate (q_w) is 385 m^3/d, in order to sustain a Solids' Retention Time (SRT) of about sixteen days. Air is only introduced into the aerobic unit to sustain an oxygen concentration of around 2 mg/l. The aforementioned oxygen concentration is reached by assigning a value for the oxygen mass transfer coefficient (Kla) of 200 (1/d).

The clarifier sub-model is not included in the model. Instead, it is assumed that no reactions are taking place in it, and its particulates' separation efficiency (SE) is relatively constant (Le Moullec et al., 2011; Hajaya, 2019). SE was calculated from the benchmark model to be 0.998 (particulate mass in the underflow/ particulate mass in the overflow). SE is used to evaluate particulate concentrations in the clarifier overflow (X_{OF}) and underflow (X_{UF}) by the following equations:

$$X_{UF} = \frac{SE.X_2.(R_2.q+1)}{R_2.q+q_W} \quad (1)$$

$$X_{OF} = \frac{(1-SE).X_2.(R_2.q+1)}{q+q_W} \quad (2)$$

where X_2 is the concentration (mg COD/l) of any particulate in the aerobic unit and its effluent.

2.2 Mathematical Model

The WWTP mathematical model follows the change in a group of variables as they pass through the system shown in Figure 1. As indicated in the BSM1 benchmark (Alex et al., 2008), this benchmark model uses the framework of the International Water Association (IWA) Activated Sludge Model 1 (ASM1) (Henze et al., 2000).

Table 1 lists these state variables with their rates; S refers to soluble concentrations and X refers to particulate concentrations.

Table 1. State variables in the benchmark model and their associated rates (Alex et al., 2008); a: Chemical Oxygen Demand.

Variable	Symbol	Rate
Soluble inert organics	S_I (mg COD[a]/l)	$r_{SI} = 0$
Readily biodegradable (soluble) substrate	S_S (mg COD/l)	$r_{Ss} = \frac{-1}{y_H}(P_1 + P_2) + P_7$
Particulate inert organics	X_I (mg COD/l)	$r_{XI} = 0$
Slowly biodegradable (particulate) substrate	X_S (mg COD/l)	$r_{Xs} = (1 - f_P)(P_4 + P_5) - P_7$
Active heterotrophic biomass	X_{BH} (mg VSS COD/l)	$r_{XBH} = P_1 + P_2 - P_4$
Active autotrophic biomass	X_{BA} (mg VSS COD/l)	$r_{XBA} = P_3 - P_5$
Non-biodegradable particulates	X_P (mg COD/l)	$r_{Xp} = f_P(P_4 + P_5)$
Dissolved oxygen	S_O (mg Oxygen/l)	$r_{So} = -\frac{1-y_H}{y_H}P_1 - \frac{4.57-y_A}{y_A}P_3$
Nitrate	S_{NO} (mg N/l)	$r_{SNO} = \frac{1-y_H}{2.86y_H}P_2 + \frac{1}{y_A}P_3$
Free and ionized ammonia	S_{NH} (mg N/l)	$r_{SNH} = \left(-i_{XB} - \frac{1}{y_A}\right)P_3 - i_{XB}(P_1 + P_2) + P_6$
Soluble biodegradable organic nitrogen	S_{ND} (mg N/l)	$r_{SND} = P_8 - P_6$
Particulate biodegradable organic N	X_{ND} (mg N/l)	$r_{XND} = (i_{XB} - i_{XP}f_P)(P_4 + P_5) - P_8$
Alkalinity	S_{ALK} (mol/l)	$r_{SALK} = -\frac{i_{XB}}{14}P_1 + \left(\frac{1-y_H}{14\times2.86\times y_H} - \frac{i_{XB}}{14}\right)P_2 - \left(\frac{1}{7y_A} + \frac{i_{XB}}{14}\right)P_3 + \frac{P_6}{14}$

The various processes shown in Table 1 are defined and their mathematical models, along with the rates governing all the different state variables (S and X) in the benchmark model are listed in Table 2.

Table 2. The processes found in the basic benchmark model (Alex et al., 2008).

Process	Mathematical Model	Symbol
Aerobic growth of heterotrophs	$\mu_H \frac{S_s}{S_s+K_s}\frac{S_O}{S_O+K_{OH}}X_{BH}$	P_1
Anoxic growth of heterotrophs	$\mu_H \frac{S_s}{S_s+K_s}\frac{K_{OH}}{S_O+K_{OH}}\frac{S_{NO}}{S_{NO}+K_{NO}}\eta_G X_{BH}$	P_2
Aerobic growth of autotrophs	$\mu_A \frac{S_{NH}}{S_{NH}+K_s}\frac{S_O}{S_O+K_{OA}}X_{BA}$	P_3
Decay of heterotrophs	$b_H X_{BH}$	P_4
Decay of autotrophs	$b_A X_{BA}$	P_5
Ammonification of soluble organic nitrogen	$k_a S_{ND} X_{BH}$	P_6
Hydrolysis of entrapped organics	$k_h \frac{X_s/X_{BH}}{X_s/X_{BH}+K_X}\left[\frac{K_{OH}}{S_O+K_{OH}} + \eta_h \frac{S_{NO}}{S_{NO}+K_{NO}}\frac{K_{OH}}{S_O+K_{OH}}\right]X_{BH}$	P_7
Hydrolysis of entrapped organic nitrogen	$P_7 \frac{X_{ND}}{X_S}$	P_8

Definitions and values (which are used in the simulation) of the kinetic and stoichiometric parameters shown in Table 2 are listed in Table 3.

Table 3. Kinetic and stoichiometric parameters used in the simulation (Alex et al., 2008).

Parameter	Definition	Value
μ_H	Max. specific growth rate for Heterotrophs (d^{-1})	4.0
μ_A	Max. specific growth rate for Autotrophs (d^{-1})	0.5
K_S	Half saturation constant for Heterotrophs (mg COD/l)	10
K_{OH}	Half saturation constant for O_2 Heterotrophs (mg O_2/l)	0.2
K_{NO}	Half saturation constant for Heterotrophs (mg NO_3-N/l)	0.5
η_G	Correction for Anoxic Heterotrophic growth (-)	0.8
K_{OA}	Half saturation constant for O_2 Autotrophs (mg O_2/l)	0.4
K_{NH}	Half saturation constant for Autotrophic. (mg NH_3-N/l)	1.0
b_H	Decay constant for Heterotrophs (d^{-1})	0.3
b_A	Decay constant for Autotrophs (d^{-1})	0.05
k_a	Ammonification rate (l.COD/mg.d)	0.05
k_h	Max. specific Hydrolysis rate (mg COD/mg VSS COD.d)	3.0
K_X	Half saturation constant for Hydrolysis (mg COD/mg COD biomass)	0.1
η_h	Correction for Anoxic Hydrolysis (-)	0.8
y_H	Heterotrophic yield coefficient (mg VSS COD/mg COD)	0.67
y_A	Autotrophic yield coefficient (mg VSS COD/mg N)	0.24
f_p	Particulate yielding biomass fraction (-)	0.08
i_{XB}	Nitrogen fraction in biomass (mg N/mg VSS COD)	0.08
i_{XP}	Nitrogen fraction in biomass products (mg N/mg VSS COD)	0.06

Finally, Table 4 lists the characteristics of the wastewater being treated in the WWTP, which represents the flow-weighted average influent concentrations during a week of dry weather operation (Alex et al., 2008).

Table 4. Wastewater characteristics used in the simulations, which represent the flow-weighted average influent concentrations during a week of dry weather operation (Vanhooren and Nguyen, 1996).

Variable	Value
S_{Ii}	30 mg COD/l
S_{Si}	70 mg COD/l
X_{Ii}	52 mg COD/l
X_{Si}	200 mg COD/l
X_{BHi}	28 mg COD/l
X_{BAi}	0.25 mg COD/l
X_{Pi}	5.0 mg COD/l
S_{Oi}	0 mg Oxygen/ l
S_{NOi}	0.25 mg N/ l
S_{NHi}	30.0 mg N/ l
S_{NDi}	7.0 mg N/ l
X_{NDi}	11.0 mg N/ l
S_{ALKi}	10.0 mol/l

Both anoxic and aerobic units are assumed to be completely mixed, with constant liquid densities and volumes. Processes shown in Table 2 are only taking place within the units. Based on the aforementioned analysis, the following equations can be used to dynamically describe the behavior of all the soluble (S) and particulate (X) constituents in the plant; the subtext denotes the unit in the system:

For the anoxic unit (unit 1):

$$\frac{dS_1}{dt} = \frac{q}{V_1}S_i + \frac{R_1q}{V_1}S_2 + \frac{R_2q}{V_1}S_2 - \left(\frac{q}{V_1} + \frac{R_1q}{V_1} + \frac{R_2q}{V_1}\right)S_1 + r_{S1} \cdots (3)$$

$$\frac{dX_1}{dt} = \frac{q}{V_1}X_i + \frac{R_1q}{V_1}X_2 + \frac{R_2q}{V_1}X_{UF} - \left(\frac{q}{V_1} + \frac{R_1q}{V_1} + \frac{R_2q}{V_1}\right)X_1 + r_{X1} \cdots (4)$$

For the aerobic unit (unit 2):

$$\frac{dS_2}{dt} = \left(\frac{q}{V_2} + \frac{R_1q}{V_2} + \frac{R_2q}{V_2}\right)S_1 - \left(\frac{q}{V_2} + \frac{R_1q}{V_2} + \frac{R_2q}{V_2}\right)S_2 + r_{S2} \cdots (5)$$

$$\frac{dX_2}{dt} = \left(\frac{q}{V_2} + \frac{R_1q}{V_2} + \frac{R_2q}{V_2}\right)X_1 - \left(\frac{q}{V_2} + \frac{R_1q}{V_2} + \frac{R_2q}{V_2}\right)X_2 + r_{X2} \cdots (6)$$

As mentioned before, oxygen is supplied only to the aerobic unit, with the following rate ($r_{Air\text{-}in}$):

$$r_{Air-in} = K_L(S_O^{SAT} - S_{O2}) \cdots (7)$$

where S^{SAT}_O is oxygen saturation concentration = 8 mg/l, (at 26 °C and 1 atm) (Rittmann and McCarty, 2001), and S_{O2} is the oxygen concentration in the aerobic reactor (mg/l). In order to establish the anoxic conditions, the value of this rate is zero in the anoxic unit.

2.3 Mathematical Model for QAC Fate and Effect

As discussed above, QACs negatively impact the biological processes responsible for wastewater treatment in WWTPs, with their fate and effect being connected to the processes of biological reactions' inhibition, adsorption, and their biological degradation.

QACs are mainly removed in activated sludge WWTPs through sorption and biodegradation (Ren et al., 2011; Zhang et al., 2011; Zhang et al., 2015). Sorption takes place with the biomass in the system or organic substances due to their strong affinity to organic and inorganic particles (Ismail et al., 2010; Ren et al., 2011). Biodegradation is achieved by a specific group of microorganisms during the aerobic biological wastewater treatment, with it depending on QAC concentration, structure, microbial community, and prevailing conditions (Sütterlin et al., 2008; Zhang et al., 2011; Hajaya and Pavlostathis, 2012; Yang et al., 2015). Additionally, QACs might not be utilized by microorganisms if they are introduced at low concentrations (Hora et al., 2020). On the other hand, a high concentration will inhibit the biological reactions in the WWTP system. In general, QACs' concentrations between 10 and 40 mg/l are inhibitory to activated sludge systems (Reynolds et al., 1987), with nitrification being the most vulnerable biological process (Zhang et al., 2011).

The biodegradation of QACs will take place after an acclimation period and under conditions where readily degradable COD is somewhat limited (Zhang et al., 2011; Hajaya and Pavlostathis, 2012), both of which are not considered as instantaneous processes. Therefore, in this work, in order to reflect the scenario under consideration, the microbial community in the WWTP is assumed to be unacclimated to high concentrations of QACs, and will be affected by the processes of microbial inhibition, in addition to adsorption.

The targeted QAC compound is chosen to represent a commercially available mix that is used in a multitude of household and industrial disinfectants, which have been studied before (Hajaya et al., 2011; Hajaya and Pavlostathis, 2012; Yang et al., 2015). The mix is comprised from three QACs (alkyl benzyl dimethyl ammonium chloride) that have a different number of carbons in their alkyl chain (12, 14, and 16).

2.3.1 QACs Inhibition

QACs' inhibition to heterotrophic bacteria responsible for COD removal and denitrification is well-documented, and can be assumed to follow the competitive inhibition model (Hajaya et al., 2011; Hajaya and Pavlostathis, 2012; Yang et al., 2015; Conidi et al., 2019). This mood of inhibition is mathematically represented by increasing the half saturation constants for heterotrophs (K_s and K_{NO}) as a result to an increase in the inhibitory compound concentration (Rittmann and McCarty, 2001), resulting in a decreased overall reaction and growth rates:

$$\bar{K} = K(1 + \frac{I}{K_I}) \quad (8)$$

where $\bar{K}$ is the inhibited, apparent half saturation constant (mg substrate/l), K is the uninhibited half saturation constant (mg substrate/l), I is the competitive inhibitor concentration, and K_I is the competitive inhibition coefficient. Units for I and K_I are specific to the concentration of the competitive inhibitor. For COD utilization, QACs inhibit through their total concentration in the unit, while for nitrate reduction they inhibit through their soluble concentration (Hajaya and Pavlostathis, 2012). Values for the competitive inhibition coefficients are 14.9 mg QAC/l and 0.27 mg QAC/l, for COD utilization and nitrate reduction, respectively. These values are for unacclimated heterotrophic bacteria (Hajaya and Pavlostathis, 2012).

For ammonia oxidizing autotrophic bacteria, QACs inhibit the biological reactions through a non-competitive inhibition mechanism (Hajaya and Pavlostathis, 2012; Yang et al., 2015). This mood of inhibition is mathematically represented by reducing the maximum specific growth rate for autotrophs (μ_A) as a result to an increase in the inhibitory compound concentration (Rittmann and McCarty, 2001), resulting in a decreased overall reaction and growth rates:

$$\bar{\mu}_A = \frac{\mu_A}{1+\frac{I}{K_I}} \quad (9)$$

where $\bar{\mu}_A$ is the inhibited, apparent maximum specific growth rate (1/d), μ_A is the uninhibited maximum specific growth rate (1/d), I is the non-competitive inhibitor concentration, and K_I is the competitive inhibition coefficient. Units for I and K_I are specific to the concentration of the competitive inhibitor. For ammonia oxidizing autotrophic growth, QACs inhibit through their autotrophic biomass adsorbed concentration (Hajaya and Pavlostathis, 2012). Value for the non-competitive inhibition coefficients is 0.0785 mg/g VSS-COD. This value is for the unacclimated autotrophic, ammonia oxidizing bacteria (Hajaya and Pavlostathis, 2012). The susceptibility to QACs for the biological processes in the WWTP can be deduced from the value of the inhibition coefficient for each reaction; reactions with low values of inhibition coefficients will be more susceptible, affected at concentrations of the inhibitor far less that those affecting reactions with higher inhibition coefficients.

2.3.2 Adsorption

The main interaction by which QACs affect the microbial group in WWTPs is adsorption (Ismail et al., 2010; Zhang et al., 2011; Conidi et al., 2019), for its phase distribution will dictate the level of its bioavailability (and inhibition) in the system (Hajaya and Pavlostathis, 2012). The adsorption behavior of the QACs mix used in this investigation has been identified to follow the Freundlich isotherm (Hajaya et al., 2011):

$$q_e = K_F Ce^n \quad (10)$$

where q_e is QAC concentration on the biomass at equilibrium (mg/g VSS COD), Ce is QAC concentration in the liquid-phase at equilibrium (mg/l), K_F is the adsorption capacity factor (mg/g VSS COD) $(l/mg)^n$, and n is the Freundlich intensity parameter. Values for K_F and n were reported to be 11.4 (mg/g VSS COD) $(l/mg)^n$ and 0.69, respectively (Hajaya et al., 2011). QACs are assumed to undergo an instantaneous equilibrium in the WWTP units.

In the simulation, QACs' biomass association and liquid phase concentrations are followed by equating them to the total QACs' concentration. This is done by linearizing the isotherm in Eq. 10, as seen in Figure 2, and performing the subsequent mass balance.

$$q_e \cong K_P Ce \quad (11)$$

$$S_Q^T = Ce + X.q_e \quad (12)$$

$$q_e = \frac{S_Q^T}{X+\frac{1}{K_P}} \quad (13)$$

$$Ce = \frac{S_Q^T}{1+X.K_P} \quad (14)$$

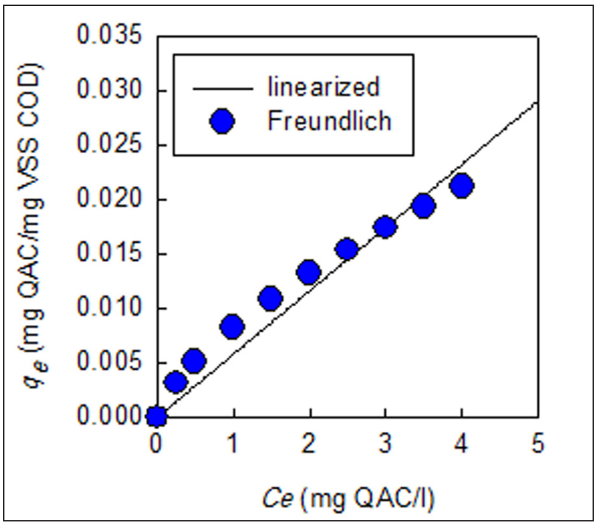

Figure 2. Linearized vs. Freundlich isotherm for the QACs mix.

where K_p is the linear adsorption coefficient for the QAC mix (mg QAC/mg VSS COD) (l/mg), S_Q^T is the total QACs concentration (mg QAC/l), and X is the total biomass available for adsorption in the WWTP (mg VSS COD/l). K_p was found to be 0.0058± 0.0002 (mg QAC/mg VSS COD) (l/mg); best estimate ± standard error. The value also considered the change in units to better suite units used in the benchmark model: (mg QAC/mg VSS COD) = (mg QAC/g VSS)/1400, 1.4 is the COD/VSS ratio (Parker et al., 2008). Furthermore, the linearization of the adsorption isotherm will result in an explicit expression for both of q_e and C_e.

2.4 Plant Simulated Operation:

The main purpose of the work presented here is to investigate the possibility of maintaining a continuous and adequate performance of a WWTP, while treating QAC-containing wastewater, by changing a group of the plant operational parameters. These changes are directed mainly to reduce the inhibitory effects by achieving an increase in microbial growth and utilization rates to overcome the reduction in their value, and/or increasing the biomass concentration in the system in order to limit the bioavailability of QACs (Conidi et al., 2019).

The WWTP depicted in Figure 1 was simulated while treating wastewater with the characteristics shown in Table 4. First, the operation treating QAC-free wastewater was simulated in order to establish the baseline performance of the plant. Second, The QAC mix was then introduced into the influent wastewater at concentrations of 2, 4, 6, 8, and 10 mg/l, individually. Plant operation was then simulated for ten days at each of the QAC concentrations in order to show the effect on the plant performance. This period of time was chosen to represent the initial response of an unacclimated WWTP to the presence of QACs at different initial concentrations. Finally, a group of operational parameters' values were changed, individually, while maintaining the others at their baseline values, in order to investigate their effectiveness in mitigating the effect of QACs on the WWTP performance.

Table 5 shows the parameters to be manipulated and the ratios and values that they will be changed to.

Table 5. Operational parameters to be manipulated and the ratios and values that they will be changed into; a: baseline operation value.

Operational parameters changed at each QAC concentration	Values changed
Solids recycle flow rate	R_2: 1[a], 1.5, 2, 4, and 6
Nitrate recycle flow rate	R_1: 1, 4, 5[a], 6, and 8
Influent wastewater flow rate	q: 0.25q, 0.5q, 0.75q, 1.0q[a], and 1.5q
Oxygen supply rate	*Kla*: 200[a], 230, 260, 290, 320 (1/d)

Changes in the solids' recycle ratio (R_2) were made to enhance the biomass concentration in order to limit QACs' bioavailability, while changes in the nitrate recycle (R_1) were made to enhance the growth rate of the two microbial groups in the plant. Values of the influent wastewater (q) were changed in order to limit the level of exposure to the QACs, while changes in the oxygen mass transfer coefficient (Kla) were made to increase the rate of oxygen supply to enhance the growth rate. These parameters were chosen because their alteration does not require modifying the existing layout or structure of the WWTP. The range of their values is, however, system-specific, and must be chosen within a window that insures a stable operation of the WWTP.

In order to simulate the system, the group of ODEs representing the behavior of the WWTP system was solved simultaneously in order to simulate the operation of the system. The equations were solved using the fourth-order Runge–Kutta procedure in MATLAB (The MathWorks Inc., Natick, MA), with a maximum time step of 0.5 day.

3. Results and Discussion

3.1 Baseline, QACs-Free Performance

The simulated operation for the WWTP was performed for thirty days of continuous and QAC-free, operation. Effluent steady state concentrations for S_{NH} and S_{NO} were 1.92 and 13.1 mg N/l, respectively, X_{BA} and X_{BH} of 151.2 and 2587.2 mg VSS COD/l, respectively, and the COD of 48.1 mg/l. The simulation results were comparable to the results of the benchmark study that had a similar unit sizes and feed wastewater composition and flow rate (Alex et al., 2008), and to results found in the literature for work that used the benchmark model in a wide group of applications (Sochacki et al., 2009; Ostace et al., 2011; Zeng and Liu, 2015; Harja and Naşcu, 2019; Wang et al., 2020)

3.2 Initial QACs Exposure

Figure 3 shows the effect of varying the non-ideal mixing parameters on the concentration of nitrogen compounds in the system.

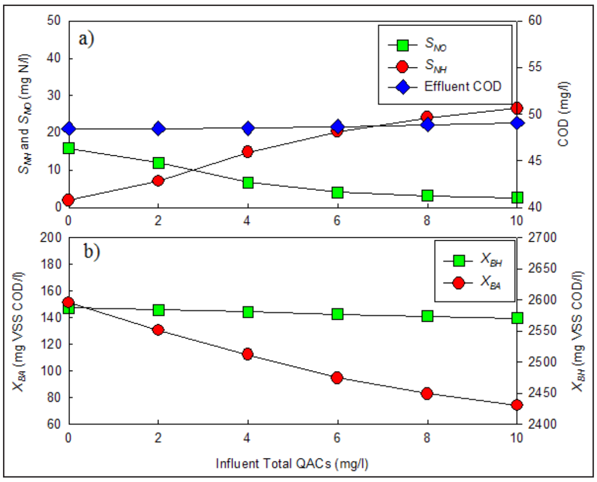

Figure 3. Effect of treating QACs-containing wastewaters at various concentrations after operating for 10 days: a) on the effluent S_{NH}, S_{NO}, and total COD, and b) on X_{BA} and X_{BH}.

As seen in the previous figure, with increasing QACs' concentration in the influent wastewater, the nitrification performance of the system has drastically dropped, resulting in an increase in S_{NH} concentration, and a decrease in S_{NO} concentration. Typically, in WWTPs, ammonia is oxidized under aerobic conditions to nitrate by autotrophic nitrifying by two consecutive biological reactions. (Madigan and Martinko, 2006; Tchobanoglous et al., 2007). However, due to QACs' inhibition, both of the biologically mediated nitrification reactions along with the microbial growth rate were inhibited. This also resulted in decreasing the autotrophic population in the system (Figure 3b).

QACs' inhibition to nitrification is well documented in the literature (Zhang et al., 2011; Hajaya and Pavlostathis, 2012; Yang et al., 2015; Conidi et al., 2019). However, as discussed above, the WWTPs will cope with the presence of QACs in their influent wastewaters, with the effectiveness of the process reaching pre-BAC exposure levels, but not before going through an operational period that will drastically affect the plant's nitrogen removal efficiency as it is clearly seen in Figure 3a. Modifications to operational parameters should be attempted during this period in order to reduce the effect on ammonia oxidation.

On the other hand, both of the COD utilization and growth of heterotrophs were not affected in QACs at the levels found in the system feed. This can be seen clear in the relatively constant effluent COD concentration (Figure 3a) and heterotrophic biomass concentration (Figure 3b) in the system while treating QAC-containing wastewater. Similarly, this observation was also reported in the literature (Zhang et al., 2011; Hajaya and Pavlostathis, 2012; Yang et al., 2015; Conidi et al., 2019).

Therefore, the attempted mitigation actions by operational parameters' manipulations should be directed towards minimizing the effect of QACs on the nitrification process.

3.2 Possible Mitigations Actions

As discussed above, actions should be directed towards maintaining an adequate level of nitrification during the initial QACs' exposure period, in order to provide a time window for the plant to recover (through microbial acclimation, biodegradation, or adsorption), and continue its operation. The following sections discuss the various measures suggested to provide such time window, and represent the resulting difference in the performance between modified and unmodified operation while treating QAC-containing wastewater. This difference is evaluated as follows at the same QAC concentration:

$$\overbrace{\text{Difference}(\Delta)}^{\text{At the same QAC conc.}} = (S \text{ or } X)^{\text{At base line parameter}}_{\text{At the same QAC conc}} - (S \text{ or } X)^{\text{Changed parameter value}}_{\text{At the same QAC conc}} \quad (15)$$

3.2.1. Changing the Solids' Recycle Ratio R_2

Figure 4 shows the predicted difference in operation resulting from the simulated operation of the WWTP while treating QACs-containing wastewater at different solid recycle ratios (R_2), evaluated through Eq. 15.

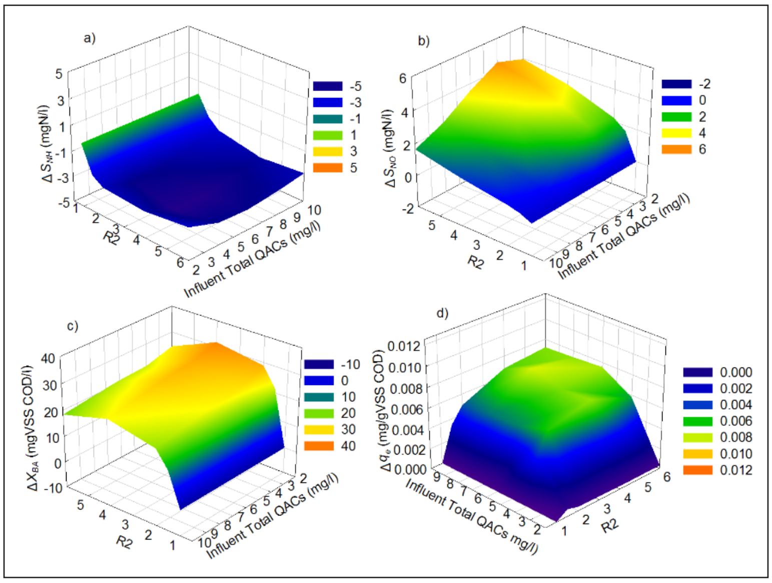

Figure 4. Difference in operation (Eq. 15) resulting from simulated operation of the WWTP while treating QACs-containing wastewater at different solids recycles ratios (R_2). A: difference in effluent S_{NH}, B: difference in effluent S_{NO}, C: difference in X_{BA}, and D: difference in q_e

As shown in Figure 4a, compared to the baseline value (R_2 = 1) increasing the solids' recycle ratio is projected to successfully reducing the effluent S_{NH} at all QAC concentrations, by up to 5 mg N/l.

This corresponded to a predictable increase in S_{NO}, less than 6 mg N/l. This more likely is attributed to a marginal enhancement in the denitrification process (Figure 4b), brought by the expected increase in heterotrophic bacteria biomass concentration of around 30 mg VSS COD/l (at R_2 = 4, at all QAC concentrations), as seen in Figure 4c. The predicted slight enhancement in Ammonia removal occurred despite the slight increase in qe, by less than 0.08 mg/g VSS COD, which is associated with the autotrophs fraction of the system's biomass (Figure 4d).

QACs are known to completely inhibit nitrification at concentrations higher than 2 mg/l (Yang et al., 2015; Conidi et al., 2019). Predicted enhancements brought by the increase of R_2 were marginal. However, they allowed for maintaining some nitrification ability and autotrophic biomass at higher concentrations (more than 2 mg/l). Additionally, this could be used in conjunction with another parameter to yield an effective mitigation measure.

3.2.2. Changing the Nitrate Recycle Ratio R_1

The predicted difference in operation resulting from the simulated operation of the WWTP while treating QACs-containing wastewater at different nitrate recycle ratios (R_1), evaluated through Eq. 1, is shown in Figure 5.

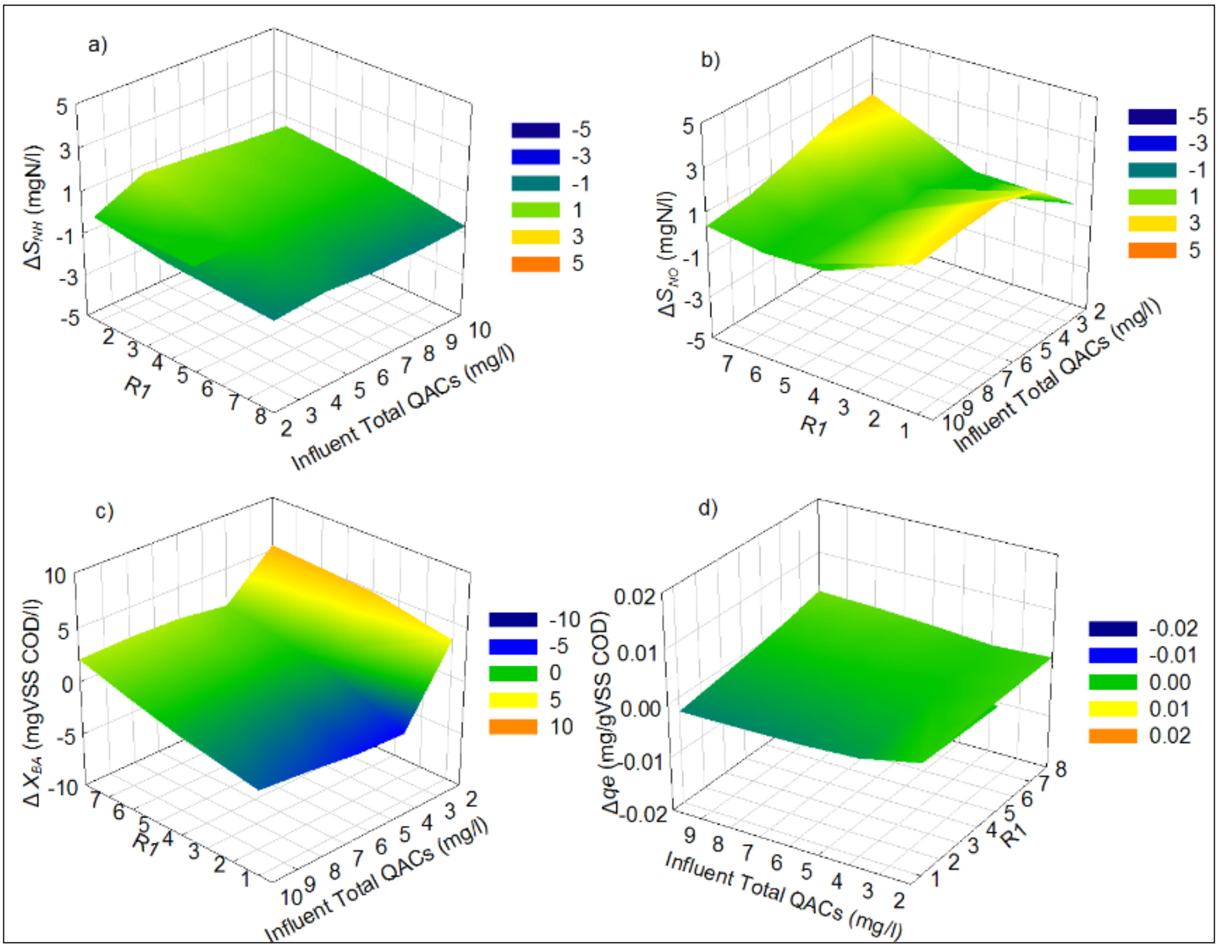

Figure 5. Difference in operation (Eq. 15) resulting from simulated operation of the WWTP while treating QACs-containing wastewater at different nitrate recycles ratios (R_1): a) difference in effluent S_{NH}, b) difference in effluent S_{NO}, c) difference in X_{BA}, and d) difference in q_e

As seen in Figure 5a, changing the nitrate recycle ratio compared to the baseline value (R_1 = 5 was not successful in improving the nitrification process, yielding slightly worse S_{NH} by almost 1 mg N/l. S_{NO} increased (by almost 5 mg N/l) when R_1 was either increased or decreased from a value of 5, as seen in Figure 5b, since this value is the best for the nitrate recycle for this system (Alex et al., 2008). Unchanged values S_{NH} were evident despite an increase in X_{BA}, up to 10 mg VSS COD/l. However, this projected increase was shown at low QAC concentrations (less than 3 mg/l), as seen in Figure 5c. Differences in qe were not projected to change and were maintained at relatively constant levels, as seen in Figure 5d. The previous projections in performance differences indicate that changing R_1 will have almost no effect in mitigating the effects of QACs on the system during its initial exposure to it.

3.2.3. Changing the Influent Flow Rate (q)

The effect of operation at different flow rate (q) fractions on the predicted difference in the simulated operation of the WWTP while treating QACs-containing wastewater (evaluated through Eq. 15) is shown in Figure 6.

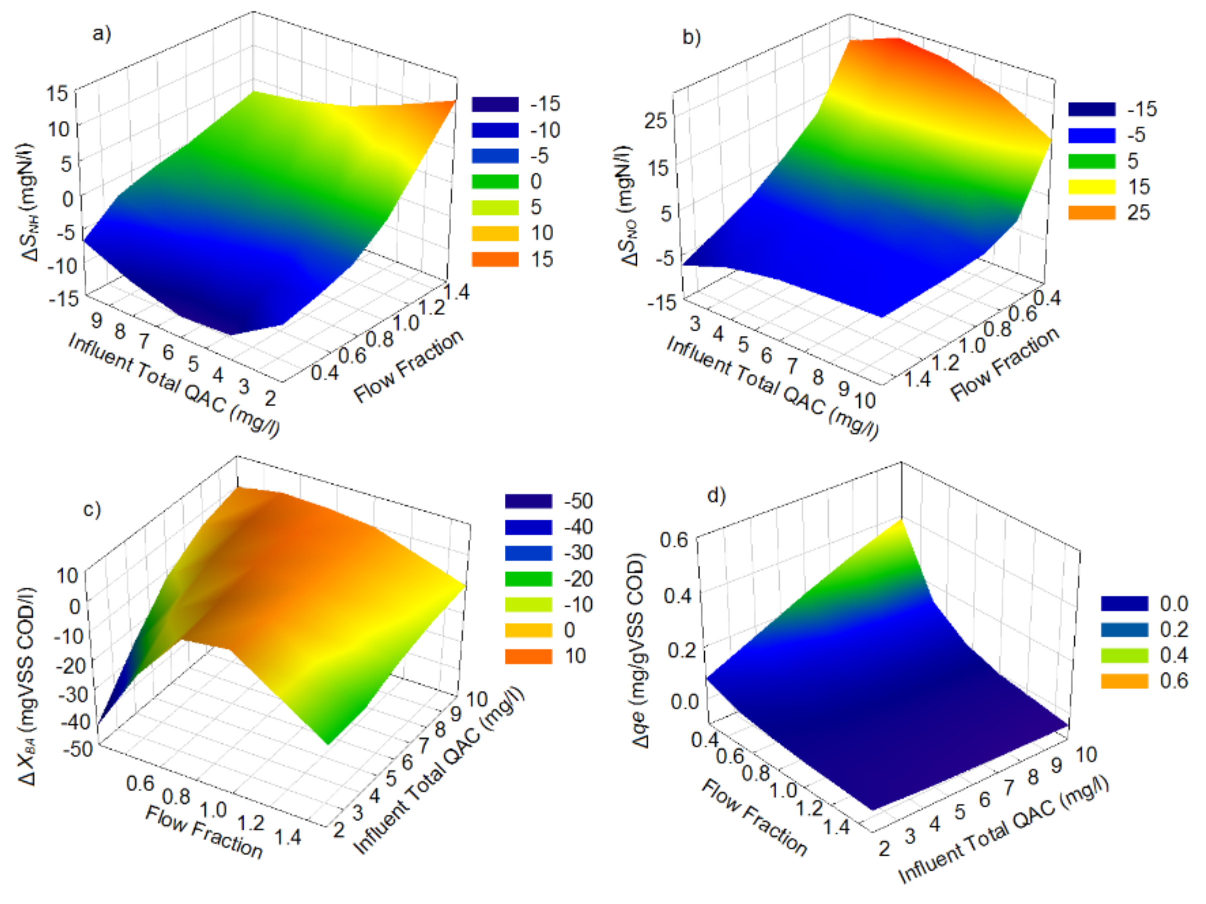

Figure 6. Difference in operation (Eq. 15) resulting from simulated operation of the WWTP while treating QACs-containing wastewater at different flow rate (q) fractions: a) difference in effluent S_{NH}, b) difference in effluent S_{NO}, c) difference in X_{BA}, and d) difference in q_e

As predicted by the simulation, increasing the influent QACs- containing wastewater did indeed reduce the nitrification performance in the system. This can be seen by increasing the effluent S_{NH}, up to almost 15 mg N/l (Figure 6a). However a decreased S_{NO} by only 5 mg N/l (Figure 6b) can be attributed to the increase in heterotrophic bacteria (from 2570 to 3320 mg VSS COD/l), which enhanced the denitrification process, as the influent wastewater flow rate is increased. This increase did not affect qe (which is associated to the autotrophs) as seen in Figure 6d. On the other hand, values of X_{BA} at the higher flow rate decreased by almost 20 mg VSS COD/l (Figure 6c). This could explain the reduction in nitrification performance.

As the flow rate was reduced, effluent S_{NH} is projected to drop up to almost 5 mg N/l (Figure 6a), which is attributed to a combination of increased of X_{BA} (up to 10 mg VSS COD/l) and reduced nitrogen load brought by a reduction in the influent wastewater. However, this enhancement is limited to drop in the feed flow rate fraction of 0.8. This reduction will also result in increasing S_{NO} by only 5 mg N/l (Figure 6b) at the same fraction limit. Changing to a smaller fraction of flow rate will eventually result in increasing S_{NO} by 25 mg N/l (Figure 6 b) , due to the decreased heterotrophic biomass concentration as a consequence of the reduced feed (from 2570 to 1667 mg VSS COD/l). qe increased drastically, between 0.2 and 0.6 mg/g VSS COD, due to the reduction in available biomass for adsorption (Figure 6d). Biomass levels in the system will affect the distribution of QACs, and ultimately affect their fate (Ren et al., 2011; Yang et al., 2015).

The aforementioned predictions for the system performance as a response to changing the influent flow rate of QAC-containing wastewater indicate that increasing the flow rate will have severe effects, similar to those resulting from extremely decreasing it (less than 0.8). The best course of action is a reduction in flow rate, for no more than a fraction of 0.8 of the original influent QACs-containing wastewater.

3.2.4. Changing the Oxygen Supply Rate

Figure 7 shows the difference in operation resulting from the simulated operation of the WWTP while treating QACs-containing wastewater at different oxygen supply rates achieved by changing the oxygen mass transfer coefficient (Kla), evaluated through Eq. 15.

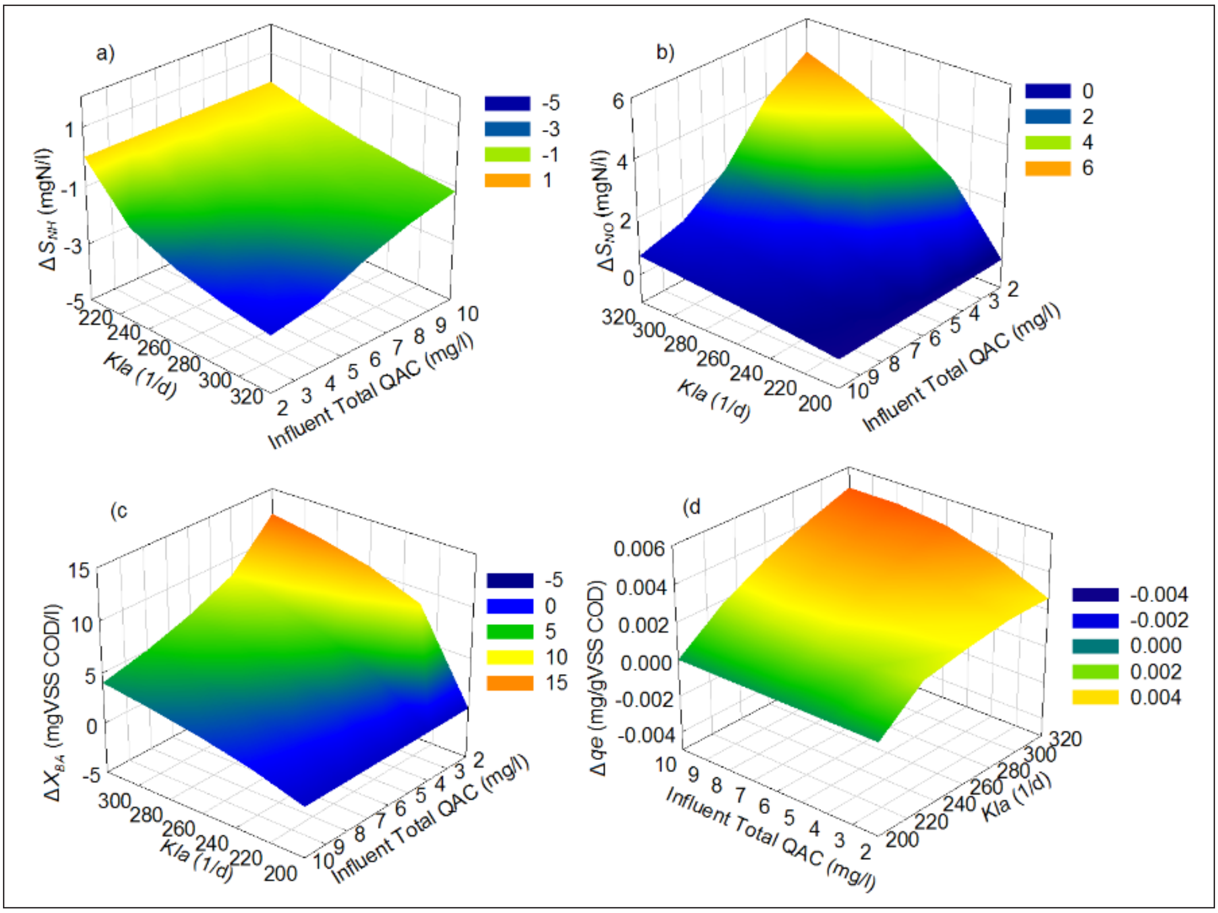

Figure 7. Difference in operation (Eq. 15) resulting from simulated operation of the WWTP while treating QACs-containing wastewater at different oxygen supply rates achieved by changing the oxygen mass transfer coefficient (Kla): a) difference in effluent S_{NH}, b) difference in effluent S_{NO}, c) difference in X_{BA}, and d) difference in q_e.

Compared to the baseline value at Kla of 200 (1/d), increasing the oxygen supply rate was capable of enhancing the system's nitrification performance by reducing S_{NH} between 3 and 5 mg N/l at Kla values between 260 and 320 (1/d), and up to a QACs' concentration of 6 mg/l (Figure 7a). The same range saw an increase in S_{NO}, between 4 and 5 mg N/l. The same could be said for X_{BA} which is projected to have an increase between 5 and 15 mg VSS COD/l (Figure 7c). S_{NO} increased (up by 6 mg N/l) at Kla values higher than 260 (1/d), remaining unchanged otherwise, as seen in Figure 7b. This is explained by the negative effect of oxygen on the denitrification process, whose rate is negatively affected by the presence of oxygen (see P2 in Table 2).

The increases in biomass also meant an increase in qe as seen in Figure 7 D. Enhancements brought by increasing the oxygen supply rate will increase oxygen concentration in the system, thus directly increasing biological reactions that utilize oxygen (Rittmann and McCarty, 2001).

On the other hand, changing Kla was not effective in mitigating the effects of QACs at concentrations higher than the aforementioned range (up to 6 mg/l). Therefore, it can be said that increasing the rate of oxygen (by changing Kla) can be used to combat the effect of QACs-containing wastewater, but to a specific limit.

4. Conclusion

The main purpose of the work presented here is to probe possible variations in a group of operational parameters of the WWTP in order to modify its operation to help reduce the initial adverse effects on the treatment, resulting from elevated QACs' concentrations in the influent. This scenario is expected as the usage of QACs-containing sanitizers has increased globally to prevent the spread of COVID-19 disease. The following conclusions were found:

The used model representing QACs' inhibition was able to successfully predict the drop in the system performance, which was mainly its nitrification ability, at each tested QACs' concentration.

Changing the solids' recycle ratio R_2 allowed for maintaining some nitrification ability and autotrophic biomass at higher concentrations (more than 2 mg/l). Best results were at $R_2 = 4$.

Manipulations in the nitrate recycle ratio (R_1) will have almost no effect on mitigating the effects of QACs on the system during initial exposure.

Increasing the influent flow rate q will negatively affect the performance, and decreasing it will help recover the performance. However, in order to maintain a stable WWTP, the reduction in q should not exceed a fraction of 0.8. This effect was predicted for QACs' concentrations below 10 mg/l.

Enhancing the oxygen transfer rate by changing Kla was effective in mitigating the effect of QACs up to a concentration of 6 mg/l. Additionally, benefits of increasing Kla were detected only at a range of 260 to 320 (1/d).

The previous predictions provided a preliminary insight into actions that can be helpful in managing the WWTP effluent during its initial QACs exposure period. As a result and as discussed in the literature, the microbial community in the plant will overcome the presence of QACs and continue a regular operation.

It must be added that this work considered changing one parameter while maintaining the others at the baseline value. Tackling the challenge by considering multiple actions towards these parameters (simultaneous change) could be more effective in achieving the main purpose, and should be considered for future works.

Finally, this work provided a framework for the simulation of WWTPs that could receive inhibitory material in their influents.

References

Alex, J., Benedetti, L., Copp, J., Gernaey, K.V., Jeppsson, U., Nopens, I., Pons, M.N., Rieger, L., Rosen, C., Steyer, J.P., Vanrolleghem, P., Winkler, S. (2008). Benchmark simulation model no. 1 (BSM1). Report by the IWA Taskgroup on benchmarking of control strategies for WWTPs.

Chen, M., Zhang, X., Wang, Z., Liu, M., Wang, L., Wu, Z. (2018). Impacts of quaternary ammonium compounds on membrane bioreactor performance: acute and chronic responses of microorganisms. Water Research 134: 153-161.

Conidi, D., Andalib, M., Andres, C., Bye, C., Umble, A., Dold, P. (2019). Modeling quaternary ammonium compound inhibition of biological nutrient removal activated sludge. Water Science and Technology 79 (1): 41-50.

Cross, J. and Singer, E.J. (1994). Cationic surfactants: analytical and biological evaluation. Marcel Dekker, Inc., New York.

Cucinotta, D. and Vanelli, M. (2020). WHO declares COVID-19 a pandemic. Acta bio-medica: Atenei Parmensis 91(1): 157-160.

Ding, W.-H. and Liao, Y.-H. (2001). Determination of alkylbenzyldimethylammonium chlorides in river water and sewage effluent by solid-phase extraction and gas chromatography/mass spectrometry. Analytical chemistry 73(1): 36-40.

Environmental Protection Agancy (2020). "List N: Products with Emerging Viral Pathogens AND Human Coronavirus claims for use against SARS-CoV-2", www.epa.gov (May 30, 2020).

Ferrer, I. and Furlong, E.T. (2001). Identification of alkyl dimethylbenzylammonium surfactants in water samples by solid-phase extraction followed by ion trap LC/MS and LC/MS/MS. Environmental Science and Technology 35(12): 2583-2588.

Hajaya, M. (2019). Identifying the Effect of Non-Ideal Mixing on a Pre-Denitrification Activated Sludge System Performance through Model Based Simulations. Jordanian Journal of Engineering and Chemical Industries 2(1): 15-32.

Hajaya, M.G. and Pavlostathis, S.G. (2012). Fate and effect of benzalkonium chlorides in a continuous-flow biological nitrogen removal system treating poultry processing wastewater. Bioresource Technology 118: 73-81.

Hajaya, M.G., Tezel, U., Pavlostathis, S.G. (2011). Effect of temperature and benzalkonium chloride on nitrate reduction. Bioresource Technology 102(8): 5039-5047.

Harja, G. and Nașcu, I. (2019). Control of an activated sludge wastewater treatment process based on a Calibrated and modified BSM1 Model. 2019 20th International Carpathian Control Conference (ICCC).

Henze, M., Gujer, W., Mino, T., Loosdrecht, M.v. (2000). Activated Sludge Models ASM1, ASM2, ASM2d, and ASM3. IWA Scientific and Technical Report 9. IWA Publishing, London, UK.

Hora, P., Pati, S.G., McNamara, P.J., Arnold, W.A. (2020). Increased Use of Quaternary Ammonium Compounds during the SARS-CoV-2 Pandemic and Beyond: Consideration of Environmental Implications. Environmental Science and Technology Letters 7(9): 622-631.

Ismail, Z.Z., Tezel, U., Pavlostathis, S.G. (2010). Sorption of quaternary ammonium compounds to municipal sludge. Water Research 44(7): 2303-2313.

Jardak, K., Drogui, P., Daghrir, R. (2016). Surfactants in aquatic and terrestrial environment: occurrence, behavior, and treatment processes. Environmental Science and Pollution Research 23(4): 3195-3216.

Kemper, J.M., Walse, S.S., Mitch, W.A. (2010). Quaternary amines as nitrosamine precursors: a role for consumer products? Environmental Science Technology 44(4): 1224-1231.

Le Moullec, Y., Potier, O., Gentric, C., Leclerc, J. (2011). Activated sludge pilot plant: Comparison between experimental and predicted concentration profiles using three different modelling approaches. Water Research 45(10): 3085-3097.

Madigan, M.T. and Martinko, J.M. (2006). Brock Biology Of Microorganisms. 11th ed., Pearson Prentice Hall, Upper Saddle River, NJ.

Marnie, C. and Peters, M. (2020). "ANMF Evidence Brief Covid-19: Cleaning and disinfection of hospital surfaces and equipment " Australian Nursing and Midwifery Federation, anmf.org.au (May. 30, 2020).

Martínez-Carballo, E., Sitka, A., González-Barreiro, C., Kreuzinger, N., Fürhacker, M., Scharf, S., Gans, O. (2007). Determination of selected quaternary ammonium compounds by liquid chromatography with mass spectrometry. Part I. Application to surface, waste and indirect discharge water samples in Austria. Environmental Pollution 145(2): 489-496.

Mitch, W.A. and Sedlak, D.L. (2004). Characterization and fate of N-nitrosodimethyl amine precursors in municipal wastewater treatment Plants. Environmental Science and Technology 38(5): 1445-1454.

Ostace, G.S., Cristea, V.M., Agachi, P.Ș. (2011). Extension of Activated Sludge Model No 1 with two-step nitrification and denitrification processes for operation improvement. Environmental Engineering Management Journal 10(10): 1529-1544.

Parker, W.J., Jones, R.M., Murthy, S. (2008). Characterization of the COD/VSS ratio during anaerobic digestion of waste activated sludge: experimental and modeling studies. Proceedings of the Water Environment Federation 10: 524-533.

Pati, S.G. and Arnold, W.A. (2020). Comprehensive screening of quaternary ammonium surfactants and ionic liquids in wastewater effluents and lake sediments. Environmental Science: Processes and Impacts 22(2): 430-441.

Ren, R., Liu, D., Li, K., Sun, J., Zhang, C. (2011). Adsorption of quaternary ammonium compounds onto activated sludge. Journal of water resource and protection 3(2): 105-113.

Rittmann, B.E. and McCarty, P.L. (2001). Environmental biotechnology: principles and applications. McGraw-Hill, New York, NY.

Reynolds, L., Blok, J., De Morsier, A., Gerike, P., Wellens, H., Bontinck, W. (1987). Evaluation of the toxicity of substances to be assessed for biodegradability. Chemosphere 16(10-12): 2259-2277.

Ruan, T., Song, S., Wang, T., Liu, R., Lin, Y., Jiang, G. (2014). Identification and composition of emerging quaternary ammonium compounds in municipal sewage sludge in China. Environmental Science and Technology 48(8): 4289-4297.

Sochacki, A., Knodel, J., Geißen, S., Zambarda, V., Miksch, K., Bertanza, G. (2009). Modelling and simulation of a municipal WWTP with limited operational data. Proceedings of a Polish-Swedish-Ukrainian Seminar: 23-25

Sütterlin, H., Alexy, R., Coker, A., Kümmerer, K. (2008). Mixtures of quaternary ammonium compounds and anionic organic compounds in the aquatic environment: elimination and biodegradability in the closed bottle test monitored by LC–MS/MS. Chemosphere 72(3): 479-484.

Pereira, B. M. P. and Tagkopoulos, I. (2019). Benzalkonium Chlorides: Uses, Regulatory Status, and Microbial Resistance. Applied and Environmental Microbiology 85(13): 1-13. DOI: 10.1128/AEM.00377-19.

Tchobanoglous, G., Burton, F.L. and Stensel, H.D. (2007). Wastewater Engineering: Treatment and Reuse. 4th Ed., McGraw-Hill Professional, New York, NY.

Tezel, U. and Pavlostathis, S. (2011). Role of quaternary ammonium compounds on antimicrobial resistance in the environment. In book: Antimicrobial resistance in the environment: 349-387. DOI: 10.1002/9781118156247.ch20.

Thomas, P., Baldwin, C., Bissett, B., Boden, I., Gosselink, R., Granger, C.L., Hodgson, C., Jones, A.Y., Kho, M.E. and Moses, R. (2020). Physiotherapy management for COVID-19 in the acute hospital setting: clinical practice recommendations. Journal of Physiotherapy 66(2): 73-82.

Tullo, A. and Bettenhausen, C. (2020). "Disinfectant Demand from Coronavirus Concerns Challenges Specialty Chemical Supply Chain. Chemical and Engineering News 98(15).

Van Doremalen, N., Bushmaker, T., Morris, D.H., Holbrook, M.G., Gamble, A., Williamson, B.N., Tamin, A., Harcourt, J.L., Thornburg, N.J., Gerber, S.I. (2020). Aerosol and surface stability of SARS-CoV-2 as compared with SARS-CoV-1. New England Journal of Medicine 382(16): 1564-1567.

Vanhooren, H. and Nguyen, K. (1996). Development of a simulation protocol for evaluation of respirometry-based control strategies. Report University of Gent and University of Ottawa.

Wang, D., Ha, M., Qiao, J., Yan, J., Xie, Y. (2020). Data-based composite control design with critic intelligence for a wastewater treatment platform. Artificial Intelligence Review 53: 3773-3785.

Wieck, S., Olsson, O., Kümmerer, K. (2018). Not only biocidal products: washing and cleaning agents and personal care products can act as further sources of biocidal active substances in wastewater. Environment international 115: 247-256.

World Health Organization (2020). Water, sanitation, hygiene and waste management for COVID-19: technical brief, 03 March 2020 Geneva: WHO; 2020.

Yang, J., Tezel, U., Li, K., Pavlostathis, S.G. (2015). Prolonged exposure of mixed aerobic cultures to low temperature and benzalkonium chloride affect the rate and extent of nitrification. Bioresource Technology 179: 193-201.

Zeng, J. and Liu, J. (2015). Economic model predictive control of wastewater treatment processes. Industrial and Engineering Chemistry Research 54(21): 5710-5721.

Zhang, C., Cui, F., Zeng, G.-m., Jiang, M., Yang, Z.-z., Yu, Z.-g., Zhu, M.-y., Shen, L.-q. (2015). Quaternary ammonium compounds (QACs): a review on occurrence, fate and toxicity in the environment. Science of the Total Environment 518: 352-362. DOI: 10.1016/j.scitotenv.2015.03.007.

Zhang, C., Tezel, U., Li, K., Liu, D., Ren, R., Du, J., Pavlostathis, S.G. (2011). Evaluation and modeling of benzalkonium chloride inhibition and biodegradation in activated sludge. Water Research 45(3): 1238-1246.

Zu, Z.Y., Jiang, M.D., Xu, P.P., Chen, W., Ni, Q.Q., Lu, G.M. Zhang, L.J. (2020). Coronavirus disease 2019 (COVID-19): a perspective from China. Radiology 296(2): 15-25.

JJEES

Jordan Journal of Earth and Environmental Sciences

JJEES (2021) 12 (1): 13-21
ISSN 1995-6681

Novel Spectrophotometric Method with Enhanced Sensitivity for the Determination of Nitrite in Vegetables

Abdulqawi Numan[1,2], Anass Al-Nedhary[3],
Mahfoudh Al-Hamadi[4], Shaif Saleh[5*], Fares Ghaleb[4], Mansour Galil[6,2]

[1]*Sana'a University, Faculty of Education, Department of Science Curricula and Teaching Methodologies, Yemen.*
[2]*Al-janad University for Science and Technology, Faculty of Medical Sciences, Department of Pharmacy, Yemen.*
[3]*Sana'a University, Khawlan Branch, Faculty of Education, Department of Chemistry, Yemen.*
[4]*Sana'a University, Faculty of Science, Department of Chemistry, Yemen.*
[5]*University of Aden, Faculty of Science, Department of Chemistry, Yemen.*
[6]*Taiz University, Faculty of Applied Sciences, Department of Chemistry, Yemen.*

Received 3rd March 2020; Accepted 1st of September 2020

Abstract

The aim of the present work is to develop a novel, sensitive, fast, and cost-effective spectrophotometric method for the detection and quantitation of nitrite ions in vegetables. The method is based on the diazotization-coupling reaction of nitrite with solid sulfanilic acid and N-(1-naphthyl) ethylenediamine dihydrochloride in acidic medium. The final product is an azo dye with a maximum absorption at 542 nm. Variables such as amounts of solid diazo-coupling reagents, pH, and mass of charcoal, are optimized. The method detection and quantitation limits are respectively 0.010 mg L^{-1} and 0.030 mg L^{-1}. The precession of the method reported as %RSD is below 5%, and the linear range is extended between 0.05 and 1 mg L^{-1} with R^2 reaching 0.9999. The performance criteria of the proposed method under the most optimal conditions are validated and found to be superior compared to the performance of two selected reference methods and also to the results of the same method when diazo-coupling reagents are used as solutions. The proposed and validated method is used to quantitate nitrite in four leafy and root vegetables marketed in Yemeni. The method's recovery in the four tested vegetables is between 98.00% and 102.00% which is an indication of the high extraction efficiency and sensitivity of the developed method.

Keywords: Nitrite, Sulfanilic acid, N-(1- naphthyl) ethylenediamine dihydro chloride, Vegetables, Spectrophotometry.

1. Introduction

Nitrite is one of the reactive species of nitrogen that has received increased attention in the recent years due to possible adverse and beneficial effects associated with it. Nitrite has been linked to the formation of N- nitrosamines in acidic media including the stomach via its reactions with secondary amines and amides (Santamaria, 2006); (Sindelar and Milkowski, 2012). The lower molecular weight N-nitrosamines have been unequivocally proven to be carcinogenic to humans and animals (Straif et al., 2000; Preussmann, 1983); Bryan et al., 2012); (Bogovski and Bogovski, 1981). Thus, nitrite is considered as a precursor of N-nitrosamine formation.

Despite the above established knowledge, the direct link between nitrite in the diet and gastric cancer, however, has not been proven conclusively as concluded by three recent review and meta-analysis articles (Bryan et al., 2012; Parvizishad et al., 2017; Song et al., 2015). The association of nitrite with methaemoglobinaemia is also questionable (Merino, 2009a). Studies on the curative effect of nitrite to humans have been on the rise. Recent review articles concluded that the dietary intake of nitrite proved to be an alternative pathway for the formation of nitric oxide (NO) which is a potent cardiovascular relaxant and vasodilator (Machha and Schechter, 2011); Jackson et al., 2018; Lundberg and Weitzberg, 2009). Nitrite may also serve as a plasma biomarker for NO bioavailability (Lundberg and Weitzberg, 2009; Bryan, 2006).

Despite the positive shift in the appreciation of the role of nitrite, the daily consumption of nitrite is still regulated in many countries. The proposed acceptable daily intake (ADI) of nitrite is estimated to be 0.06 mg kg^{-1} bodyweight which is translated to be 3.6 mg day^{-1} for 60 kg person (SCF, 1995).

The ubiquitous nature of nitrite and the complexity of the matrices present a challenge for scientists to develop an adequate method for the detection and quantitation of nitrite. A variety of analytical methods have been developed and applied for the determination of nitrite in food, water, vegetables, biological fluids, and other matrices. These methods include spectrophotometry (Moorcroft et al., 2001; Ozcan and Akbulut, 2007), chromatography (Gennaro and Bertolo, 1989; Cheng and Tasng, 1998; Bosch et al., 1995; Sui and Henshall, 1998), polarographic method (Ximenes et al., 2000), flow injection analysis (Ensafi and Kazemzadeh, 1999; Kazemzadeh and Ensafi, 2001), and capillary electrophoresis (Jimidar et al., 1995; Gaspar et al., 2005). Two review articles (Moorcroft et al., 2001; Wang et al., 2017), have summarized scientific endeavors to assess the level of nitrite ions in

Corresponding author email: shamq2002@yahoo.com

various matrices. Generally speaking, each method has its limitations and advantages. Spectrophotometric based-methods that are classified into three categories: Griess Assay methods, nitrosation procedures and catalytic methods are by far the most popular approaches for the determination of nitrite due to their simplicity and feasibility (Wang et al., 2017). Even though Griess Assay has been used extensively for the detection of nitrite with dozens of color producing reagents (diazo-coupling agents) available for the reaction with nitrite, this approach suffers from interferences and low sensitivity. The performance of spectrophotometric methods in general is compromised by the addition of access reagents that causes unnecessary dilution. Thus, the present work aims at developing and validating a spectrophotometric method based on the use of a new combination of diazotizing and coupling agents; sulfanilic acid and N-(1-naphthyl) ethylenediaminedihydrochloride (NEDD) in solid forms to determine nitrite ions in vegetables. In this study, this method is applied for nitrite quantitation in four leafy and root vegetables (mint, coriander, white radish, and carrots). This approach and to the best of the authors' knowledge has not been reported previously.

2. Methodology

2.1. Chemicals and Reagents

All chemicals and reagents used in the present work were of analytical grade. The charcoal, hydrochloric acid 37%, sodium nitrite, sodium hydroxide (99.9%), sulfanilamide (99%) and sulfanilic acid (99%) were from BDH. The N-(1-naphthyl) ethylenediamine. 2HCl (99%) and Methyl anthranilate (99%) were purchased from Merck and Himedia respectively. De-ionized water (with specific conductance of 0.05 µS cm^{-1}) was produced in-house, and was used for the preparation of all solutions.

2.2. Instruments

Spectrophotometer (UV/Visible) model Spectroscan 60DV, Biotech Engineering, was used for all absorbance measurements. Deionized water was prepared in-house using DirectQ3 (Millipore-USA). Electronic balance, model no: E51120-4, Biotech Engineering and pH meter, Biotech Engineering were also used.

2.3. Preparation of Nitrite Standards and Reagents Solutions

2.3.1. Nitrite Stock Standard Solution

The stock standard solution of nitrite (400 mg L^{-1}) was prepared by placing 0.15 g of sodium nitrite in a 250 mL volumetric flask and de-ionized water was then added to the mark. The stock solutions were kept in a refrigerator at 4 °C. All other working standard solutions were then made fresh from the 400 mg L^{-1} stock solution by making the appropriate dilution using de-ionized water.

2.3.2. Hydrochloric Acid and Sodium Hydroxide

HCl solution was prepared by diluting an appropriate volume of the concentrated HCl reagent in de-ionized water to make 0.1 M. The 2N NaOH solution was prepared by weighing an appropriate amount of the solid pellets in de-ionized water to make a final concentration of 2N.

2.3.3. Preparation of the Color Producing Reagents (diazo-coupling reagents)

Sulfanilic acid (SA), sulfanilamide, and NEDD were prepared by weighing 0.6 g, 1 g and 0.6 g respectively into three separate volumetric flasks. De-ionized water was added to the flasks. Methyl anthranilate was prepared by diluting 0.5 mL in 100 mL of alcohol.

2.4. Vegetable Samples

Two leafy plants (mint, and coriander) and two root vegetables (carrots and white radish) were used for this study. These vegetables are amongst the most common cultivated crops in Yemen. A total of twenty samples (five samples for each vegetable) were collected between February and December, 2013 which represnt the dry and rainy seasons. The five samples of each kind of vegetable represented five local markets (Ali Muhssan, Bab al Qa'a, Bab Alyemen, Shumailah and Daris markets) where all the market located in the capital Sana'a. The markets and samples were chosen randomly. The vegetables are brought fresh from suburb areas and other governorates on a dialy basis.

2.5. Development and Validations Procedures

The performance criteria of the developed method included linearity, accuracy, precision (repeatability), detection limit, quantitation limit and stability (robustness) were validated. The validation of these parameters was done as follows:

2.5.1. Comparison and Selection of Color Reagents Used in Nitrite Determination Methods

For the sake of comparison, two published combinations of diazo-coupling reagents used for spectrophotometric determination of nitrite ions were selected based on their stability and sensitivity. The first combination involved sulfanilic acid with methyl anthranilate (Narayana and Sunil, 2009). In this paper, it is named as "Ref. method 1". The second diazo-coupling reagents were sulfanilinamide with NEDD as color reagents (Merino, 2009b), and it was given the name of "Ref. method 2". These two names were used throughout this paper. The results of the two reference methods were compared with each other and also with the results of our developed method in which sulfanilic acid with NEDD were used as diazo-coupling reagents.

2.5.1.1. Nitrite Determination Using "Ref. Method 1" (Narayana and Sunil, 2009):

A volume of 10 mL of working nitrite standards 8 to 80 mg L^{-1} were transferred into a series of 100 mL calibrated flask. To each flask, 10 mL of 0.1 M HCl and 10 mL of 0.6% sulfanilic acid were added, then the solution was mixed properly. Thereafter, 10 mL of 1% methyl anthranilate and 10 mL of NaOH (2N) were added, and the contents were diluted to 100 mL using de-ionized water. After the formation of the yellow colored dye, the λ_{max} was determined by scanning the absorbance in the range of 380-800 nm. Finally, the absorbance of the solutions was measured at λ_{max} (410 nm) against the corresponding reagent blank.

2.5.1.3. Nitrite Determination Using Sulfanilic Acid with NEDD as Diazo-coupling Reagents (the proposed method)

The volumes of 10 ml of working nitrite standards of 0.5 to 10 mg L^{-1} were transferred into a series of 100 mL calibrated flasks. To each flask, 10 mL of 0.1 M HCl, 10 mL of 0.6% sulfanilic and 10 mL of 0.6% NEDD were added and diluted to 100 mL using de-ionized water. After the formation of the pink colored dye, the λ_{max} was determined by scanning the absorbance in the range 380-800 nm. Finally, the absorbance of the solutions at λ_{max} (542 nm) was measured against the corresponding reagent blank.

2.6. Optimization and Development of the Procedures

For the purpose of enhancing the sensitivity and suitability of the method, few parameters were optimized to establish the best conditions. These variables included charcoal mass, pH, physical state and quantity of the diazo-coupling reagents, and pH. .

2.7. Application of the Developed Method for Nitrite Determination in Vegetables

The application of the developed method and the validation for the quantitation of nitrite in four kinds of leafy and root vegetables were done as follows:

2.7.1. Preparation of Test Sample (nitrite extraction)

A weight of 250 g of root vegetables and 100 g of leafy vegetables were rinsed with tap water and then with de-ionized water. After cutting the vegetable samples into small parts, they were ground by a blender, and were filtered, and washed using de-ionized water. After shaking, a volume of 50 mL of the samples was then centrifuged using Compact Laboratory Centrifuges Digital LC 8 (Chemglass Life Science) and the supernatant was collected into a glass bottle. The pigments were removed from the sample by adding an approprate amount of charcoal, and were shaken properly and centrifuged. The supernatant was collected from which a volume 10 mL was transferred into separate flasks. To each flask, 1 mL of 0.1 M HCl, 6 mg of sulfanilic acid and 6 mg of NEDD were added, and the content was shaken by hand until all reagents were dissolved. The absorbance of the pink-colored dye was measured at 542 nm against the corresponding reagent blank. Each sample was analyzed in triplicates, and the result was expressed as mg kg^{-1} fresh weight of vegetable.

2.7.2. Spiking and Recovery Calculations

For calculating the method recovery and studying the matrix effects, 0.05 to 1 mg L^{-1} of nitrite spiked samples were prepared and thereafter the nitrite concentrations were measured. The differences between the pairs of results obtained from the spiked and unspiked samples were used to calculate the recovery

2.7.3. Preparation of Spiked Samples of Nitrite

Spiked samples with the concentrations of 0.05 to 1mgl^{-1} were prepared by adding various volumes (5.5 to 110 µL) of 100 mg L^{-1} nitrite standard solutions to 10 mL of the filtrated vegetable sample. Each spiked sample was treated with 1 mL of 0.1 M HCl, 6 mg of sulfanilic acid and 6 mg of NEDD to develop the color, and then the solution was shaken. Absorbance of the pink- colored dye was measured at 542 nm against the corresponding reagent blank.

3. Results and Discussion

3.1. Method Development for NO_2^- Determination

The development of the proposed spectrophotometric method for nitrite determination in vegetables was based on a modifed Geris reaction in which a diazotization reaction took place between nitrite ion and sulfanilic acid in an acidic medium. The product was coupled with NEDD to produce an azo dye as proposed in the scheme bellow.

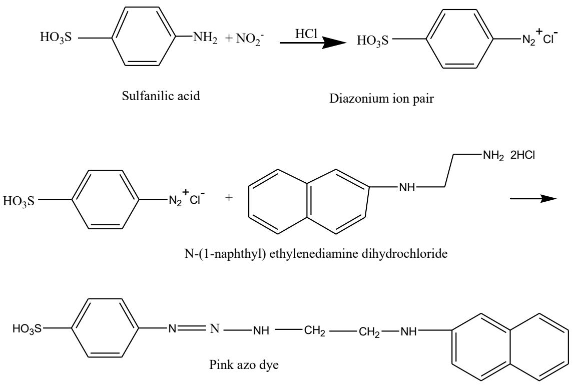

Scheme showing a proposed chemical structure of the pink azo dye produced by the reaction of sulfanilic acid and NEDD with NO_2^-

Both reactions were done at room temperature. Figure 1 below depicts the visible spectra obtained from the proposed method and the two referencemethods. Noticeably, in the Ref. method 1, the amount of nitrite standard was 80 mg L-1 since it was difficult to get equivalent absorbance to that generated by Ref. method 2, and the proposed method in which only 4 mg L^{-1} of nitrite standard have to be used. The azo dyes produced by the proposed method and Ref. method 2 showed maximum abornbances at longer wavelengths (542 and 543 nm respecttively) compared to that obtained from Ref. method 1 where the maximum absorbance was observed at 410 nm. The molar absorptivities of the products from the the proposed method, Ref. method 2 and Ref. methods 1 were 7.50 x10^3, 7.07 x10^3 and 6.47 x10^2 L mol^{-1} cm^{-1} respectively. The molar absorptivity data revealed that the method proposed in the present work showed a higher value compared to both reference methods. Further comparision was also made in Table 1 showing some initial analytical merits of the proposed method against the two refrence methods.

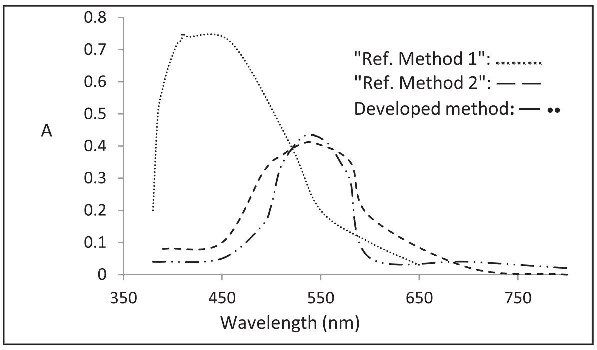

Figure 1. Visible spectra of azo dyes that were produced by the two reference methods and the developed method.

Table 1. Comparison Table between some initial performance criteria of the developed method with the two reference methods.

NO.	Method	λ_{max} (nm)	Equation	R^2	LOD mg L^{-1}
1	"Ref. method 1"	410	y = 0.009x + 0.006	0.9997	1.10
2	"Ref. method 2"	543	y = 0.103x - 0.003	0.9994	0.092
3	Proposed method	542	y = 0.108x + 0.007	0.9998	0.090

LOD = 3.3 × sd/s, where sd is the standard deviation of the blank and s is the slope of the calibration curve. R^2 was calculated from the respected calibration curves of the three methods.

Even though, the performances of the proposed method and Ref. method 2 look similar under initial experimental conditions, the data uneqivocally proved that the proposed method has LOD that is 12 times less than that of the Ref. method 1. With possible further fine tunning, the analytical merits of the proposed method could be even improved to make the proposed method a better alternative for nitrite determination. Therefore, further development and validation steps as discussed in the following sections were considered to improve the performance of the proposed method.

3.2. Optimization of the Proposed Method

The kinetics study of the various diazo-coupling reagents used in Gries reactios for nitrite detrmination reported previously (Fox, 1979) indicated that optimum conditions for each diazo-coupling reagents varried and should be determined experimentally. Thus, For enhancing the sensitivity and suitability of the proposed method for the determination of nitrite in vegetables, different variables such as the quantity of charcoal, pH, the physical state (liquid or solid) and amount of diazo-coupling reagents were optimized to establish the most optimal experimental conditions. The optimization processes are discribed as follows:

3.2.1 Effect of Quantity of Charcoal on the Method's Performance

Pigments from vegetables' extract may cause interferences in nitrite determination and thus compromise the method performance (Wang et al., 2017). Some earlier works (Prasad and Chetty, 2008; Mao et al., 2009) used activated charcoal for pegment removal prior to the spectrophotometric assessment of nitrite in vegetables. Although, activated charcoal is effective in pigment removal, its cost is higher than charcoal. Thus, the latter was selected as an alternative in the proposed method. To test the effectiveness of charcoal and find out its optimum mass for the removal of pigments from cooriander, carrots, mint and white radesh, various amounts of charcoals (0.1-1 g)were used. As might be expected, the extracts of colored and leafy vegetables needed higher amounts of charcoal than the juicy or colorless vegetables. An amount of 0.300 g charcoal was enough to remove the pigment from the 10 mL white radish extract, while the same volume of the extracts of mint, coriander and carrots required 0.600 g of charcoal. For further investigations, nitrite recovery calculations in the presence of three different amounts of charcoal are shown in Table 2.

Table 1. Recoveries results of nitrite ions standards after applying different amounts of charcoal.

NO.	Nitrite actual Conc. mg l^{-1} (n =3)	%Recovery after using 0.1 g charcoal	%RSD	%Recovery after using 0.5 g charcoal	%RSD	% Recovery after using 1 g charcoal	%RSD
1	0.05	99.54	0.40	97.70	0.41	97.76	0.42
2	0.20	100.92	0.40	101.84	0.40	102.30	0.42
3	0.40	100.46	0. 30	99.31	0.32	102.76	0.40
4	0.80	100.92	0.35	100.92	0.30	102.07	0.35
5	1.00	98.25	0.30	100.09	0.30	98.25	0.35

Recovery = [(calculated Conc.(mg L^{-1})/actual Conc.(mg L^{-1})] × 100, n = number of replications.

3.2.2. pH Effect on Nitrite Ions Determination

In general, the determination of nitrite in foodstuffes based on Griess reaction requires a careful control of the pH for both diazotization and coupling reactions to prevent the converion of nitrite to nitrous acid or nitrous oxide (Hsu et al., 2009). Even though the pH optimum value varries according to the type of diazo-coupling reagents and needs to be determined experimentally, the sulfonic acid diazotization reaction has to be done in acidic media (Fox, 1979; Narayana and Sunil, 2009; Rider and Mellon, 1946). In the proposed method, the optimum pH for the azo dye formation as a result of the diazo-coupling reactions was determined as shown in Figure 2.

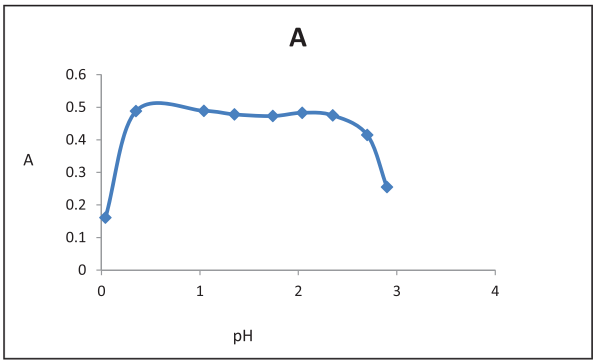

Figure 2. pH Effect on nitrite ions determination using the developed method.

Thee results showed that the suitable pH values were in the range of (0.35-2.35) which corresponded to a maximum absorption. Unlike the case when sulfonic acid and methyle anthranilate were used as dizo-coupling reagents (Narayana and Sunil, 2009), where a higher molar concentraion (up to 2 M) HCl was used, the diazo-coupling reactions in the proposed method did not work at pH values lower than 0.35. At these extreem pH, the formed azo dye was degraded and the appearance of a dark color in the solution was observed. Beyond pH 2.35, the absorbance of the formed azo dye was less, indicating unfaverable conditions for the dye formation. It should be mentioned that all pH measurments were done in HCl solution rather than in buffer system to simplify the diazonium ion formation and the subsequent coupling of the formed ion with NEDD

3.2.3. Minimizing the Dilution Factor Through Using Solid Diazo-coupling Reagents:

Enhancing the method sensitivity relies heavily on the concentration of color-producing reagents. Consequently, we tried to minimize the effect of dilution by adding volumes of higher concentrations of the color-producing reagents; sulfanilic acid and NEDD. This attempt, however, failed due to the solubility problem. For this reason, a different approach has been used in which the solid reagents were added directly to the reaction vessel. Interestingly, this approach overcame the solubility problem and resulted also in minimizing the volume of the needed hydrochloric acid (HCl) where only a volume of 1 mL of 0.1M HCl was enough to adjust the pH. The advantages of this approach is not limited to minimizing the dilution-factor effect, but also, the preparation steps are less, and the method is economic, simpler and environmental friendly. This attempt has not been reported previously in the determination of nitrite ions, as far as the researchers know.

3.2.4. Quantity of Coupling Reagents

The amounts of sulfanilic acid and NEDD were also optimized. The investigation was carried out using concentrations of nitrite (0.05 to 1 mg L^{-1}) which covered the method range. The results in Table 3 confirmed that the amount of 6 mg of each sulfanilic acid and NEDD was sufficient to generate repeatable linear results over the method range.

Table 3. Effect of the quantity of coupling reagents.

Nitrite actual Conc. mg L^{-1}	Quantity of sulfanilic acid (mg)	Quantity of NEDD (mg)	A
0.05	6	6	0.056
0.05	12	12	0.057
0.05	18	18	0.057
0.40	6	6	0.440
0.40	12	12	0.440
0.40	18	18	0.440
1.00	6	6	1.080
1.00	12	12	1.080
1.00	18	18	1.090

Experiments were done at pH = 2.

The investigation was done at pH 2. Higher amounts of reagents have no effect on the results. The lack of repeatability of nitrite determination using Griess reaction is attributed to the presence of excessive nitrite ions compared to the concentration of the diazo-coupling reagents (Nicoholas and Fox, 1973).

With all optimum conditions in hand, confirmation experiments were carried out to check if these optimized conditions would have improved the calibration sensitivity and LOD of the developed method. Table 4 compared the results of the developed method under optimum and initial conditions.

Table 4. Data comparison under initial and optimum conditions.

NO.	Method	Condition	*Reagent's phase	Calibration curve equation	R^2	LOD mg L^{-1}
1	Proposed method in the present work	Initial (no optimization)	As as solution	y = 0.108x + 0.005	0.9998	0.090
2	Developed method in the present work	Optimal conditions	Added as solid	y = 1.1x + 0.004	0.9999	0.010

**Reagents: sulfanilic acid and NEDD*

The calibration sensitivity and LOD under optimum conditions were substantially improved more than nine times. It is also evident from the data (when compared to Table 1), that the developed method under optimum conditions is 120 times more sensitive than Ref. method 1, and its LOD is 110 times lower. Furthermore, the developed method has a calibration sensitivity nine times better than that of Ref. method 2, and the detection limit is 111 times lower.

3.3. Validation Study

Method validation is an essential step to ensure the accuracy and validity of the data obtained by the developed method. Various performance criteria were validated as outlined below:

3.3.1. Precision (repeatability)

The repeatability (intraday precision) of the developed method was calculated at three different concentrations covering the method range (0.05 1 mg L^{-1}), in triplicate. Results of the method precision, as % RSD, were shown in Table 5.

Table 5. Results of repeatability studies.

Sample	Nitrite actual Conc. mg L^{-1}	Absorbance (n =3)	Calculated Conc. mg L^{-1}	% Recovery	Average % RSD	Acceptable % RSD (AOAC 1998)
SMP _1	0.05	0.059	0.051	102.00	4.78	15 (for 100 ppb)
	0.05	0.057	0.049	98.00		
	0.05	0.054	0.046	92.00		
SMP _2	0.40	0.460	0.420	105.00	4.74	11 (for 1 mg L^{-1})
	0.40	0.450	0.411	102.75		
	0.40	0.420	0.383	95.75		
SMP _3	1.00	1.030	0.946	94.60	4.26	11 (for 1 mg L^{-1})
	1.00	1.090	1.001	100.10		
	1.00	1.120	1.029	102.90		
Overall Average % RSD					4.59	

% Recovery = (Calculated conc. in mg L^{-1}/actual Conc. mg L^{-1}) × 100

The low values of % RSD were indicative of the high repeatability of the method. The average % RSD values of the developed method (%4.59) are within the accepted limit suggested by the AOAC Manual for the Peer-Verified Methods program (AOAC 1998) and very close to the reported value (%4.51) using capillary electrohoresis (Oztekin et al., 2002)

3.3.2. Accuracy

Accuracy of the developed method was also calculated and shown in Table 6.

Table 6. Accuracy of the developed method.

Name of sample	Nitrite Actual Conc. mg L^{-1}	Absorbance (n = 3)	Calculated Conc. mg L^{-1}	% Recovery	% RSD	% Bias
Blank	Negligible	Negligible				
STD_1	0.05	0.062	0.0487	97.40	4.2	-2.60
STD_2	0.10	0.119	0.0992	99.20	3.7	-0.80
STD_3	0.20	0.230	0.1975	98.75	3.5	-1.25
STD_4	0.40	0.450	0.3924	98.10	3.8	-1.90
STD_5	0.60	0.680	0.5961	99.35	3.8	-0.65
STD_6	0.80	0.900	0.7910	98.87	3.5	-1.13
STD_7	1.00	1.120	0.9858	98.58	4.0	-1.42

% Recovery = (Calculated concentration in mg L^{-1} /actual Conc. mg L^{-1}) × 100
% Bias = % Recovery - % 100 , calculated concentration in mg L^{-1} was calculated from the linear regression equation (y = 1.1x + 0.004), n = number of replications.

The method showed a small bias which indicated that errors affecting the accuracy of the developed method were under control.

3.3.3. Method Linearity

The linearity of the developed method was tested by constructing a calibration curve of the data in Table 6. The obtained results shown in Figure 3 indicated that the developed method possessed high linearity with R^2 = 0.9999 within the method linear range (0.05 – 1 mg L^{-1}). The linearity of the developed method (0.9999) was close to the linearity of HPLC method (Chou et al., 2003) reported previously (1.000) and similar to the value reported by Kmel and co-workers (Kmel et al., 2019). It should be indicated that the average recovery of the standards used to construct the calibration curve was 98.61% (%RSD 3.80) which indicated a high accuracy method.

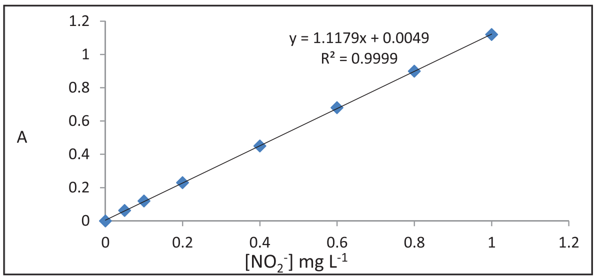

Figure 3. Calibration curve of nitrite standard solutions using the developed method.

3.3.4. Limits of Detection (LOD) and Quantification (LOQ)

Nitrite concentrations in the lower part of the linear range of the calibration plot were used to determine the limit of detection (LOD) and limit of quantification (LOQ). They were determined from the slope of the calibration plot(s) and standard deviation (sd) of the blank using the following two equations (Jimidar et al., 1995):

LOD = 3.3 × sd/s

LOQ = 10 × sd/s

The LOD and LOQ were 0.010 and 0.030 mg L^{-1}, respectively, for nitrite, which indicated that the sensitivity of the method was adequate enough to detect nitrite level well below the safe limit (European Commission, 1995). The above LOD is much lower than that reported for Capillary electrophoresis methods for nitrite in vegetables (Jimidar et al., 1995) and the multichannel contineous flow analyzer accredited by the Solvenion Accreditation Board (Susin et al., 2006).

3.3.5 Recovery Calculation of Nitrite in Vegetables:

Table 7 (a-d) sumarizes the recovery calculations of nitrite in the matricies of the four selected vegetables (carrots, white radish, mint and coriander). The overall recovery of proposed method ranged between 98.00% and 102.00%. This is an indication of the high sensitivity and suitability of the method to determine nitrite in root and leafy vegetables.

Table 7 (a). Recovery results of nitrite in carrots sample.

Sample	Spiked Conc. ppm	Abs.	A. Spiked sample-A. unspiked	Calculated Conc. (ppm)	% Recovery	% Bias
Unspiked sample	0.00	0.056				
Spiked sample_1	0.05	0.114	0.058	0.050	100.00	0.00
Spiked sample_2	0.20	0.281	0.225	0.204	102.00	2.00
Spiked sample_3	0.40	0.491	0.435	0.397	99.25	-0.75
Spiked sample_4	0.80	0.921	0.865	0.794	99.25	-0.75
Spiked sample_5	1.00	1.131	1.075	0.987	98.70	-1.30

Table 7 (b). Recovery results of nitrite in white radish sample

Sample	Spiked Conc. ppm	Abs.	A. Spiked sample-A. unspiked	Calculated Conc. (ppm)	% Recovery	% Bias
Unspiked sample	0.00	0.110				
Spiked sample_1	0.05	0.167	0.057	0.049	98.00	-2.00
Spiked sample_2	0.20	0.330	0.220	0.199	99.50	-0.50
Spiked sample_3	0.40	0.545	0.435	0.397	99.25	-0.75
Spiked sample_4	0.80	0.975	0.865	0.794	99.25	-0.75
Spiked sample_5	1.00	1.195	1.085	0.996	99.60	-0.40

Table 7 (c). Recovery results of nitrite in mint sample.

Sample	Spiked Conc. ppm	Abs.	A. Spiked sample-A. unspiked	Calculated Conc. (ppm)	% Recovery	% Bias
Unspiked sample	0.00	0.090				
Spiked sample_1	0.05	0.147	0.057	0.049	98.00	-2.00
Spiked sample_2	0.20	0.310	0.220	0.199	99.50	-0.50
Spiked sample_3	0.40	0.530	0.440	0.402	100.50	0.50
Spiked sample_4	0.80	0.960	0.870	0.798	99.75	-0.25
Spiked sample_5	1.00	1.190	1.100	1.010	101.00	1.00

Table 7 (d). Recovery results of nitrite in coriander sample.

Sample	Spiked Conc. ppm	Abs.	A. Spiked sample-A. unspiked	Calculated Conc. (ppm)	% Recovery	% Bias
Unspiked sample	0.00	0.130				
Spiked sample_1	0.05	0.187	0.057	0.049	0.049	-2.00
Spiked sample_2	0.20	0.355	0.225	0.204	0.204	2.00
Spiked sample_3	0.40	0.570	0.440	0.402	0.402	0.50
Spiked sample_4	0.80	0.995	0.865	0.794	0.794	-0.75
Spiked sample_5	1.00	1.200	1.070	0.982	0.982	-1.80

3.4. Real sample analysis

Table 8. summarizes the results of nitrite assessment in vegetables.

Table 8. Nitrite concentration in some vegetable samples from different markets.

Sample Source	mg.kg^{-1}			
	Carrots	White radish	Mint	Coriander
ALI MUHSSAN MARKET sample1_1	0.13	4.94	1.19	3.29
ALI MUHSSAN MARKET sample1_2	0.13	4.95	1.24	3.24
ALI MUHSSAN MARKET (Spiked sample)	0.15	4.92	1.20	3.24
BAB AL QA'A MARKET	0.02	4.19	0.71	2.14
BAB ALYEMEN MARKET	0.08	3.95	0.98	1.93
SHUMAILAH MARKET	0.38	2.18	1.27	1.47
DARIS MARKET	0.10	4.31	1.04	3.35
Average	0.14±0.11	4.20 ± 0.98	1.09 ± 0.20	2.80 ± 0.72

4. Conclusion

This paper presented the development and validation of a spectrophotometric method for the determination of nitrite in vegetables. The method was based on the use of sulfanilic acid with NEDD in solid forms added directly to reaction vessels containing HCl and nitrite solutions. The method showed higher performance criteria compared to those of two methods used as references. The developed method was successfully applied for the determination of nitrite in green leafy and root vegetables.

Acknowledgment

The authors express their gratitude to Al-Saeed Foundation for partial financial support of the project. Sincere thanks also go to Yemeni Jordanion University for allowing the researchers to use their equipment.

References

AOAC (Association of Official Analytical Chemists (1998). AOAC Peer-Verified Methods Program, Manual on polcies and procedures, Arlington, Va. USA.

Ayaz, A., Topcu, A., Yurttagul, M. (2007). Survey of nitrate and nitrite levels of fresh vegetables in Turkey. Journal of Food Technology 5(2): 177-179.

Bogovski, P. and Bogovski, S. (1981). Species in which n-nitroso compounds induce cancer. International Journal of Cancer 27(4): 471-474. PMID: 7275353

DOI: 10.1002/ijc.2910270408.

Bosch Bosch, N., Garcia Mata, M., Penuela, M. J., Ruiz Galan, T., Lopez Luiz, B. (1995). Determination of nitrite levels in refrigerated and frozen spinach by ion chromatography. Journal of Chromtography A 706(1-2): 221-228. doi.org/10.1016/0021-9673(95)00153-E.

Bryan, N. (2006). Nitrite in nitric oxide biology: Cause or consequence?: A systems-based review. Free radical biology and medicine. 41(5): 691-701. PMID: 16895789. DOI: 10.1016/j.freeradbiomed.2006.05.019.

Bryan, N. S., Alexander, D. D., Coughlin, J. R., Milkowiski, A. L., Boffetta, P. (2012). Ingested nitrate and nitrite and stomach cancer risk: an updated review. Food Chemistry Toxicology 50: 3646-3665. PMID: 22889895. DOI: 10.1016/j.fct.2012.07.062.

Cheng, C. F. and Tasng, C .W. (1998). Simultaneous determination of nitrite, nitrate and ascorbic acid in canned vegetable juices by reverse-phase ion-interaction HPLC. Food dditives and Contaminants 15 (7): 753-758.

Chou, S., Chung , J., Hwang, D. A. (2003). A high performance liquid chromatography method for determining nitrate and nitrite levels in vegetables. Journal of food and Drug Analysis 11(3): 233-238.

Ensafi, A. A. and Kazemzadeh, A. (1999). Simultaneous determination of nitrite and nitrate in various samples using flow injection with spectrophotometric detection. Analytica chimica acta 382 (1-2): 15-21.

Fox, J. B. Jr. (1979). Kinetics and mechanisms of the Griess reaction. Analytical Chemistry 51(9): 1493-1502.

Gaspar, A., Juhasz, P., Bagyi, K. (2005). Application of capillary zone electrophoresis to the analysis and to a stability study of nitrite and nitrate in saliva. Journal of Chromatography A. 1065(2): 327-331. PMID: 15782979. DOI: 10.1016/j.chroma.2004.12.085.

Gennaro, M.C. and Bertolo, P. L. (1989). Determination of the principal anionic components in wines and soft drinks, by ion interaction reversed-phase high-performance liquid chromatography. Journal of Chromatography A 472: 433-440. doi.org/10.1016/S0021-9673(00)94146-3.

Hsu, J. Arcot, J., Lee, N. A. (2009). Nitrate and nitrite quantification from cured meat and vegetables and their estimated dietary intake in Australians. Food Chemistry 115(1): 334-339.

Jackson, J.K., Patterson, A. J., MacDonald, W. L. K., Oldmeadow, C., McEvoy, M. A. (2018). The role of inorganic nitrate and nitrite in cardiovascular disease risk factors: a systematic review and meta-analysis of human evidence. Nutrition Rview 76(5): 348-371. PMID: 29506204. DOI: 10.1093/nutrit/nuy005.

Jimidar, M., Hartmann, C., Cousement, N., Massart, D. L. (1995). Determination of nitrate and nitrite in vegetables by capillary electrophoresis with indirect detection. Journal of Chromatography A 706(1-2): 479-492.

Kazemzadeh, A. and Ensafi, A. A. (2001). Sequential flow injection spectrophotometric determination of nitrite and nitrate in various samples. Analitica Chemica Acta 442(2001): 319–326.

Kmecl, V., Znidarcic, D, Franic, M., Ban, S. G. (2019). Nitrate and nitrite contamination of vegetables in the Slovenian market. Food Additives and Contaminants: Part B 12 (2): 216-223.

Lundberg, J. O. and Weitzberg, E. (2009). NO generation from inorganic nitrate and nitrite: Role in physiology, nutrition and therapeutics. Archives of pharmacal research 32(8): 1119-1126. doi: 10.1007/s12272-009-1803-z.

Machha, A. and Schechter, A. N. (2011). Dietary nitrite and nitrate: a review of potential mechanisms of cardiovascular benefits. European journal of nutrition 50: 293-303.

Mao, Y., Hua, S., Fen. J. (2009). Determination of nitrates in fresh vegetables and fruits by UV-Spectrophotometry. Journal of Huazhong Agricultural University 28(1): 102-105.

Merino, L. L. (2009a). Nitrate in Foodstuffs:Analytical standardisation and Monitoring and Control in Leafy Vegetables, M.Sc. Thesis, Swedish University of Agriculture Sciences.

Merino, L. L. (2009b). Development and validation of a method for determination of residual nitrite/nitrate in foodstuffs and water after zinc reduction. Food Analytical Methods 2(3): 212-220.

Moorcroft, M. J., Davis, J., Compton, R. G. (2001). Detection and determination of nitrate and nitrite: a review. Talanta 54(5): 785-803. PMID: 18968301. DOI: 10.1016/s0039-9140(01)00323-x.

Narayana, B. and Sunil, K. A., A Spectrophotometric Method for the Determination of Nitrite and Nitrate. Euraasian Journal of Analytical Chemistry 4(2): 204-2012.

Nicholas, R. N. and Fox, J. B. Jr. (1973). Critical evaluation of the AOAC method of analysis for nitrite in meat. Journal of Association of Official Analytical Chemists. 56(4): 922-925. doi.org/10.1093/jaoac/56.4.922.

Ozcan, M. M. and Akbulut, M. (2007). Estimation of Minerals, Nitrate and Nitrite Contents of Medicinal and Aromatic Plants Used as Spices, Condiments and Herbal Tea. Food Chemistry 106(2): 852-858.

Oztekin, N., Nutku, M.S., Erim, F. B. (2002). Simultaneous determination of nitrite and nitrate in meat products and vegetables by capillary electrophoresis. Food Chemistry 76(1): 103-106.

Parvizishad, M., Dalvand, A., Mahvi, A. H., and Goodarzi, F. (2017). A Review of Adverse Effects and Benefits of Nitrate and Nitrite in Drinking Water and Food on Human Health. Health Scope 6(3): e214164. DOI : 10.5812/jhealthscope.14164.

Prasad, S. and Chetty, A. A. (2008). Nitrate-N determination in leafy vegetables: Study of the effects of cooking and freezing. Food Chemistry 106(2): 772-780.

DOI: 10.1016/j.foodchem.2007.06.005.

Preussmann, R. (1983). Public health significance of environmental N-nitroso compounds. International Agency for Research on Cancer (IARC) Scientific Publications 45: 3-17.

Ranasinghe, R. and Marapana, R. (2018). Nitrate and nitrite content of vegetables: A review. Journal Pharmacognosy and Phytochemistry 7(4): 322-328. Rider, B. F. and Mellon, M. G. (1946). Colorimetric determination of nitrites. Industrial and Engineering Chemistry 18(2): 96-99.

Santamaria, P. (2006). Nitrate in vegetables: toxicity, content, intake and EC regulation. Journal of the Science of Food and Agriculture 86(1): 10-17.

SCF (Scientific Committee on Food, 1995). Opinion on nitrate and nitrite, expressed on 22 September 1995 (Annex 4 to Document III/5611/95) (Ed.) European Commission, Brussels, p 20.

Sindelar, J. J. and Milkowski, A. (2012). Human safety controversies surrounding nitrate and nitrite in the diet. Nitric Oxide 26(4): 259-66. doi: 10.1016/j.niox.2012.03.011.

Song, P., Wu, L., Guan, W. (2015). Dietary nitrates, nitrites, and nitrosamines intake and the risk of gastric cancer: a meta-analysis. Nutrients 7(12): 9872-9895. doi: 10.3390/nu7125505.

Straif, K., Weiland, K. S., Bungers, M., Holthenrich, D., Taeger, D., Yi, S., Keil, U. (2000). Exposure to high concentrations of nitrosamines and cancer mortality among a cohort of rubber workers. Occupational and Environmental Medicine 57(3): 180–187. doi: 10.1136/oem.57.3.180.

Sui, D. C. and Henshall, A. (1998). Ion chromatographic determination of nitrate and nitrite in meat products. Journal of Chromatography A 804(1-2):157-60.

doi: 10.1016/s0021-9673(97)01245-4.

Susin, J., Kmecl, V., Gregorcic, A. (2006). A survey of nitrate and nitrite content of fruit and vegetables grown in Slovenia during 1996–2002. Food Addiives andt Contaminants 23(4): 385-390. doi: 10.1080/02652030600573715.

Wang, Q., Yu, L., Liu, Y., Lin, L., Lu, R., Zhu, J., He, L., Lu, Z. (2017). Methods for the detection and determination of nitrite and nitrate: A review. Talanta 165: 709-720. doi: 10.1016/j.talanta.2016.12.044.

Ximenes, M., Rath, S., Reyes, F. (2000). Polarographic determination of nitrate in vegetables.Talanta 51(1): 49-56. doi: 10.1016/s0039-9140(99)00248-9.

Zhou, Z-Y., Wang, M-J., wang, J-S. (2000). Nitrate and nitrite contamination in vegetables in China. Food Reviews Inernational 16(1): 61-76. doi.org/10.1081/FRI-100100282.

JJEES

Jordan Journal of Earth and Environmental Sciences

JJEES (2021) 12 (1): 22-35
ISS`N 1995-6681

Assessment of the Suitability of Urban Residential Roof Catchments for Rainwater Capturing in Umuahia, Southeastern Nigeria

Ubuoh Emmanuel*, Kanu Samuel, Uzonu Ugona

Michael Okpara University of Agriculture, College of Natural Resources and Environmental Management, Department of Environmental Management and Toxicology, Nigeria.

Received 22nd April 2020; Accepted 1 September 2020

Abstract

Rainwater is an alternative source of potable water supply for urban dwellers in Abia State- Nigeria; however, little is known about the suitability of roof catchments for capturing rainwater. The current work focuses on the seasonal evaluation of rainwater captured from four sampled roof catchments (SRC_1-$_4$), namely Asbestos, Aluminum, Corrugated iron, and Harvey-tiles that are commonly used for roofing and atmospheric rain during rain events. One hundred and event samples of harvested rainwater from four different rooftops in three layouts are analyzed for selected physicochemical parameters and metals. The results of the analysis were subjected to mean separation and were compared with water-quality guidelines to evaluate the suitability for consumption and a correlation of parameters was established. Water quality and pollution indices were computed for rainwater quality and rooftop pollution status. Analysis of pH and Zn^{2+} in rainwater from the Asbestos and corrugated roofs during rain events were above the WHO permissible limits for drinking water. Tracers from the roofs that negatively correlated may have been originated from the atmosphere, and the positive correlation attributed to the kinetic energy of rainfall that impinged on the roofing material. Rainwater quality index from the roofs was greater than the 1.0 critical limit. The pollution index revealed strongly-polluted samples from the Asbestos rooftop, moderately-polluted samples from the Aluminum and Corrugated rooftops, and slightly- polluted samples from the Harvey-tile rooftop. The roofs exhibited a decreasing abundance of contaminants in the samples in the order of: Asbestos ≥ Corrugated ≥ Aluminum ≥ Harvey Tile. This, then, calls for designing first-flush devices, a regular maintenance of the RWH systems, and avoidance of catchments capable of releasing contaminants into the harvested rainwater.

Keywords: Rainwater, harvesting, Catchment, suitability, Water, pollution, index, Urban, environment

1. Introduction

The practice of domestic rainwater harvesting (DRWH) is an old tradition adopted in many parts of the world, in addition to being a new technology that is growing in popularity worldwide (Chukwuma et al., 2014). Several studies have explored the implementation of rainwater harvesting (RWH) technologies in response to the growing water demand in developed and developing countries (Chiang et al., 2015; Kahinda et al., 2007). Currently and because of the environmental and economic advantages, RWH systems are receiving increased attention as alternative sources of potable water, particularly in semi-arid areas (Kahinda et al., 2007), and urban areas as well (Teston et al., 2018; Campisano et al., 2017; Gurung and Sharma, 2014;Cook et al., 2013).

Generally, in a rainwater harvesting system, the household water saving is subjected to the amount of water harvested in wet seasons (Amos et al., 2018; Rahman and Eslamian, 2016; Abdulla and Al-Shareef, 2009; Hoque et al., 2004). For example, Herrmann and Schmida (2000) reported that, the installation of rainwater harvesting systems increased water saving from 30%to 60% depending on the roof area in Germany. Therefore, rainwater is a valuable source of water and is quite safe for drinking when harvested and stored in a properly installed and maintained water catchment systems (Mohammad et al., 2020; Olaoye and Olaniyan, 2012; Ubuoh et al., 2012). Accordingly, Ubuoh and Ekpo (2017), Chang et al. (2004) reported that many roofing materials can be serious sources of non- point pollution.

Chang et al. (2004) in Texas reported that residential roofing materials can negatively influence the rainwater quality and that the quality of harvested rainwater improved with roof flushing. Nicholson et al. (2009) compared harvested rainwater quality from different roof catchments and concluded that the quality of rain varied based on the type of roofs used. Roof surfaces in urban settlements also contribute excess nutrients and toxic metals to receiving waters (Van -Metre and Mahler, 2003).

Above all, the level of pollutants that may emanate from roof runoff depends on the roof materials, age, orientation and, slope of the roofs, atmospheric depositions, rain events, and meteorological conditions (Martinson and Thomas, 2005). Studies investigating roof-harvested rainwater quality were conducted in Australia, Canada, Denmark, India, etc. (Despins et al., 2009). Most of these locations are in temperate climate regions, where dry periods between consecutive rain events are relatively short. These significant

Corresponding author email: ubuohemmanuel@yahoo.com

differences in weather conditions such as rain intensity and depth, rain distribution, dry periods between consecutive rain events, and forms of rain (light, heavy) may affect the quality of roof-harvested rainwater (Friedler et al., 2017).

Though some studies have examined the importance of various urban functions as sources of metals by Ezemonye et al. (2016), IKhioya et al. (2015), Aladenola and Adebayo (2009), Akhionbare (2009), Efe (2006), but none particularly paid attention to Harvey tile roof and rainwater pollution index. In Umuahia, public water supply has been a problem leading to commercial private boreholes. This has resulted in the high water bills due to the high cost of operations. Therefore, people relied on the storage of rainwater from rooftops including emerging Harvey tile roof without knowing the characteristic compositions meant for human consumption.

The study then has focused on the determination of the quality of rainwater from roof catchments using water quality and pollution indices to identify rooftops' suitability for rainwater harvesting for human consumption. The result will aid the State Ministry of Water Resources, Ministry of Environment, and Sister Agencies to take proactive steps toward harnessing rainwater as an alternative water supply in urban areas in developing countries that constantly suffer from water crises.

2. Materials and Methods

2.1. Study Area

The study was carried out in Umuahia Municipal, the capital city of Abia State. The area is a typical humid tropical area with its location at the intercept of latitude 05^0 29'N and longitude 7^{0}33'E, and altitude, at the highest point of about 205m (Ozabor and Nwagbara, 2018) with a population of 147,167 (NPC, 2006). Annual rainfall totals vary from about 1900 mm to 2400 mm (Ozabor and Nwagbara, 2018). The high intensity tropical rainfall in the area produces a high volume of overland flow and run-off that possess high erosive energy (Nwilo et al., 2011). This rainfall is of the double maxima type with peaks in July and September. In recent times, September has been the month with the highest amount of rainfall as against July whereas December has the lowest amount (NRCRI, 2016). Air temperature ranges between 21°C and 34°C, and relative humidity ranges from 60% to 83% (NRCRI, 2016).According to Ishaku et al. (2010), the rainfall pattern generally decreases as distance increases from the coastal areas of the South to the Sahelian semi-arid lands of the North (Figure 1).

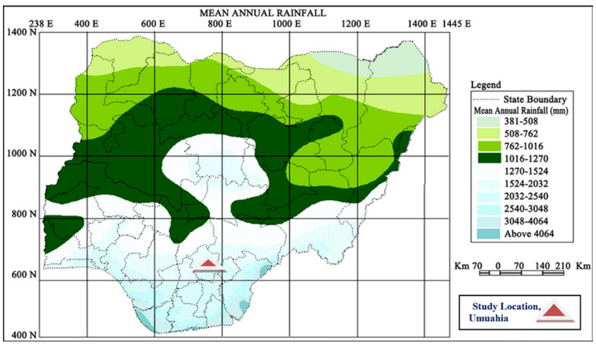

Figure 1. Map of Nigeria Showing Mean Annual Rainfall Pattern in Umuahia, Abia State. Source: Ishaku et al. (2010).

2.2 Experimental Design

A random sampling technique was adopted for the study within the three layouts: New town layout, Eghem layout, and Uzo Avoiteyi layout because they all had the roof catchments of interest (Figure 2). The technique was employed in selecting the sampled households with the four identified roof types, with the atmosphere as control from each of the layout, containing twelve buildings in the study area. The four types of the existing roof materials were designated, sample roof catchments (SRC): Asbestos (SRC_1), Aluminum (SRC_2), Corrugated iron (SRC_3), and Harvey-Tiles (SRC_4). Sample containers were rinsed with the sterile water and drained before they were used to collect the samples from the different roof types and directly from the atmosphere, during April as onset of rain, in July as peak of rain, and during October as late rain (cessation), 2017, respectively, with 108 rain samples from the four roof catchments and nine from the atmosphere constituting a total of 170 rainwater samples (New town layout:36, Eghem layout: 36, Uzo Avoiteyi layout:36) for the three rain events .Care was taken to ensure that the samples were representative of the water to be examined, and that no accidental contamination occurred during the sampling. The rainwater samples were harvested using stainless basins placed on elevated- wooden stands above the ground surface for rooftops rainwater and atmospheric rain at different intervals of rainfall. The samples were then crammed and put into clean polythene bottles, which were corked and labeled according to the different roof catchments. They were then placed in freezers that contained ice blocks.

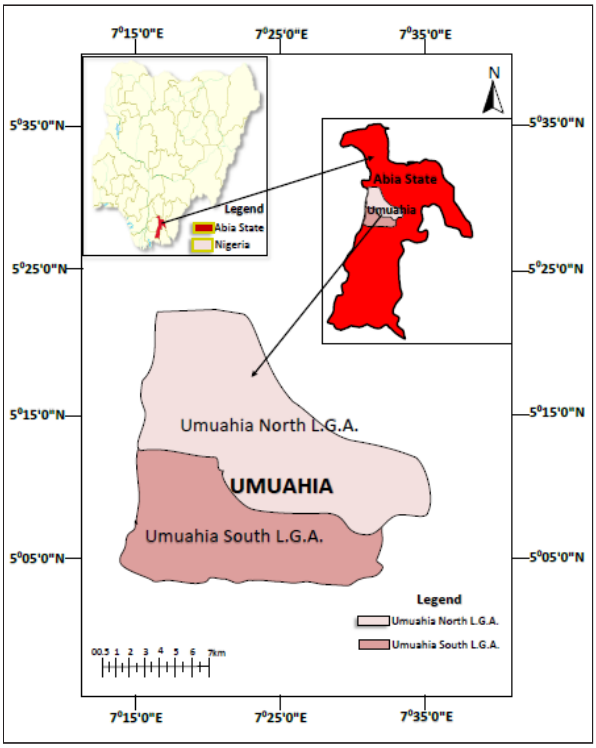

Figure 2. Map of Abia State showing the Study Area. Source: LA-cute consults, after Ishaku et al. (2010).

3. Physicochemical Analysis of Rainwater Samples

The pH was determined on-site using HannapH meter, Model 211.Total acidity was measured using titrimetric methods (Ademoroti, 1996). Electrical Conductivity was determined using Suntex 120 conductivity meter (USEPA, 1997). Nitrate (NO_3^-) was determined using the phenol disulphuric acidic method adopted by Ubuoh et al. (2016). Sulphate (SO_4^{2-}) was determined using the colorimeter at 440nm. A blank without $BaCl_2$ was prepared and run at the same wavelength. The total dissolved solids were determined by the HACH 44600-00 Conductivity/TDS meter. The concentrate of (Cl^-) was obtained by reference to a calibration curve using standard sodium chloride solution (Stern, 2006).

4. Heavy Metals' Determination

The determination of heavy metals such as Cu^{2+}, Pb^{2+}, Fe^{2+}, Zn^{2+} were carried out using the flame atomic absorption Spectrophotometer Perkin-Elmer A Analyst 200 (USA) described by APHA (1998).

5. Data Analysis

The results of data collected were subjected to descriptive statistics which illustrated the means and standard deviation from replicates of collected data. Means of the collected data were afterward subjected to mean separation using Ducan Multiple Range Test (DMRT). Means of the tested parameters were subjected toTwo-Tailed Pearson Correlation to illustrate the degree of relationship between the observed variables from difference roof catchments and atmospheric rain as control in the stud area.

6. Application of Water Quality Index and Water Pollution Index

6.1 Water Quality Index (WQI)

Water quality index was developed and used by Horton (1965); it is expressed mathematically as follows:

$$P_{ij} = (max \frac{C_i}{L_{ij}})^2 + (min_{C_i}/L) \quad \text{............................ Equ. 1}$$

Initially, WQI was developed by Horton (1965) and was adopted by authors including Andreea-Mihaela (2018) in Romania, Ubuoh et al. (2013) in Nigeria, Shweta et al. (2013), Chaturvedi, and Bassin (2010), in India, Lumb et al. (2002) in Great Bear, Polkowska et al. (2005) in Poland. Horton (1965) used multiple items of water qualities as expressed as Ci's and permissible levels of the respective item expressed as L_{ij}'s then the pollution index, Pij is expressed as a function of the relative values of Ci/L_{ij} (Horton, 1965). Here, i is the number of the i^{th} item of the water quality, and j is the number of the j^{th} water use. Each value of (C_i/L_{ij}) shows the relative pollution contributed by the single item. A value of 0.1 is the critical value for each (Ci/L_{ij}).

i. Values greater than 0.1 indicate that the water requires some treatment prior to use for a specific purpose.

i i. Combining the mean value of C_i/L_{ij} into a common index, values over 1.0 signify a critical condition under which proper treatment is needed for portable water.

6.2 Water Pollution Index (WPI)

A pollution index (PI) of individual parameters can be equally used as adopted by Amadi et al. (2013), Udousoro and Ikpeme (2013), Ubuoh et al. (2013); it is expressed mathematically as:

$$\mathbf{WPI} = \frac{\sqrt{(C_I|S_i)^2 \max + (C_I|S_i)^2 \min}}{2} \quad \text{.. Equ. 2}$$

Where,

C_i is the mean value as determined in rainwater

S_i is the drinking water quality guideline (WHO, 2011).

The results of the water quality index based on water tracers were then interpreted with the help of the pollution index classification in Table 1.

Table 1. Parameter classification based on Pollution index (PI).

Class	PI	STATUS
1	<1	No pollution
2	1-2	Slightly polluted
3	2-3	Moderately-polluted
4	3-4	Strongly-polluted
5	>5	Seriously-polluted
Source: Juahir et al. (2008)		

7. Results and Discussions

Characteristics of the roof-harvested runoff mean values over all roof types during April, July, and October rain events are presented in Table 2.

7.1 Physicochemical Characteristics of Harvested Rainwater from Roof Catchments during Rain Events

The mean pH of harvested rainwater samples from the different roof catchments during onset of rain ranged from 6.20 to 6.75, with the mean pH of 6.55, which is less than the 6.90 pH value of the atmospheric rain (control), indicating that rainwater from the Asbestos and corrugated roofs was slightly acidic, signifying no cations from the roof and atmosphere ($Ca^{2+} + Mg^{2+} + K^{+}NH^{4+}$) to neutralize the acidity of rainwater (Mouli et al., 2005; Tang et al., 2005).

For July, pH ranged from 6.55 to 6.90, with a mean pH of 6.73, and the atmospheric rain having a 6.90 pH value. In October, pH ranged from 6.40 to 6.85 with the mean pH of 6.64, which is less than the 6.85 pH value of the atmospheric rain. During the three rain events, the mean pH of the harvested rainwater samples from the different roof catchments ranged from 6.20 to 6.90, with the Asbestos roof being more acidic below the values 6.5-8.5, 6.0-9.0mg/l of the WHO/ FME_{NV} permissible limits for drinking water. The Harvey roof and control showed results within the permissible limits respectively .The results of the low pH from the Asbestos roof during onset of rain disagrees with the pH value 7.6 for the rainwater harvested from Asbestos roof in the Ibadan metropolis by Olubanjo (2016). As for rainwater harvested from aluminum and corrugated iron rooftops, pH ranged from 6.55to 6.70, 6.35 to 6.60, with the corrugated rooftops recording the lowest values above the permissible limit for drinking water. The result is different from the findings of Chukwuma et al. (2013), Akharaiyi et al. (2007) who reported pH values in the rainwater from galvanized iron rooftops being below the WHO maximum permissible value. The pH values obtained in this study agreed with the results of Simmons et al. (2001) who reported a pH range between 5.2 and 11.4 for harvested rainwater. However, they disagreed with Ikhioya et al. (2015) who reported that pH in rainwater harvested from Aluminum-roofing sheet fell within the WHO allowable limit during the early rain event. It is also observed that the pH of rain increased to normal with the increase in the rain intensity during the peak period. This result of pH is in line with the finding of Rahman et al. (2019) who observed that the value of pH has increased to a normal value with the increase in the duration of rain. Accordingly, the tendency of the roofing materials to release and exhibit pH is in a decreasing order: Asbestos ≥ Corrugated iron roof≥ Aluminum roof≥ Harvey-tiles. From the results, the samples during the onset of rain were more acidic than those of the July and October rain (Table 2). This is suspected to be due to the built- up of dry deposition of gases in the atmosphere and catchments respectively. The result is in tandem with the findings of Akhionbare (2009); Boller and Steiner (2002); Gadd and Kennedy (2001), who reported that low pH in the harvested rainwater during early rain is due to the dry deposition of aerosols/gases emitted from human activities during the first-flush event. Kale (2016), reported that rainwater harvested in July had a higher pH value compared with the other months, which indicates that there was less CO_2 in the air.

Table 2. Physicochemical properties and heavy metals in harvested rainwater from different roof catchments during rain events.

CATCHMENT	pH	Acidity (mg/l)	TDS (mg/l)	EC (µhosm/cm)	NO_3^- (mg/l)	SO_4^{2-} (mg/l)	Cl^- (mg/l)	Cu^{2+} (mg/l)	Pb^{2+} (mg/l)	Fe^{2+} (mg/l)	Zn^{2+} (mg/l)
Onset of Rain : April											
Asbestos roof: SRC_1	6.20^{e}	28.58^{a}	46.00^{a}	64.00^{a}	2.66^{a}	13.16^{a}	14.03^{a}	ND	0.04	ND	1.16^{b}
Aluminum roof: SRC_2	6.55^{c}	22.19^{c}	28.50^{c}	52.00^{c}	0.22^{c}	3.86^{c}	9.18^{c}	0.07	ND	0.22^{b}	0.43^{c}
Corrugated iron:SRC_3	6.35^{d}	25.09^{b}	39.00^{b}	57.50^{b}	0.66^{b}	5.20^{b}	10.42^{b}	0.001	ND	0.40^{a}	4.35^{a}
Harvey tile roof:SRC_4	6.75^{b}	14.43^{d}	16.00^{d}	26.50^{d}	0.13^{cd}	1.09^{d}	6.45^{d}	ND	ND	ND	0.22^{cd}
Atmosphere Rain: (Control)	6.90^{a}	10.01^{e}	8.00^{e}	13.00^{e}	0.05^{d}	0.47^{d}	4.13^{e}	ND	ND	ND	0.03^{d}
Mean	6.55	20.06	27.50	42.60	0.74	4.76	8.84	0	0.008	0.044	1.238
S.E	0.05	0.31	0.71	1.00	0.06	0.42	0.23	0.04	0.00	0.03	0.12
Peak ofRain : July											
Asbestos roof: SRC_1	6.55^{c}	22.27^{a}	29.00^{a}	43.50^{a}	0.46^{a}	3.30^{a}	4.98^{a}	ND	ND	ND	1.42^{b}
Aluminum roof: SRC_2	6.70^{b}	13.44^{c}	19.00^{c}	32.00^{c}	0.08^{c}	0.06^{c}	2.32^{c}	ND	ND	0.10	0.09^{c}
Corrugated iron:SRC_3	6.60^{c}	19.33^{b}	23.00^{b}	36.00^{b}	0.21^{b}	0.11^{b}	3.40^{b}	ND	ND	ND	1.37^{a}
Harvey tile roof:SRC_4	6.90^{a}	8.98^{d}	7.00^{d}	12.00^{d}	0.04^{c}	ND	1.15^{d}	ND	ND	ND	0.04^{c}
Atmospheric Rain: (Control)	6.90^{a}	9.43^{d}	5.00^{d}	9.00^{d}	ND	ND	0.83^{d}	ND	ND	ND	ND
Mean	6.73	14.76	16.6	26.5	0.158	0.694	2.536	0	0	0.02	0.584
S.E	0.03	0.27	0.89	1.44	0.04	0.07	0.19	0.00	0.00	0.01	0.06
Late Rain: October											
Asbestos roof: SRC_1	6.40^{d}	24.48^{a}	37.05^{a}	55.50^{a}	1.24^{a}	6.58^{a}	9.51^{a}	ND	ND	ND	0.69^{b}
Aluminum roof: SRC_2	6.60^{b}	19.93^{c}	24.00^{b}	28.50^{c}	0.14^{c}	1.26^{c}	4.19^{c}	ND	ND	0.14^{b}	0.26^{c}
Corrugated iron:SRC_3	6.50^{c}	22.28^{b}	25.50^{b}	44.00^{b}	0.41^{b}	1.71^{b}	4.99^{b}	ND	ND	0.18^{a}	1.78^{a}
Harvey tile roof:SRC_4	6.85^{a}	10.22^{d}	13.00^{c}	19.00^{d}	0.09^{c}	0.22^{d}	2.65^{d}	ND	ND	ND	0.08^{d}
Atmospheric Rain : (Control)	6.85^{a}	9.33^{e}	7.00^{d}	11.00^{e}	0.04^{c}	0.08^{e}	1.35^{e}	0.10^{a}	ND	ND	ND
Mean	6.64	17.106	21.3	31.6	0.384	1.97	4.52	0.02	0	0.064	0.562
S.E	0.04	0.17	0.71	1.61	0.05	0.05	0.22	0.02	0.00	0.01	0.01
WHO 6.5-8.5	200	250	200	40	250	250	0.5	0.01	0.30	0.3	
FME_{NV} 6.0-9.0	-	500	-	10	500	250	0.1	0.05	1.0	5.0	

Means with the same superscript are not significantly different (P ≥ 0.05) TDS=Total Dissolved Solid: EC=Electrical Conductivity: NO_3^-=Nitrate: SO_4^{2-}=Sulphate: Cl^-=Chloride: S.E=Standard Error of Means: WHO=World Health Organization: FME_{NV} = Federal Ministry of Environment

Chloride (Cl^-) the in rainwater harvested during onset of rain ranged from 6.45to 14.03 mg/l with the atmospheric rain recording 4.13 mg/l, and a mean of 8.842 mg/l. During peak rain, chloride in the harvested rainwater ranged from 1.15to 4.98 mg/l, with a mean of 2.536 mg/l and the atmospheric rain recorded 0.83 mg/l. According to Daifullah and Shakour (2003), chloride ions originate from human activities such as industrial emission, automobile exhaust etc. Ultimately, Cl^- values of the analyzed harvested rainwater samples were below the250 mg/l WHO/FMEnv allowable limits for portable water, with Asbestos recording the highest value, while Harvey tile recorded the lowest value. The study is in tandem with the finding of Eruola et al. (2010) who observed that the highest concentration of chloride in rainwater came from the Asbestos roof and was followed by Aluminum, Zinc, and atmospheric rainwater respectively. During rain events, Cl^- in the rainwater from the four different roofs was in a decreasing order as follows: Asbestos ≥ Corrugated iron ≥ Aluminum ≥Harvey tile (Table 2). This implies that the rainwater harvested from the Asbestos rooftop recorded the highest chloride, while the Harvey–tile rooftop showed the least value. Meanwhile, chloride ions in very small concentrations or as an impurity in raw water can cause active corrosion (Egereonu, 2006).

7.2 Heavy Metal Concentrations in Harvested Rainwater from Roof Catchment during Rain Events

According to Table 2, during the onset of rain event, Cu^{2+} ranged from zero to 0.07mg/l, with the Asbestos and Harvey-tile rooftops recording a zero value, while the Aluminum roof exhibited the highest value, with a mean of 0.04mg/l. The results of Cu^{2+}during onset of rain from roofs are lower than 0.460 - 0.820mg/l obtained from the Aluminum-Asbestos roofs by Olubanjo (2016). The copper in rainwater from roofs was below the0.5mg/l, 0.1 mg/l WHO/FMEnv permissible limits, with a decreasing abundance of Aluminum ≥ corrugated iron and Asbestos, Harvey tile. Asbestos rooftops and atmospheric rain recorded zero respectively. Olubanjo (2016) recorded 0.560 mg/l of Cu^{2+}in atmospheric rain compared to zero in the current study. The result is in tandem with the finding of Akhionbare (2009) who reported highest concentrations of Cu^{2+}in rainwater from the Aluminum roofing sheet during the first flush. Only Asbestos roof recorded Pb^{2+}: 0.04mg/l, a mean value of 0.008 mg/l, while the other sampled rooftops and atmospheric rain recorded none respectively. The result is in agreement with the finding of Ezemonye et al. (2016) who reported a higher concentration of Pb^{2+}in the rainwater samples from the Asbestos roof than other rooftops. The higher value of Pb could be due to the tendency of Pb to strongly adhere to particles (Dannecker et al., 1990). The Aluminum roof runoff samples recorded Fe^{2+} (0.22mg/l), while the galvanized roof samples recorded (0.40mg/l), with a mean of 0.044mg/l respectively, while others recorded none. Elevated values of Fe in the aluminum, and galvanized metal roof runoff samples may be due to the erosion of zinc roofing material, galvanized gutters and bulk atmospheric deposition (Chang et al., 2004; Uzoma and Sangodoyin, 2000).

The SRC1^{-4} and atmospheric rain recorded Zn^{2+}: 1.16mg/l, 0.43mg/l, 4.35mg/l, 0.22mg/l, 0.03mg/l respectively, with the mean of 1.238 mg/l. The highest value of Zn^{2+} was found in the rainwater from the corrugated iron roofing sheet. The result agreed with the finding of Chizoruo and Onyekachi (2016), who reported the highest Zn^{2+}concentration in rainwater from the galvanized iron rooftop in Orlu, Imo State, Nigeria.

Table 3. Pearson correlation matrix of physicochemical parameters of harvested rainwater from rooftops during rain events.

Tracer	pH	Acidity (mg/l)	TDS (mg/l)	EC (μhosm/cm)	**NO_3^-(mg/l)**	**SO_4^{2-}(mg/l)**
April: Onset of rain						
pH	1					
Acidity	-0.987**	1				
TDS	-0.999**	0.992**	1			
EC	-0.967**	0.995**	0.976**	1		
NO_3^-	-0.815	0.750	0.791	0.682	1	
SO_4^{2-}	-0.917*	0.878	0.902*	0.829	0.973**	1
Cl^-	-0.986**	0.978**	0.982**	0.955*	0.864	0.951*
July: Peak rain						
pH	1					
Acidity	0.973**	1				
TDS	-0.992**	0.964**	1			
EC	-0.990**	0.944*	0.997**	1		
NO_3^-	-0.863	0.935*	0.890*	0.853	1	
SO_4^{2-}	-0.637	0.736	0.693	0.648	0.918*	1
Cl^-	-0.954*	0.984**	0.967**	0.945*	0.974**	0.821
October: Late rain						
pH	1					
Acidity	0.992**	1				
TDS	0.965**	0.957*	1			
EC	0.965**		0.966**	1		
NO_3^-	-0.817	0.746	0.869	0.892*	1	
SO_4^{2-}	-0.828	0.767	0.891*	0.879*	0.990**	1
Cl^-	-0.907*	0.868	0.965**	0.951*	0.965**	0.975**

***. Correlation is significant at the 0.01 level (2-tailed).*
**. Correlation is significant at the 0.05 level (2-tailed).*

In the peak of rain, the result shows that Cu^{2+}andPb^{2+}were not detected across the roof catchments and atmospheric rain. Iron was only detected from the Asbestos roof runoff samples at 0.10 mg/l. Ikpoba (2002) observed that the lowest value of Fe2 in rainwater in July could be because the rain runs off on the roofs and washed off some Iron, which is part of the material used in their manufacturing. The Zn^{2+}ranged from 0.69to 1.42 mg/l with the Asbestos roof samples having the highest value and the Harvey-tile runoff samples having the lowest value, with a mean zinc of 0.584 mg/l that is less than the 0 mg/l value of the atmospheric rainwater. The highest value of Zn^{2+} was suspected to come from the eroded particles of zinc washed off by runoff water from the Corrugated Iron Sheet rooftop. Accordingly, zinc found in water could be attributed to the weathering of the Corrugated Iron sheets and industrial pollution (Eruola et al., 2010). Gromaire et al. (2002) reported that the elevated zinc in rainwater was related to zinc gutters, and the roofing as well as the galvanized iron roofing. Zinc levels found in the harvested rainwater samples do not cause any concern except for those of the corrugated Iron sheet rooftop during the early rain as the samples recorded concentrations higher than the WHO limits of 0.3 mg/l although these were still below the limit stated by FMEnv (5.0 mg/l). An overdose of zinc can depress the immune system, cause anemia, and copper deficiency, and decrease the high density lipoprotein cholesterol in the blood (Akhter et al., 2002). Moreover, Zinc causes an undesirable taste in water at a high accumulation.

During late rain,Cu^{2+} and Pb^{2+} were not detected across the SRC_{1-4}, except in the atmospheric rain as control which recorded 0.10 mg/l. Lead was also not detected in the harvested rain samples from SRC_1, SRC_3, SRC_3, SRC_4 and atmospheric rain respectively. Iron was detected in $SRC_2$and SRC_3 at 0.14 mg/l and 0.18 mg/l respectively, and was not detected in SRC_1, SRC_4 and the control respectively. The results show that Zn^{2+} ranged from 0.08 to 1.78 mg/l with SRC_1 having the highest value of 1.78 and SRC_4 the lowest value (0.08 mg/l), with a mean of 0.562 mg/l (Table 2). The highest concentration of dissolved Zn^{2+} and Fe^{2+} in the metal sheets suggests that either metal roofs galvanized iron or aluminum act as a potential source of the soluble fraction of heavy metals compared to other roof types (Ayenimo et al., 2006). Similarly, the maximum concentration of the sampled metals was observed in the Asbestos roof compared to other roofing materials. This observation agrees with the report of Gadd and Kennedy (2001) who suggested that the galvanized metal roofs contribute more zinc to the roof runoff. This report implies that products used in roofs appear to have a direct influence on the potential for the release of these soluble metals into storm-water. This implies that the Asbestos roofing sheet yielded to the heavy contaminants more than the Harvey tile sheet being the best for July rain event.

7.3 Correlation between Physicochemical Characteristics during the Onset of Rain

The correlation (r) was used to analyze the relationship between rainwater characteristics from four different roof catchments to analyze the strength of the relationship by using the value of r to understand the sources of the rainwater contaminants during rain events. The Pearson's correlation coefficients for the contents of pH, acidity, TDS, EC, NO_3^-, SO_4^{2-}, and Cl^-in the harvested rainwater from roof catchments during rain events are presented in Table 3.

A negative correlation was found between pH and acidity (r^2=-0.987**),TDS(r^2=-0.999**), EC(r^2=-0.967**), SO_4^{2-} (r^2=-0.917*) and Cl^-(r^2-0.986**), indicating that the parameters from the harvested rainwater may have a similar source or properties such as the atmosphere, i.e. due to the anthropogenic activities (air quality),outside the roof catchments. Acidity was positively but highly correlated with TDS, EC and Cl^-: r^2=0.992**, 0.995**, 0.978** respectively. The strong positive correlation between acidity and TDS, EC and Cl^-further emphasizes a common pathway and origin; this could be attributed to the kinetic energy of rainfall that impinges on the roof materials (Chukwuma et al., 2014). The TDS was positively but strongly correlated with EC (r=0.976**), SO_4^{2-}(r=0.902*), Cl^-=0.982**). The EC was positively and strongly correlated with Cl^-(r=0.955*), NO_3^- was positively and strongly correlated with SO_4^{2-}(0.973**) and SO_4^{2-} was positively and strongly correlated with Cl^-(r=0.951*). These positive correlations are indications that rainwater from the rooftops was acidic signifying the atmospheric composition of the area. In the same vein, Zunckel et al. (2003) found a strong correlation between the presence of contaminants in the catchments area and rainwater quality. The result agrees with Ramlall et al. (2015) who observed that SO_2 and NOx in the atmosphere are related to industrial activities and the combustion of fossil fuels. These compounds undergo oxidation in the atmosphere in combination with ozone, forming strong acids (sulphuric and nitric acids) which, when dissolved in rainwater, decrease its pH (Ubuoh et al., 2016).

7.4 Correlation between Physicochemical Characteristics during the Peak of Rain

During July, pH was positively and strongly correlated with acidity: (r^2=0.973**), while it was negatively and strongly correlated with TDS, EC, Cl^- (r^2=-0.992**, 0.990**,-0.954*) respectively which is suspected to come from the atmosphere through human activities. Acidity was positively and strongly correlated with TDS, EC, NO_3 Cl^-(r^2=0.964**, 0.944*, 0.935*, 0.984**) respectively, TDS was positively correlated with EC, NO_3^- and Cl^- : r^2=0.997**, 0.890*, 0.967** respectively. EC was positively correlated with Cl (r^2=0.945*) and $NO_3$was positively and strongly correlated with SO_4^{2-} (r^2= 0.918*), Cl^-(r^2=.974**). This correlation between nitrate and sulphate in rainwater from rooftops is attributed to the atmospheric composition of acid precursors due to anthropogenic activities. These results agree with the finding of Keller and Pitblado, (1986) who reported that the levels of sulfate in rainwater from rooftops and surface water correlate with emissions of sulfur dioxide from anthropogenic sources. The positive correlations signify that rooftops also contributed to the physicochemical contaminants in the rainwater through the weathering of the catchments despite the heavy rain that cleansed the rooftops and atmosphere respectively. Roof material and its features may also have a significant impact on rainwater runoff quality (Friedler et al., 2017). This is due to the reactions between rooftops and substances in the atmosphere as the result of human activities in the area (Cotton and Pielke 2007). Negative correlations revealed between most measured physicochemical parameters in the rainwater may probably be attributed to the scouring and transport of dry matter accumulated on the roof surfaces (Friedler et al., 2017). The result of the correlation is in line with the report that rainwater and roof drainage pollution is caused by constituents existing in the atmosphere (Hu et al., 2003; Khare et al., 2004) and/or accumulated on the roof area. Accordingly, acid pollutants in the atmosphere (e.g., H_2SO_4, HNO_3) mainly originate from the combustion of fossil fuels in automobiles and from heating in buildings, and the industry (Hu et al., 2003; Kulshrestha et al., 2003; Lee et al., 2000).

7.5 Correlation between Physicochemical Characteristics during Late Rain

During late rain, the pH was highly positively correlated with acidity (r^2=0.992**), TDS (r^2=0.965**), EC (r^2= 0.965**) and was highly negatively correlated with Cl^-(r^2=0.907*). Acidity was positively correlated with TDS (r^2=0.957*), EC (r^2= 0.940*), NO_3^- and SO_4^{2-} were strongly correlated with Cl^-: .965**, 0.975** respectively.

Table 4. Pearson correlation matrix of metal in harvested rainwater from roofs during rain events.

Metal/rain event	Cu^{2+} (mg/l)	Pb^{2+}(mg/l)	Fe^{2+}(mg/l)	Zn^{2+} (mg/l)
April: Onset of rain				
Cu^{2+}	-			
Pb^{2+}	.-	1		
Fe^{2+}	.-	-0.382	1	
Zn^{2+}	.-	-0.024	0.821*	1
July: Peak of rain				
Cu^{2+}	-			
Pb^{2+}	-	-		
Fe^{2+}	-	-	1	
Zn^{2+}	-	-	0.373*	1
October: Late rain				
Cu^{2+}	1			
Pb^{2+}	.-			
Fe^{2+}	-0.403	.-	1	
Zn^{2+}	-0.430	.-	0.681	1

**. Correlation is significant at the 0.05 level (2-tailed)*
***. Correlation is significant at the 0.01 level (2-tailed).*

7.6 Correlation between Heavy Metals during Onset of rain

Lead (Pb^{2+}) was negatively but very weakly correlated with Fe^{2+} and Zn^{2+}:r^2=-0.382, -0.024 respectively (Table 4). Fe^{2+} was positively and moderately correlated with Zn^{2+} (r^2=0.821*). This is an indication of the influence of the roof types in the area. The result is in line with the finding of Friedler et al. (2017) who observed that the type of roof also affected the concentrations of some heavy metals in the harvested rainwater during the onset of rain.

7.7 Correlation between Heavy Metals during Peak of rain

The correlation analysis between metals in the harvested rainwater during the month of July recorded a very weak negative correlation between Fe^{2+} and Zn^{2+} (r^2 =0.373) (Table 4). This is thought to come from the corrugated iron roofing sheet through the weathering process during heavy rain. This result is in line with the findings of Ubuoh et al. (2016); Akhionbare (2009) who reported that corrugated iron roofing sheet recorded the highest concentration of Zn^{2+} in the harvested rain water after the first flush (AFF), because corrugated iron roofing sheets are known for their faster weathering (Akhionbare, 2009; Quek and Forester, 1993).

7.8. Correlation between Heavy Metals during Late Rain

The correlation between heavy metals in the rainwater harvested during late rain indicated that Cu^{2+} was weakly and negatively correlated with Fe^{2+} (r^2= -0.403) and Zn^{2+} (r^2=-0.430) and Fe^{2+} had a positive correlation with Zn^{2+} (r^2=0.681) (Table 4).

Table 5. Temporal variability of harvested rain quality during rain events.

Rain Events	Physicochemical Characteristics						Heavy **Metals**				
	pH	Acidity	TDS	EC	NO_3^-	SO_4^{2-}	Cl^-	Cu^{2+}	Pb^{2+}	Fe^{2+}	Zn^{2+}
April : onset of rain	6.55	20.06	27.50	42.60	0.74	4.76	8.84	0.07	0.01	0.04	1.24
July :peak of rain	6.73	14.76	16.6	26.5	0.158	0.694	2.536	0	0	0.02	0.6
October :late rain	6.64	17.106	21.3	31.6	0.384	1.97	4.52	0.02	0	0.06	0.6

Temporal variability of rainwater harvested during April, July, and October rain events indicates that the chemical parameters increased during the onset of rain, decreased during the peak of rain, and increased again during the late rain as cessation (Table 5). The result is in line with the observations of Balogun et al. (2016); Ubuoh et al. (2012); Mendez et al. (2010) who opined that the concentration of contaminants in roof runoff are highest at the beginning of the rain event compared to subsequent events of similar magnitudes. Accordingly, Leonard et al. (2015) classified the beginning of rain as onset, middle, and cessation respectively. Jamal et al. (2009) also opined that the concentration of various pollutants were higher in the first spill of rain in comparison with the next spills. Teemusk and Mander (2007) found out that values of pollutants were found to be higher in moderate rain, while in samples taken during a heavy rainstorm; the components were less concentrated, as the rain helped wash the contaminants.

8.1 Rainwater Quality Index (RWQI)

The water quality Index was computed for rainwater sampled from the four rooftop catchments in regard to the physicochemical characteristics and heavy metals (tracers) for onset, peak, and late rain events to give the weighted values (Ci/Lij) and the overall RWQI) (Table 6).

Table 6. Rainwater Quality Index (RWQI) of each parameter from different roof catchments during rain events.

Tracer	(WHO) Li	Asbestos (SRC_1)		Aluminum (SRC_2)		Corrugated (SRC_3)		Harvey Tile (SRC_4)	
		C_i	Ci/Lij	C_i	Ci/Lij	Ci	Ci/Lij	Ci	Ci/Lij
Onset of rain (April)									
pH	8.5	6.20	0.73	6.55	0.77	6.35	0.75	6.75	0.79
Acidity (mg/l)	100	28.58	0.29	22.19	0.22	25.19	0.25	14.43	0.14
TDS (mg/l)	250	46.00	0.18	28.50	0.11	39.00	0.16	16.00	0.10
EC(µhosm/cm)	100	64.00	0.64	52.00	0.52	57.50	0.58	26.50	0.27
NO_3^-(mg/l)	40	2.66	0.07	0.22	0.006	0.66	0.02	0.13	0.003
SO_4^{2-}(mg/l)	250	13.16	0.05	3.86	0.02	5.20	0.02	1.09	0.004
Cl^-(mg/l)	250	14.03	0.06	9.18	0.04	10.42	0.04	6.45	0.03
Cu^{2+}(mg/l)	1.0	ND	ND	ND	ND	ND	ND	ND	ND
Pb^{2+}(mg/l)	0.01	0.04	4.0	ND	ND	ND	ND	ND	ND
Fe^{2+}(mg/l)	0.3	ND	ND	0.22	0.73	0.40	1.30	ND	ND
Zn^{2+} (mg/l)	3.0	1.16	0.37	1.16	0.14	4.35	1.45	0.22	0.10
RWQI	-	-	6.47	-	2.54	-	2.79	-	1.37
Peak of Rain (July)									
pH	8.5	6.55	0.77	6.70	0.79	6.60	0.78	6.90	0.81
Acidity (mg/l)	100	22.27	0.22	13.44	0.13	19.33	0.19	8.98	0.09
TDS (mg/l)	250	29.00	0.17	19.00	0.08	23.00	0.09	7.00	0.03
EC(µhosm/cm)	100	43.50	0.44	32.00	0.32	36.00	0.36	12.00	0.12
NO_3^-(mg/l)	40	0.46	0.01	0.08	0.002	0.21	0.005	0.04	0.001
SO_4^{2-}(mg/l)	250	3.30	0.01	0.06	0.0002	0.11	0.0004	ND	ND
Cl^-(mg/l)	250	4.98	0.02	2.32	0.009	3.40	0.01	1.15	0.005
Cu^{2+}(mg/l)	1.0	ND	ND	ND	ND	ND	ND	ND	ND
Pb^{2+}(mg/l)	0.01	ND	ND	ND	ND	ND	ND	ND	ND
Fe^{2+}(mg/l)	0.3	ND	ND	0.10	0.3	ND	ND	ND	ND
Zn^{2+} (mg/l)	3.0	1.42	0.47	0.09	0.07	1.37	0.46	0.04	0.01
RWQI	-	-	2.11	-	1.66	-	1.90	-	1.066
Late rain (October)									
pH	8.5	6.40	0.75	6.60	0.78	6.50	0.76	6.85	0.81
Acidity (mg/l)	100	24.48	0.24	19.93	0.20	22.28	0.22	10.22	0.10
TDS (mg/l)	250	37.05	0.19	24.00	0.12	25.50	0.13	13.00	0.07
EC(µhosm/cm)	100	55.50	0.56	28.50	0.29	44.00	0.44	19.00	0.19
NO_3^-(mg/l)	40	1.24	0.03	0.14	0.004	0.41	0.01	0.09	0.002
SO_4^{2-}(mg/l)	250	6.58	0.03	1.26	0.005	1.71	0.007	0.22	0.0009
Cl^-(mg/l)	250	9.51	0.04	4.19	0.02	4.99	0.02	2.65	0.01
Cu^{2+}(mg/l)	1.0	ND	ND	ND	ND	ND	ND	ND	ND
Pb^{2+}(mg/l)	0.01	ND	ND	ND	ND	ND	ND	ND	ND
Fe^{2+}(mg/l)	0.3	ND	ND	0.14	0.47	0.18	0.6	ND	ND
Zn^{2+} (mg/l)	3.0	0.69	0.23	0.26	0.09	1.78	0.59	0.08	0.03
RWQI		-	2.1	-	2.0	-	2.8	-	1.2
ND: Not detected, RWQI: Rainwater quality index									

The result indicates that during the onset of rain, individual parameters such as pH, acidity, TDS, and EC from the four rooftops were greater than 0.1. This connotes that rainwater from roof catchments needs some treatment before consumption. For example, Pb^{2+} (4.0) from the Asbestos roof was greater than the critical value of 1.0, demanding a proper treatment of rainwater before use. Based on the overall tracers in the harvested rainwater from the different roof catchments during a n early rain event, rooftops recorded water quality indices that range between 1.4 and 6.5, which is greater than the critical 1.0 limit used for the assessment of water contamination; the roof catchments are put in a decreasing order as follows: Asbestos (6.5) ≥ Corrugated iron (2.8) ≥ Aluminum roof (2.5) ≥ Harvey-tile roof (1.4). This implies that the rainwater harvested from the Asbestos roof is more contaminated than the Harvey-tile rainwater during the early rain events.

During the peak of rain, regarding TDS in the samples from SRC_{2-4}only EC, NO_3 SO_4^{2-}, Cl^-; Fe^{2+} and Zn^{2+} from SRC_2 were greater than the 0.1 value, which calls for little treatment for human consumption, while others did not require any treatment for human consumption (Table 6). Meanwhile, the overall tracers from the rainwater from the roof catchments during the peak of rain event, rooftops recorded water quality indices that ranged approximately from 1.07 to 2.11, which is greater than the critical limit of 1.0 used for WPI judgment. There is a decreasing abundance of contaminants in the samples from the four different catchments in the order of: Asbestos (2.11) ≥ Corrugated iron (1.90) ≥ Aluminum roof (1.7) ≥ Harvey tile roof (1.07). This implies that the rainwater harvested from The Asbestos roof is more polluted than that of the Harvey-tile roof which is less polluted during the peak of rain event. During late rain, acidity, TDS, EC Fe^{2+} and Zn^{2+} from some roofs were greater than the 0.1 value which means that the rainwater required little treatment for human consumption, while others did not require any treatment for human consumption (Table 6). The overall tracers in the rainwater harvested from the roof catchments during the late rain event recorded water quality indices that ranged between 1.21 and 2.78, which is greater than the critical limit of 1.0 used for WPI judgment, having a decreasing order as follows: Corrugated iron (2.8) ≥ Asbestos (2.1) ≥ Aluminum roof (2.0) ≥ Harvey-tile roof (1.2). This indicates that the rainwater harvested from the corrugated iron roof is more contaminated than that of the Harvey-tile roof during the cessation of rain events (Figure 3).

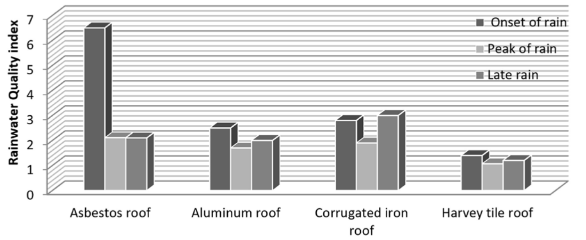

Figure 3. Rainwater Quality Index from rooftops during the rain events.

8.2 Rainwater Pollution Index (RWPI)

Total pollution indices and class status based on each rainwater characteristic during rain events are presented in Table 7.

Table 7. Rainwater Pollution Index (RWPI) for each rainwater characteristic during rain events.

Rainwater Quality	Total pollution index Onset of rain)	Pollution Class status (PCS)	Total pollution index (peak of rain)	Pollution Class status(PCS)	Total pollution index (Late rain)	Pollution Class status (PCS) (Table 1)
pH	3.04	STP	3.15	STP (4)	3.1	STP (4)
Acidity (mg/l)	0.9	NOP (1)	0.63	NOP (1)	0.8	NOP (1)
TDS (mg/l)	0.51	NOP (1)	0.4	NOP (1)	0.51	NOP (1)
EC(µhosm/cm)	2.01	MOP (3)	1.24	SLP (2)	1.5	SLP (2)
NO_3^-(mg/l)	0.1	NOP (1)	0.02	NOP (1)	0.05	NOP (1)
SO_4^{2-}(mg/l)	0.09	NOP (1)	0.012	NOP (1)	0.043	NOP (1)
Cl^-(mg/l)	0.17	NOP (1)	0.044	NOP (1)	0.09	NOP (1)
Cu^{2+}(mg/l)	ND	-	ND	-	ND	-
Pb^{2+}(mg/l)	4	STP (4)	ND	-	ND	-
Fe^{2+}(mg/l)	2.03	MOP (3)	0.3	NOP (1)	1.1	SLP (2)
Zn^{2+} (mg/l)	2.03	MOP (3)	1.01	SLP (2)	0.94	NOP (1)

PCS: Pollution class status, STP: Strongly polluted, NOP: No pollution, MP: Moderately polluted ,SLP: Slightly polluted

The pH and Pb^{2+} indicate a strong pollution suspected to be due to atmospheric pollution by human activities and soil-dust in the atmosphere (Ubuoh et al., 2016), and air pollution in form of CO_x, NO_x, and SO_x leading to acid rain formation (Ubuoh et al, 2012; Bogan et al., 2009; Menz and Seip, 2004; Velikova et al., 2000). Acidic rainwater will cause corrosiveness on the zinc roof (Ubuoh and Ekpo, 2017), and has a high solubility against heavy metals such as Pb (Bogan et al., 2009). The Pb in water can result to the formation of $Pb(OH)_2$ (Khayan et al., 2019), making it hazardous to environment (Patunru, 2015). The higher the level of Pb in rainwater, the bigger the chances for the public to suffer health disorders through drinking rainwater (Khayan et al., 2019 ; Alli, 2015; Al-othman et al., 2013), and the high the level of Pb in urine of the consumers of rainwater (Khayan et al., 2019). Acidity, TDS, NO_3^-, SO_4^{2-}, and Cl^-indicated no pollution. Moderate pollution was observed concerning EC, Fe^{2+}, Zn^{2+} during the onset of rain respectively (Table 7). During the peak of rain, pH indicated a strong pollution suspected to be due to urban air pollution. while acidity, TDS, NO_3^-, SO_4^{2-},

Cl^- and Fe^{2+} recorded no pollution, and EC and Zn^{2+}recorded slight pollution respectively. In the late rain, pH indicates a strongly polluted samples, while acidity, TDS, NO_3^-, SO_4^{2-}, Cl^- Zn^{2+}indicated no pollution. EC and Fe^{2+} showed a slight pollution. No pollution was observed concerningCu^{2+} during the rain events, and during the peak, and late rain events, no pollution was observed regardingPb^{2+}. The result of Cu is inconsistent with the findings of Udousoro and Unanaowo (2015) who reported that atmospheric rainwater at Urua Akpan- Andem, Akwa Ibom State, Nigeria shows a strong pollution concerning Cu^{2+} due to the commercial activities and heavy traffic flow. Ultimately, the results of rainwater pollution classes recorded during the rain events are as follows: strongly polluted rainwater (STP) constituted 14.3%, samples with no pollution (60.7%), moderately polluted samples (MOP) (10.7%), and the slightly polluted samples constituted (14.3%).

Table 8. Rainwater pollution index for roof catchments on temporal rain events.

Roof types	The Month of Rain Event				
	April	July	October	Mean	Ordering
Asbestos Roof (SRC_1)	6.46	2.11	2.07	3.55	4th
Aluminum Roof (SRC_2)	2.54	1.66	1.98	2.06	2nd
Corrugated Roof (SRC_3)	2.79	1.90	2.78	2.49	3rd
Harvey Tile (SRC_4)	1.37	1.07	1.21	1.22	1st
Total	13.16	6.74	8.04	9.32	-
Mean	3.29	1.69	2.01	-	-

It is observed that all of the selected roof catchments recorded values higher than the critical value of 1.0 used for judgment of unpolluted water, which implies that rainwater from these roof catchments in the study area must be subjected to treatment before any potable water use (Table 8). However, the pollution was at different levels during the months. In April: Harvey tile ≤ Aluminum ≤ Corrugated ≤ Asbestos, in July: Harvey tile ≤ aluminum ≤ Corrugated ≤ Asbestos, while in October: Harvey tile ≤ Aluminum ≤ Asbestos ≤ Corrugated. However, Harvey tile roof was observed to be the most suitable while July is observed as the most suitable period for rainwater harvesting. Asbestos roof recorded the worst water quality due to heavily loaded contaminants throughout the three rain events (Figure 4). This result disagrees with Opare (2012) who reported that the corrugated iron sheet is the most suitable for rainwater harvesting. The result is in line with the findings of Ezemonye et al. (2016); Ikhioya et al. (2015), who reported that rainwater harvested from Asbestos rooftop had more parameters and the highest contaminants. Differences that occur in the pollution index of rainwater from rooftops between April, July, and October may be due to the type of roof, human activities, and the intensity of the rain. Solids and dusts that are deposited on the roof were flush off in the early rain, reduced in July, and gradually built -up in October. The flush off' effect of the rain has cleared the contaminants on the roof of the building. Hence, the reading is decreasing with the increase of rain duration (Chu et al., 2001).

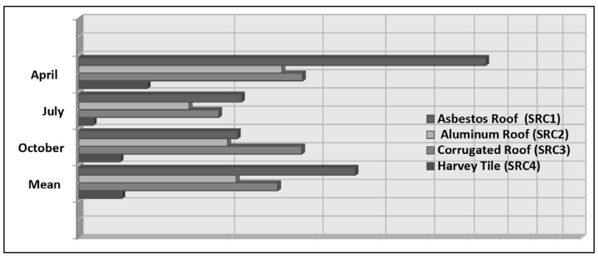

Figure 4. Rainwater pollution index of different roof catchments during rain events.

From the rainwater pollution index (RWP1) by roof catchments, Asbestos recorded 3.6 (i.e. strongly polluted), Aluminum 2.1 (moderately polluted), Corrugated 2.5 (moderately polluted) and Harvey-tile roof 1.2 (slightly polluted), with a decreasing abundance of contaminants in the samples from the four catchments in the order of: Asbestos ≥ Corrugated ≥ Aluminum ≥ Harvey Tile. This signifies that the Harvey-tile rooftop is the best, while the Asbestos rooftop is the worst for rainwater harvesting respectively. These results disagreed with the observation that rainwater harvested from rooftops is often considered unpolluted (Meera and Ahammed, 2006; Gonçalves et al., 2003) or at least being of a relatively good quality compared with the runoff from surface catchments (Göbel et al., 2007). The result is consistent with the observation by Adeniyi and Olabanji (2005) who raised disagreement about the quality of rooftop runoff ranging from good or acceptable to contaminated, and stated that rainwater quality is dependent on the roofing material (Adeniyi et al., 2002; Zobrist et al., 2000), environmental conditions, and atmospheric pollution (Friedler et al., 2017; Van -der Sterren et al., 2013).

4. Conclusion

Rainwater was collected from Asbestos, Aluminum, Corrugated iron and Harvey-tile roofs which are commonly used material for roofing houses, as well as from the atmospheric rain as control during early, peak and late rain. The samples were taken from the three selected housing locations (layouts), whenever rainfall occurs at different locations. However, apart from pH, other physiochemical properties and metals: Cu^{2+}, Pb^{2+} and Fe^{2+} were below the WHO/FMEnv permissible limits for drinking water. Physicochemical characteristics and heavy metals from the roofing sheets' samples were considerably higher than in the atmospheric rain during rain events: April> July < October. Positive and negative correlations existed between most examined rainwater tracers from rooftops, where the positive correlation is assumed to have originated from the weathering of roof catchments or probably from the scouring and transport of dry matter accumulated on the roof surface during the antecedent dry period. A negative correlation is also assumed to have resulted from the environmental conditions (air-borne dust and mists, bird droppings, and other debris), that accumulated in rain water via rooftop. The results indicated that the contamination of rainwater originated from the atmosphere outside the roof catchments; the common pathway and origin may be attributed to the kinetic energy of rainfall that impinged on the roof materials. Except for the Harvey-tile roof, the Zn^{2+} values in the rainwater samples from the Asbestos, Aluminum, and corrugated roofs were above the permissible limits of the 0.3mg/l set by the WHO, which produces the undesirable taste of the rainwater alongside health risks as a result of a Zn^{2+}overdose. From RWP1, roof catchments exhibited a decreasing abundance of contaminants in the order of: Asbestos ≥ Corrugated ≥ Aluminum ≥ Harvey-Tile, signifying that rooftops resulted in slightly-polluted samples and strongly-polluted ones, with the Harvey-tile being the best and Asbestos being the worst for rainwater harvesting. For urban dwellers that intend to harvest rainwater using roofs, Harvey-tile roofing sheets that are environmentally friendly should be recommended for the roofing of houses. However, if not feasible due to their high cost, Aluminum roofing sheets should be an alternative. However, the use of Asbestos is not recommended as its fibers can cause the Asbestosis disease. The use of Asbestos as a roofing sheet should be discouraged by developers and compliance must be enforced. Ultimately, Nigerians should be properly enlightened on the risks associated with the use of some roof materials that are not environmentally friendly .For roofs that are nontoxic, the operation and maintenance (O and M) strategy of the catchments must be strictly adhered to.

Conflict of interest: The authors declare that they have no conflict of interest.

Acknowledgement:

The authors are grateful to the residents of three layouts: New town layout, Eghem layout, and Uzo Avoiteyi layout for their cooperation and assistance during the course of field work. The authors are thankful to the entire lecturers in the Department of Environmental Management and Toxicology, Michael Okpara University of Agriculture, Umudike Nigeria, who helped in restructuring the title of the paper. We also wish to appreciate Mr. Paul, a laboratory Technologist who helped during the analyses.

References

Abdulla, F. A. and Al-Shareef, A. W. (2009). Roof rainwater harvesting systems for household water supply in Jordan. Desalination 243: 195–207.

Ademoroti, C. M. O. (1996). Standard methods for water and effluents analysis. Foludex Press Ltd., Ibadan 3: 29-118.

Adeniyi, I.F. and Olabanji, I.O. (2005). The physicochemical and bacteriological quality of rainwater collected over different roofing materials in Ile-Ife, South-western Nigeria. Chemistry and Ecology 21(3): 149-166.

Akharaiyi, F.C. Adebolu, T.T., Abiagom, M.C. (2007). A Comparison of Rainwater in Ondo State, Nigeria to FME Approved Drinking Water Quality Standard. Research Journal of Microbiology 2: 807-815.

Akhionbare, S. M.O. (2009). Evaluation of Heavy metal concentrations from different roof catchments in a semi-urban community. Global Journal of Engineering and Technology 2: 223-228.

Akhter, P., Akram, M., Orfi, S. D., Ahmad, N. (2002). Assessment of Dietary Zinc Ingestion in Pakistan. Nutrition 18: 274-278.

Aladenola, O.O. and Adeboye, O.B. (2009). Assessing the Potential for Rainwater Harvesting. Water Resource Management 24: 2129–2137.

Alli, L.A. (2015). Blood level of cadmium and lead in occupationally exposed persons in Gwagwalada, Abuja, Nigeria Interdisciplinary Toxicology 8(3): 146–150.

Al-Othman, A.M., Al-Othman, Z. A., El-Desoky, G. E., Mourad, A. M. A., Mohamed, A. H, Giesy, J.P. (2013). Lead in drinking water and human blood in Riyadh City, Saudi Arabia. Arabian Journal of Geosciences 6(10): 3103-3109. DOI 10.1007/s12517-012-0551-4.

Amadi, A.N., Dan-Hassan, M. A., Okoye, N.O., Ejiofor I.C., Aminu T. (2013). Studies on pollution hazards of shallow hand dug wells in Erena and environs, North-Central Nigeria, Environment and Natural Resources Research 3(2): 69-77.

Amos, C. C., Rahman, A., Karim, F., Gathenya, J. M. (2018). A scoping review of roof harvested rainwater usage in urban agriculture: Australia and Kenya in focus. Journal of Cleaner Production 202: 174-190. https://doi.org/10.1016/j.jclepro.2018.08.108.

Andreea-Mihaela, D. (2018).Water Pollution and Water Quality Assessment of Major Trans-boundary Rivers from Banat (Romania). Journal of Chemistry 2018: 1-8. https://doi.org/10.1155/2018/9073763

APHA (1998). Standard Methods for the Examination of Water and Wastewater. 20th Ed. Washington, D.C: American Public Health Ass. WPCF and AWWA.

Ayenimo, J. G., Adekunle, A. S., Makinde, W. O. Ogunlusi., G. O. (2006). Heavy metal fractionation in roof run off in Ile-Ife, Nigeria. International Journal of Environmental Sciences and Technology 3(3): 221-227.

Balogun, I. I., Adebayo O. S., Bosede, O. O. (2016). Assessment of rainfall variability, rainwater harvesting potential and storage requirements in Odeda Local Government Area of Ogun State in South-western Nigeria. Cogent Environmental Science 2(1): 113859. doi.org/10.1080/23311843.2016.1138597.

Bogan, R. A. J., Ohde, S., Arakaki, T., Mori, I., McLeod, C .W. (2009). Changes in rainwater ph associated with increasing atmospheric carbon dioxide after the industrial revolution. Water, Air, and Soil Pollution 196(14): 263-271.

Boller, M. A. and Steiner, M. (2002). Diffuse emission and control of copper in urban surface runoff. Water Science and Technology 46(6-7): 173-181.

Campisano, A., Butler, D., Ward, S., Burns, M. J., Friedler, E., DeBusk, K., Han, M. (2017). Urban rainwater harvesting systems: Research, implementation and future perspectives. Water Research 115: 195–209.

Chang, M., McBroom, M.W., Beasley, R.S. (2004) Roofing as a source of non-point water pollution. Journal of Environmental Management 73 (4): 307-315.

Chaturvedi, M.K. and Bassin, J. K. (2010) "Assessing the water quality index of water treatment plant and bore wells, in Delhi, India". Environmental Monitoring and Assessment 163: 449–453.

Chiang, J. C. H., Swenson, L. M., Kong, W. (2015). Role of seasonal transitions and the westerlies in the interannual variability of the East Asian summer monsoon precipitation

Geophysical Research Letters.10.1002/2017GL072739.

Chizoruo, I. F. and Onyekachi, I.B. (2016). Roof runoff water as source of pollution: a case studyof some selected roofs in orlu metropolis, Imo state, Nigeria. International Letters of Natural Sciences 50: 53-61.

Chu, C.P., Chang, B.V., Liao, D.S., Lee, D.J. (2001). Observations on changes in ultrasonically treated waste-activated sludge. Water Research 35(4):1038-1046. doi: 10.1016/s0043-1354(00)00338-9.

Chukwuma, E. C., Ogbu, K. N., Okonkwo, I. F. (2013) Quality assessment of direct harvested rain water in parts of Anambra State, Nigeria. International Journal of Agriculture and Biosciences 2(3): 120-123.

Chukwuma, J. N., Nnodu, V. C., Okoye, A. C., Chukwuma, E. C. (2014). Assessment of Roof Harvested Rainwater in Parts of Anambra State for Environmental Pollution. Monitoring British Biotechnology Journal 4(10): 1105-1114.

Cook, S., Sharma, A., Chong, M., (2013). Performance Analysis of a Communal Residential Rainwater System: a case study in Brisbane, Australia. Water Resources Management 27 (14): 4865-4876. DOI 10.1007/s11269-013-0443-8.

Cotton, W. R. and Pielke, R.A. Sr. (2007).Human Impacts on Weather and Climate. 2nd ed. New York: Cambridge University Press.

Daifullah, M.A.A. and Shakour, A.A. (2003). Chemical Composition of Rainwater in Egypt. AJEAM –RAGEE 6: 32 – 43.

Dannecker W., Au, M., Stedimann, H. (1990). Substances load in rainwater runoff from different streets in Hamburg. The Science of the Total Environment 93: 385-392. DOI: 10.1016/0048-9697(90)90129-i.

Despins, C., Farahbakhsh, K., Leidl, C., 2009. Assessment of rainwater quality from rainwater harvesting systems in Ontario, Canada. Journal of Water Supply: Research and Technology-AQUA 58 (2): 117-134.

Efe, S.I. (2006). Quality of Rainwater Harvesting for Rural Communities of Delta State, Nigeria. The Environmentalist 26(3): 175-181.

Egereonu, U.U. (2006). Physicochemical Assessment of Rainwater from two Rain gauged Stations in the Rainforest Region, Anambra State, Nigeria. Journal of Chemical Society 31(1-2): 43-48.

Eruola, A. O., Ufoegbune, G. C., Awomeso, J. A., Adeofun, C. O., Idowu, A. O. Sowunmi, A. (2010). Qualitative and Quantitative Assessment of Rainwater Harvesting from Rooftop Catchments: Case Study of Oke-Lantoro Community in Abeokuta, Southwest, Nigeria. European water 32: 47-56.

Ezemonye, M. N., Isueken, C. O., Emeribe, C.N. (2016). Physicochemical and Bacteriological Characteristics of Rainwater Harvested from Rooftops in Esan-West Local Government Area of Edo State, Nigeria. Journal of Applied Sciences and Environmental Management 20(3): 748–757.

Forster, J. (1996). Patterns of roof runoff contamination and their potential implications on practice and regulations of treatment and local infiltration. Water Science and Technology 33(6): 39-48.

Friedler, E. D., Gilboa, Y., Muklada, H. (2017). Quality of Roof-Harvested Rainwater as a Function of Environmental and Air Pollution Factors in a Coastal Mediterranean City (Haifa, Israel). Water 9(11), 896. https://doi.org/10.3390/w9110896.

Gadd, J. and Kennedy, P. (2001). House Runoffs: is it clean as we think? Second South Pacific Storm Water Conference.

Göbel, P., Dierkes, C., Coldewey, W.G. (2007). Storm water runoff concentration matrix for urban areas. Journal of Contaminant Hydrology 91(1-2): 26 - 42. doi: 10.1016/j.jconhyd.2006.08.008

Gonçalves, F., Andrade, M., Forti, M., Astolfo, R., Ramos, M., Massambani, O., Melfi, A. (2003). Preliminary estimation of the rainfall chemical composition evaluated through the scavenging modeling for north-eastern Amazonian region (Amapa State, Brazil). Environmental Pollution 121: 63–73.

Gromaire, M.C., Chebbo, G., Constant, A. (2002.) Impact of zinc roofing on urban runoff pollutant loads: the case of Paris. Water Science and Technology 45(7): 113–122.

Gurung, T.R. and Sharma, A. (2014). Communal Rainwater Tank Systems Design and Economies of Scale. Journal of Cleaner Production 67: 26-36.

Herrmann, T. and Schmida, U. (2000) Rainwater utilisation in Germany: efficiency, dimensioning, hydraulic and environmental aspects. Urban Water 1(4): 307-316.

Hoque, B.A., Hoque, M.M., Ahmed, T., Islam, S., Azad, A.K., Ali, N., Hossain, M., Hossain, M.S. (2004). 'Demand-based Water Options for Arsenic Mitigation: An Experience from Rural Bangladesh'. Public Health 118: 70 –77.

Horton, R. K. (1965). An Index Number System for Rating Water Quality. Journal of Water Pollution Control Federation 37: 300-306.

Hu, G. P., Balasubramanian, R., Wu, C. D. (2003). Chemical characterization of rainwater at Singapore. Chemosphere 51: 747–755.

Ikhioya, P. E., Osu, C. I., Obuzor, G. U. (2015). Physiochemical characteristic of Harvested Rain water from Bodo Community in Rivers State, Nigeria. Journal of Applied Sciences and Environmental Management 19(4): 671–677.

Ikpoba, I. T. (2002). Natural Gas Flaring in Nigeria – Clarifications of Environmental Issues, Standards and Flare-Down Policy. Society of Petroleum Engineers Workshop on Gas Flaring, 14th March, 2002, Abuja, Nigeria.

Ishaku, H. T., Rafee, M., Majid (2010). X-Raying Rainfall Pattern and Variability in Northeastern Nigeria: Impacts on Access to Water Supply. Journal of Water Resource and Protection 2: 952-959.

Ishisone, M. (2004). Gas Flaring in the Niger Delta: the Potential Benefits of its Reduction on the Local Economy and Environment. Available at: http://socrates.berkely.edu/es196/projects/2004final/ishisone.pdf (visited last on 27/05/11).

Jamal, R., Kamel, A., Adnan, A., Rida, A. (2009). Quality Assessment of Harvested Rainwater for Domestic Uses. Jordan Journal of Earth and Environmental Sciences 2(1): 26 -31.

Juahir, H., Ekhwan, T.M., Zain, S.M., Mokhtar, M.B., Jalaludin, Z. Jan, K.M. (2008). The use of chemometrics analysis as cost-effective tool in sustainable utilization of water resources in Langat river catchment. American-Eurasian Journal of Agricultural and Environmental Sciences 4(1): 258-265.

Kahinda, J.M.M., Taigbenu, A.E., Boroto, J.R. (2007). Domestic rainwater harvesting to improve water supply in rural South Africa. Physics and Chemistry of the Earth 32: 1050–1057.

Kale, V. S. (2016). Consequence of temperature, pH, turbidity and dissolved oxygen water. Quality Parameters 3(8): 186–190.

Keller, W. and Pitblado, J.R. (1986). Water quality changes in Sudbury area lakes: a comparison of synoptic surveys in 1974–76 and 1981–83. Water Air Soil Pollution 29: 285–296.

Khare, P., A. Goel, D. P., Behari, J. (2004). Chemical characterization of rainwater at a developing urban habitat of Northern India. Atmospheric Research 69 (3-4): 135-145. Doi: 10.1016/j.atmosres.2003.10.002.

Khayan, K., Husodo, A. H., Astuti, I., Sudarmadji, S., Djohan, T. S. (2019). Rainwater as a Source of Drinking Water: Health Impacts and Rainwater Treatment. Journal of

Environmental and Public Health 2019, Article ID 1760950. doi.org/10.1155/2019/1760950.

Kulshrestha, U. C., Kulshrestha, M. J., Sekar R., Sastry, G. S. R., Vairamani, M. (2003). Chemical characteristics of rainwater at an urban site of south-central India. Atmospheric Environment 37 (21): 3019–3026.

Lee, B. K., Hong, S. H., Lee, D. S. (2000). Chemical composition of precipitation and wet deposition of major ions on the Korean Peninsula. Atmospheric Environment 34(4): 563-575.

Leonard, K. A., Edmund, I. Y., Kwasi, P., Ernest, O. A., Jeffrey, A., Michael, B., Samue, N. A. C. (2015).Variability in Rainfall Onset, Cessation and Length of Rainy Season for the Various Agro-Ecological Zones of Ghana . Climate 3: 416-434.

Lumb, A., Halliwell, D., Sharma, T. (2002). "Canadian water quality index to monitor the changes in water quality in the Mackenzie river–Great Bear. Proceedings of the 29th Annual Aquatic Toxicity Workshop, (Oct. 21-23), Whistler, B.C., Canada. 2002.

Martinson, D. B. and Thomas, T. H. (2005). Quantifying the First Flush Phenomenon. In Proceedings of the 12th International Conference on Rain Water Catchment Systems. New Delhi: International Rainwater Catchment Systems Association.

Meera, V. and Ahammed, M.M. (2006).Water quality of rooftop rainwater harvesting systems: A review. Journal of Water Supply Research and Technology-aqua 55: 257–268. DOI: 10.2166/AQUA.2006.0010

Mendez, B.C., Brigit, R.A., Kerry, K., Micheal, E.B., Mary, K. (2010). Effect of Roof Material on Water Quality for Rainwater Harvesting Systems. Texas water Development Board Report, p. 2

Menz, F. C. and Seip, H. M. (2004). Acid rain in Europe and the United States: an update. Environmental Science and Policy 7(4): 253–265.

Mohammad, A. A., Ataur, R., Zhong, T., Bijan, S., Muhammad, M. K., Shafiq, S. (2020). Suitability of Harvested Rainwater for Human Consumption: A Scoping 9 Review. Journal of Cleaner Production 248: 1-47. DOI: 10.1016/j.jclepro.2019.119226.

Mouli, P. C., Mohan, V. S Reddy, S. J. (2005). Rainwater chemistry at a regional representative urban site: influence of terrestrial sources on ionic composition. Atmospheric Environment 39: 999–1008.

Muhamad, A. B. Muhamad, A. Muzaffar, Z. A. (2016). Water Quality Assessment of Rainwater Collected from Rooftop at UTM. Journal of Environmental Engineering and hydrology 3: 1-11.

National Root Crop Research Institute, (NRCRI) (2016). Meteorological Data. Nigeria Tribune Newspaper 18: 17-19.

Nicholson, N., Clark, S.E., Long, B.V., Spicher, J. Steele, K.A. (2009). Rainwater harvesting for non-potable use in gardens: a comparison of runoff water quality from green vs. traditional roofs. In: Proceedings of World Environmental and Water Resources Congress - Great Rivers Kansas City, Missouri.

NPC (2006). National Population Census Figures. NPC Abuja.

Nwilo, P. C., Olayinka, D. N., Uwadiegwu, I., Adzandeh, A. E. (2011). An assessment and mapping of gully erosion hazards in Abia State: A GIS approach. Journal of Sustainable Development 4(5): 196-211.

Olaoye, R.A. and Olaniyan, O.S. (2012). Quality of rain water from different roof materials. International journal of Engineering and Technology 2(8): 1413-1414.

Olubanjo, O.O. (2016). Evaluation of Quality of Rainwater Harvested from Different Roof Catchments Systems. Journal of Sustainable Technology 7(1): 1-20.

Opare, S. (2012). Rainwater harvesting: an option for sustainable rural water supply in Ghana. GeoJournal 77(5): 695-705.

Ozabor, F. and Nwagbara, M. O. (2018). Identifying Climate Change Signals from Downscaled Temperature Data in Umuahia Metropolis, Abia State, Nigeria. Journal of Climatology and Weather Forecasting 6: 215.

Patunru, A. (2015). Access to safe drinking water and sanitation in Indonesia. Asia and the Pacific Policy Studies 2(2): 234–244.

Polkowska, Z., Astel, A., Walna, B., Malek, S., Mdrzycka, K., G´orecki, T., Siepak, J., Namie´snik, J. (2005). Chemometric analysis of rainwater and throughfall at several sites in Poland. Atmospheric Environment 39: 837–855.

Quek, U. and Forster, J. (1993). Trace metals in roof runoff. Water Air and Soil Pollution 68(3- 4): 373–89.

Rahman, A. and Eslamian, S. (2016). Rainwater tanks as a means of water reuse and conservation in urban areas. Urban Water Reuse Handbook, pp. 805-814.

Rahman, M. M., Rahman, M. A., Haque, M. M., Rahman, A. (2019). Sustainable water use in construction. In: Tam, V. W. Y. and Le, K. N. (Eds.), Sustainable Construction Technologies Life-cycle Assessment (pp. 211-235). doi.org/10.1016/B978-0-12-811749-1.00006-7.

Ramlall, C., Varghese, B., Ramdhani, S., Pammenter, N.W., Bhatt, A., Berjak, P. (2015). Effects of simulated acid rain on germination, seedling growth and oxidative metabolism of recalcitrant-seeded Trichilia dregeana grown in its natural seed bank. Physiologia Plantarum 153: 149–160. DOI: 10.1111/ppl.12230.

Shweta, T., Bhavtosh, S., Prashant, S., Rajendra, D. (2013). Water Quality Assessment in Terms of Water Quality Index. American Journal of Water Resources 1(3): 34-38.

Simmons, G., Hope, V. Lewis, G., Whitmore, J., Gao, W. (2001). Contamination of potable roof-collected rainwater in Auckland, New Zealand. Water Resources 35(6): 1518–1524.

Stern, N. (2006). The Economics of Climate Change: The Stern Review. 1st Ed. HM Treasury, London.

Tang, A., Zhuang, G., Wang, Y., Yuan, H., Sun, Y. (2005). The chemistry of precipitation and its relation to aerosol in Beijing. Atmospheric Environment 39: 3397–3406.

Teemusk, A. and Mander, Ü. (2007). Rainwater runoff quantity and quality performance from a green roof: The effects of short-term events. Ecological Engineering 30(3-2): 271-277.

Teston, A., Celimar, A. T., Enedir, G.I., Ernani, Benincá, C. (2018). Impact of Rainwater Harvesting on the Drainage System: Case Study of a Condominium of Houses in Curitiba, Southern Brazil. Water 10(8): 1-16. https://doi.org/10.3390/w10081100.

Ubuoh, E. A., Akhionbare, W. N. A., Akhionbare, S.M.O., Ikhile, C. I. (2012). Evaluation of the Spatial Variation of Rainwater Quality in Parts of AkwaIbomState of Nigeria Using Chloropleth Map. Indian Journal of Educational Information Management 1(8): 328-336.

Ubuoh, E. A. and Ekpo, F. E. (2017). Characterization by Principal Component Analysis (PCA) of the Chemistry of Atmospheric Precipitation in oil and non-oil producing Communities of Akwa Ibom State, Nigeria. CARD International Journal of Environmental Studies and Safety Research 2(1): 2536-7285.

Ubuoh, E. A., Akhionbare, S. M., Ogbuji, O., Akhionbare, W.N. (2013). Effectiveness of Water Quality Index in Assessing Water Resources Characteristics in Izombe Oguta L o c a l Government Area of Imo State, Nigeria. International journal of Advanced Biological Research 3(1): 31-35.

Ubuoh, E. A., Kanu, C. Mpamah, I. C. (2017). Assessment of Air Quality Status Using Pollution Standard Index in Udeagbala Industrial Area, Abia State, Nigeria.IIARD International

Journal of Geography and Environmental Management 3(3): 47-57.

Ubuoh, E.A., Kanu, C., Ikwa, L. O. (2016). Comparative Analysis of ambient air quality status in Residential, Commercial and Industrial settlements in Bayelsa state, Nigeria. International Journal of Agriculture and Rural Development 19(2): 2766-2773.

Udousoro, I. I. and Unanaowo, A.E. (2015). Rainwater Quality Assessment in Uyo Metropolis using Water Quality Index. Nigerian Journal of Chemical Research 20: 1-8.

Udousoro, I.I. and Ikpeme, N. E. (2013). Chemometric characterisation of surface water quality in Uruan, Nigeria. International Journal of Chemical Studies 1: 102.

USEPA (2005). U.S. Environmental Protection Agency, Managing Wet Weather with Green Infrastructure. Municipal Handbook, Rainwater Harvesting Policies EPA-833-F-08-010.

USEPA (1997). Manganese. Washington, DC, US Environmental Protection Agency, Integrated Risk Information System (IRIS). Available at http://www.epa.gov/iris/subst/0373.htm

Utsev, J. T. (2012). Variability of rainwater quality due to roofcharacteristics. Global journal of engineering research 11(2): 77-84.

Uzoma, V.C. and Sangodoyin, A.Y. (2000). Rainwater chemistry as Influenced by atmospheric deposition of pollutants in southern Nigeria. Environmental Management and Health 11 (2): 149–156. doi.org/10.1108/09566160010321569

Van -der Sterren, M., Rahman, A., Dennis, G.R. (2013).Quality and quantity monitoring of five rainwater tanks in Western Sydney, Australia. Journal of Environmental Engineering 139: 332–340.

Van Metre, P. C. and Mahler, B. J. (2003). The contribution of particles washed from rooftops to contaminant loading to urban streams. Chemosphere 52(10): 1727-1741.

Velikova, V., Yordanov, I., Edreva, A. (2000). Oxidative stress and some antioxidant systems in acid rain-treated bean plants. Plant Science 151(1): 59–66.

WHO (2011). Guidelines for drinking-water quality, 4th Edition, World Health Organization, Geneva.

Zobrist, J., Muller, S. R., Ammann, A., Bucheli, T. D., Mottier, V., Ochs M., Schoenenberger R., Eugster, J., Boller, M. (2000). Quality of roof runoff for groundwater infiltration. Water Research 34: 1455–1462.

Zunckel, M., Saizar, C., Zarauz, J., (2003). Rainwater composition in northeast Uruguay. Atmospheric Environment 37 (12): 1601-1611.

JJEES

JJEES (2021) 12 (1): 36-43
ISSN 1995-6681

Jordan Journal of Earth and Environmental Sciences

An Overview of Solid Waste in Nigeria: Challenges and Management

*Odiana Sylvester and Olorunfemi Ikudayisi

University of Benin, Faculty of Life Sciences, Department of Environmental Management and Toxicology, Nigeria.

Received 18 June 2020, Accepted 3 September 2020

Abstract

Waste can be seen as material originating from animal and human activities, and when discarded as useless and unwanted, it attracts pathogens. The ineffective management of solid waste by individuals, homes, consumers, and waste management companies in Nigeria can be attributed to inadequate information on the benefits of waste management and poor implementation of government policies. This study is a descriptive research based on observation and secondary data gathered from news print and journals. The review sheds light on the concept of solid waste and management in Nigeria, recent studies in solid-waste management in Nigeria, solid-waste menace in Nigeria, methods for the control of land pollution in Nigeria due to improper waste disposal and challenges of municipal solid-waste management. Public and private partnership and public awareness should be encouraged to enhance solid-waste management. Thus, the sustenance of a healthy environment requires a careful attention to the environment which includes proper management of solid waste whose rate of generation in Nigeria has been put at an average value of 0.49 kg/capita/day.

Keywords: Waste, Menace, Environment, Management, Awareness.

1. Introduction

The environment is very crucial for the existence of every creature. In addition to serving as a place of abode to any creature, it also contributes, to a large extent, to the quality of life of creatures (Oreyomi, 2005). The environment can be seen as the total factors that surround and influence an organism at a given time and place. The failure of the numerous efforts to address the problem of environmental health hazards in developing nations has been attributed to various factors including unhealthy socio-cultural practices, poor environmental sanitation education and awareness, low literacy level, bad governance, disregard to the rule of law and other forms of indiscipline (Omotosho, 2005). Solid wastes are abandoned materials and could be garbage, sludge from a waste-treatment plant, discarded materials resulting from industrial, commercial, mining, agricultural operations, and those resulting from community activities such as waste tires, scrap metal, latex paints, furniture toys, appliances and vehicles, empty aerosol cans, paint cans and compressed gas cylinders, and construction and demolition debris. (Bamgbose et al., 2000). However, most of the waste commonly known as garbage, which consists of everyday items being discarded by the public, is generally regarded as municipal solid waste. It covers all thrown-away materials including products of packaging, grass clippings, furniture, clothing, bottles, food scraps, newspapers, appliances and batteries (Afon, 2006; Bassey et al., 2006). The quantity and rate of solid waste generation in a place is largely dependent on the population, level of industrialization, socio-economic status and the kinds of commercial activities (Dauda and Osita, 2003).

Humans have suffered in no small way from diseases associated with solid wastes and the contamination of the subsurface water by the leachate from solid wastes heavily laden with toxic chemicals and pathogenic organisms which contaminate the water and make it unfit for human consumption (Adedibu, 2008).

Solid-waste management entails the collection, storage, transportation, treatment, recycling, recovery, and disposal of waste in such a way as to render them innocuous to human and animal life, ecology, and the environment as a whole (Fafioye and John-Dewole, 2013). The problem of waste management is a primordial and poses threats in developing countries in Africa, particularly Nigeria. Municipal waste-management problems in Nigeria cut across concerns for human health, air, water, and land pollution among others. The analysis of the key problem affecting the efficient management of municipal waste is critical for developing a workable solution in an emerging economy like Nigeria's (Abila and Kantola, 2013). Waste management is not properly done in most towns in Nigeria. Most parts of urban areas do not benefit from public waste disposal services, which makes residents sort for other options such as burying or burning their waste therefore disposing it haphazardly.

Given the fact that waste management in developing countries is an ongoing challenge due to weak institutions and policies including the environmental laws, a chronic under-funding, the rapid urbanization and industrialization, the situation in the urban areas of Nigeria may not be different from other towns in the developing world. These challenges

Corresponding author email: odiana09@yahoo.com

along with the lack of understanding by different factors that contribute to the hierarchy of waste management may affect the treatment of wastes. It is imperative therefore, to examine the menace of solid waste generated in urban areas in Nigeria and the ways they can be curbed.

2. Concept of Solid Waste and Management in Nigeria

Waste could be any material which has been used and is no longer wanted as the valuable or useful part of it has been taken out (Oyeniyi, 2011). Solid waste can be defined as non-liquid and non-gaseous products of human activities, regarded as useless. It could take the form of garbage and sludge (Leton and Omotosho, 2004). Waste generated by human activities since time immemorial has continued to be a threatening problem and a growing one that is of major concern to every nation around the world (Oyelola and Babatunde, 2008). The rapid increase in the volume and types of solid and hazardous waste, due to the continuous economic development, urbanization and industrialization is becoming a burgeoning problem for most governments in ensuring an effective and a sustainable management of wastes (Ogu, 2000; Igoni et al., 2007). Waste generation encompasses those activities in which materials are identified as being no longer of value and are either thrown away or gathered together for disposal. When living standards rise, people consume more, so waste increases. The best place to sort waste materials for recovery is at the source of generation (Ezigbo, 2012).

According to Areme et al. (2007) cited in Ikemike (2015), waste generated in the country is characterized by a high percentage (60-80%) of domestic and commercial waste in relation to others. This gives waste a high density and makes it very attractive to flies, cockroaches, rats, and other vermin. Also, Mshelia (2015) opined that solid wastes are generally very diverse and are usually made up of complex mixtures of biodegradable and non-biodegradable matters. The biodegradable nature that characterizes solid waste in Nigeria is similar to what is obtainable in countries with similar economic and demographic characteristics including India, Bangladesh and Ghana (Akinwonmi et al., 2012). In Nigeria today, among the pressing environmental and public health issues are the problems of solid waste generation, control, and disposal (Okwesili et al, 2016). Although the problem of solid waste disposal is as old as man's existence that is inextricably linked to the generation of waste, the truth is that in many cities, it has become so intractable that even the government is overwhelmed (Momodu et al., 2011). The volume of solid waste generated continues to increase at a faster rate than the ability of the agencies to improve the financial and technical resources needed to balance this growth (Olukanni and Mnenga, 2015). The rate of solid waste generation in Nigeria has been put at an average value of 0.49 kg/capita/day (Nnaji, 2015). The average rate of waste generation in some Nigerian cities is shown in the Table 1 below:

Table 1. Quantity of municipal solid waste generated in some cities across Nigeria.

Cities	Population Estimation	Estimated kg/ capita/day	Tonne/ day	Tonne/ year
Minna	346,524	0.68	235	86007
Enugu	817,757	0.74	605	220876
Birnin kebbi	128,403	0.65	83	30463
Lagos	21,000,000	0.92	119320	7051800
PortHarcort	1,363,596	0.85	1159	423055
Bauchi	493, 730	0.68	336	122543
Abuja	1,857,298	0.95	1764	644018
Ibadan	3,565,108	0.72	2566	936910
Kaduna	1,582,102	0.70	1107	404227
Onitsha	561,066	0.69	387	141304
Sokoto	563,861	0.68	383	139950
Jos	816,824	0.73	596	217642
Benin City	1,125,058	0.78	877	320304

Source: Ike et al. (2018)

Table 1 above shows that Lagos with an estimated population of 21 million and generation rate of 0.92 kg/ capita/day, generates about seven million tons of waste annually. When compared with generation rates around the world, Nigeria, similar to other third world countries generate tons of waste, but is unable to deal with it effectively due to poor management practices. Moreover, the amount of waste generated is very necessary in determining and planning waste-treatment facilities and management (Ike et al., 2018).Wastes contain a lot of valuable resources in the form of nitrogen, phosphorus, potassium etc which are useful (Hammed et al., 2011). Almost all substances that are designated as waste possess potential resource utilization in that within the waste stream, there exists some degree of residual value for alternative uses. Waste represents valuable resources as ground covers to reduce erosion, and as fertilizers to nourish the crops and can also be a source of energy (Adekunle et al., 2011).

Different types of vehicles are used for solid-waste collection in Nigeria. The compactor trucks, side loaders, rear loaders, mini trucks, tippers, skip trucks and open back trucks are the commonly used collection trucks. It was observed that 60% of the available trucks are always out of service. The few available trucks breakdown frequently due to overuse (Agunwamba et al., 2003). Cities in Nigeria, being among the fast growing cities in the world, are all faced with the problem of solid waste generation (Onibokun and Kumuyi, 1996). The need for proper collection, adequate treatment and sanitary disposal of solid waste by man has risen as populations migrated from disperse geographical areas into communal living areas. Waste generation, both domestic and industrial, continues to increase globally in tandem with the growth in population and consumption patterns of towns and cities (Emelumadu et al., 2016). Based on the available literature, it has been confirmed that if current trends continue, the world may see a five-fold increase in waste generation by the year 2025 (Okalebo et al., 2014).

One of the consequences of population growth is waste. It therefore becomes a serious problem that needs attention from the government or agencies responsible for this (Olu-Olu and Omotosho, 2007; Schwarz-Herion et al, 2008; Adejobi and Olorunnimbe, 2012).

Waste management comprises the collection, transport, segregation, recycling, and disposal of wastes in an environmentally acceptable manner (Ekanem et al., 2013; Elenwo, 2015).

A sustainable environment and improved waste management offer opportunities for income generation, health improvements and reduced vulnerability (Adetunji et al., 2015). This could hardly be attained in some of the developing countries, most especially in Nigeria because of non- readiness, uncoordinated and laissez faire attitudes toward better ways of solid-waste disposal methods in spite of the high rate of urbanization and growth in commercial and industrial activities (Afangideh et al., 2012).

3. Recent Studies on Solid Waste Management in Nigeria

The unprecedented increase in world population growth rate particularly in developing countries coupled with the technological advancements, waste disposal and management constitute serious problems for societies. In cities going through rapid urbanization, the problems and issues of solid-waste management are of immediate importance (Momoh and Oladebeye, 2010). Nigerian cities and towns are currently facing serious environmental challenge due to poor solid-waste management. Solid waste is generated at a rate beyond the capacity of authorities to handle for the sake of maintaining a sustainable urban environment. This has resulted in a poor solid-waste management system that portends serious environmental crises in most Nigerian towns and cities (Abel and Afolabi, 2007).

Babayemi and Dauda (2009) reported high waste-generation rates in Abeokuta without a corresponding efficient technology to manage the wastes. Out of 201 sampled respondents in Abeokuta Ogun State, (35.8%) used waste collection services, (64.2%) used other waste disposal options, (16.4%) used both, (68.7%) and (58.7%) were aware of waste-collection services and waste-management regulations, respectively.

Okeniyi and Anwan (2012) reported that amongst the average wastes generated per day in Covenant University Ota, food waste exhibited the highest percentage of (26.2%), followed by polythene bags (19.3%); plastic bottles (13.6%), metal cans (11.5%), paper (10.5%), plastic food packages (7.2%), other combustible wastes (5.6%) and polystyrene food pack (5.6%).

Ogu (2000) interviewed 591 households in Benin-City, Nigeria and found out that three-fifth of the respondents had no solid-waste collection service. This is attributed to inadequate resources, and the privatization scheme set up in 1995 to address the environmental issues. The current study stresses the need for private partnership with government in providing adequate delivery services to the public.

Onwughara et al., (2010) examined the disposal habits, and the environmental impact of solid-waste management in Umuahia, Abia State, Nigeria. They gave an overview of the various management practices and the necessary rules for achieving a sound management with a population of about 1.2 million people who produced 250 metric tons of waste in 2005 and 350 metric tons of waste in 2007 daily. The study revealed that (80.0 %) of the solid wastes was generated from market traders consisting of mixed wastes containing hazardous and non-hazardous components which are separated, treated, or recycled before disposal by the municipality.

Onwughara et al., (2010) examined the disposal habits, and the environmental impact of solid-waste management in Umuahia, Abia State, Nigeria. They gave an overview of the various management practices and the necessary rules for achieving a sound management with a population of about 1.2 million people who produced 250 metric tons of waste in 2005 and 350 metric tons of waste in 2007 daily. The study revealed that (80.0 %) of the solid wastes was generated from market traders consisting of mixed wastes containing hazardous and non-hazardous components which are separated, treated, or recycled before disposal by the municipality.

The solid-waste generation scenario in Nigeria has been of great concern to the government and waste generations have been known to pose hydra-headed problem beyond the scope of the local and city councils (Awomuti, 2008). The reason is centered on the fact that major streets experience a continual presence of solid waste from varying sources. Although studies have been conducted on various aspects of the phenomena in Nigeria; however, most of the studies are confined to the much larger and older cities, while the situation in smaller and newer cities, which may be experiencing faster urbanization, is being neglected.

4. Solid-Waste Menance in Nigeria

It was observed that residents in many urban areas of Nigeria do not carry out efficient solid- waste management practices. They dispose their waste in burrow pits, road sides, and drainages. This finding is consistent with the work of Ogwueleka (2003) in Nsukka Nigeria, who reported that people dump waste at any vacant plot, public space, and river or burn them in their backyard, thereby polluting the air. Babayemi and Dauda (2009) reported a high waste generation rate in Abeokuta without a corresponding efficient technology to manage the wastes. Nkwocha et al., (2011) assessed the efficiency of solid-waste collection services in Owerri's municipality and found out that the level of efficiency in waste collection was only about 61%; a situation they attributed to a wide range of socio-economic and technical factors. Ogwueleka (2009) also investigated solid-waste management involving nine cities in Nigeria and discovered that a great majority of the total solid wastes generated in the cities are organic in nature and there is gross inefficiency in the solid waste management practically in all the cities. The poor performance was attributed to the inadequate funding, personnel, equipment, and technological constraints. Motorists are frequently seen throwing their refuse on the road as they pass by. The wastes disposed by residents in these manners were not only domestic but include other types such as medical waste which is more hazardous to man. Usually, the sites of disposal were close to the houses and markets where food items were sold. This can increase the risk of contamination of these food items. It could be observed that some residents in Nigeria dump their waste into nearby drainages; around their surroundings which are mostly unattended or throw their garbage on the roadside. This finding agrees with the study of Puopie and Owusu-Ansah (2014); Nabegu (2010). Anyanwu and Adefilia (2014) reported in their work that people have the habit of dumping their refuse within a close range to their residence or where they carry out their daily activities and it accounts for huge heaps of accumulated refuse found along the road-sides, streets, and gutters. This also agrees with the report of Ogbonna et al. (2002); Samuel et al. (2013); Naphtali and Vimtim (2016); Opara et al. (2016); Opara and Uwakwe (2016) that most people dispose their solid waste in any open space which contribute to the improper management of waste. This further explains why people tend to disregard the use of designated official dump-sites and create alternative points. Strict laws against indiscriminate disposal of waste should therefore be enacted and enforced so as to discourage people from such practices

These attitudes lead to the degradation of the environment and create a breeding ground for pathogens which could cause serious health problem. It has been reported that the exposure to poorly disposed food wastes leads to health hazards due to the decaying matter which provides suitable material for harmful insects, rats and other creatures to thrive and rapidly aid the cause and spread of diseases including cholera, diarrhea, dysentery, guinea worm and typhoid fever (Komolafe, 2011). This finding was similar to the documentation by Fafioye and John-Dewole (2013) in their study on the 'Effect of Solid Waste Management on the People of Iseyin Community in Oyo State, Nigeria'. In Nigeria, poorly-disposed waste creates a lot of problems on the roads especially during rainy seasons when drains are blocked thereby hindering the free flow of water which results in waterlogging or the flooding of the roads. This corresponds with the report of Manton et al. (2016).

5. Control of Land Pollution due to Improper Solid-Waste Disposal

According to Egunjobi (2004), in the early times (pre-colonial days) up untill the 1970s, the disposal of refuse and other waste did not pose any significant problems. The population was small and enough land was available for the assimilation of waste. Solid waste has started to constitute a problem with the urban growth. Also, it has resulted partly from the national increase in population and more importantly from immigration. In view of the problems associated with control of land pollution in Nigeria; the following aspects can be determined:

1. Public enlightenment: In Nigeria, public awareness on sustainable waste management is still very poor and the efforts by the agencies to raise the awareness are still very low. Municipal members are not well informed on the adverse effects of the indiscriminate and improper disposal of waste and also the benefits of such act (Abila and Kantola 2013). Fafioye and John-Dewole (2013) reported that the knowledge community occupants have about the environment, waste management and control is inadequate, and accounts for the poor environmental management. Akpala (2006) also reported that the poor attitude towards the keeping and maintenance of hygienic environment stems from the inadequate knowledge of the inhabitants on safe and hygienic waste handling and management. Therefore, in order to curb land pollution due to improper disposal of waste, people should be adequately enlightened.
2. Solid-waste management method: It is include waste minimization, reuse, and recycling before thinking of disposal. Sridhar and Hammed (2014) observed that a school in Abeokuta collected worn out tires and used them as a fence around their playground. Individuals in urban areas should sort items that can be reused before disposing them as waste thereby reducing the volume of solid waste in the environment. Solid wastes that cannot be reused should be sorted and taken to industries for recycling. These recyclable wastes can find their way to big industries. Aluminum can be recycled into cooking pots. Plastic can be transformed into plates, spoons, chairs, and other household materials. Broken bottles can be transformed into usable bottles for industries. Scavengers in the various operating fields can recover both ferrous and non-ferrous metals. Blacksmiths, welders and artisans can recycle these metals for the construction of metal gates and hand-held tools such as cutlasses, hoes, spades and piercing instruments (Nzeadibe and Eziuzor, 2006). In this era of a massive waste generation and diminishing raw materials, reuse and recycling should be encouraged. Recyclable materials can be obtained by local residents or by cart pushers thereby creating jobs for themselves. The activities of the cart pushers are popular among the residents of unserved areas although formal waste-management authorities regard them as illegal (Afon, 2007). However, the public attitude towards informal waste workers is usually negative and is characterized by repression, particularly of the cart pushers and, sometimes, the landfill scavengers (Medina, 2000). These scavengers are primarily waste workers who collect and dispose of household refuse for a fee, from places not served by the formal refuse collection system (Medina, 2005; Afon, 2007). Solid waste that can be recycled is, however, thrown away indiscriminately in most towns. This agrees with the findings of Otitoju (2014) that the solid wastes collected from the streets of Nigerian urban centers are dumped in open dumps without the due recourse of sorting them at sources of waste generation and disposal. Modebe et al. (2009) in their study in Awka Nigeria, showed that most of the households did not recycle their solid waste. Also, Ogwueleka (2003) reported that less than 60% of (MSW) generated is collected in developing countries. However, 60% of waste generated in the households can be recycled, if a proper waste-recycling system is put into place (Nkwocha and Okeoma, 2009; Adogu et al., 2015).

3. Composting: It is a method through which solid waste in Nigeria can be curbed. It is the biological process of breaking up organic waste such as food waste, manure, leaves, grass trimmings, paper worms and general household wastes into an extremely useful humus-like substance by various micro-organisms including bacteria and fungi in the presence of oxygen (Bellamy, 2007). The waste materials generated in Nigeria can be classified as municipal solid waste (MSW) which is a heterogeneous mixture of various kinds of solid wastes including biodegradable food waste and non-biodegradable solid waste such as polythene bags, glass, rags, metal items etc. Most of the wastes are from residential houses that generate majorly all waste food articles, vegetable peelings, fruit peelings etc. These wastes are organic in nature and therefore decompose quickly as such they are good for composting. Manure obtained from the compost is more beneficial to the soil than the inorganic fertilizer. It produces a good yield, lasts longer, softens the soil, and adds vital humus and a natural pesticide for the soil (Ladan, 2014). It is reported in the work of Ladan (2014) that in Katsina metropolis, composting can be a sustainable method of waste management.
4. Management Improvement: Waste management agencies should be headed and administered by professional environmental managers who are well-trained environmental practitioners rather than being politicians who are not adequately knowledgeable about environmental matters. This will facilitate the making of right decisions on waste management (Uwadiegwu and Chukwu, 2013).
5. Strengthening Waste Management Agencies: Strengthening a public waste-management agency requires that the government should be committed to the cleanliness of the town by beefing up the personnel strength of the agency, improving the circulation infrastructure and logistics. These will enable the agency to operate at a high level of efficiency (Uwadiegwu and Chukwu 2013).

6. Challenges of Municipal Solid-Waste Management in Nigeria

The problems affecting municipal solid-waste management in Nigeria are diverse and numerous, and are related to economical, technological, psychological and political aspects in the country. In view of the challenges of municipal solid waste management in Nigeria; the following challenges can be determined:

1. Poor Funding: This is one of the major problems constraining the waste-management sector (Ogu, 2000). The incapability of purchasing new waste-collection trucks, the limited staff, poor vehicle maintenance, unsubsidized waste-storage containers, and the inability to purchase equipment among others are all attributed to the shortage of capital. Actualizing waste-management projects requires a consistent funding to achieve answers to the strategies yet to be implemented (Abila and Kantola 2013). More importantly, economic or financial constraints may result in the populace patronizing cart pushers who are not able to get to the approved designated dump sites where the solid waste are expected to be managed properly (Igbinomwanhia and Ohwovoriole, 2012).
2. Poor Legislation and Implementation of Policy: The constitutional strength of solid-waste management policy is weak and ineffective. Also the implementation of this policy is not monitored adequately. The efforts by state and local environmental protection agencies in Nigeria to completely rid streets and neighborhoods of indiscriminate wastes have not yet achieved the much desired success (Kofoworola, 2007).
3. Cultural Belief: Wastes are viewed as an invaluable and unwanted materials rather than wealth. Wastes are not seen as valuable materials that can be recycled for actual use, material recovery and energy recovery. The value of waste to people enhances the actualization of the process involved in the management of waste (Abila and Kantola, 2013).
4. Urbanization: As a result of urbanization and the rapid population growth in the country, wastes are generated faster than they are collected, transported, and disposed. This problem of urbanization has also complicated the problem of waste management as land becomes scarce, human settlements encroach upon landfill spaces, and government in some cases encourage new development directly on top of operating on recently closed landfills (Ikemike, 2015).
5. Poor management strategies: Waste management in the country is hindered by exhausted waste collection services, and by inadequately managed and uncontrolled dumpsites and the problems are worsening day by day. The effectiveness of waste collection initiated by both the public and private sectors is largely controlled by location, the ability and willingness of the owner of the waste to pay the amount charge (Olukanni and Mnenga, 2015). Most of the times, people are not willing to pay. Most waste in Africa is not collected by municipal collection systems because of poor management, fiscal irresponsibility, equipment failure, or inadequate waste-management budgets (Bartone, 1991; Opara et al., 2016).
6. Population growth: The ever increasing challenges of rapid population growth rate and poor planning, has not only affected solid-waste volume but they also made solid-waste management strategies incapable of keeping pace with the rate of generation. Education, income and socio-economic status are other important factors influencing per-capita solid-waste generation (Abel, 2009).

7. Conclusions

A healthy environment in most places in Nigeria has been compromised by an indiscriminate disposal of solid waste as such, it requires efficient management since solid-waste generation occurs as a result of human activities. The need for an adequate waste-management strategy in any community cannot be overemphasized, because inadequate waste management creates a negative impact on the environment and human health. Solid-waste management in Nigeria can be achieved through public enlightenment, composting, management improvement and strengthening and supporting waste- management agencies. Efficient solid-waste management can, however, be affected by poor funding, poor management strategies, population growth, Poor legislation and implementation of policies. Thus, the goal of the sustenance of a healthy environment requires paying a careful attention to the environment which entails a proper management of solid waste.

8. Recommendations

In view of the problems associated with poor solid-waste management in Nigeria; the following recommendations are made:

1. Public awareness campaigns via electronic and print media, by the chiefs and community leaders, etc. should be launched so as to enlighten the general public regarding the effects of poor waste disposal and the need for effective waste management.
2. The public and private partnership should be highly encouraged to participate in effective solid-waste management for the sustenance of a healthy environment.
3. The government should encourage more research projects in the area of waste management.
4. There should be comprehensive environmental legislation that relates to environmental sanitation offences.
5. There should be adequate and proper town planning for effective solid-waste management for example, there is a big need to provide a good access to roads to ease the evacuation of solid waste from all the nooks and crannies of the town.
6. Solid Waste Management in Nigeria should be the concern of everybody not one agency by itself.
7. There should be provision for sanitary landfill facilities for a proper deposition of solid waste. This will help minimize pests, disease, air pollution, ground and surface water pollution and also improve aesthetic values.

References

Abel, O.A. and Afolabi, O. (2007). Estimating the quantity of solid waste generation in Oyo, Nigeria. Waste Management and Research 25(4): 371-379.

Abel, O.A. (2009). An Analysis of Solid Waste Generation in a Traditional African City: The Example of Ogbomoso, Nigeria. Environment and Urbanization SAGE Journals 19(2): 527-537.

Abila, B. and Kantola, J. (2013). Municipal Solid Waste Management Problems in Nigeria: Evolving Knowledge Management Solution. International Journal of Environmental, Chemical, Ecological, Geological and Geophysical Engineering 7(6): 303-308.

Adedibu, A. A. (2008). Environmental Problems Associated with Urbanization of Rural Areas in Nigeria. Environmental Issues 15:229–235.

Adejobi, O. S. and Olorunnimbe, R. O. (2012). Challenges of Waste Management and Climate Change in Nigeria: Lagos State Metropolis Experience. African Journal of Science and Research 7(1): 346-362.

Adekunle, I. M., Adebola, A. A., Aderonke, K. A., Pius, O. A., Toyin, A. A. (2011). Recycling of organic wastes through composting for land applications: A Nigerian experience. Waste Management Resources 29(6): 582-93.

Adetunji, M.A., Atomode, T.I., Isah, I.O. (2015). Assessment of solid waste management in Lokoja, Nigeria. Jordan Journal of Earth and Environmental Sciences 7(2): 103-108.

Adogu, P.O.U., Uwakwe, K.A., Egenti, N.B., Okwuoha, A.P., Nkwocha, I.B., (2015). Assessment of waste management practices among residents of Owerri Municipal Imo State Nigeria. Journal of Environmental Protection 6(5): 446-456.

Afangideh, A.I., Joseph, K. U., Atu, J. E. (2012): Attitude of urban dwellers to waste disposal and management in Calabar, Nigeria. European Journal of Sustainable Development 1(1): 22-34.

Afon, A.O. (2007). Informal sector initiative in the primary sub-system of urban solid Waste management in Lagos, Nigeria. Habitat International 31(2): 193-204.

Afon, A.O. (2006). Estimating the quantity of solid waste generation in Oyo, Oyo State, Nigeria. Journal of Institute Town Planners 19(1): 49-65.

Agunwamba, J.C., Egbuniwe, N., Ogwueleka, T.C. (2003). Least cost management of solid waste collection. Journal of Solid Waste Technology and Management 29(3): 154-16.

Akinwonmi, A. S., Adzimah, S. K., Karikari, C. M. (2012). Assessment of solid waste management in Tarkwa municipality Ghana: time series approach. Journal of Environment and Earth Science 2(10): 139-147.

Akpala, C. O. (2006). Health Implications of poor urban planning in South-Eastern Nigeria. Journal of Environmental Research and Managements 3(4): 46-51.

Anyanwu, N. C. and Adefila, J. O. (2014). Nature and Management of Solid Waste in Karu Nasarawa State, Nigeria. American International Journal of Contemporary Research 4(11): 149-159.

Awomuti, A. A. (2008). An Analysis of waste generation rate and pattern in Ilorin, Nigeria. Lapai. International Journal of Management and Social Sciences 1(1): 171-183.

Babayemi, J. O. and Dauda, K. T. (2009). Evaluation of solid waste generation, categories and disposal options in developing countries: A case study of Nigeria. Journal of Applied. Science 13(3): 83-88.

Bamgbose, O.A., Arowolo, T.A., Oresanya, O., Yusuf, A.A. (2000). Assessment of urban solid waste management practices in Lagos, Nigeria. African Science 1(1): 23-31.

Bartone, C. R. (1991). Institutional and management approaches to solid waste disposal in large Metropolitan Areas. Waste Management and Research 9 (6): 525-536.

Bassey, B. E., Benka, M. O. Aluyi, H.S.A, (2006). Characterization and management of solid medical wastes in the Federal Capital Territory, Abuja, Nigeria. African Health Sciences 6(1): 58-63.

Bellamy, P. (2007). Academics Dictionary of Environment, Academic Publishers, India: New Delhi, pp. 101.

Dauda, M. and Osita, O. O. (2003). Solid Waste Management and Re-use in Maiduguri, Nigeria: Towards the Millennium Development Goals. 29th WEDC International Conference, Abuja, Nigeria. Pp. 20-23.

Egunjobi, J. K. (2004). Solid waste management in an increasingly urbanized Nigeria. Ado Ekiti, Proceedings of the National Practical Training Workshop.

Ekanem, C.H., Ekanem, H.E., Eyenaka, F.D., Isaiah, E.A. (2013). Zero waste: an innovation for less polluting emission processes, resources management, practices and policies. Mediterranean Journal of Social Sciences 4 (8): 53-64.

Elenwo, E.I. (2015). Solid waste management practices in

Port Harcourt metropolis: problems and prospects. Journal of Geographic Thought and Environmental Studies 13(1): 60-81.

Emelumadu, O. F., Azubike, O. C., Nnebue, C.C., Azubike, N.F., Sidney-Nnebue, N.Q. (2016). Practice, pattern and challenges of solid waste management in Onitsha metropolis, Nigeria. American Journal of Public Health Research 4(1): 16-22.

Ezigbo, C.A. (2012). Management of solid waste in Nigeria challenges and proposed solution. Sacha Journal of Environmental Studies 2 (1): 159-169.

Fafioye, O.O. and John-Dewole, O.O. (2013) A Critical Assessment of Waste Management Problems in Ibadan South-West Local Government Area, Ibadan, Nigeria. Greener Journal of Environmental and Management Studies 2(2): 060-064.

Hammed, T.B., Soyingbe, A.A., Adewole, D.O. (2011). An abattoir waste water management through composting: A case study of Alesinloye waste recycling complex. International Journal of Interdisciplinary Social Sciences 6(2): 67-78.

Igbinomwanhia, D.I. and Ohwovoriole, E.N. (2012). A study of the constraints to residential solid waste management in Benin metropolis, Nigeria. Journal of Emerging Trends in Engineering and Applied Sciences 3(1): 103-107.

Igoni, A. H.,Ayotamuno, M.,Ogaji, S. O. T, Probert, S. D. (2007).Municipal solid waste in Port Harcourt, Nigeria. Applied Energy 84(6): 664-670.

Ike, C. C., Ezeibe, C. C., Anijiofor, S. C., Daud, N., Nik, N. (2018) Solid waste management in Nigeria: problems, prospects, and policies. Journal of Solid Waste Technology and Management 44(2): 163-172. DOI: https://doi.org/10.5276/JSWTM.2018.163.

Ikemike, D.O. (2015). Effective Solid Waste Management: A Panacea to Disease Prevention and Healthy Environment in Bayelsa State, Nigeria. International Journal of Academic Research in Education and Review 3(3): 65-75.

Kofoworola, O.F. (2007). Recovery and recycling practices in municipal solid waste management in Lagos, Nigeria. Waste Management 27(9): 1139-1143.

Komolafe, S.F. (2011). Sustainable Solid Waste Management - A Possible Solution to Environmental and Sanitation Problems in the Ancient City of Ibadan, Nigeria. Journal of Environmental Science and Technology 4(2):119-122.

Ladan, S.I. (2014). Composting as a sustainable waste management method in Katsina metropolis, Northern Nigeria. International Journal of Bioscience, Biochemistry and Bioinformatics 4(1):11-13.

Leton, T.G. and Omotosho, O. (2004). Landfill Operations in the Niger Delta Region of Nigeria. Engineering Geology 73(1-2): 171-177.

Manton, D.J. Kigun, P.A. Ogalla, M. (2016). Integrated solid waste management: a palliative to existing waste management challenges in Jabi-District Abuja. Ethiopian Journal of Environmental Studies and Management 9(6): 769-779.

Medina, M. (2000). Scavenger cooperatives in Asia and Latin America. Resources, Conservation and Recycling 31 (1): 51-69.

Medina, M. (2005). Serving the unserved: informal refuse collection in Mexico. Waste Management and Research 23 (5): 390-397.

Modebe, I.A., Onyeonoro, U.U., Ezeama, N.N., Ogbuagu, C.N., Agam, N.E. (2009). Public health implication of household solid waste management In Awka South East Nigeria. The Internet Journal of Public Health 1(1): 1-6.

Momodu, N.S., Dimuna, k. O., Dimuna, J.E. (2011). Mitigating the impacts of solid wastes in Urban Centers in Nigeria. Journals of Human and Ecological Sciences 1(34): 125-133.

Momoh, J.J. and Oladebeye, D. H. (2010). Assessment of awareness, attitude and willingness of people to participate in household solid waste recycling programme in Ado-Ekiti, Nigeria. Journal of Applied Sciences in Environmental Sanitation 5 (1): 93-105.

Mshelia, A.D. (2015). Solid waste management: An urban environmental sanitation problem in Nigeria. Sky Journal of Soil Science and Environmental Management 4(3): 034-039.

Nabegu, A. (2010). An analysis of municipal solid waste in Kano Metropolis. Kamla-Raj Journal of human ecology 31(2): 111-119.

Naphtali, G. and Vimtim, E. (2016). The use of geographic information system in site sustainability analysis for waste disposal in Mubi Town. Sky Journal of Soil Science and Environmental Management 5(2): 026-032.

Nkwocha, E.E. and Okeoma, I.O. (2009). Street littering in Nigeria towns: towards a framework for sustainable urban cleanliness. African research review 3(5): 147-164.

Nkwocha, E. E., Pat-Mbano, E. C., Dike, M. U. (2011). Evaluating the efficiency of solid waste collection services in Owerri municipality, Nigeria. International Journal of Science and Nature 2(1): 89-95.

Nnaji, C. C. (2015). Status of municipal solid waste generation and disposal in Nigeria: Management of Environmental Quality. An International Journal 26(1): 53-71.

Nzeadibe, T. C. and Eziuzor, O. J. (2006). Waste scavenging and recycling in Onitsha urban area, Nigeria. CIWM Scientific and Technical Review 7 (1): 26-31.

Ogbonna, D. N., Ekweozor, I. K. E, Igwe F.U. (2002). Waste management: a tool for Environmental Protection in Nigeria. AMBIO: A Journal of the Human Environment 31(1): 55-57. https://doi.org/10.1579/0044-7447-31.1.55.

Ogu, V.I. (2000). Private sector participation and municipal waste management in Benin City, Nigeria. Environmental and Urbanization 12 (2): 103-117.

Ogwueleka, T. C. (2009). Municipal solid waste characteristics and management in Nigeria. Iranian Journal of Environmental Health Science and Engineering 6(3): 173-180.

Ogwueleka, T.C. (2003). Analysis of urban solid waste in Nsukka, Nigeria. Journal of Solid Waste Technology and Management 29 (4): 239-246.

Okalebo, S. E., Opata, G. P., Mwasi, B. N. (2014). An analysis of the household solid waste generation patterns and prevailing management practices in Eldoret town, Kenya. International Journal of Agricultural Policy and Research 2(2): 76-89.

Okeniyi, J. O. and Anwan, E. U. (2012). Solid wastes generation in Covenant University, Ota, Nigeria: Characterisation and implication for sustainable waste management. Journal of Environmental Science 3(2): 419-424.

Okwesili, J., Chinyere, N., Iroko, N. C. (2016). Urban solid waste management and environmental sustainability in Abakaliki urban, Nigeria. European Scientific Journal 12(23): 155-183.

Olukanni, D. O. and Mnenga, M. U. (2015). Municipal Solid Waste Generation and Characterization: A Case Study of Ota, Nigeria. International Journal of Environmental Science and Toxicology Research 3(1): 1-8.

Olu-Olu, O. and Omotosho, B. J. (2007). Waste Disposal and Waste Management in Ado-Ekiti, Nigeria. The Social Sciences 2(2): 111-115.

Omotosho, O. S. (2005). Nigerian Environmental Issues; A Statistical Approach. Journal of Environmental Research 4(6): 54-59.

Onibokun, A. G. and Kumuyi, A. J. (1996). Urban Poverty in Nigeria: Towards Sustainable Strategies for its Alleviation. Center for African Settlement Studies and Development, Ibadan, Nigeria. CASSAD Monograph Series 10. PP.1-2.

Onwughara, I. N., Nnorom, I. C., Kanno, O. C. (2010). Issues of roadside disposal habit of municipal solid waste: Environmental impacts and implementation of sound management practices in developing country Nigeria. International Journal of Environmental Science 1(5): 409-418.

Opara, J.A. and Uwakwe, F. (2016). Environmental waste management and sustainable development in developing countries. International Journal of Applied Science and Engineering 4(2): 51-60.

Opara, J.A, Akuei, J., Sempewo, J. (2016). Environmental health efficiency and urbanization: The case solid waste management in Bor municipality of South Sudan. International Journal of Bioinformatics and Biological Sciences 4 (1): 19-33.

Oreyomi M.K, (2005). Principles and Practice of Environmental Health. 2nd Ed. Kingston Press.

Otitoju, T. A. (2014). Individual attitude toward recycling of municipal solid waste in Lagos, Nigeria. American Journal of Engineering Research 3(7): 78-88.

Oyelola, O. and Babatunde, A. I. (2008). Characterization of domestic and market solid waste at source in Lagos metropolis, Lagos, Nigeria. African Journal of Environmental Science and Technology 3(12): 430-437.

Oyeniyi, B.A. (2011). "West Management in contemporary Nigeria: the Abuja example". Netherlands. International Journal of Politics and Good Governance 2(22): 1-18.

Puopie, l. F. and Owusu-Ansah, J. (2014). Solid waste management in Ghana: the case of Tamale metropolitan Area. Journal of Environment and Earth Science 4(17): 129-147.

Samuel, E. S., Gemson, G. S., Ezebuiro, V. O. (2013). Attitude of primary healthcare workers towards solid waste management in Taraba State. African Journal of Educational Research and Administration 6(1): 121-129.

Schwarz-Herion, O., Omran, A., Rapp, H. P. (2008). A Case study on successful municipal solid waste management in industrialized countries by the example of Karlsruhe City, Germany. Journal of Engineering Annals 6(3): 266-273.

Sridhar, M. K. C. and Hammed, T. B. (2014). Turning Waste to Wealth in Nigeria: An Overview. Journal Human Ecology 46(2): 195-203.

Uwadiegwu, B. O. and Chukwu, K. E. (2013). Strategies for effective urban solid waste management in Nigeria. European Scientific Journal 9 (8): 297-308.

JJEES

JJEES (2021) 12 (1): 44-49
ISS`N 1995-6681

Jordan Journal of Earth and Environmental Sciences

Assessment of Microorganisms Isolated from Steeping Maize (*Zea mays* L.) and Sorghum (*Sorghum bicolour* L.) on the Hydrolysis of some Hydrocarbon Products

Adewale Olalemi*, Daniel Arotupin, Oluwadamilola Ojuolape, Funso Ogunmolu

Federal University of Technology, Department of Microbiology, Ondo State, Nigeria.

Received 13 July 2020; Accepted 4 September 2020

Abstract

In this work, the degradative ability of microorganisms isolated from steeping maize and sorghum on some hydrocarbon products namely petrol, diesel, engine oil, and kerosene is investigated. The steeping microorganisms were isolated and identified by standard microbiological methods, while its physicochemical parameters were determined. In addition, all the isolates were screened for their ability to utilize some hydrocarbon products. The microbial utilization was monitored by measuring the absorbance of each of the isolates in culture media in which the hydrocarbon products served as carbon sources. The associated bacterial isolates included *Bacillus subtilis*, *Erwinia herbicola* and *Lactobacillus plantarum*, while the fungal isolates were *Aspergillus flavus*, *A. niger*, *A. repens*, *Neurospora crassa*, *Penicillium italicum,* and *Candida krusei*-yeast. The pH values ranged from 4.07 to 5.09 (maize), 4.18 to 5.66 (sorghum); titratable acidity (TTA) ranged from 0.06 to 2.44% (maize), 0.19 to 2.32% (sorghum). Whilst the steeping water turned turbid, the colour of the grains changed from yellow to pale, and from red to brown. All the microbial isolates utilized the hydrocarbon products with the exception of *Erwinia herbicola* on diesel. Therefore, cereals steeping water could be a reservoir of microorganisms with the potential to bioremediate environments polluted with hydrocarbon products.

Keywords: Hydrocarbons, Steeping, Bioremediate, Maize, Sorghum

1. Introduction

Microbial degradation is important in the elimination of spilled petroleum products from the environment. Many bacteria and fungi have been demonstrated to have the ability to degrade specific fractions of petroleum compounds. Mixed cultures of bacteria and fungi have been used to degrade petroleum-derived hydrocarbon mixtures (Diaz et al., 2002), but single cultures of fungi have been found more effective than mixed cultures of bacteria and fungi or using traditional techniques involving bacteria (Okerentugba and Ezeronye, 2003; Ojumu et al., 2004). Fungi digest hydrocarbons through the secretion of extracellular enzymes, and they have the ability to grow in environments with low pH, nutrients and water activity. These group of fungi include *Articulospora, Aspergillus*, *Candida*, *Cladosporium*, *Fusarium*, *Helminthosporium*, *Mucor*, *Penicillium*, *Rhodosporium*, *Saccharomyces*, *Trichoderma*, *Umbelopsis*, *Varicosporium* (Ojumu et al., 2004; Ezeji et al., 2005; Akinyosoye et al., 2011). Bacteria capable of utilizing hydrocarbon compounds as a source of nutrients include *Achromobacter*, *Acinetobacter*, *Arthrobacter*, *Bacillus*, *Brevibacterium*, *Corynbacterium*, *Flavobacterium*, *Micrococcus*, *Pseudomonas* (Ijah and Abioye, 2003; Ojumu et al., 2004; Ojo, 2006; Olalemi and Arotupin, 2012).

Maize (*Zea mays* L.) constitutes a staple food in many parts of the world. In Africa, it has become the most important staple food crop. Maize can be cooked or roasted to become palatable during consumption. Also, it is cooked to be served as a vegetable in side dishes, salads, garnishes as well as cornbread, cornflakes, and other baked products (Nuss and Tanumihardjo, 2010). The flour of maize is common in home cooking and industrialized food products. Maize starch can be hydrolysed and treated enzymatically to produce syrups used as sweeteners, and it may also be fermented and distilled to produce alcohol (Nuss and Tanumihardjo, 2010). The corn steep liquor is the watery by-product of maize wet-milling process and is widely used in the biochemical industry, and in research as a medium for culturing microorganisms. It has been demonstrated to be a potential resource for the bioremediation of soils polluted with hydrocarbon (Salam and Ishaq, 2019).

Sweet sorghum may be used to produce syrups, bread, beverages and ethanol (Nuss and Tanumihardjo, 2010; Maryke, 2010). Fermentation refers to the processes involving the production of ethanol by yeasts or organic acids by lactic acid bacteria. The process is a form of energy-yielding microbial metabolism in which an organic substrate, usually a carbohydrate, is incompletely oxidised and acts as the electron acceptor (Adams, 1990). The fermentation of maize and sorghum grains contribute significantly to food technological processes in most low- and middle-income countries including Nigeria (Inyang and Idoko, 2006; Omemu et al., 2007).

Corresponding author email: waleolas2002@yahoo.com

This study is aimed at determining the degradative ability of microorganisms isolated from steeping maize and sorghum on some hydrocarbon products such as petrol, diesel, engine oil and kerosene. It also aims at isolating and identifying microorganisms associated with fermenting maize and sorghum grains; and determining the ability of the isolates to utilize various hydrocarbon products.

2. Materials and Methods

2.1 Collection of Samples and Fermentation

Maize and sorghum samples were obtained from Oja-Oba in Akure, Ondo State, Nigeria. The samples were transported immediately in sterile black polythene bags to the Microbiology Research Laboratory. Impure grains were sorted and discarded, while the clean and apparently healthy grains were stored at ambient temperature. Fifty grams of each of maize and sorghum were weighed using a weighing balance (Triple beam 700/800 series, 2610g-5lb 2oz capacity) and were poured into a separate clean, sterile fermenter. Approximately, 150 ml of sterile distilled water was poured into each fermenter until the grains were fully submerged. Fermentation of the grains was allowed to take place for a period of seven days under appropriate conditions.

2.2 Determination of pH and Total Titratable Acidity

The pH of the steeping water was determined using Hanna multi-meter instrument (HI 98107). The total titratable acidity (TTA) was determined by titrating 0.1 N sodium hydroxide (NaOH) against 10 ml of steeping water containing three drops of phenolphthalein. The total titratable acidity was calculated and expressed as percentage by multiplying the molarity and volume of NaOH used and dividing it by the volume of the sample. The pH and %TTA were determined daily over the period of seven days

2.3 Enumeration and Identification of Bacterial and Fungal Population

One millilitre each of the steeping water was diluted in a ten-fold serial dilution. An aliquot of 1 ml from the third, fourth, and fifth dilutions was pour-plated with freshly prepared media: Nutrient agar (NA) and Potato Dextrose agar (PDA). The agar plates were incubated at 37°C for twenty-four hours (NA); 25°C for seventy-two hours (PDA) and were observed for growth. The discrete colonies of bacteria and fungi were counted, calculated and expressed as colony-forming units per millilitre (CFU/ml) and spore-forming units per millilitre (SFU/ml) respectively. The isolates were sub-cultured repeatedly to obtain pure isolates, and were characterized using standard microbiological techniques.

2.4 Determination of Rates of Utilization of Refined Petroleum Products by Isolated Bacteria and Fungi

Refined petroleum products including petrol, kerosene, diesel, and engine oil were obtained from Total Petrol Station along Oba Adesida road, Akure, Ondo State, Nigeria. Czapek broth was prepared containing; 3 g $NaNO_3$, 1 g K_4HPO_4, 0.5 g $MgSO_4.7H_2O$, 0.5 g KCl, 0.01 g $FeSO_4.7H_2O$, 1 g peptone and 1000 ml distilled water with 1% refined petroleum product (petrol, diesel, kerosene, engine oil) as the only source of carbon. A positive control was also prepared with 30 g sucrose as the carbon source. The prepared media were inoculated with 0.1 ml of a nutrient broth of twenty-four-hour old cultures of isolated bacteria. The setup was incubated at 30°C for five days. Turbidity produced as a result of bacterial growth was monitored visually on a daily basis and the absorbance reading at 650 nm on UNICO 1100RS spectrophotometer was determined. Similarly, the Czapek agar (20 g agar added to the prepared broth) was inoculated with a 9 mm diameter culture disc of a forty-eight-hour old culture of isolated fungi and was incubated at 30°C for five days. Nutrient utilization was measured by determining the radial diameter of the fungal growth.

2.5 Statistical Analysis

The data obtained were subjected to general descriptive statistics and the single factor analysis of variance (ANOVA), while the significant means were separated with the new Duncan's multiple range test (DMRT) at 5% confidence level (p = 0.05) using Statistical Package for Social Sciences (SPSS) Version 20.

3. Results

3.1 The pH and Total Titratable Acidity of the Steeping Water of Maize and Sorghum

The epicarp of the yellow maize and red sorghum grains was hard before fermentation and the steeping water was clear. As fermentation progressed, the maize turned pale and sorghum turned brown with the epicarp of both grains becoming soft, and the colour of the steeping water turning turbid. The values of pH of the steeping water ranged from 4.07 to 5.09 (maize) and 4.18 to 5.66 (sorghum) (Figure 1). Also, the values of pH decreased steadily as the fermentation progressed, the total titratable acidity (%) increased steadily. TTA ranged from 0.06 to 2.44% (maize) and 0.19 to 2.32% (sorghum) (Figure 2).

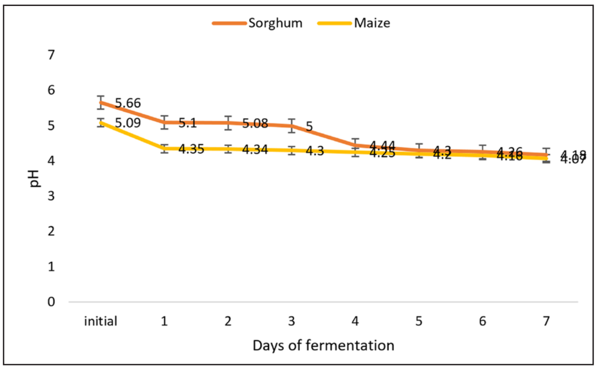

Figure 1. pH of the steeping water of maize and sorghum grains.

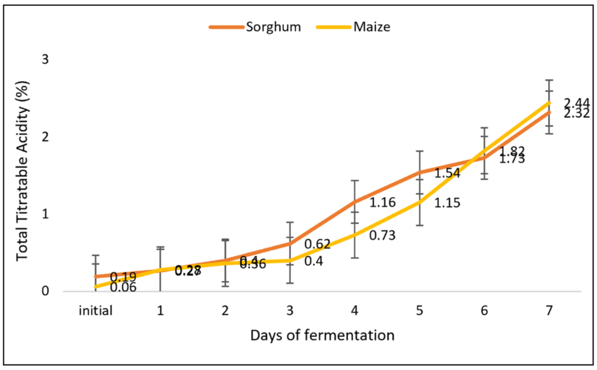

Figure 2. Total titratable acidity (%) of the steeping water of maize and sorghum grains.

3.2 Detection of Bacteria and Fungi in the Steeping Water of Maize and Sorghum Grains

Three bacterial isolates were detected in the steeping water of maize and sorghum. Isolate A was observed to be Gram-positive, motile, spore former, catalase-positive and hydrolysed starch. Isolate B was observed to be Gram-positive, motile, spore former, catalase-positive and does not utilize citrate. Isolate C was observed to be Gram-negative, motile, spore former, catalase-positive and does not produce indole (Table 1). On the basis of these Gharacteristics, isolates A, B, and C were tentatively identified as *Bacillus subtilis*, *Lactobacillus plantarum* and *Erwinia herbicola* respectively. *Bacillus subtilis* (47%) had the highest percentage of occurrence in the steeping water of maize and sorghum, followed by *Lactobacillus plantarum* (41%) and *Erwinia herbicola* (12%) was the least (Table 2). Furthermore, six fungal isolates were detected in the steeping water of maize and sorghum. Based on their morphological characteristics, the isolates were tentatively identified as *Aspergillus flavus*, *A. niger*, *A. repens*, *Candida krusei*, *Neurospora crassa,* and *Penicillium italicum*. Interestingly, *Neurospora crassa* (33%) had the highest percentage of occurrence in the steeping water of maize and sorghum, while *Candida krusei* (5%) had the least (Table 3).

Table 1. Morphological and biochemical characteristics of bacterial isolates from the steeping water of maize and sorghum grains.

Characteristics	Isolates		
	A	B	C
Morphological			
Colour	Creamy	Creamy	Creamy
Surface	Rough	Rough	Rough
Cell shape	Rod	Rod	Rod
Cell arrangement	Pairs	Singly	Singly
Colony morphology	Opaque	Opaque	Opaque
Biochemical			
Gram reaction	+	+	-
Catalase	+	+	+
Motility	+	+	+
Spore	+	+	-
Urease	-	+	-
Oxidase	-	+	-
Indole	+	+	-
Citrate	+	-	+
Hydrogen sulphide	+	+	+
Carbohydrate utilization			
Starch hydrolysis	+	+	-
Glucose	+	+	+
Galactose	+	+	+
Fructose	+	+	+
Maltose	+	+	+
Lactose	-	+	+
Sucrose	+	+	+
Arabinose	+	-	+
Mannitol	+	+	+
Sorbitol	-	-	-

Key: + = Positive; - = Negative; Probable organisms: A – Bacillus subtilis; B – Lactobacillus plantarum; C – Erwinia herbicola

Table 2. Occurrence of bacterial isolates in the steeping water of maize and sorghum.

Isolated bacteria	Maize (n=10)	Sorghum (n=10)	Occurrence (%)
Bacillus subtilis	8	7	47
Erwinia herbicola	3	1	12
Lactobacillus plantarum	5	8	41

Key: Values represent the number of times the bacterial isolates were detected in the samples (n) of the steeping water of maize and sorghum.

Table 2. Occurrence of fungal isolates in the steeping water of maize and sorghum grains.

Isolated fungi	Maize (n=10)	Sorghum (n=10)	Occurrence (%)
Aspergillus flavus	3	5	14
Aspergillus niger	5	4	16
Aspergillus repens	6	7	22
Candida krusei	3	0	5
Neurospora crassa	9	10	33
Penicillium italicum	4	2	10

Key: Values represent the number of times the fungal isolates were detected in the samples (n) of the steeping water of maize and sorghum.

3.3 Utilization of Refined Petroleum Products by Bacterial and Fungal Isolates

The growth of bacterial isolates in media containing refined petroleum products measured at 650 nm absorbance revealed that *Bacillus subtilis*, *Lactobacillus plantarum*, and *Erwinia herbicola* grew heavily in petrol-based media. *Bacillus subtilis* exhibited the highest ability to utilize the refined petroleum products, whereas *Erwinia herbicola* demonstrated the least ability to utilize the products and exhibited no growth in diesel-based media. In addition, all the bacterial isolates exhibited moderate growth in kerosene- and engine oil-based media and minimal growth in diesel-based media. After forty-eight hours, bacterial growth in the control medium containing sucrose declined, whereas growth in media containing refined petroleum products continued even after ninety-six hours (Figure 3).

The growth of fungal isolates measured as radial diameter (cm) in media containing refined petroleum products showed that *Aspergillus flavus*, *A. niger*, *A. repens*, *Candida krusei*, *Neurospora crassa* and *Penicillium italicum* had the ability to utilize the refined petroleum products. Although, at forty-eight hours, the fungal growth in the control medium containing sucrose was greater than that in the media containing refined petroleum products. Generally, *A. flavus*, *A. repens*, *Neurospora crassa* and *Penicillium italicum* exhibited heavy growth in media containing refined petroleum products. Interestingly, *A. flavus* exhibited the highest ability to utilize petrol- and kerosene-based media, while *Neurospora crassa* showed the highest ability to utilize engine oil- and diesel-based media. On the other hand, *A. niger* and *Candida krusei* had a minimal growth in media containing refined petroleum products (Figure 4).

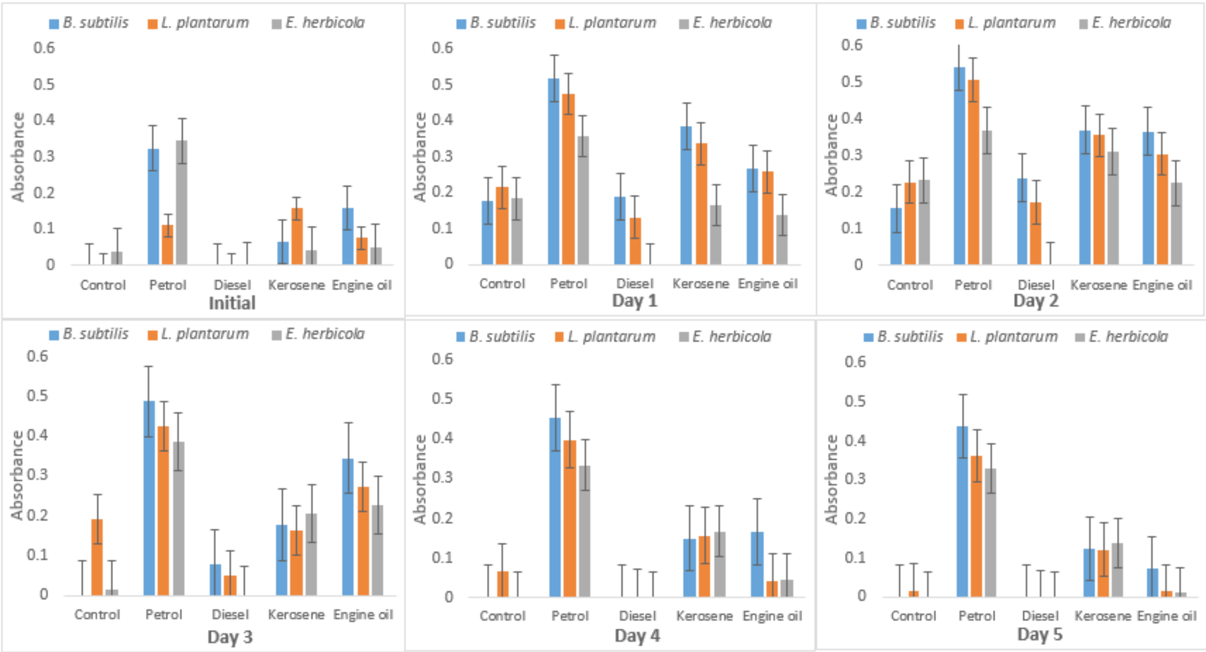

Figure 3. Growth of bacteria in media containing refined petroleum products measured at 650 nm absorbance.

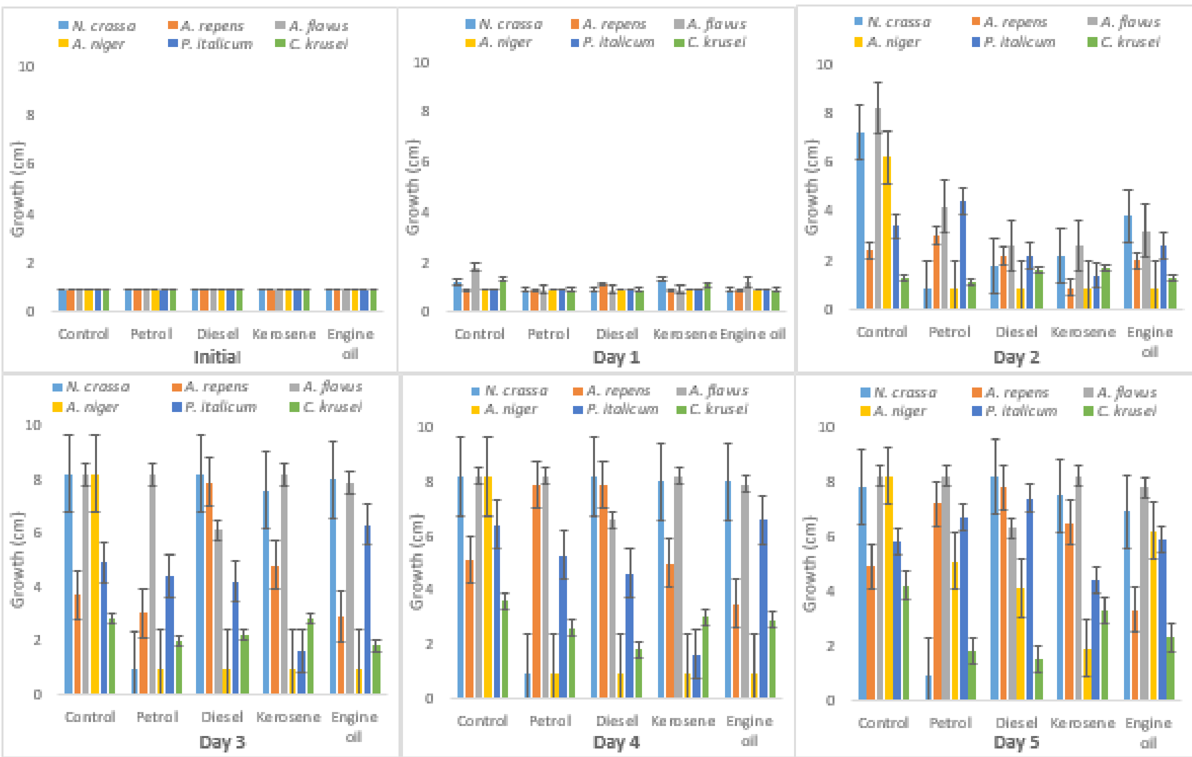

Figure 4. Growth of fungi measured as radial diameter (cm) in media containing refined petroleum products.

4. Discussion

This study investigates microorganisms associated with fermenting maize and sorghum grains. It examines whether their ability to utilize the carbon in some hydrocarbon products (such as petrol, diesel, engine oil and kerosene) as a basic source of carbon for growth may be useful especially for the remediation of environments polluted with refined petroleum products. The pH of the steeping water of maize and sorghum grains decreased steadily, while the total titratable acidity (TTA) increased as the fermentation progressed over the period of study. The decreasing pH and the increasing TTA may be a result of the accelerated growth of lactic acid bacteria in the steeping water. Studies have demonstrated that a decrease in pH and accumulation of lactic acid bacteria are common during the fermentation of foods (Choi et al., 1994; Inyang and Idoko, 2006; Akpinar-Bayizit et al., 2007). The lactic-acid bacteria hydrolyses the starch in the grains to produce acid which eventually reduces the pH and increases the TTA of the steeping water. The decrease in pH gives rise to conditions favourable for the souring of the fermented grains (Akpinar-Bayizit et al., 2007).

In this study, the bacteria detected in the steeping water of maize and sorghum grains were *Bacillus subtilis*, *Lactobacillus plantarum* and *Erwinia herbicola.* Counts of *Lactobacillus plantarum* were moderate at the onset of the fermentation of the grains, but increased as the fermentation progressed. This may likely be a result of acidification in the steeping water. This observation is in agreement with Abegaz (2007) who observed increasing counts of lactic-acid producing bacteria attributed to the acidification of the fermentation medium. However, the decrease in the counts of lactic-acid producing bacteria at the later stages of fermentation may be attributed to the depletion of available nutrients in the cereal slurry (Muyanja et al., 2003). Fungi detected in the steeping water of maize and sorghum were *Aspergillus flavus*, *A. niger*, *A. repens*, *Candida krusei*, *Neurospora crassa* and *Penicillium italicum.* Species of *Aspergillus* and *Penicillium* were eliminated during the early steeping period and after twenty-four hours of fermentation of the grains. This observation may likely be due to the reduction in pH and the acidification of the fermentation medium (Abegaz, 2007).

The rates of utilization of refined petroleum products by *Bacillus subtilis*, *Lactobacillus plantarum* and *Erwinia herbicola* varied. All the bacterial isolates utilized petrol, diesel, engine oil, and kerosene suggesting that the organisms can adapt, survive, and grow easily in the refined petroleum-based medium, except for *Erwinia herbicola* which could not utilize diesel at all. The decline in bacterial growth in the control medium containing sucrose after forty-eight hours may likely be attributed to the exhaustion of carbon and other nutrients necessary for growth. On the other hand, the massive bacterial growth after ninety-six hours in the media containing refined petroleum products may not be unconnected with the high number of carbon atoms per molecule of hydrocarbons in the refined petroleum products (Collins, 2007). In this study, *Bacillus subtilis* exhibited the highest ability to utilize the refined petroleum products and this is in agreement with many studies that have demonstrated the high ability of *Bacillus subtilis* in the degradation of petroleum hydrocarbon (Ijah and Abioye, 2003; Ijah and Antai, 2003; Olalemi and Arotupin, 2012). The findings of this investigation points to *Bacillus subtilis*, *Lactobacillus plantarum* and *Erwinia herbicola* as promising isolates in the clean-up of petroleum hydrocarbon pollutants. The rates of utilization of refined petroleum products by *Aspergillus flavus*, *A. niger*, *A. repens*, *Candida krusei*, *Neurospora crassa* and *Penicillium italicum* were generally high suggesting that hydrocarbons in petroleum products do not resist attack by fungi.

Aspergillus flavus, *A. repens*, *Neurospora crassa* and *Penicillium italicum* exhibited the highest degradative ability as a result of their high cell densities with a concomitant visual increase in the radial diameter of their spread. This observation is in agreement with Ezeji et al. (2005) who reported that the species of *Aspergillus* and *Penicillium* are often implicated in the degradation of petroleum hydrocarbons. These findings suggested that *Aspergillus flavus*, *A. niger*, *A. repens*, *Candida krusei*, *Neurospora crassa*, and *Penicillium italicum* are potential fungi for the degradation of petroleum hydrocarbon products.

5. Conclusions

The findings of this study demonstrate the degradative ability of bacteria (*Bacillus subtilis*, *Lactobacillus plantarum* and *Erwinia herbicola*) and fungi (*Aspergillus flavus*, *A. niger*, *A. repens*, *Candida krusei*, *Neurospora crassa,* and *Penicillium italicum*) isolated from steeping maize and sorghum grains on hydrocarbon products such as petrol, diesel, engine oil and kerosene. Further understanding of this essential low-cost approach and metabolic processes of these organisms on the hydrocarbons would increase the possibilities of developing techniques that may be useful for the remediation of an environment polluted with refined petroleum products.

Acknowledgement:

The authors are grateful to the Department of Microbiology, School of Sciences, Federal University of Technology, Akure, Ondo State, Nigeria for providing a conducive research environment and items used for this study.

References

Abegaz, K. (2007). Isolation, Characterization and Identification of Lactic Acid Bacteria Involved in Traditional Fermentation of Borde, An Ethiopian Cereal Beverage. African Journal of Bacteriology 6: 1469-1478.

Adams, M.R. (1990). Tropical Aspects of Fermented Foods. Trends in Food Science and Technology 1: 141-144.

Akinyosoye, F.A., Arotupin, D.J., Olalemi, A.S. (2011). Effect of Refined Petroleum Products Ccontamination on Fungal Population and Morphology of Cowpea (Vigna unguiculata (L.) walp) Cultivated on Agricultural Soil Sample. Nigerian Journal for Microbiology 25: 2302-2311.

Akpinar-Bayizit, B., Tulay, O., Lutfiye, Y. (2007). Study on the Use of Yoghurt, Whey, Lactic Acid and Starter Culture on Carrot Fermentation. Journal of Food Nutritional Science 57: 147-150.

Choi, S., Beuchart, L.R., Perkins, L.M. and Nakayama, T. (1994). Fermentation and Sensory Characteristics of Kimichi Containing Potassium Chloride as Partial Replacement of Sodium Cchloride. International Journal of Food Microbiology 21: 335-340.

Collins, C. (2007). Implementing Phytoremediation of Petroleum Hydrocarbons. Methods in Biotechnology 23: 99–108.

Diaz, M.P., Boyd, K.G., Grigson, S.J.W., Burgess, J.G. (2002). Biodegradation of Crude Oil across a Wide Range of Salinities by an Extremely Halotolerant Bacterial Consortium MPD- M, Immobilized onto Polypropylene Fibers. Biotechnology and Bioengineering 79: 145-153.

Ezeji, E.U., Anyanwu, B.N., Onyeze, G.O.C. Ibekwe, V.I. (2005). Studies on the Utilization of Petroleum Hydrocarbon by Microorganisms Isolated from Oil – Polluted Soil.

International Journal of Natural Applied Science 1: 122–128.

Ijah, U.J.J. and Abioye, O.P. (2003). Assessment of Physicochemical and Microbiological Properties of Soil 30 Months after Kerosene Spill. Journal of Research in Science and Management 1(1): 24–30.

Ijah, U.J.J. and Antai, S.P. (2003). Removal of Nigerian Light Crude Oil in Soil over a 12- Month Period. International Bioremediation and Biodegradation 51: 93-99.

Inyang, C.U. and Idoko, C.A. (2006). Assessment of the

Quality of 'Ogi' made from Malted Millet. African Journal of Biotechnology 5: 2334-2337.

Maryke, L. (2010). Ecogeographical Distribution of Wild, Weedy and Cultivated Sorghum biocolor (l.) Moench in Kenya: Implications for Conservation and Crop-to-Wild Gene Flow.

Genetic Resources and Crop Evolution 57: 243-253.

Muyanja, C.M., Narvhus, J.A., Treimo, J., Langsrud, T. (2003). Isolation, Characterization and Identification of Lactic Acid Bacteria from Bushera, A Ugandan Traditional Fermented Beverage. International Journal of Food Microbiology 80: 201-210.

Nuss, E.T. and Tanumihardjo, S.A. (2010). Maize: A Paramount Staple Crop in the Context Of Global Nutrition. Comprehensive Reviews in Food Science and Food Safety 9: 417-436.

Ojo, O.A. (2006). Petroleum-Hydrocarbon Utilization by Native Bacterial Population from a Wastewater Canal in Southwest Nigeria. African Journal of Biotechnology 5: 333-337.

Ojumu, T.V., Bellow, O.O., Sonibare, J. (2004). Evaluation of Microbial System for Bioremediation of Petroleum Refinery Effluent in Nigeria. African Journal of Biotechnology 4: 31-35.

Okerentugba, P.O. and Ezeronye, O.U. (2003). Petroleum Degrading Potentials of Single and Mixed Microbial Cultures Isolated from Rivers and Refinery Effluent in Nigeria. African Journal of Biotechnology 2: 288-292.

Olalemi, A.S. and Arotupin, D.J. (2012). Effect of Refined Petroleum Products Contamination on Bacterial Population and Physicochemical Characteristics of Cultivated Agricultural Soil. Journal of Microbiology, Biotechnology and Food Science 2: 684-700.

Omemu, A.M., Oyewole, O.B., Bankole, M.O. (2007). Significance of Yeast in the Fermentation of Maize for 'Ogi' Production. Food Microbiology 24: 571-576.

Salam, L.B. and Ishaq, A. (2019). Biostimulation Potentials of Corn Steep Liquor in Enhanced Hydrocarbon Degradation in Chronically Polluted Soil. Biotechnology 9(2): 46. doi: 10.1007/s13205-019-1580-4.

JJEES

JJEES (2021) 12 (1): 50-61
ISS`N 1995-6681

Jordan Journal of Earth and Environmental Sciences

Differential Morphological Growth Responses of *Chromolaena odorata* under Heavy Metal Influence

Gloria Omoregie[1,3*] and Beckley Ikhajiagbe[2,3,4]

[1]Federal University of Petroleum Resources Effurun, Department of Environmental Management and Toxicology, Nigeria.
[2]University of Benin, Department of Plant Biology and Biotechnology, Nigeria
[3]University of Benin, Environmental Biotechnology and Sustainability Research Group, Department of Plant Biology and Biotechnology, Nigeria
[4]University of Benin, Applied Environmental Biosciences and Public Health Research Group, Department of Microbiology, Nigeria

Received 12 January 2020; Accepted 6 September 2020

Abstract

The differential growth responses and morphological changes exhibited by *Chromolaena odorata* in heavy metal-polluted soil were investigated. This was with a view to providing information on the test plant growth adaptation potential during heavy-metal exposure. Fresh- stem cuttings of *C. odorata* were propagated in Manganese, Cadmium, Copper, Lead and Zinc-polluted soils. Heavy-metal (HMs) concentration in soil was based on the respective ecological screening value/benchmark for each metal. The ESV values for the HMs were 50, 4, 100, 50 and 50 mg/kg respectively. Heavy-metal concentrations for the study were 1, 3 and 5 times their respective ESV. The control experiment consisted of plants grown in metal-free soil. The plants were observed for eight months. There was a compensatory growth response of the test plant under heavy-metal exposure. Although growth suppression in some plant parameters occurred as a result of heavy-metal exposure, there were enhanced growth responses with regards to some other parameters. Although, plant height was reduced from 132.2 cm in the control plants to 88.21 – 111.4 cm in the heavy metal-exposed plants, there was > 25% increase in the number of leaves of heavy metal-exposed plants compared with the control plants. The plant showed compensatory growth responses necessitated by heavy metals. Generally, significant foliar chlorosis and necrosis, leaf curling and folding, leaf loss/senescence, refoliation capacity and unique patterns of display of foliar scorching were reported. Despite general growth suppression, the capacity of the plant to subsist at heavy metal concentrations five times higher than benchmark values was noted; an indication that the test plant might be tolerant to heavy metals, and can be used for phytoremediation studies.

Keywords: Heavy metals, *Chromolaena odorata*, growth response, morphology, phytoremediation.

1. Introduction

Studies have proved that heavy-metal pollution is gradually becoming an environmental disaster because of the alarming increase of metal presence in our environment. Apparently it devastates the ecosystems and deleteriously affects the health of plants, animals and human beings. Consequently, it is very essential to control metal pollution in our environments and remediate metal-polluted sites. The plant employed for the study was *Chromolaena odorata*; it is an invasive species that belongs to the family *Asteraceae*; its common name is Siam weed genus *Chromolaena* and the species is *odorata*.

Heavy metals (HMs) at polluted environment are introduced by anthropogenic activities such as metal- mine dumps, dumping of high metal contaminants in unsuitably secured landfills, addition of fertilizers to soils, inorganic materials, animal manures, compost, pesticides, bio-solids and atmospheric settlement (Basta et al., 2005; Khan et al., 2008; Cirlakov´a, 2009; Zhang et al., 2010).

In soil, toxic levels of HM can impede normal plant activities, disrupt metabolic processes (Hall, 2002), deterring functional groups of significant cellular molecules (Hossain et al., 2012). Heavy-metal toxicity can interrupt the functionality of pigments or enzymes which are essential biomolecules (Ali et al., 2013), adversely affecting the nature of the cytoplasmic membrane (Farid et al., 2013). This results in the suppression of vital events in plants such as respiration, photosynthesis as well as enzymatic activities (Hossain et al., 2012). Results from several analyses have confirmed that heavy metals can affect productivity level in the soil as well as the ecological geochemistry. In addition, heavy metals are constantly added to soils with the wild rate of Industrialization (Okoye, 1991).

Several processes are accessible for heavy-metal removal from the environment. Examples are chemical, physical and biological processes. Biological processes seem to be more reliable because they are environmentally friendly and retain the quality of environments during and after the remediation process. Moreover, biological methods are cheaper than physical and chemical techniques. Biological remediation of metal uses microorganisms to remediate metal-polluted environments. Plants (phytoremediation) can also do likewise (Petarca and Cioni 2011). An example of such plants is *Chromolaena odorata*. According to Omoregie et al. (2020) *Chromolaena odorata* significantly accumulated heavy

Corresponding author email: omoregie.gloria@fupre.edu.ng

metals in different plant parts (leaves, stem, and roots) with the availability of heavy metal in organic forms, implying that the plant had the capacity for heavy-metal sequestration. In phytoremediation processes, plants are grown to decrease the concentrations of heavy metals in polluted soils to recommendable levels in the environment (Henry, 2000; Zheng et al., 2002). Heavy metals can be transported to the above ground plant parts which are eventually removed when these plants are harvested from the site with traditional remediation practices (Blaylock et al., 1997). However, for a successful phytoremediation, it is necessary to have plants capable of generating high biomass and simultaneously accumulating large levels of pollutants from the soil (Tu et al., 2000; Shen et al., 1997). Previous studies have shown *C. odorata* to be capable of generating high biomass with concomitant capacities for bioaccumulation of large concentrations of heavy metals from the soil (Uyi et al., 2014; Ikhajiagbe, 2016; Ikhajiagbe and Akendolor, 2016; Anoliefo et al., 2017; Omoregie and Ikhajiagbe, 2019).

Chromolaena odorata or siam weed belongs to the Asteraceae family, and it is a recurrent and invasive shrub that is extensively distributed, and is still increasing its range. Being a shrub, sometimes it behaves like a lianascent plant. It has simple leaves lacking stipules and is opposite-decussate. The leaves are rhomboid-ovate to ovate with an acute apex and a cuneate base. Petiole is usually between 1 and 3 cm long, the lamina is between 5 and 14 cm long and between 2.5 and 8 cm wide. The plant grows in a wide range of soil pH (Gareeb, 2007). It spreads and colonizes lands in a short time while resulting in more remediating capacity (Taiwo et al., 2011). Moreover, it flourishes in disturbed areas with suitable light and temperature (Gareeb, 2007).

Different environmental stress conditions are always reflected in plant morphology. The level of concentration of heavy metals in the environment puts fort adverse effect on plants (Gorlach and Gambus, 1992; Obata and Umebayashi, 1997). Plant adaptation to stressed environmental conditions and high-contamination concentrations is a usual occurrence reflected in plant morphology (Nkongolo et al., 2008; Kraner et al., 2010). These changes are critical for understanding plant behavior as a necessary input during the selectivity of plant for specific metal-remediation strategies. The objective of this study is to investigate the plant-growth performance and any morphological changes expressed by *Chromolaena odorata* in heavy-metal polluted soil.

2. Materials and Methods

The study was carried out in a well-ventilated Screen House in the Department of Plant Biology and Biotechnology, University of Benin (Ugbowo Campus), Nigeria. The soils used in the study were top-layered garden soils (0 – 10 cm) previously collected from ten random spots in the Departmental Botanic Garden, and were pooled together to form a composite soil sample and were sun-dried to constant weight. The samples of soil used (an ultisol) were taken to the Lab for the determination of selected physical and chemical characteristics prior to use according to methods described by Bray and Kurtz (1945 a and b); Nelson and Sommers (1982); APHA (1985); Osuji and Nwoye (2007).

In order to determine soil pH, 20ml distilled water was added to 20g of the sieved soil sample and was allowed to stand for thirty minutes. The mixture was intermittently stirred with a glass rod. The pH was determined by inserting the pH meter (Model 238 PHS-3C), and the soil conductivity was read through a hand 239 held conductivity meter (HI 70039P, Hanna Instruments). For determination of total organic carbon (TOC), 2.5 ml of 1N $K_2Cr_2O_7$ solution was added to 0.5g of soil sample in a conical flask and was swirled gently to disperse the sample in the solution. Thereafter, 5 ml concentrated H_2SO_4 was added rapidly, into the flask and swirled gently until the sample and reagents were mixed and were finally swirled vigorously for about a minute. The flask was allowed to stand in a fume cupboard for thirty minutes. Five to ten (5 to 10) drops of the indicator were added and the solution titrated with 0.5N $FeSO_4$ to maroon colour. A blank determination was carried out to standardize the dichromate (Nelson and Sommers, 1982; Osuji and Nwoye, 2007). TOC was calculated as follows:

$$\text{TOC (\%)} = \frac{(\text{meq K2Cr2O7} - \text{meq Fe SO4}) \times 0.003 \times 100 \times 1.3}{\text{Weight of sample (g)}}$$

Where,

meq $K_2Cr_2O_7$ = 1N X 2.5 ml

meq $FeSO_4$ = 0.5 N X Volume of titrant in ml

0.03 = Milliequivalent weight of carbon

1.30 = Correction factor

During the mechanical analysis (particle size distribution) of the soil sample, 100g of soil was weighed out and placed in a one-liter-shaking bottle. To this, 50 ml Calgon solution, 3 ml of N sodium hydroxide and 200 ml of water were added. The mixture was, then, properly shaken for three hours and transferred quantitatively to the mechanical analysis cylinder. The volume was made up to the first (1130 ml.) mark with water. The cylinder was shaken by inverting it a few times, and was later placed on the bench and the time read. After 4.5 min., the hydrometer was inserted, and at after five minutes, the scale was read. Whenever there was more froth on the surface of the liquid, one or two drops of amyl alcohol were added before inserting the hydrometer. The hydrometer was then withdrawn, and the process was repeated five hours later. With 100 g of the soil sample being used for the determination, the results gave directly the percentage silt and clay (1st reading) and clay (2nd reading).

Nitrogen in the soil was determined by Kjeldahl digestion, and the resulting ammonium ion was measured calorimetrically. Elements such as iron and manganese, which may interfere in the alkaline medium during colorimetric determination, were first complexed with sodium potassium tartrate. The Ammonia was determined calorimetrically as the indophenol blue complex by reaction with alkaline sodium phenate and sodium hypochlorite.

For the determination of exchangeable acidity, 50 ml of the M KCI was added to 5 g of soil in a 150 ml plastic bottle, and was then shaken mechanically for one hour. This was filtered using Whatman filter paper No.1 into a 250 ml conical flask. Thereafter three drops of the indicator were then added and titrated against the 0.05 M NaOH until the colorless solution turned to pink. The pink color was neutralized with 0.05 M HCI. Then 10 ml of 1 M NaF was added to restore the pink color. The set up was titrated against 0.05 m HCI until colorless.

Calculations:

Exchange Acidity = 0.05 m x Titre x 20 meq/l00 g soil

$$\mathrm{Al} = \frac{0.05 \text{ m x } 20 \text{ x } 26.98 \text{ meq/l00 g soil}}{8.99}$$

Exchangeable bases (Na, K and Ca) were determined by weighing 5g soil into a plastic bottle. Thereafter, 100 ml of neutral 1 M ammonium acetate was added, and the mixture was shaken mechanically for thirty minutes. and filtered using No. 42 Whatman filter paper, into a 100 ml volumetric flask. This was made up with the acetate to the mark. Then, Na (589-nm wavelength) and K (766.5nm wavelength) were determined with a Flame Photometer, and Ca and Mg by the Atomic Absorption Spectrophotometer.

2.1 Soil Pollution with Metal Samples

Twenty (20) kg of the soil was filled into experimental buckets previously prepared for the study. The soils were polluted with Mn, Cd, Pb, Cu, and Zn in their respective chloride forms. The reported ecological screening values (ESV) of the metals were: 50, 4, 50, 100, and 50 mg/kg respectively (Efroymson et al., 1997). The metals were therefore divided into three concentrations each on the basis of their reported ESV as once, thrice and five times their respective ESVs. Successful soil pollution with the respective metal concentrations was achieved by dissolving each measured quantity in distilled water used to properly irrigate the soil up to its water holding capacity, which was earlier determined to be 190.3 ml/kg soil. The control soil was not amended with metal. The experimental buckets that held the soils were not perforated in order to ensure that the metals did not percolate further into the soil.

2.2 Propagation of Chromolaena odorata

Equal-sized stem cuttings of *C. odarata* (2.0 - 2.3 cm thick; 30 cm long) were obtained from a fallow land near the University of Benin Senior Staff Quarters, Ugbowo, and were propagated vertically into the soil at an angle of 45 degrees, with 15 cm of stem cutting buried into the soil.

2.2.1 Husbandry and Analyses

The plants in experimental bags were constantly weeded, and carefully irrigated every other day with 500 ml of water (pH 6.6 – 6.8) especially during dry and hot days. Care was taken to ensure that loamy soil moisture level was adequate for plant development, following procedures laid out by USDA (1998).

2.2.2 Plant parameters considered

Above- and Below-ground Parameters

The test plants were observed throughout the experiment for some plant-growth parameters including mean plant height which was measured by a tape rule, the number of leaves per plant, leaf length, petiole length, internode, as well as stem girth which was determined by a Vernier caliper. Leaf area was determined using an android application (Leaf-IT) following the methods prescribed by Julian et al. (2017). The below-ground parameters determined were the number of primary root branches and length of main root.

2.2.3 Morphological Stress Responses

Morphological measurements of the plant in response to the experimental conditions were recorded on a periodic basis. Those measurements include the color observations, color, shape, form or the appearance of the leaves and the stem of the plant as well as the positioning of the flowers and nodes. Care was also taken to ensure that the progression of chlorosis was recorded. In this case, whenever chlorosis was noted, the leaf was immediately tagged so that chlorotic progress would be followed up till the leaf became entirely chlorotic. The progress of chlorosis measured in hours was provided. The same procedure was followed to describe the progress of necrosis. The rate at which the plant lost its leaves as well as which portion of the plant lost any leaf was also taken into note. Thereupon, every plant was divided into three major plant-shoot partitions as described by Ikhajiagbe and Guobadia (2016).

According to Ikhajiagbe and Guobadia (2016), the leaves which are located in the plant part from the soil level measuring up till 45 cm above soil level, were said to be in the plant's upper partition (or the old leaves), whereas those within the plant part measuring 45 cm downwards from the apical meristem were said to be in the plant's upper partition (or young leaves). The middle partition in this study referred to the plant part in between the upper and lower partitions. Leaves herein were referred to as the intermediate leaves. Haven followed this demarcation based on partitioning, changes with regard to necrosis, senescence, leaf browning, or any other physical observation, was made and reported on time basis.

Care was taken to ensure that the total number of leaves that folded, curled or showed signs of foraging were taken into consideration and as such were counted and presented as the percentage of the total number of leaves that appeared in the plant at any given time. These were therefore presented in the result sections as the percentage of folded leaves, the percentage of curled leaves as well as the severity of leaf foraging. For the latter, a severity score chart was developed. For a severity score of 5, it implied that more than 20% of plant total leaves showed signs of foraging. A severity score of 4 meant that 10 – 20% of plant total leaves showed signs of foraging. A 5 – 10% occurrence equaled a severity score of 3. A severity score of 2 meant that 1 – 5% of the plant total leaves showed signs of foraging. When there were no signs of foraging, a severity score of zero sufficed.

2.2.4 Refoliation

In the present study, because it was possible that when plants lost their leaves, they refoliated, the researcher decided to tag defoliated nodes and followed up with the time in hours taken for every defoliated node to eventually regrow. Therefore, refoliation percentage or recovery percentage as herein referred to was presented in the result section to mean the time in hours taken between defoliation of a node and the re-emergence of a bud at the node position.

2.2.5 Progression of Necrosis and Chlorosis

In order to appreciate the presentation of chlorotic and necrotic symptoms in treated and control plants, the total number of leaves, that showed both chlorotic and necrotic symptoms, was counted on a weekly basis. And then presented as graphs.

2.2.6 Statistical Analyses

A complete randomized experimental design was adopted for the study. A single-factor analysis of variances (ANOVA) was used to analyse data having assumed the homogeneity of the entire experimental plot when soils were pooled before use. Least significant differences (LSD) were used to separate treatment means at a 95% confidence limit. Statistical analyses were performed using the SPSS® version 23 as well as the PAST® version 2.17c according to Hammer et al. (2001) where necessary.

3. Results

The physical and chemical properties of the soil before pollution are presented in Table 1.

Table 1. Physical and chemical properties of soil before pollution. These are background mean concentrations (n = 5), (mean±S.E.M).

Parameters	Mean (n = 5)
Ph	5.97 ± 0.67
Electric conductivity (µs/cm)	301.21 ± 23.01
Total organic carbon (%)	0.49 ± 0.09
Total Nitrogen (%)	4.18± 1.06
Exchangeable acidity (meq/100g)	0.22 ± 0.08
Na (meq/100g)	10.90 ± 2.11
K (meq/100g)	1.48 ± 0.62
Ca (meq/100g)	14.32 ± 3.10
Mg (meq/100g)	12.01 ± 3.22
NO^-_2 (mg/kg)	164.34 ± 23.03
NO^-_3 (mg/kg)	286.16 ± 18.16
Soil texture	
Clay (%)	5.43 ± 0.88
Silt (%)	7.36 ± 1.74
Sand (%)	84.81 ± 12.12
Heavy metals	
Fe (mg/kg)	1011.92 ± 73.38
Cd (mg/kg)	<0.001
Mn (mg/kg)	17.03 ±3.22
Pb (mg/kg)	0.03 ± 0.01
Cu (mg/kg)	3.93 ± 0.01
Zn (mg/kg)	30.12 ± 3.06

The impact of heavy metals on the selected above-ground parameters of *Chromolaena odorata* after six months of planting and the application of treatment showed highly significant changes in the average plant height as well as the number of plant root (P<0.01) (Table 2). In regard to plant height, there were significant decreases compared to the control. Although plant height in the control was 142.2 cm in the Mn-exposed plant, it ranged from 84.44 to110.30 cm. Similarly, in the Cu-exposed plants, the highest plant height was obtained in Cu +1ESV (ht = 98.43cm). There was a significant increase in the number of leaves per plant in the metal-exposed plants when compared to the control. As for leaf length, there were no significant changes in the number of leaves per plant in both control and metal-exposed plants, although these changes differed among metals. For example, increases were recorded for Cu-exposed plants but not recorded for Pb, Zn, and Cd-exposed plants. Leaf length ranged from 5.21 to 7.85 cm. There were significant changes in leaf area when compared between control and metal-exposed plants. Leaf area in the control plant was 18.87cm. This significantly increased in Mn-exposed plants (21.49 to 23.96 cm^2) as well as in Zn-exposed plant (18.89 to 23.32cm^2). The changes in Pb Cu and Cd-exposed plant were minimal (P>0.05). There were significant changes in the average number of primary branches by plant as affected by Cd. However, changes were only minimal (P>0.05) in pants exposed to Pb, Mn, and Cu.

As presented in Table 3, the percentage of foliar folding ranged from 3.8 – 9.4 % (p>0.05) in both experiments and control plants in the upper-plant partition. Although foliar folding was not reported in the control plants, as well as in Mn and Pb-exposed plants, over 5 % of the leaves of the Cu and Zn-exposed plants showed signs of foliar folding. These folded leaves eventually recovered from this folding characteristic. There was no evidence of foliar folding at the lower-plant portions. Leaves of the upper partition were more curled (< 53 %) than those of the intermediate partition (< 36 %). Leaves of the Cd-exposed plants were more curled (16.6 – 36.3 %); Mn-exposed leaves (11.5 – 25 %). The results eventually showed that leaves in the upper partition of both control and HM-exposed plants lost less than 10 % of foliage to the foragers. The least foraging occurred in the older plant partition.

Generally, all plants showed signs of curling. However, most of the curled cleaves in both control and metal-affected plants recovered from the curling anomaly, herein referred to as recovery time. Plants therefore differed significantly in their recovery period (Figure 1). All curled leaves recovered from the anomaly within twelve days, which was not statistically different from the control implying that these heavy metals may not have accelerated foliar curling. However, Cd-exposed leaves showed a significant delay (p < 0.05) (< 19 days).

Some morphological disposition of the leaves of the metal-exposed plants showed somewhat similar manifestations of metal toxicity. In the Mn-exposed leaves, these appeared first on the leaf's left margin and on the right (but not always prominent), and it progressed throughout the entire leaf (Figure 2). Cu-exposed leaves predominantly showed foliar scorching beginning from the lower right margin of the leaf (Figure 3), whereas in the Pb-exposed leaf, scorching progressed mainly from the upper right margin of the leaf (Figure 4). Scorching in the Zn-exposed leaves progressed from the left leaf margin (Figure 5), whereas for the Cd-exposed leaves, burning was mainly restricted to foliar tips (Figure 6).

Table 2. Effects of treatment on above-ground parameters of the test plant after 6 months of sowing.

Treatment	Average Plant height(cm)	*No. of Leaves/ Plant	Leaf length (cm)	Leaf Area (cm^2)	Petiole length (cm)	Internodal distance (cm)	*No. of primary nodes	*Average No of pry. Branches	Stem girth (mm)
Control	142.2±1.00	252±10	5.71±1.2	18.87±0.51	2.01±0.11	8.02±0.03	4±0	7±0	23.01±1.00
Mn+1ESV	84.44±1.10	261±10	5.52±1.5	21.49±0.82	1.82±1.00	7.92±1.59	4±1	5±0	23.02±1.00
Mn+3ESV	100.1±1.40	240±11	5.45±0.5	21.96±2.40	2.03±1.00	9.31±0.53	3±1	7±1	12.03±1.01
Mn+5ESV	110.3±1.05	256±11	7.33±0.64	23.96±3.68	1.84±1.13	7.73±1.28	2±1	6±1	20.04±0.12
Cd+1ESV	112.2±1.00	295±14	6.85±0.7	21.92±1.45	2.03±1.1	6.42±0.72	3±0	8±1	18.01±0.99
Cd+3ESV	103.1±3.50	303±13	5.55±0.11	18.45±1.34	2.04±.056	7.82±0.31	4±0	8±1	22.51±0.56
Cd+5ESV	110.3±1.20	274±14	5.82±0.51	17.71±1.11	1.82±0.62	7.61±0.67	3±1	9±0	23.02±0.44
Pb+1ESV	104.2±0.5	268±5	5.05±0.68	16.74±1.35	1.82±0.77	7.04±0.06	3±0	5±0	17.01±1.0
Pb+3ESV	79.12±1.52	359±6	6.65±0.71	17.93±2.40	1.81±0.56	7.52±0.90	3±1	6±0	17.04±1.00
Pb+5ESV	85.33±1.95	285±5	5.55±0.4	24.80±5.20	2.01±0.88	9.01±0.09	4±1	5±0	20.03±2.12
Cu+1ESV	98.43±1.01	319±8	7.85±0.70	20.41±3.4	2.53±0.10	8.02±0.34	4±1	5±1	17.03±0.97
Cu+3ESV	93.22±0.61	297±11	6.75±0.41	19.88±4.2	2.51±0.94	6.53±0.36	3±1	6±0	18.51±0.34
Cu+5ESV	87.43±0.88	335±12	6.65±0.18	16.21±3.4	2.04±0.33	7.21±0.93	4±1	5±1	15.02±0.12
Zn+1ESV	88.21±0.98	298±13	5.12±0.46	18.89±1.56	1.83±0.92	7.54±0.06	4±0	6±1	20.03±0.01
Zn+3ESV	111.4±0.91	248±11	5.15±0.45	23.32±1.30	1.84±0.12	8.93±0.41	3±0	4±0	20.04±1.00
Zn+5ESV	96.22±0.10	313±17	5.21±0.50	23.32±1.32	2.51±0.23	9.72±0.55	3±1	6±1	21.02±0.55
p-values	0.000	0.000	0.091	0.042	0.075	0.001	0.021	0.018	0.031
LSD(0.05)	16.3	11.7	2.66	2.46	1.66	2.00	1.6	1.67	2.60

**Expressed to the nearest integer. **Results expressed as Mean ± SEM 0.05*

Table 3. Foliar morphological changes during 10 – 25-week periods of *Chromolaena odorata* growth.

Conc. of contaminant in soil	Percentage of folded leaves			Percentage of curled leaves			Severity of foraging signs on leaves (see severity score key)		
	UP	IP	OP	UP	IP	OP	UP	IP	OP
Control	4.0±0.2	0.0±0.0	0.00	0.79±1.3	0.0±0.0	0.0±0.0	3.22±1.20	3.61±0.38	0.21±0.05
Mn+1ESV	0.38±0.1	0.0±0.0	0.00	0.77±3.1	1.15±1.9	0.0±0.0	3.83±1.21	3.22±1.50	0.12±0.55
Mn+3ESV	0.83±0.7	0.0±0.0	0.00	4.17±13.4	2.50±5.5	0.06±0.04	0.63±0.11	1.24±1.00	0.02±1.51
Mn+5ESV	0.44±0.2	0.0±0.0	0.00	0.88±4.2	0.44±1.1	0.0±0.0	0.94±0.11	0.24±0.01	0.23±0.04
Cd+1ESV	0.52±1.4	0.0±0.0	0.00	5.42±2.4	1.69±1.6	0.08±0.07	0.11±0.21	0.73±0.94	0.14±0.02
Cd+3ESV	0.66±0.9	0.0±0.0	0.00	1.65±9.1	0.66±2.5	0.0±0.0	3.23±2.20	3.61±0.88	0.12±0.02
Cd+5ESV	0.72±0.4	0.36±0.9	0.00	7.30±6.5	0.36±7.1	0.0±0.0	3.42±2.1	2.51±1.56	0.03±0.21
Pb+1ESV	0.75±1.2	0.0±0.0	0.00	0.75±5.2	0.61±0.3	0.0±0.0	3.44±2.54	3.34±2.10	0.44±0.00
Pb+3ESV	0.84±0.2	0.0±0.0	0.00	2.79±9.8	1.11 ±2.8	0.0±0.0	3.04±1.11	3.64±0.31	0.12±0.00
Pb+5ESV	0.85±0.2	0.0±0.0	0.00	2.98±12.2	1.28±4.3	0.0±0.0	3.23±1.23	2.12±0.57	0.01±0.00
Cu+1ESV	0.94±0.3	0.0±0.0	0.00	1.25±9.9	0.31±0.3	0.0±0.0	3.31±2.11	3.14±2.10	0.01±0.00
Cu+3ESV	0.63±0.1	0.51±1.8	0.00	0.40±4.2	0.64±1.1	0.0±0.0	2.34±1.56	2.42±0.11	0.01±0.00
Cu+5ESV	0.00±0.0	0.60±3.1	0.00	00.0±0.0	0.84±0.0	0.0±0.0	0.82±0.01	0.03±0.00	0.13±0.01
Zn+1ESV	1.01±0.8	0.75±0.8	0.00	2.013±9.3	0.0±0.0	0.0±0.0	3.23±2.1	3.22±1.48	0.24±0.12
Zn+3ESV	0.81±0.8	0.90±0.6	0.00	2.82±12.3	0.0±0.0	0.0±0.0	2.81±1.45	2.51±0.80	0.02±0.01
Zn+5ESV	1.60±9.0	0.64±1.2	0.00	0.96±5.4	0.0±0.0	0.0±0.0	2.74±1.3	2.12±1.50	0.03±0.01
Significance	P>0.05	P<0.05	NA	P<0.05	P<0.05	P>0.05	P<0.05	P<0.05	P>0.05
(LSD (0.05)	8.3	0.42	NA	11.7	9.8	NA	0.67	0.51	0.11

** Mean ± S.EM 0.05*

Key:
Foliar partitions - UP Upper foliar partition, IP intermediate partition, OP older leaf partition

Percentage of plant total leaves showing signs of foraging	Severity score	Percentage of plant total leaves showing signs of foraging	Severity score
>20%	5	1 – 5%	2
10 - 20 %	4	<1%	1
5 - 10%	3	None	0

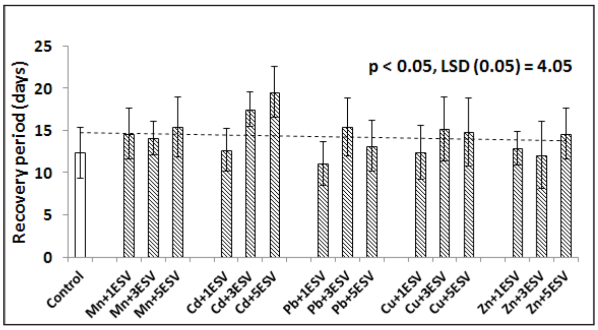

Figure 1. Period required for foliar recovery from curled symptoms.

Figure 2. Presentation of foliar scorching in Mn-exposed leaves.

Figure 3. Cu-exposed leaves showing scorching symptoms.

Figure 4. Pb-exposed leaves presenting position of scorching in leaves.

Figure 5. Scorching in Zn-exposed leaves.

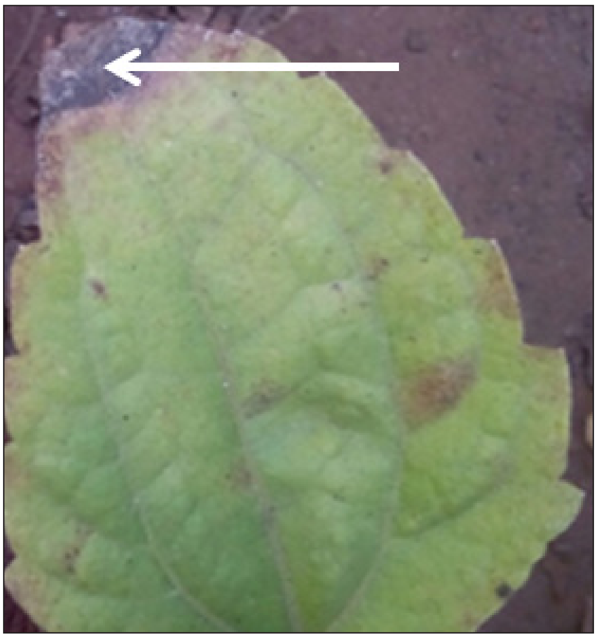

Figure 5. Scorching in Zn-exposed leaves.

Table 4 presents the percentage of chlorosis and necrosis after three months of exposure to heavy metals. The results show that chlorosis and necrosis were significantly elevated by the HM presence in the soil. This incident was mostly pronounced in the plant's lower partition, where older leaves usually existed (13 – 30 %), compared to both intermediate (3 – 14 %) and upper-plant partitions (1 – 6 %) respectively in that order. There was neither chlorosis nor necrosis at the upper-plant partition. The results also showed that the occurrence of chlorosis in the control plant were on the sixth day (Table 4), whereas necrosis occurred two days later. Generally, as observed, foliar necrosis usually occurred two days following the confirmation of foliar chlorosis (Table 4).

Table 4. Percentage of Chlorosis and necrosis 3 months after sowing according to foliar partitions. (Mean ± SEM).

Conc. of contaminant in soil	Plant partition/Chlorisis (%)			Total necrotic leaves (%)	Chlorosis period (days)	Necrosis period (days)
	Lower	Middle	Upper			
Control	9.09±0.15	3.64±0.55	0±0.00	11.92±4.72	6.32±2.22	8.12±٤,٠٠
Mn+1ESV	19.61±4.42	7.84±1.45	3.92±1.16	29.86±2.89	4.14±1.09	6.03±3.91
Mn+3ESV	31.25±2.16	10.42±4.27	4.17±1.23	43.18±5.27	4.21±1.34	6.41±3.88
Mn+5ESV	23.07±5.31	9.62±0.60	1.92±0.08	35.02±8.67	4.33±1.54	6.04±3.92
Cd+1ESV	16.67±2.88	6.67±2.89	0±0.92	24.11±5.16	4.43±1.87	5.22±2.27
Cd+3ESV	29.09±8.67	5.45±0.77	3.64±1.29	37.63±3.15	4.22±1.67	5.31±2.91
Cd+5ESV	17.31±2.67	3.85±0.75	1.92±0.98	24.16±9.87	3.02±0.85	5.42±2.99
Pb+1ESV	21.82±3.15	7.27±2.36	0.00±0.00	27.11±8.67	4.33±1.99	6.13±3.92
Pb+3ESV	22.95±5.10	14.75±0.45	0.00±0.00	32.88±1.21	4.14±1.21	5.22±3.27
Pb+5ESV	20.41±3.09	10.26±5.51	6.12±2.08	33.02±5.59	4.43±1.71	6.31±3.81
Cu+1ESV	24.56±5.05	8.77±3.64	0±0.00	31.66±0.57	5.11±2.00	7.41±4.02
Cu+3ESV	22.60±6.05	7.55±2.50	3.77±2.21	33.03±1.39	4.24±1.77	6.04±4.22
Cu+5ESV	16.18±2.04	2.94±0.91	2.94±1.19	21.67±0.10	5.03±3.21	7.12±4.19
Zn+1ESV	15.87±1.50	3.17±0.29	1.59±0.54	19.18±1.09	5.01±3.49	6.33±4.71
Zn+3ESV	13.79±4.32	8.62±1.51	3.45±2.12	24.93±5.21	3.24±2.10	5.24±4.53
Zn+5ESV	13.73±4.41	9.83±0.29	1.96±1.23	26.81±5.07	4.11±2.72	6.03±5.23
Significance	0.018	0.024	0.015	0.000	0.029	0.038
(LSD(0.05)	7.2	6.12	3.24	8.63	1.17	2.26

Table 4. Percentage of Chlorosis and necrosis 3 months after sowing according to foliar partitions. (Mean ± SEM).

After six months, the presentation of chlorosis and necrosis was similar to that presented after three months (Table 4). Although the occurrence of both chlorosis and necrosis was enhanced by HM- pollution, the percentage of total plant leaves reported to be chlorotic during the sixth month was less compared to the results obtained during the third month (Tables 4 and 5); whereas 2.19 % of the lower-partition control-plant leaves were chlorotic, 3.39 – 12.56 % of the same leaves were chlorotic when-exposed to HM. The most prominent region of necrosis occurrence is reported in Table 5. In the control, this was observed as burning patches, which expanded to occupy the entire leaf. However, for the Cd-exposed leaves, necrosis was observed to spread from leaf tips, and it was accompanied by similar burning patches. In the Zn-exposed plants, foliar necrosis was mainly restricted to the left leaf margin.

Figure 7 presents the percentage of leaf senescence six months after sowing. A significantly higher percentage of the HM-exposed leaves detached from the parent plant, compared to the control. Cd-exposed leaves were the most senesced (4.63 – 16.74 %), compared to 5.45 % reported for the control leaves (Figure 7).

The time taken for refoliation of defoliated nodes is provided in Figure 8. It took ninety-three hours for the control plants to produce leaves at defoliated nodes. However, this refoliation time delayed when the plant was-exposed to Cd (123 hrs.).

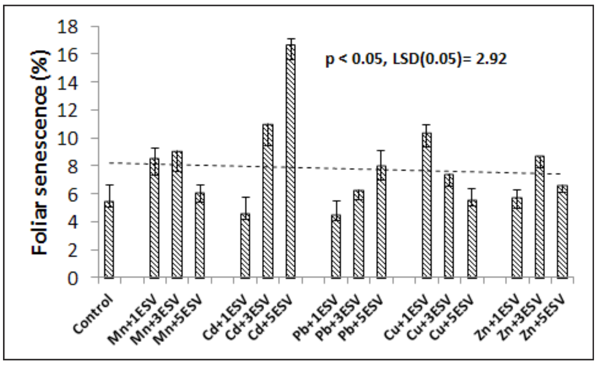

Figure 7. Percentage of leaf senescence 6 months after sowing.

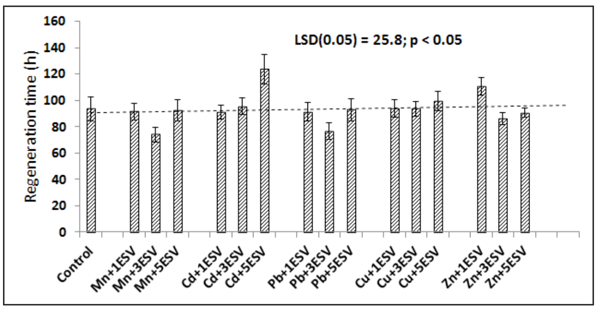

Figure 8. Time taken for the replacement of a new leaf from a defoliated node during the post-flowering period of plant development.

Table 5. Percentage of chlorosis and necrosis 6 months after sowing according to foliar partitions. (Mean ± S.E.M).

Conc. of contaminant in soil	Plant partition/Chlorosis			Total necrotic leaves (%)	Chlorosis period (days)	Necrosis period (days)	Most prominent region of necrosis
	Lower	Middle	Upper				
Control	2.19±0.32	3.17±0.29	2.35±0.60	8.71±1.45	7.05±1.23	9.12±3.23	Burning patches, expands to occupy entire leaf
Mn+1ESV	5.81±1.40	3.75±1.29	1.53±1.29	11.09±2.60	5.25±2.12	7.32±0.22	Similar to control, marginal and patches
Mn+3ESV	8.03±1.47	4.02±0.03	0.81±0.53	11.68±3.40	5.05±2.12	7.33±3.34	
Mn+5ESV	8.31±0.31	5.54±0.93	1.33±0.54	14.02±1.45	5.23±2.34	8.12±4.34	
Cd+1ESV	7.79±0.41	5.08±0.13	2.03±0.05	13.96±3.60	4.31±1.23	5.44±0.23	Spread from leaf tips accompanied with similar burning patches
Cd+3ESV	6.62±1.54	3.96±0.06	0.33±0.05	11.01±1.45	4.31±2.34	6.02±1.11	
Cd+5ESV	8.28±0.05	4.38±0.65	0.36±0.05	13.62±1.12	4.22±3.23	5.11±0.12	
Pb+1ESV	8.58±1.72	5.62±1.07	2.24±0.41	15.69±4.60	4.14±1.20	6.32±3.23	Progression from the right leaf margin inwards
Pb+3ESV	8.62±1.45	2.51±0.88	1.00±0.06	11.92±0.56	5.41±3.65	7.22±0.09	
Pb+5ESV	11.49±1.69	8.09±0.15	3.41±0.71	22.98±7.89	4.01±2.00	6.33±2.76	
Cu+1ESV	3.39±0.90	2.19±0.32	0.94±0.91	8.12±0.33	4.22±1.02	7.24±1.23	Progression from the right leaf margin inwards
Cu+3ESV	6.07±1.12	4.86±1.48	0.81±0.05	11.42±2.11	6.03±4.77	8.22±2.12	
Cu+5ESV	8.28±0.46	2.69±1.19	0.33±0.05	10.63±1.90	5.44±2.4	8.11±0.12	
Zn+1ESV	4.69±0.10	4.36±0.62	1.00±0.73	9.06±1.99	4.22±1.90	6.41±0.34	Majorly restricted to the left leaf margin
Zn+3ESV	8.87±0.90	4.34±0.58	0.81±1.12	13.99±2.45	4.11±2.16	7.22±2.23	
Zn+5ESV	12.56±0.05	2.88±1.54	1.64±0.11	16.42.03±3.35	4.23±2.47	7.32±4.33	
Significance	0.031	0.027	0.018	0.029	0.033	0.028	NA
LSD(0.05)	1.63	1.43	1.10	3.06	0.55	2.57	NA

** Results above are for chlorosis, but as observed herein, all chlorotic leaves turned necrotic*

Table 6 shows bivariate correlation among the selected morphological characteristics of the test plant. Plant leaf number negatively correlated with the percentage of foliar chlorosis/necrosis; implying therefore that a reduction in plant leaves may have been a result of the former (r = 0.66, p<0.01). The percentage of the occurrence of chlorosis was significantly correlated with the occurrence of necrosis (r = 1.00, p<0.01); indicating that nearly every chlorotic leaf turned necrotic.

Table 6. Bivariate correlation among selected morphological characteristics of the test plant.

	PLHT	NLVS	LVA	NCR	CHL	RCV	SEN	REGT	RTBR
PLHT	1	-0.22	-0.08	-0.02	-0.02	0.017	0.172	0.129	0.406
NLVS	-0.224	1	-0.52*	-0.66**	-0.66**	0.207	-0.07	0.028	-0.1
LVA	-0.076	-0.52	1	0.469*	0.469*	0.074	0.259	-0.34	0.153
NCR	-0.015	-0.66**	0.469*	1	1	-0.22	0.085	-0.19	0.099
CHL	-0.016	-0.66**	0.469*	1**	1	-0.22	0.085	-0.19	0.099
RCV	0.0165	0.207	0.074	-0.22	-0.22	1	0.355	-0.35	0.117
SEN	0.1721	-0.07	0.259	0.085	0.085	0.355	1	-0.18	0.316
REGT	0.1289	0.028	-0.34	-0.19	-0.19	-0.35	-0.18	1	0.005
RTBR	0.4059	-0.1	0.153	0.099	0.099	0.117	0.316	0.005	1
RTLN	-0.028	0.038	-0.23	-0.27	-0.27	-0.13	0.027	0.447*	-0.09

**Correlation is significant at 0.05, **Correlation is significant at 0.01*
PLHT - Plant height, NLVS - No of leaves per plant, LVA - Leaf area, NCR - Total foliar percentage necrosis, CHL - Total foliar percentage chlorosis, RCV - Plant recovery from curling, SEN - Incident of Senescence, REGT - Foliar regeneration time, RTBR - No of pry root branches, RTLN - Root length.

Figure 9 shows that the plant characteristics including the number of leaves, chlorosis occurrence, necrosis occurrence, and leaf area were loaded on component 1, and these were basically related to the plant leaf. This implied that the plant leaf was the most disposed factor responsible for determining the effects of HM on morphology. The impact on foliar abundance was mostly associated with copper pollution. With a Kaiser-Meyer-Olkin (KMO) measure of sampling adequacy, being a factor of 0.51 (Figure 9), and a highly significant Bartlett's Test of sphericity (p<.0.01), the results of the Principal component analysis (PCA) was deemed reliable. The results of cluster analyses showed a presentation of two groups; one group was predominantly Mn and Pb, and the other was predominantly Cd and Cu (Figure 10). The control was a standout in the first group with Mn and Pb as predominates. Plant responses in soils polluted with Mn at ecological screening value (ESV) was more closely related to those exposed to soils polluted with Cu at three times the ESV compared to other plants in their respective metal-exposed conditions.

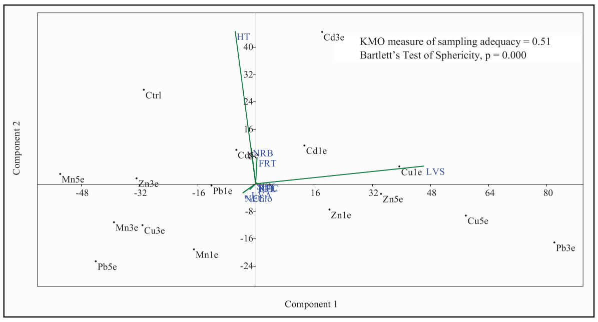

Figure 9. Principal component analysis (PCA) biplot showing association between selected morphological characteristics of the test plant (letters in blue) and their respective soil heavy-metal concentrations (letters in black).

Key:
Soil metal concentrations: Cu1e – plant response in soil polluted with Cu at 1 ESV; Cd3e – plant response in soil polluted with Cd at 3 ESV, Mn5e – plant response in soil polluted with Mn at 5 ESV, respectively and so on.
Plant morphological characteristics: HT - Plant height, NLV - No of leaves per plant, LVA - Leaf area, NEC - Total foliar percentage of necrosis, CHL - Total foliar percentage of chlorosis, REC - Plant recovery from curling, SEN - Incident of Senescence, FRT - Foliar regeneration time, NRB – No. of pry root branches, RTL - Root length.

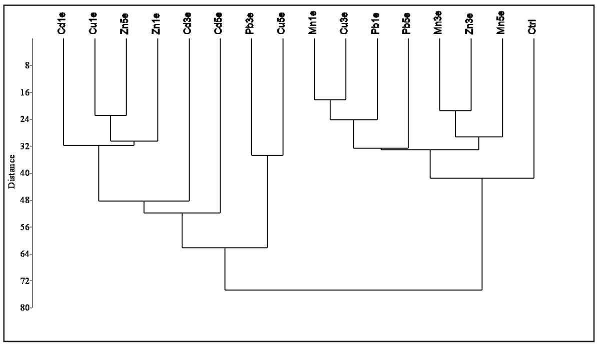

Figure 10. Dendrogram from cluster analyses of showing association among plants exposed to various heavy-metal concentrations.

Key:
Cu1e – Plant response in soil polluted with Cu at 1 ESV; Cd3e – plant response in soil polluted with Cd at 3 ESV, Mn5e – plant response in soil polluted with Mn at 5 ESV, respectively and so on.

4. Discussion

Heavy metals available for plant uptake are in soluble forms which are easily solubilized by root exudates in the soil. Even though plants need soluble heavy metals for their growth and development, extreme concentrations can become injurious to plants. Metals cannot be broken down when they exceed maximum concentrations in plants as such has an adverse effect on plants, such effect could be the inhibition of cytoplasmic enzymes and damage to cell structures due to oxidative stress or growth inhibition. The toxic effects of heavy metals lead to a drop in plant growth which from time to time results in the death of plants. (Jadia and Fulekar, 2009; Schaller and Diez, 1991). Decline in the growth parameters of plants growing on heavy metal-polluted soil can be credited to the reduction in photosynthetic activities, activities of some enzymes and plant mineral nutrient (Kabata-Pendias and Pendias, 2001)

The effects of heavy-metal (HM) pollution on plant morphological features were different for each plant part; whereas there was a growth suppression in some parts (e.g. height), there was enhancement in others (e.g. leaf number). This has pointed to compensatory growth responses. In this study, growth parametric compensation refers to the ability of the test plant to enhance the development of certain parameters when other parameters have been growth-sup by the presence of the stressor provided that the parameter in question has similar contribution to plant growth and development processes. This perhaps may not be unconnected to a possible ability by the plant for metal exclusion (Hossain et al., 2009). As reported in the study, the capability for the test plant to survive in HM-polluted soil is a clear indication for tolerance, which is notably its capacity for compensatory growth in the face of HM-induced stress (Peralta-Videa et al., 2004).

The aerial parts of the plant show visual symptoms of leaf curling in response to heavy-metal pollution, cadmium toxicity also causes leaf curling and stunted growth as reported by Alloway and Ayres (1997); Fontes and Cox (1998); Moreno et al. (1999); Kabata-Pendias and Pendias (2001); Emamverdian et al. (2015). Leaf curling was reported as a prominent morphological feature in the study. It was difficult to link leaf curling with metal pollution in the upper-plant partition since it also significantly appeared in the control. However, leaf folding, and curling symptoms were HM-associated in the intermediate partition. The mechanism behind this could not be explained. It is therefore suggested that this may just be an indicative characteristic that plant biologists might use to suggest HM toxicity. Although in very minute concentrations, some heavy metals like Zinc are important mitopromotors for cell division, Pandey and Upadhyay (2010); Saha (2015) have both showed that heavy metals in high concentrations were mitodepressive, and prompted a multiplicity of chromosomal abnormalities. Consequently, the development of cell and cellular organelles becomes negatively impaired thus leading to impaired plant structure, leaf curling, and rolling in the young leaves.

From the morphological observation, it was clear that chlorosis, necrosis, and wilting are visual signs of metal toxicity (Sanitá di Troppi and Gabbrielli, 1999; Pandey and Upadhyay, 2010; Kekere et al., 2011; Ikhajiagbe and Chijioke-Osuji, 2012; Ikhajiagbe et al., 2013; Saha, 2015). Zenginand and Munzuroglu (2005); Pandey and Singh (2009); Pandey and Upadhyay (2010); Ikhajiagbe (2016); Ikhajiagbe and Ogwu (2020) reported the inhibition of chlorophyll occasioned by heavy metal accumulation in plant leaves. Pandey and Singh (2009); Saha (2015) also reported suppression in the activities of protease and RNase, which decreased photosynthetic pigments, changed chloroplast structure, and decreased enzyme activities for the assimilation of carbon(IV)oxide. Chlorosis may also arise partly from an induced iron (Fe) deficiency as hydrated Zn^{2+} and Fe^{2+} ions have similar radii (Marschner, 1986). Excess in Zn can also give rise to Mn and Cu deficiencies in plant shoots. There have been general chlorosis and necrosis in HM-exposed plants irrespective of the type of metal. Although this morphological anomaly occurred also in the control, but the magnitude of chlorosis and necrosis in the HM-exposed leaves was significant. The presentation of leaf browning was reported, but it was difficult to link this to HM toxicity, as this same anomaly was reported in the control, although with minimal differences in magnitude. Also, the leaves which showed browning symptoms eventually recovered at some point or another. According to previous studies, it is evident that soils polluted with Pb, Zn, Mn, Cu, and Cd showed the same peculiar symptoms such as leaf chlorosis, necrotic lesions, reduction in *C. odorata* height and leaf area (Zhu and Alva, 1993; Taylor and Foy, 1985, Guo et al., 2008; Wojcik and Tukiendorf, 2004, WHO, 1992, Lee et al., 1996; Baryla et al., 2001, Gupta and Gupta, 1998; Elamin and Wilcox, 1986; Bachman and Miller, 1995, Harmens et al., 1993; Fontes and Cox, 1998).

Leaves of *C. odorata* showed common patterns of display of foliar scorching. In the control, burning patches appeared which expanded eventually to occupy the entire leaf. Although burning patches appeared all over the leaves in the Mn-exposed plant, the majority of this phenomenon, however, predominantly occurred from the left leaf margin and was accompanied by burning patches scattered on the surface of the leaf. Scorching in Zn-exposed leaves was mainly restricted to the left leaf margin. For those plants exposed to Cd pollution, the majority of leaf scorching spread from leaf tips accompanied with similar burning patches. This occurrence was similar for Cu and Pb-exposed leaves, which progressed from the left leaf margin inwards. No possible ecophysiological explanation has been attributed to this phenomenon; however, the fact that these leaves also showed diversity of presentation in leaf scorching or burning patterns implied a genetic or environmental influence. Yadav (2010) proposed that genetic manipulations of plant antioxidant systems can help plants ameliorate toxic effects of heavy metals and as such enable the plants to present a huge diversity of morphological features in response to metal toxicity. Generally, however, metal toxicity induces deficiency of essential ions causing leaf discolorations, with the upper and lower leaflets turning brown or purple before they die (Reichman, 2002; Asati et al., 2016; Van Assche and Clijsters, 1990; Meharg, 1994).

There was a significant leaf loss/senescence in HM-exposed plants compared to the control, with Cd initiating the highest foliar loss. However, the capacity for each plant to refoliate at defoliated nodes was reported; Mn-exposed plants refoliated better than others (in approx. < 75 hrs), while Cd-exposed plants were slowest to refoliate (approx. >120 hrs). Plants adjust to conditions of defoliation and the associated reduction in whole-plant photosynthetic rates by altering resource allocation patterns and reducing relative growth rates. In contrast, a transient period of modified physiological function frequently accompanies the plant defoliation followed by a recovery of steady-state plant function (Bhandal and Malik, 1988). A large decrease in the photosynthesis/transpiration ratio of the canopy (i.e., water-use efficiency) is also associated with this pattern of plant defoliation (Hopkins, 1999). Therefore, when plants begin to show quick signs of refoliation, it becomes a plus. In terms of plant refoliation capacity, information on the time, which a defoliated bud takes to refoliate, can be a very useful tool in presenting plant's survival capability with net assimilation.

5. Conclusions

Plants grown in heavy metal-polluted soil expressed several morphological changes including stunted growth, leaf distortions, chlorotic and necrotic lesions. These were common features exhibited by *C. odorata* in this study. Although a significant presentation of morphological anomalies due to exposure to elevated amounts of heavy metals has been reported in the study, the capacity of the plant to subsist has also been reported. Despite the exposure of plants to toxic levels of metals, these plants have developed a very potential mechanism to combat such adverse environmental heavy-metal toxicity problems. These capacities lie in their metabolism, physiology or in their ability for morphological adaptation. Minimal differences in morphology between metal-impacted and control plants indicated that the test plant might be a tolerant plant to heavy metals and thus, can be used for phytoremediation studies.

Acknowledgement

The authors are grateful to Tertiary Education Trust Fund (TETFund) and Needs Assessment for funding this research. The support of the Environmental Biotechnology and Environmental Sustainability Research Group, Department of Plant Biology and Biotechnology, and University of Benin is greatly acknowledged.

References

Ali, S., Farid, M., Shakoor, M. B., Ehsan, A., Zubair, M., Hanif, M. S. (2013). Morphological, physiological and biochemical responses of different plant species to Cd stress. International Journal of Chemical and Biochemical Sciences 3:53–60.

Alloway, B.J. and Ayres, D. C. (1997). Chemical Principles of Environmental Pollution. Blackie Academic and Professional, Glasgow. doi.org/10.1177/1420326X9500400319.

Anoliefo, G.O, Ikhajiagbe, B, Omoregie, E.S., Aimiebenomor, R.A., Okoye, P.C. (2017). Plant growth response and nitrate reductase activities of roots of *Chromolaena odorata* in a model spent lubricating oil-polluted soil. Studia Universitatis Babeș – Bolyai, Biologia, LXII (2): 97-106. doi:10.24193/subbbiol.2017.2.09

APHA (1985). Standard method for the examination of water and waste water. American Public Health Association, Washington DC. 256p

Asati A., Pichhode M., Nikhil K. (2016). Effect of Heavy Metals on Plants: An Overview. International Journal of Application or Innovation in Engineering Management 5(3): 56-66.

Bachman, G. R. and Miller, W. B. (1995). Iron chelate inducible iron/manganese toxicity in zonal geranium. Journal of Plant Nutrition18: 1917–1929.

Baryla, A., Carrier, P., Franck, F.., Coulomb, C., Sahut, C., Havaux, M. (2001). Leaf chlorosis in oilseed rape plants (Brassica napus) grown on cadmium-polluted soil: causes and consequences for photosynthesis and growth. Planta. 212: 696–709.

Basta, N. T., Ryan, J. A., Chaney, R. L. (2005).Trace element chemistry in residual-treated soil: key concepts and metal bioavailability. Journal of Environmental Quality 34(1): 49– 63.

Bhandal, I. S. and Malik, C. P. (1988). Potassium estimation, uptake, and its role in the physiology and metabolism of flowering plants. International Review of Cytology 110: 205-254.

Blaylock, M.J., Dushenkov, S., Zakharova, O., Gussman, C., Kapulnik, Y., Ensley, B.D., Salt, D.E., Raskin, I. (1997). Enhanced accumulation of Pb in Indian mustard by soil-applied chelating agents. Environmental Science and Technology 31: 860-865.

Bray, R.H. and Kurtz, L.T. (1945a). Soil chemical analysis. Soil Science 59: 39-45.

Bray, R.H. and Kurtz, L.T. (1945b). Determination of total organic and available form of phosphorus in soils. Soil Science 59: 45-49.

Cirlakov´a, A. (2009). Heavy metals in the vascular plants of Tatra Mountains. Oecologia Montana 18: 23–26.

Efroymson, R. A., Will, M. E., Suter II, G. W., Wooten, A. C. (1997). Toxicological Benchmarks for Screening Contaminants of Potential Concern for Effects on Terrestrial Plants: 1997 Revision. ES/ER/TM-85/R3. U.S. Department of Energy, Office of Environmental Management. 123p.

Elamin, O. M. and Wilcox, G. E. (1986). Effect of magnesium and manganese nutrition on muskmelon growth and manganese toxicity. Journal of American Society and Horticultural Science 111: 582–587.

Emamverdian, A., Ding, Y., Mokhberdoran, F., Xie, Y. (2015). Heavy metal stress and some mechanisms of plant defense response. The Scientific World Journal 2015: 1-18. DOI: 10.1155/2015/756120

Farid, M., Shakoor, M. B., Ehsan, A., Ali, S., Zubair, M., Hanif, M. S. (2013). Morphological, physiological and biochemical responses of different plant species to Cd stress. International Journal of Chemical and Biochemical Sciences 3: 53– 60.

Fontes, R. L. S. and Cox, F. R. (1998). Zinc toxicity in soybean grown at high iron concentration in nutrient solution. Journal of Plant Nutrition 21: 1723–1730.

Gareeb, M. (2007). Investigation in the potted *Chromolaena odorata* (L.) R.M. King and H. Robinson (Asteraceae). B.Sc. Hons Thesis, University of technology.

Gorlach, E. and Gambus, F., (1992). A study of the effect of sorption and desorption of selected heavy metals in soils on their uptake by plants. Problem Journals of Advances in Agricultural Sciences 398: 47–52.

Guo, J., Dai, X., Xu, W., Ma, M. (2008). Over expressing GSHI and AsPCSI simultaneously increases the tolerance and accumulation of cadmium and arsenic in Arabidopsis thaliana. Chemosphere 72: 1020–1026.

Gupta, U.C. and S.C. Gupta. (1998). Trace element toxicity relationships to crop production and livestock and human health: Implications for management. Communication in Soil Science and Plant Analysis 29: 1491-1522.

Hall, J. L. (2002). Cellular mechanisms for heavy metal detoxification and tolerance. Journal of Experimental Botany 53(366): 1–11.

Hammer, O., Harper, D.A.T., Ryan P.D. (2001). PAST: Paleontological statistics software package for education and data analysis. Paleontologia Electronica 4(1): 1-9.

Harmens, H., Gusmao, N.G.C. P.B., Denhartog, P.R.,Verkleij, J.A.C., Ernst, W.H. O. (1993). Uptake and transport of zinc in zinc-sensitive and zinc-tolerant *Silene vulgaris*. Journal Plant Physiology 141: 309–315.

Henry, R. J. (2000). An Overview of the Phytoremediation of Lead and Mercury, United States Environmental Protection Agency Office of Solid Waste and Emergency Response Technology Innovation office. Washington, DC, USA. 244pp

Hopkins, W. G. (1999). Introduction to Plant Physiology. 2nd edition. John Wiley and Sons Inc., New York. 512pp.

Hossain, M. A., Hossain, M. Z., Fujita, M. (2009). Stress-induced changes of methylglyoxal level and glyoxalase I activity in pumpkin seedlings and cDNA cloning of glyoxalase I gene. Austrian Journal of Crop Science 3: 53–64.

Hossain, M. A., Piyatida, P., da Silva, J. A. T., Fujita, M. (2012). Molecular mechanism of heavy metal toxicity and tolerance in plants: central role of glutathione in detoxification of reactive oxygen species and methylglyoxal and in heavy metal chelation. Journal of Botany 2012: 1-37. doi.org/10.1155/2012/872875.

Ikhajiagbe, B. and Chijioke-Osuji, C.C. (2012). Heavy metal contents and microbial composition of the rhizosphere of *Eleusine indica* within an auto-mechanic workshop in Benin City, Nigeria. Journal of the Ghana Science Association 14(2): 45–55. URL: http://www.ghanascience.org.gh/wp-content/uploads/2018/03/5-Ikhajiagbe-1.pdf.

Ikhajiagbe, B., Odigie, E. U., Okoh, B. E., Agho, E. E. (2013). Effects of sodium azide on the survival, growth and yield performance of rice (*Oryza sativa*, FARO-57 variety) in a hydrocarbon-polluted soil. The International Journal of Biotechnology 2(1): 28-41.

Ikhajiagbe, B. (2016). Possible adaptive growth responses of *Chromolaena odorata* during heavy metal remediation. Ife Journal of Science 18(2): 403–411.

Ikhajiagbe, B. and Akendolor, A. (2016). Comparative effects of pretreatment of stem cuttings of *Chromolaena odorata* (Siam weed) with sodium azide and hydroxylamide on the survival and phyoremediative performance in an oil-polluted soil. Nigeria Journal of Biotechnology 30(1): 27–39.

Ikhajiagbe, B. and Guobadia, B.O. (2016). Application of dry cell battery dust to cultivated fluted pumpkin (*Telfairiaoccidentalis*) as a pest management strategy: implications for both the plant and the consumer's health. Studia UBB 2: 13–30.

Ikhajiagbe, B. and Ogwu, M.C. (2020). Hazard quotient, microbial diversity, and plant composition of spent crude oil-polluted soil. Beni-Suef University Journal of Basic and Applied Sciences 9: 26. DOI: 10.1186/s43088-020-00052-0.

Jadia, C.D. and Fulekar, M.H. (2009). Phytoremediation of heavy metals: Recent techniques. Africa Journal of Biotechnology 8(6): 921-928.

Julian, S., Giso, P., Holger, K. (2017). Leaf-IT: An android application for measuring leaf area. Ecology and Evolution 7: 9731-9738.

Kabata-Pendias, A. and Pendias, H. (2001). Trace Elements in Soils and Plants. CRC Press, Inc. Boca Raton, Florida. 413p.

Kekere, O; Ikhajiagbe, B., Apela, B.R. (2011). Effects of crude petroleum oil on the germination, growth and yield of *Vigna unguiculata* Walp L. Journal of Agriculture and Biological Sciences 2(6): 158-165.

Khan, E., Ali, H., Sajad, M. A. (2008). Phytoremediation of heavy metals-concepts and applications. Chemosphere 7: 869–881.

Kraner, R. M., Minibayeva, F. V., Beckett, P. R., Seal, E. C. (2010). What is stress? Concepts, defintions and application in seed science. New Phytologist 188: 655-662.

Lee, C. W., Choi. J. M., Pak, C. H. (1996). Micronutrient toxicity in seed geranium (Pelargonium x hortorum Bailey). Journal of American Society and Horticultural Science 121: 77–82.

Marschner, H. (1986). Mineral Nutrition of Higher Plants. Academic Press, London. p. 674.

Meharg, A.A. (1994). Integrated tolerance mechanism-Constitutive and adaptive plant-responses to elevated metal concentrations in the environment. Plant Cell Environment 17: 989-993.

Moreno, J.L., Hernandez, T., Garcia, C. (1999). Effects of a Cadmium-Containing Sewage Sludge Compost on Dynamics of Organic Matter and Microbial Activity in An Arid Soils. Biology and Fertility of Soils 28: 230-237.

Nelson, D.W. and Sommers, L.E. (1982). Total carbon, organic carbon and organic matter. In: Methods of soil analysis, Part 2. ASA/SSSA. Madison WI. 539–579pp.

Nkongolo, K. K, Vaillancourt, A, Dobrzeniecka, S, Mehes, M, Beckett, P. (2008). Metal content in soil and black spruce (*Picea mariana*) trees in the Sudbury region (Ontario, Canada): Low concentration of arsenic, cadmium, and nickel detected near smelter sources. Bulletin Environmental Contamination and Toxicology 80: 107-111.

Obata, H. and Umebayashi, M. (1997). Effects of cadmium on mineral nutrient concentrations in plants differing in tolerance for cadmium. Journal Plant Nutrition 20: 97-105.

Okoye, B.C. (1991). Heavy metals and organisms in Lagos Lagoon. International Journal of Environment 37: 285-292.

Omoregie, G.O. and Ikhajiagbe, B. (2019). A comparative assessment of antioxidant responses of *Chromolaena odorata* during exposure to heavy metal pollution. Zimbabwe Journal of Applied Research 2: 53–61.

Omoregie, G.O, Ogofure, A.G., Ikhajiagbe, B, Anoliefo, G.O. (2020). Quantitative and qualitative basement of microbial presence during phytoremediation of heavy metal polluted soil using *Chromolaena odorata*. Ovidius University Annals of Chemistry 31(2): 145–151. DOI: 10.2478/auoc-2020-0023.

Osuji, L. C. and Nwoye, I. (2007). An appraisal of the impact of petroleum hydrocarbon on soil fertility: the Owaza experience. Africa Journal of Agricultural Research 2: 318-324.

Pandey, C. B. and Singh, L. (2009). Soil fertility under home garden trees and native moist evergreen forest in South Andaman. India. Journal of Sustainable Agriculture 33: 303-318.

Pandey, R.M. and Upadhyay, S.K. (2010). Cytological effect of heavy metals on root meristem cells of *Vicia faba* L., Toxicological and Environmental Chemistry 92(1): 89-96. DOI: 10.1080/02772240902757081.

Peralta-Videa J. R, de la Rosa, G., Gonzalez, J. H., Gardea-Torresdey, J. L. (2004). Effect of the growth stage on the heavy metal tolerance of alfalfa plants. Advances in Environmental Research 8: 679–685.

Petarca, L. and Cioni, B. (2011). Petroleum products removal from contaminated soils using microwave heating. Chemical Engineering Transactions 24: 1033-1038.

Reichman, S.M. (2002). The Responses of Plants to Metal Toxicity: A review focusing on Copper, Manganese and Zinc. Published by the Australian minerals and energy environment foundation. Published in Melbourne, Australia 55pp Published as Occasional Paper No.14.

Saha, B. (2015). Toxic Metals and Plants. Journal of Plant Biochemistry and Physiology 3(3): 1-2. DOI: 10.4172/2329-9029.1000e129.

Sanitá di Troppi, L. and Gabbrielli, R. (1999). Response to cadmium in higher plants. Environomental and Experimental Botany 41: 105-130.

Schaller, A. and Diez, T. (1991). Plant specific aspects of heavy metal uptake and comparison with quality standards for food and forage crops. In: Sauerbeck, D, Lubben, S (Eds.) Der Einfluß von festen Abfallen auf Boden, Pflanzen. Julich, Germany: KFA, 1991: 92–125.

Shen Z.G., Zhao F.J., McGrath S.P. (1997) Uptake and transport of zinc in the hyper-accumulator Thlaspi caerulescens and the non-hyperaccumulator *Thlaspi ochroleucum*. Plant Cell Environ 20: 898–906.

Taiwo, O. B., Olajide, O. A., Soyande, O. O., Makinde, J. M. (2011). Anti-inflammatory, antipyretic and antispasmodic properties of *Chromolaena odorata*. Pharmaceutical Biology 38: 367–370.

Taylor, G. J. and Foy, C. D. (1985). Differential uptake and toxicity of ionic and chelated copper in *Triticum aestivum*. Canadian Journal of Botany 63: 1271–1275.

Tu, C., Zheng, C. R., Chen, H. M. (2000). Effect of applying chemical fertilizers on forms of lead and cadmium in red soil. Chemosphere 41(1-2): 133–138.

USDA. (1998). Estimating Soil Moisture by Feel and Appearance. United States Department of Agriculture, Natural Resources Conservation Service, Program Aid No. 1619. April, 6p.

Uyi, O. O., Ekhator, F., Ikuenobe, C. E., Borokini, T. I., Aigbokhan, E. I., Egbon, I. N., Adebayo, A. R., Igbinosa, I. B., Okeke, C. O., Igbinosa, E. O., Omokhua, G. A. (2014). *Chromolaena odorata* invasion in Nigeria: A case for coordinated biological control. Management of Biological Invasions 5(4): 377–393.

Van Assche, F. and Clijsters, H. (1990). Effects of metals on enzyme activity in plants. Plant Cell environment 13: 195-206.

WHO (1992). Cadmium. Environmental Health Criteria. Geneva: World Health Organization. Vol.134

Wojcik, M. and Tukiendorf, A. (2004). Phytochelatin synthesis and cadmium localization in wild type of Arabidopsis thaliana. Plant Growth Regulators 44: 71–80.

Yadav, S.K. (2010). Heavy metals toxicity in plants: An overview on the role of glutathione and phytochelatins in heavy metal stress tolerance of plants. South African Journal of Botany 76(2): 167-179.

Zenginand, F. K. and Munzuroglu, O. (2005). Effects of some heavy metals on content of chlorophyll, proline and some antioxidant chemicals in bean (*Phaseolus vulgaris* L.) seedlings. Acta Biologica Cracoviensia Series Botanica 47(2): 157–164.

Zhang, M. K., Liu, Z. Y., Wang, H. (2010). Use of single extraction methods to predict bioavailability of heavy metals in polluted soils to rice. Communications in Soil Science and Plant Analysis 41(7): 820–831.

Zheng XS, LU AH, Gao X, et al. 2002. Contamination of heavy metals in soil present situation and method. Soils and Environmental Sciences 11(l): 79-54

Zhu, B. and Alva, A. K. (1993). Effect of pH on growth and uptake of copper by swingle citrumelo seedlings. Journal of Plant Nutrition 16: 1837–1845.

JJEES

JJEES (2021) 12 (1): 62-71
ISSN 1995-6681

Jordan Journal of Earth and Environmental Sciences

Assessment of Environmental Pollution on the Soil, Plants, and Water Chemistry of Insurgency-Inflicted Communities of Madagali, Adamawa State Nigeria

Ibrahim Bwatanglang[1*], Ezekiel Yonnana[2], Lynna Ibrahim[3], Aishatu Medugu[1], Elisha Bitrus[1]

[1]Adamawa State University, Faculty of Science, Department of Pure and Applied Chemistry, Nigeria.
[2]Adamawa State University, Faculty of Science, Department of Geography, Nigeria.
[3]Adamawa State College of Nursing and Midwifery, Department of Anatomy and Physiology, Nigeria.

Received 6 May, 2020; Accepted 19 September 2020

Abstract

In this study, soil, plant, and water samples were analyzed toward establishing the level of pollution-induced by insurgency/military action in the crisis-inflicted areas of Madagali. The respective samples taken from a crisis-free areas of Maksi (MK) were used in this study as a reference station to evaluate and establish the level of pollution buildup due to insurgency in samples collected from the crisis-inflicted communities of Angwan mission (AM), Magar (MG), and Bakin kasuwa (BK). The total concentrations of Iron (Fe), Zinc (Zn), Copper (Cu), lead (Pb), Chromium (Cr), and Cadmium (Cd) ions determined in the soil samples from the study areas based on the Pollution Index (PI) and the integrated pollution load index (PLI) showed the soil samples to be slightly-to-moderately polluted. Anthropogenic-related activities were further observed to contribute >100 % to the pollution levels in the soil samples at AM, MG, and BK respectively. The results further showed Cr, Pb, Cu, and Zn to be of a low ecological risk (Er < 40) in the samples from AM, MG, and BK. However, Cd was observed to be of a moderate-to-considerable ecological risk (40 < Er < 86) in the samples from AM and BK. On the whole, the Potential Ecological Risk Index (Ri) estimated for samples from AM, MG, and BK was observed to be of a low potential ecological risk (R_i<150). The water quality for drinking purposes according to the Water Quality Indices (WQI) is classified as good for drinking for the samples from MG (47.42), BK (36.85), and AM (28.63). Only the water samples from MK, having a value of 19.76 was observed to be of excellent quality (WQI<25). The results were observed to be significantly (p<0.5) higher in the insurgeny-inflicted areas of AM, MG, and BK compared to the values obtained from MK, the reference site.

Keywords: Heavy metal, Pollution index, Ecological risk Index, Water quality

1. Introduction

Ban Ki-moon in a statement presented at the UN's International Day for Preventing the Exploitation of the Environment in War and Armed Conflict placed emphasis on the devastating effects of war on the environment; crying out that the environment has long been a silent casualty of war and armed conflicts (https://www.theguardian.com/environment/2014/nov/06/whats-the-environmental-impact-of-modern-war). Certini et al. (2013) in their review hypothesized a possible decline in the state–state warfare, and an increase in localized warfare/insurgencies across the globe. According to the assessment, the state–state warfare will increase the levels of localized contamination of the environmental medium by chemical warfare agents. In Nigeria, hostilities, communal clashes, and insurgency are quantified to be of epic proportion; creating systematic and dire environmental consequences of similar proportions. In northeastern Nigeria, the carbon footprint from Boko Haram activities and its vices have created a devastating humanitarian crisis, disease outbreak, refugee surge, food insecurity, and water stress among others (Nwakaudu, 2012). The situation rendered 8.5 million people, among which 1.78 million are internally displaced persons (IDPs) who rely solely on humanitarian-based assistance (OCHA, 2017a). Close to 75% of water/sanitation facilities in the region are destroyed due to insurgency, with about 200 health facilities rendered useless (OCHA, 2017b).

Though, the attention of researchers is primarily drawn to several aspects of insurgency especially in northeastern Nigeria (Awortu, 2015; Chukwurah et al., 2015; Iliyasu et al., 2015; Emmanuelar, 2015; Shuaibu et al., 2015; Dunn, 2018), these efforts, however, are observed to be limited to economic, social, agricultural and health-related implications of the insurgency. The immediate environmental effects resulting from insurgency activities, with particular attention to the effects of pollutants to the soil, water, and the entire food chain are seldom investigated and reported. During Insurgency or hostilities, the greatest threat is manifested in the risk of environmental pollution and ecocide (Heiderscheidt, 2018). Research findings in war-tone countries further support these observations, bringing to the fore, the causative effects of conflict and environmental-

Corresponding author email: ibbbirma@gmail.com

based pollution (Heiderscheidt 2018). Such activities was observed to mediate the deposition of pollutants in the soils, water, and bioaccumulation in plants (Kokorīte et al., 2008; Lewis et al., 2010; Meerschman et al., 2011; Bazzi et al., 2020).

Insurgency or hostility-mediated activities were reported to lead to loss of functional properties of the biota, and were further observed to trigger economic and social crisis to the inflicted areas (Sims et al., 2019). Such activities may lead to the degradation of the soil ecosystem, generating pollutants from heavy military vehicles, explosives, gun residues, and bullet cache (Kokorīte et al., 2008; Briggs et al., 2016; Gębka et al., 2017). Studies show that Pb dust and debris are generated in surface soils at the shooting range (Chen et al., 2002; Cao et al., 2003; Levonmäki et al., 2006). Soil as a repository of contaminants can readily accumulate HMs, which if substantially accumulated in the soils, can be released to other ecosystems, such as groundwater, rivers, atmosphere, and crops (Wei and Yang 2010). Through the casualty flow, the risk from conflict-mediated pollutants through several reaction pathways could impinge heavily on the health of the population (Meerschman et al., 2011; Das, 2014; Heiderscheidt, 2018).

Against this backdrop, this present study was undertaken to ascertain the level of pollutants in the soil, plants, and water sources of insurgency/hostility areas of Adamawa State, Nigeria. The research covering the conflict zone in the state is limited by the unavailability of access to the inflicted areas for a full-scale assessment. Thus, this study was narrowed toward evaluating the environmental pollution levels in the soil, plants, and water sources of Madagali LGA of the State. Due to the non-availability of data on pollution indices in the study location before the conflict, the study will consider sampling data from crisis-prone areas and areas that experience no insurgency or hostilities around the study locations. The research work will serve as a pilot effort to experimentally study the effects of insurgency/hostilities on environmental indicators (Heavy metals, Physicochemical and bacteriological parameters) for a small number of samples and sample locations.

2. Materials and Methods

2.1 Description of the Study Area

Madagali LGA as shown in Figure 1 is located in the northern senatorial zone of Adamawa state in the northeast region of Nigeria. Situated at latitude $10^0 51^I$N and $10^0 58^I$N and longitude $13^0 36^I$E and $13^0 42^I$E, 420 meters above the sea level (Ahmed et al., 2015). Since August 2014, the area has been experiencing a series of hostilities by Boko Haram insurgency, creating humanitarian, social, and health-related crises in the region. The majority of the people living across the crisis area lack access to basic sanitation, and safe water.

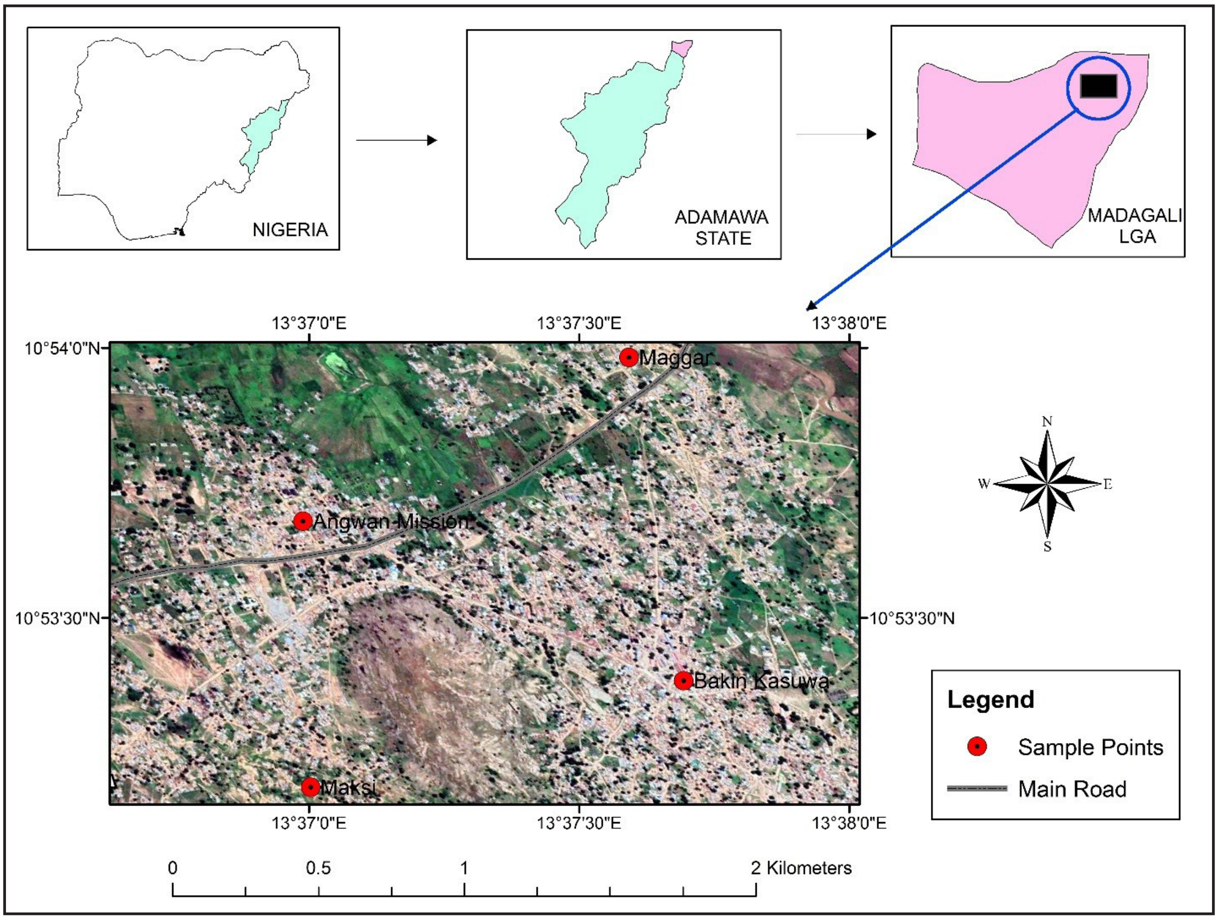

Figure 1. Map of Madagali showing the sampling points.

2.2 Sampling and Preparation

Surface soils and water samples were collected randomly across three major wards in Madagali LGA which has experienced likely changes in the soil and water quality due to frequent attacks by insurgents and military-related response action. The locations as shown in the map in Figure 1, include the Anguwan mission (AM) located at Mararaba under the Madagali ward, Bakin kasuwa/Police station (BK) located at Madagali central, and Magar (MG) situated at Wagga ward. The fourth location is Maksi (MK), a community in the Dirif unit in Bebel ward close to Mt. Maksi in Cameroun. Maksi is considered to be a community that did not experience any insurgent attacks and thus served as a reference station for the study. In each of the four sample locations, soil samples were taken randomly from six sub-points. The samples taken from the six sub-points are pooled to form a composite for each of the study locations. The samples obtained at a depth of approximately 5-10 cm were disaggregated and sieved through a 250 µm mesh. From the respective sample locations, one of the widely and popularly consumed vegetables (Sorrel) in the area was also sampled for analysis. Ten sorrel plants were taken at each of the six sub-points and were homogenized to make a composite sample for each of the four sample locations. The sorrel vegetable samples were processed following the procedure described by Aderinola et al. (2012). The water samples were collected from both hand-dug wells and boreholes located in each of the four sample locations. The samples were treated based on the method described in ASJ (2012).

Atomic Absorption Spectrophotometer (AAS) (Buck Scientific, VPG 210) was used to determine the total concentrations of Fe, Zn, Cu, Pb, Cr, and Cd in the samples. Before the analysis, sieved soil and powdered plant samples were subjected to acid-digestion using aqua regia at a ratio of 3:1 of concentrated HCl: HNO_3. While 10 ml of 8 M HNO_3 was used for the digestion of the water samples. The HMs concentrations in the soil were used for the Environmental Pollution study using the following tools: bioaccumulation (BF), pollution index (PI) and the integrated pollution index (PLI), anthropogenicity (APn%), the ecological risk factor (E_r), and the potential ecological risk factor (R_i). For the water sample analysis, Sodium (Na) and Potassium (K) were carried out using a Flame Photometer. The presence of anion such as chloride was determined using the argentometric titration method, acid-base titration using methyl orange as an indicator for the Bicarbonate (HCO_3^-) ions, Nitrate (NO_3^-), and Sulphate (SO_4^{2-}) using Sci-04 model of water LaMotte Analyzer. The pH was measured using pH meter while Dissolved Oxygen was determined using a DO meter (JENWAY 970). Total Dissolved Solids was determined using a multipurpose JENWAY portable combined TDS/ Conductivity meter. The total hardness of the water samples was determined using the titration method with EDTA, while. The turbidity of the samples is measured by Nephelometer. The data were evaluated based on a statistical description using a statistical Package for Social Sciences (SPSS) software (Version 20). The analysis was run in triplicate, and the results were expressed as Mean ± SD. Furthermore, the data analyzed were considered significant at $p < 0.05$.

2.3 Environmental Pollution Study

2.3.1 Bioaccumulation Factor

The Bioaccumulation Factor (BAF) was used to establish the transfer dynamics of the HMs in the soil to the Sorrel plants; an indicator used to determine possible contamination in plants. The units of BAF were calculated using the expression in equation 1.

$$BAF= C_{leave}/C_{Soil} \quad (1)$$

Where C_{leave} and C_{soil} are metals concentration in the Sorrel plant (mg/kg) and soil (mg/kg).

2.3.2. Assessment of Pollution Index

The integrated pollution index (PLI) reveals the overall pollution status of the soil samples. The PLI was calculated using the expression in equation 2

$$PLI= (PI_1 \times PI_2 \times PI_3 \times . . . \times PI_n)\ 1/n \quad (2)$$

Where PI is the pollution index obtained from equation 3

$$PI= C_i/C_{Rei} \quad (3)$$

Where C_i is the concentration of the ith element in soil samples (mg/kg), and C_{REi} is its corresponding reference concentration (mg/kg). Since no available information on the natural background values for heavy metals in the study location, the concentration of HMs in the surface soils from MK (insurgent free area) will be considered as the C_{REi} value. Similarly, the world average natural background values will be adopted for comparison (Turekian and Wedepohl, 1961). The PI is classified into, no pollution ($PI \leq 1$), slight pollution ($1 < PI \leq 3$), moderate pollution ($3 < PI \leq 5$), and severe pollution ($PI > 5$). The PLI is classified into seven levels: background concentration ($PLI = 0$), no pollution ($0 < PLI \leq 1$), no-to-moderate pollution ($1 < PLI \leq 2$), moderate pollution ($2 < PLI \leq 3$), moderate-to-high pollution ($3 < PLI \leq 4$), high pollution ($4 < PLI \leq 5$), or very high pollution ($PLI > 5$) (Sun and Chen, 2018)

2.3.3. Assessment of Anthropogenicity

Anthropogenicity (Apn%) directly measures the anthropogenic influence on the metal concentrations in the soil samples. It is calculated as follows:

$$APn\% = \frac{Mc}{Bn} x100 \quad (4)$$

Where M_c = measured concentration, while B_n = world average natural background values (Turekian and Wedepohl, 1961). Values taken from Maksi (MK) were equally adopted as the reference or natural background values.

2.3.4. Ecological Risk Assessment

An ecological risk assessment is used to determine the nature or potential effects of the anthropogenic-related actions of pollutants in the soil samples on public health and the environment. This is estimated using the Ecological Risk factor E_r and Potential Ecological Risk Index (R_i) proposed by Hakanson (1980), and was expressed in equation 5.

$$Er = Ti\ x \left(\frac{Cm}{Bn}\right) \quad (5)$$

Where E_r is an ecological risk factor, T_i is a toxic response factor of a certain metal. The values for each metal is in the order of Zn=1<Cr=2<Cu=Pb=5<Cd=30 (Hakanson1980). The Cm is the metal content in the soil and

Bn is a background value of metals in soil. The following terminology are used to describe the potential ecological risk factor: E_r< 40 indicates a low potential ecological risk, 40 <E_r< 80 indicates a moderate potential ecological risk, 80 <E_r< 160 indictaes a considerable potential ecological risk, 160 <E_r< 320 means a high potential ecological risk and E_r> 320 denotes a very high potential ecological risk

$$Ri = \sum E_r^i \quad (6)$$

Where R_i is the potential ecological risk calculated as the sum of the ecological risk factor for heavy metals in the soil. E_i is an ecological risk factor. The following terminology is used to describe the potential ecological risk index: R_i< 150 indicates low ecological risks, 150 ≤ R_i> 300 indicates moderate ecological risks, 300 ≤ R_i> denotes 600 considerable ecological risks, and R_i> 600 indicates a very high ecological risk

2.4 Water Quality Assessment

The water quality index (WQI) was assessed using the HMs concentrations and the physicochemical parameters in Table 1. The assessment was conducted using the expressions in equation 8 (Guettaf et al., 2017).

$$WQI = \sum_{i=1}^{n} SI_i \quad (8)$$

Where SI is the water quality sub-index determined using the equation

$$SI = RWi \; x \; qi \quad (i)$$

Where Wi is the relative weight of each parameter, and qi is the rating scale for each parameter obtained from the expressions below

$$RWi = \frac{Wi}{\sum_{n=1}^{n} Wi} \quad (ii)$$

Where Wi is the assigned weight for each parameter, and RWi is the relative weight. The Wi are assigned to reflect the relative importance of each parameter in the overall quality of water for drinking purposes

The results are presented in Table 1

$$qi = \left(\frac{Ci}{Si}\right) x \; 100 \quad (iii)$$

Where Ci is the concentration of each parameter, and Si is the corresponding standards from WHO

Table 1. The weight (Wi) and relative (RWi) for each parameter used in WQI determination

	Literature values									This study	
Parameters	WHO (2004)	Guettaf et al. (2017)	Pesce and Wunderlin (2000)	Abdul Hameed et al. (2010)	Abu Khatita et al. (2017)	Al-Mutairi et al. (2014)	Şener et al. (2017)	Tyagi et al. (2013)	Olasoji et al. (2019)	Wi	RWi
pH	6.5-8.5	3	1	2.1	2.1	0.11	4	4	4	2.5	0.05
E.C (µs/cm)	1000	3	4	2.4	ND	ND	ND	ND	ND	3.1	0.06
TDS (mg/l)	1000	5	ND	ND	ND	0.08	ND	5	ND	3.4	0.06
Turbidity (NTU)	5	ND	2	2.4	ND	ND	ND	ND	ND	2.2	0.04
Total hardness (mg/l)	100	3	1	1.1	ND	ND	ND	ND	ND	1.7	0.03
Chloride (mg/l)	250	3	ND	ND	ND	ND	3	3	1	2.5	0.05
Calcium (mg/l)	75	2	ND	ND	ND	ND	2	3	2	2.3	0.04
Magnesium (mg/l)	30	2	ND	ND	ND	ND	2	3	2	2.3	0.04
Phosphate (mg/l)	1	ND	ND	ND	ND	0.1	ND	ND	ND	0.1	0.00
Na (mg/l)	200	3	ND	1	ND	ND	2	ND	ND	2.0	0.04
DO (mg/l)	6-8	ND	4	4	4	0.17	ND	ND	ND	3.0	0.05
Nitrate (NO_3^-) (mg/l)	50	5	2	2.2	2.2	0.1	5	4	ND	2.9	0.05
Fluoride (F^-) (mg/l)	1.5	ND	ND	ND	ND	ND	ND	4	ND	4.0	0.07
Sulphate (mg/l)	250	3	ND	ND	ND	ND	4	4	ND	3.7	0.07
Cd (mg/l)	0.003	ND	ND	ND	3	ND	ND	ND	ND	3.0	0.05
Cu (mg/l)	1	ND	ND	ND	2	ND	ND	3	4	3.0	0.05
Cr (mg/l)	0.05	ND	ND	ND	3	ND	5	ND	5	4.3	0.08
Fe (mg/l)	0.3	5	ND	ND	ND	ND	ND	2	ND	3.5	0.06
Pb (mg/l)	0.01	ND	ND	ND	5	ND	5	2	ND	4.0	0.07
Zn (mg/l)	0.1	ND	ND	ND	2	ND	ND	ND	ND	2.0	0.04
										55.5	1.00

ND: Stands for not determined in the study

3. Results and Discussion:

3.1 Heavy Metal Pollution in the Surface Soil and Sorrels with their BAF

The concentration of the HMs (Pb, Cu, Cr, Zn, Fe, and Cd) in the surface soil and the Sorrel samples from AM, MG, BK, and MK wards of Madagali LGA in Adamawa statem Nigeria are presented in Figure 2. From the results in Figure 2(a), Fe was observed to be the predominant species in the surface soils across the wards, constituting a 58.3% distribution followed by Zn (29.5%) and Cu (10.6%). The least metals found in the soil samples across the wards are Cr, constituting only 0.3%. The predominant Fe in the surface soil is reported to be consistent with its behavior in association with elements such as Cr, Pb, and Cu (Edith-Etakah et al., 2017). However, when compared with the standard set by WHO, the concentrations of all the species in all the wards were below their respective permissible limits (PL) (WHO/FAO, 2001). From Figure 2, except for Cr which shows an insignificant ($p>0.05$) decrease in the soil samples from AM (0.07±0.03), the distribution of the heavy metals in the surface soils of AM, MG, and BK was observed to be significantly ($p<0.05$) higher compared to the corresponding values from the insurgent free soils of MK. A similar trend was observed in the Sorrels sampled from the study locations, showing Fe as the predominant species accounting for a 54 % abundance, to be followed by Zn (33%) and Cu (11.5%) (Figure 2b). Chromium was detected only in the samples from AM (0.06±0.04) and a 0.1% abundance was found in samples from MG (0.01±0.01). Except for Cu (in all the samples) and Cd in the samples from AM (0.25±0.01), all the other species were found to be below the PL set by WHO. The concentration of Fe, Zn, and Cu in the samples from AM, MG, and BK were observed to be significantly ($p<0.05$) higher than their corresponding values in MK. Lead was found to be significantly ($p<0.05$) higher in the samples from AM (0.22±0.02) and BK (0.02±0.02) compared to the values in MK (0.01±0.02). Chromium and Cd were not detected in the samples from MK.

However, it will suffice to conclude that geogenic and anthropogenic-related activities might be the major contributor to the HMs availability in the study locations. Factors other than agriculture may likely come into play considering the significant variation in concentrations between the conflict areas and MK. Environmental disturbances from insurgents/military-related activities may likely play additional roles in the metal buildup in these locations. Studies show that the environmental disturbances initiated by war/hostilities facilitated the changes in soil morphology, composition, and chemistry (Certini et al., 2013; Bazzi et al., 2020). In a study conducted by Gębka et al. (2016), the concentration of Hg in soil samples collected from a military-active range, in southern Baltic in 2014 and 2015 was observed to increase tenfold in soil samples collected in an area with an active gun range compared to a nonmilitary range, used as a reference point in the study. The source of the Hg, according to the study, is mercury fulminate used in the manufacturing of ammunition primers (Knobloch et al., 2013). In a related study, Meerschman et al. (2011) using about 731 data points collected from Ypres battlefield showed the source of Cu and Pb to be from war-related activities. Bullets or ammunition residues through several chemical processes, over time, release HMs into the environment medium, which is either biotransformed by plants or enriched in the soil (Lewis et al., 2010).

The empirical effect of warfare on the environment depends on some environmental attributes, largely defined in terms of the size (scale), locations (international or locally-induced war) or developmental (either by developed or developing countries) (Reuveny et al., 2010). Even though this study could be considered locally-induced, not a full-blown or large scale, it shows that war has through the wake of the hostilities increases aggregated environmental stress leading to the observed variation in the heavy metal contents in the surface soil of AM, MG, and BK compared to MK.

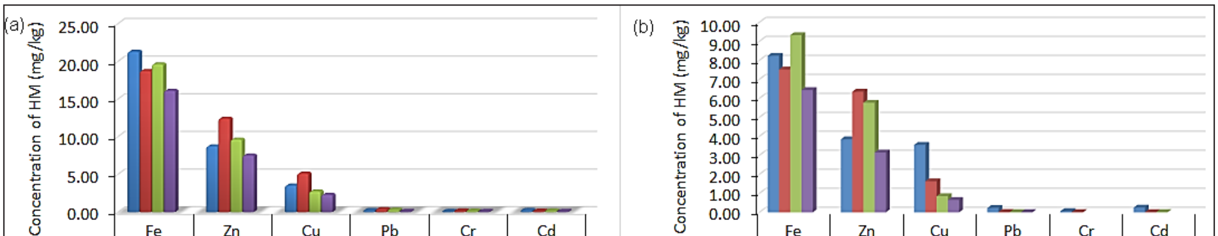

(a)

	Fe	Zn	Cu	Pb	Cr	Cd
AM	21.33	8.77	3.56	0.24	0.07	0.26
MG	18.77	12.44	5.15	0.38	0.15	0.13
BK	19.66	9.66	2.78	0.31	0.13	0.16
MK	16.14	7.55	2.33	0.09	0.08	0.09
WHO/FAO	5000	250	50	200	50	10

(b)

	Fe	Zn	Cu	Pb	Cr	Cd
AM	8.24	3.85	3.55	0.22	0.06	0.25
MG	7.52	6.35	1.63	0.02	0.01	0.01
BK	9.33	5.77	0.85	0.02	ND	0.01
MK	6.44	3.15	0.65	0.01	ND	ND
WHO/FAO	425	20	0.30	0.35	0.50	0.10

Figure 2. The concentrations of Heavy Metals in the Soil (a) and Sorrel vegetable (b) and their corresponding PL by WHO/FAO. Results are presented in Mean ±SD of three replicate analysis.

Plant-soil chemistry is an effective and sustained pathway for metal enrichment in a plant. The complexity of the interaction depends on several environmental factors that influence metal availability and variability in the soil for an efficient uptake by plants (Garba et al., 2018; Magili and Bwatanglang, 2018). The persistence of bioavailable HMs in a soil medium through several reaction mechanisms is readily transformed and transferred across the trophic levels (Ali et al., 2019). The number of research work in Nigeria reported a high accumulation of HMs from contaminated soils into plants (Akinola and Ekiyoyo, 2006; Adesuyi et al., 2015). Other studies show a direct relationship between vehicular emission, the application of agrochemicals, and other anthropogenic-related activities with heavy metals accumulated in soils and in plants (Bwatanglang et al., 2019). The estimation of metal bioavailability in soils and its contamination status in plants are also used as an indicator for assessing the environmental pollution status (Shtangeeva, 1995). While being efficient in phytoremediation, it also serves as a conduit for toxic metal mobility and can be utilized scientifically toward establishing pollution dynamics from the soil, to the food chain and public health.

From the results in Figure 3, Cu, Pb, Cd, and Cr, out of the six heavy metals analyzed, show BF of ~1 in the samples collected from AM. Only Zn, out of the six HMs analyzed in MG, Zn and Fe analyzed in BK give a BAF of 1. Furthermore, BAF of <1 was recorded in all the metal species analyzed in MK. The major contributor to heavy-metal buildup in the surface soil in the study location could be attributed to agricultural activities such as the application of agrochemicals. However, the variation in the results from the AM, MG, and BK samples compared to the least values in MK further suggest possible man-made activities that could be linked to insurgency/military-related activities. The higher contents in those locations are translated into a higher uptake by the plant and higher BAF in the insurgent areas (AM, MG, and BK) compared to the reference area (MK).

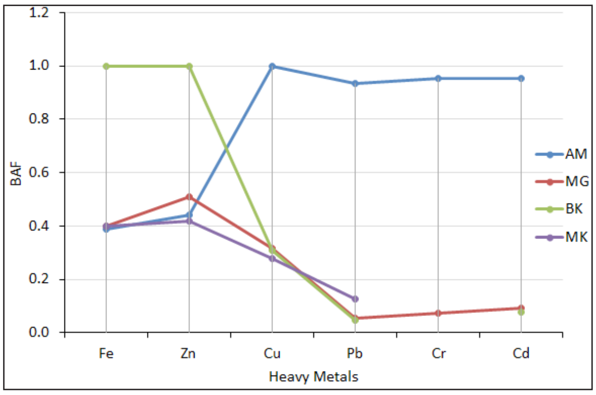

Figure 3. The Bioaccumulation Factor of the Heavy Metals for each sample locations.

3.1 Environmental Pollution Study and Potential Ecological Risk Assessment of the Heavy Metals in Surface Soil

Using MK as reference values, the PI in the soil samples obtained from the insurgent areas (AM, MG, and BK) showed the soil samples to be slightly and moderately contaminated with heavy metals (Table 2). The surface soils in AM, MG, and BK were observed to have PI≤ 3. For these locations, Fe, Zn, Cu, Cr, and Cd are the major contributors to soil pollution. The result further shows the surface soils from MG and BK to be moderately polluted with Pb (3 < PI ≤ 5). The PLI was further observed to be high (PLI ≤ 4) in AM and Bk and very high pollution (PLI > 5) in MG. In all of the locations, the major contributors to the surface soil pollution are Pb followed by Cd and Cu. The results of the pollution index show that the quality of soil in the study area is slightly-to-moderately compromised. Insurgents/military-related activities in addition to the application of agrochemicals increased the levels in AM, MG, and BK compared to the values obtained from the reference site (MK) (Certini et al., 2013; Bazzi et al., 2020).

Table 2. The Pollution Index and the Integrated Pollution Load Index (PLI) of the Heavy Metals. Established using the data from MK and World natural background value as reference values.

		Reference value (Maksi)			Reference value (Natural background value)			
Metals		AM	MG	BK	AM	MG	BK	MK
Fe	PI	1	1	1	0	0	0	0
Zn		1	2	1	0	0	0	0
Cu		2	2	1	0	0	0	0
Pb		3	4	4	0	0	0	0
Cr		1	2	2	0	0	0	0
Cd		3	1	2	1	0	1	0
PLI		4	7	4	1	1	1	0

Anthropogenicity is a numerical expression (in Percentage) employed to measure the impact of anthropogenic-related activities on the environment. The results are presented in Table 3. Using the HMs concentration at MK as a reference value, the study showed anthropogenic activities contributing more than 100 % in the surface soil at AM, MG, and BK, respectively. Lead, Cd, Cu, and Cr are the HMs most influenced by man-made activities in the surface soils at these locations. Further appraisal of the surface soils at AM, MG, BK, and MK using the world natural background values showed a much lower level of anthropogenic activity. The soil at MK experiences a lesser impact from anthropogenic activities, showing a background concentration for Fe, Pb, and Cr. The highest anthropogenicity of 31% was observed for Cd while, Zn and Cu contribute 8 % and 5% respectively. The anthropogenicity for the heavy metals in AM, MG, and BK shows Cd as the major contributor, accounting for 88%, 44%, and 52%, in that order.

The main occupation of the people residing in the study locations is agriculture; thus, it is logical to conclude that agrochemical will be the major contributor in addition to the natural geologic processes. Phosphate-based fertilizers contain high amounts of Cd ranging from trace quantities to 300 ppm on a dry weight basis (Grant and Sheppard, 2008). The source of this fertilizer, phosphate rock, contains different environmentally-hazardous elements including Cr, Cd, Pb, Hg, and As, (Atafar et al., 2010). Other studies shows a high correlation for these metals associated with phosphate in fertilizers (Ukpabi et al., 2012), and the application of fungicide for Cu enrichment (Semu and Singh, 1996). However, since the concentration of the HMs in the insurgent areas (AM, MG, and BK) is relatively higher than the values in MK, it will not be out of place to suggest additional HMs inputs from the insurgent/military-related activities (Meerschman et al., 2011; Certini et al., 2013; Gebka et al., 2016; Bazzi et al., 2020).

Table 3. The Anthropogenicity (Apn %) of the Heavy Metals in the Surface Soils. Established using the data from MK and World natural background values as the reference value.

	Reference value (Maksi)			Reference value (Natural background value)			
Metals	AM	MG	BK	AM	MG	BK	MK
Fe	>100	>100	>100	0	0	0	0
Zn	>100	>100	>100	9	13	10	8
Cu	>100	>100	>100	8	11	6	5
Pb	>100	>100	>100	1	2	2	0
Cr	84	>100	>100	0	0	0	0
Cd	>100	>100	>100	88	44	52	31

The possible risk associated with these pollutants as shown above can best be understood when subjected to the potential ecological risk assessment of the surface soil. The results of the assessments of the potential ecological risk factor (Er) and the potential ecological risk index (RI) are summarized in Table 4. The Er of the heavy metals in the soils from the study areas factored using the concentration from MK as reference values shows Cd >Pb>Cu>Cr>Zn. The Er for Cr, Pb, Cu, and Zn in the surface soils at AM, MG, and BK were found to be less than 40, wich means a low ecological risk. The surface soils at MG based on the calculated ecological risk factor (Er) of 43 are considered to be of moderate potential ecological risk for Cd, while BK and AM showed a moderate-to-considerable potential ecological risk for Cd, having Er values of 51 at BK and 86 at AM respectively. However, all the RI values estimated for the metals in the surface soil from all the study locations are of low ecological risk, having values R_i<150. Furthermore, when measured against the world's natural background values, the Ri estimated in the surface soils for all the metals, having values <150 was observed to be of no consequences, indicating a no-potential ecological risk.

Table 4. Ecological Risk factor (Er) and Potential Ecological Risk Index (Ri) of the Heavy Metals in the Surface Soil. Established using the data from MK and World natural background concentrations as the reference value.

		Reference value (Maksi)			Reference value (Natural background value)			
Metals		AM	MG	BK	AM	MG	BK	MK
Zn	E_r	1	2	1	0	0	0	0
Cu		8	11	6	0	1	0	0
Pb		14	22	18	0	0	0	0
Cr		2	4	3	0	0	0	0
Cd		86	43	51	26	13	16	9
R_i		110	81	79	27	14	16	10

3.3 Assessment of the Physicochemical Parameters and Heavy Metals in Water Samples against Recommended Permissible Limits

As shown in Table 5, there is no significant (p>0.05) difference in the mean concentration of the parameters in some of the study locations relative to the PL. Except for total hardness, phosphate, and Cd level in MG, the remaining parameters were observed to all fall below the PL set by WHO. The parameters were further observed to be of the least concentration/level in the samples from MK and fall between the optimum pH ranges for first-class drinking water (6.5-8.5).

(Tebbutt, 1998; Sen and Aksoy, 2015). Electrical conductivity (EC) is a reflection of Dissolved Solids' concentrations in water. The EC values of the water samples from the study locations vary within a range of 374–172 µS/cm. The values at the insurgent areas are significantly (p<0.05) higher than the values from the non-conflict area (MK). Similar to the trend observed for EC, the Total Dissolved Solids' (TDS) values in all the study locations were below the WHO PL (1,000 mg/l). The values at BK (186 mg/l) and MG (95 mg/l) are significantly (p<0.05) higher than the values from the non-conflict area (MK, 82 mg/l). The turbidity values of the water samples are between 8.11 and 1.01 NTU. The values in MG (8.11 NTU) are significantly (p<0.05) higher than the WHO (5 NTU) values, and were observed to follow a decreasing trend between the locations (MK<BK<AM<MG). Total hardness (TH) is a function of excessive Ca and Mg concentrations in the water body (Dirican, 2015). The highest value above the WHO limit (100 mg/l) was observed in BK (240.00 mg/l) and MG (240.11 mg/l), followed by a sample from AM (184.01 mg/l). The values in MK were the lowest (80.00 mg/l) and were further observed to be significantly (p<0.05) lower than the values in the insurgent areas. The concentration of TH in water is classified into six categories: ≤50 as soft, moderately-soft (50-100), slightly-hard (100-150), moderately-hard (150-250, hard (250-350), and very hard (>350) (Şener et al., 2017). According to this classification, the samples from MK are soft, that of AM, MG, and BK are moderately-hard (Tebbutt, 1998; Sen and Aksoy 2015). The dissolved oxygen (DO) values in the water samples range from 7.11 to 6.51 mg/L, falling within the recommended values of 6-8 mg/l for quality drinking water (Tebbutt, 1998; Sen and Aksoy, 2015; Dirican, 2015).

The availability of cations in all of the sample locations are in the order of Na>Mg> Ca>Zn>Cu>Fe>Cd>Pb>Cr, with Na as the dominant species. The cations except for Cd (0.008) in the samples from MG were observed to all fall below the PL set by WHO. The HMs in the samples from AM, MG, and BK, though found to be insignificantly (p>0.05) higher than the corresponding values in the samples from MK, could be attributed to phosphate/nitrate-based fertilizers, Cu-based fungicides (Atafar et al., 2010; Ukpabi et al., 2012), or ammunition residues (Lewis et al., 2010). The anions in this study follow the order of Cl^-> SO_4^{2-}> NO_3^->PO_4^{3-} >F^-, with chloride as the dominant species. In this category, phosphate was observed to be above the PL set by WHO. Phosphate levels range from 3.11-6.80 mg/l. The highest value was observed in a sample from BK (6.80±0.14 mg/l), while the least in MK (3.11±0.12 mg/l). Chloride, nitrate, and sulphate are the major anions that adversely alter the drinking-water quality (Şener et al., 2013) and are found to be significantly (p<0.05) higher in the samples from AM, MG, and BK compared to the samples from MK. The presence of chloride ions in the water samples could be related to anthropogenic activities or to the leaching of saline residues in the soil (Chatterjee et al., 2010). Water samples containing ≤25 mg/l of Chloride are considered class-I; and class-II, III, and IV if the chloride concentration in the water is 200 mg/l, 400, and >400 respectively. From the analysis, the water in the study locations could be categorized as class-I, (Tebbutt, 1998; Sen and Aksoy, 2015; Dirican, 2015). The concentration of nitrates in the water samples could be attributed to the nitrate-based agrochemicals or to the leaching of human or animal wastes (Guettaf et al., 2017). Water is considered class-I if it contains ≤5 mg/l of nitrate, class-II; if it contains 6-10 mg/l of nitrate, class-III and IV if it contains 11-20 and >20 mg/l of nitrate respectively. According to these limits, the water samples from the study locations having nitrate values from 3.49-7.50 could be categorized as class-I (Tebbutt, 1998; Sen and Aksoy, 2015; Dirican, 2015). The breakdown of organic materials through soil weathering processes, leaching from sulphate-containing fertilizers, atmospheric deposition and oxidative decomposition of the sulfur compound by bacteria are means of sulphate induction into the water bodies (Guettaf et al., 2017; Dirican, 2015; Şener et al., 2017; Varol and Davraz, 2015; Chatterjee et al., 2010). Sulphate below 200 mg/l in the water samples is classified as class-I, class-II if it is 200 mg/l. If 400 or >400 mg/l they are categorized class-III and IV respectively (Dirican, 2015). The water samples from all the study locations based on the concentration of sulphate are classified as class-I (Tebbutt, 1998; Sen and Aksoy, 2015; Dirican, 2015).

3.4 Water Quality Assessment

The water quality index (WQI) values are classified into five types namely, excellent water (0< WQI<25), good water (25< WQI<50), poor water (50 < WQI< 75), very poor water (75< WQI< 100), and water unsuitable for drinking (WQI > 100) (Guettaf et al., 2017). The WQI values were estimated using the assigned weighted values in Table 1 and equations 8. From the result in Table 5, the quality of water for drinking purposes is good for samples from MG (47.42), BK (36.85), and AM (28.63) respectively. Only the water samples from MK, having a value of 19.76 were observed to be of excellent quality (WQI<25). Anthropogenic-related activities from agrichemical and environmental disturbances created during insurgency may have introduced additional levels of contaminants into the water body. This may equally explain the low WQI values registered in the three study locations inflicted by insurgency (AM, MG, and BK). Total hardness, phosphate level, and the presence of Cd in addition to the cumulative effects from sulphate, nitrate, and chloride could be the possible reasons for the observed drop in water quality from AM, MG, and BK.

Table 5. Physicochemical and Heavy-Metal Analysis in Water Samples from the Study Locations and the WHO Standards.

Parameters	AM	BK	MG	MK	WHO
pH	7.10±0.05	7.20±0.10	7.69±0.12	7.05±0.11	6.5-8.5
E.C (µs/cm)	174.00±0.20*	374.00±0.03*	189.00±1.05*	172.00±0.15	1000
TDS (mg/l)	87.12±1.06*	186.00±0.04*	95.01±0.11*	82.02±0.14	500
Turbidity (NTU)	2.00±1.10	2.00±0.07	8.11±0.09*	1.01±2.12	5.0
Total hardness(mg/l)	184.01±0.05*	240.00±0.11*	240.11±0.12*	80.00±0.13	100
Chloride (mg/l)	106.00±0.82	64.51±0.15	42.54±0.11	54.95±1.01	250
Calcium (mg/l)	0.06±0.03	0.09±0.02	0.05±0.01	0.05±0.02	75
Magnesium(mg/l)	0.09±0.03	1.15±0.02*	1.14±0.04*	0.08±0.03	30
Phosphate (PO_4^{3-}) (mg/l)	6.70±0.12*	6.80±0.14*	6.41±0.13*	3.11±0.12	1.0
Na (mg/l)	5.5±0.11*	4.1±1.55	4.2±1.05	4.1±0.06	200
DO (mg/l)	7.0±0.04	6.51±0.11	6.71±0.72	7.11±1.09	6-8
Nitrate (NO_3^-) (mg/l)	7.50±0.11*	6.30±0.42*	6.20±0.51*	3.49±0.19	50
Fluoride (F^-) (mg/l)	0.11±0.51	0.16±1.05	0.21±0.13	0.10±0.51	1.5
Sulphate (mg/l)	26.00±0.11*	25.11±0.41*	31.21±0.01*	20.11±0.15	500
Cd (mg/l)	0.002±0.01	0.001±0.01	0.008±0.02	0.001±0.02	0.003
Cu (mg/l)	0.04±0.01	0.09±0.02	0.06±0.03	0.01±0.08	1.0
Cr (mg/l)	ND	0.004±0.03	ND	ND	0.05
Fe (mg/l)	0.02±1.50	0.02±0.03	0.03±0.11	0.02±0.11	0.3
Pb (mg/l)	ND	0.008±0.005	ND	ND	0.01
Zn (mg/l)	0.05±0.03	0.07±0.01	0.09±0.03	0.03±0.03	0.1
WQI	28.63	36.85	47.42	19.76	
Quality	Good	Good	Good	Excellent	

**Denoted level of significance to the reference value at MK*

4. Conclusions

Environmental disturbances created during insurgent hostilities leave behind salient but causative effects, releasing toxic substances which often take a longer time to be manifested, and whose consequences are often undervalued and underreported. Environmental pollution induced by toxic substances through several reactive pathways may induce changes in the functional properties and quality of the soil and water, thus increasing the likelihood of health risk to the public on the long run. These observations necessitated an investigation using a small sample-size reported in this work. The distribution of HMs in the surface soils and sorrel plants in samples from AM, MG, and BK were observed to be significantly ($p<0.05$) higher than in samples from MK. The Pollution Index (PI) values showed the soil samples to be slightly-to-moderately polluted. With >100 % of the HMs availability in the samples derived from anthropogenic-related activities. The study further revealed the Ecological Risk Index (Ri) for samples from AM, MG, and BK as a low potential ecological risk (R_i<150), however, it revealed a moderate-to-considerable ecological risk (40<Er<86) concerning Cd levels. The WQI shows the samples from MK, having WQI≤19 to be of an excellent quality compared to the samples from AM, MG, and BK (<28WQI<47). The overall assessment conducted in this study shows that the environmental indicators analyzed were significantly (p<0.5) higher in the crisis-inflicted areas (AM, MG, and BK) compared to the reference station (MK). Though the study was limited by the unavailability of access to all the insurgent communities for full-scale assessment, the results however establish a possible link toward pollution buildup from conflict/military-related activities which suggest that if the insurgents' hostilities are not tamed, they will create additional stress on the environment, increasing public exposure to contaminants whose effects overtime will supersede the immediate impact initiated during the crisis. Therefore, further research is, however, encouraged to cover a larger number of sample sizes across the northeastern state of Nigeria, especially in communities where data on the environmental indicators exist before the insurgency. The effort will provide additional information toward marshaling out an ecological and remediatory intervention plan in the affected areas.

References

Abdul Hameed M. J., A., Haider, S.A., Bahram, K. M. (2010). Application of water quality index for assessment of Dokan lake ecosystem, Kurdistan region, Iraq. Journal of water resource and protection 2(9): 792-798.

Abu Khatita, A. M. Shaker, I. M., Shetaia, S. A. (2017). Water quality assessment and potential health risk of Manzala lake-Egypt. Al Azhar Bulletin of Science 9: 119-136.

Aderinola, O. J. and Kusemiju, V. (2012). Heavy metals concentration in Garden lettuce (Lactuca sativa L.) grown along Badagry expressway, Lagos, Nigeria. Transnational Journal of Science and Technology 2(7): 115-130.

Adesuyi, A.A., Njoku, K.L., Akinola, M.O. (2015). Assessment of Heavy Metals Pollution in Soils and Vegetation around Selected Industries in Lagos State, Nigeria. Journal of Geoscience and Environment Protection 3(7): 11-19. DOI: 10.4236/gep.2015.37002.

Ahmed, H. A. Ahmed, K. S., Jamilu, M. (2015). Stream Sediment Survey of an Area around Madagali, Northeastern Nigeria. Researcher 7(10): 56-69.

Akinola, M.O. and Ekiyoyo, T.A. (2006). Accumulation of lead, cadmium and chromium in some plants cultivated along the bank of river Ribila at Odonla area of Ikorodu, Lagos state, Nigeria. Journal of Environmental Biology 27(3): 597-599.

Ali, H., Khan, E., Ilahi, I. (2019). Environmental chemistry and ecotoxicology of hazardous heavy metals: environmental persistence, toxicity, and bioaccumulation. Journal of chemistry 2019: 1-14 https://doi.org/10.1155/2019/6730305

Al-Mutairi, N., Abahussain, A., El-Battay, A. (2014). Spatial and temporal characterizations of water quality in Kuwait Bay. Marine pollution bulletin 83(1): 127-131.

Analytical science journal (ASJ). (2012). Vol.no 1, official journal of institute of public Analyst of Nigeria (IPAN).

Atafar, Z., Mesdaghinia, A., Nouri, J., Homaee, M., Yunesian, M., Ahmadimoghaddam, M., Mahvi, A. H. (2010). Effect of fertilizer application on soil heavy metal concentration. Environmental monitoring and assessment 160(1-4): 83.

Awortu, B.E. 2015. Boko Haram Insurgency and the Underdevelopment of Nigeria. Research on Humanities and Social Sciences 5(6): 213-220.

Bazzi, W., Abou Fayad, A. G., Nasser, A., Haraoui, L. P., Dewachi, O., Abou-Sitta, G., Nguyen, V. K., Abara, A., Karah, N., Landecker, H., Knapp, C., McEvoy, M. M., Zaman, M., Higgins, P. G., Matar, G. M. (2020). Heavy metal toxicity in armed conflicts potentiates AMR in A. baumannii by selecting for antibiotic and heavy metal co-resistance mechanisms. Frontiers in Microbiology 11: 68. doi.org/10.3389/fmicb.2020.00068

Briggs, C., Shjegstad, S.M., Silva, J.A.K., Edwards, M.H. (2016). Distribution of chemical warfare agent, energetics, and metals in sediments at a deep-water discarded military munitions site. Deep Sea Research Part II: Topical Studies in Oceanography 128: 63–69.

Bwatanglang, I. B., Alexander, P., Timothy, N. A. (2019). Vehicle-derived heavy metals and human health risk assessment of exposure to communities along Mubi-Yola highway in Adamawa State (Nigeria). Journal of Scientific Research and Reports 23(1): 1-13.

Cao, X., Ma, L. Q., Chen, M., Hardison, D. W., Harris, W. G. (2003). Weathering of lead bullets and their environmental effects at outdoor shooting ranges. Journal of environmental quality 32(2): 526-534.

Certini, G. Scalenghe, R. Woods, W. I. (2013). The impact of warfare on the soil environment. Earth Science Reviews 127: 1-15.

Chatterjee, R., Tarafder, G., Paul, S. (2010). Groundwater quality assessment of Dhanbad district, Jharkhand, India. Bulletin of engineering geology and the environment 69(1): 137-141.

Chen, M., Daroub, S. H., Ma, L. Q., Harris, W. G., Cao, X. (2002). Characterization of lead in soils of a rifle/pistol shooting range in central Florida, USA. Soil and Sediment Contamination 11(1): 1-17.

Chukwurah, D. C., Eme, O., Ogbeje, E. N. (2015). The implication of Boko Haram Terrorism on Northern Nigeria. Mediterranean Journal of Social Sciences 6(3): 376-377.

Das, O. (2013). Environmental protection in armed conflict: Filling the gaps with sustainable development. Nordic Journal of International Law 82(1): 103-128. https://doi.org/10.1163/15718107-08201006.

Dirican, S. (2015). Assessment of water quality using physico-chemical parameters of Çamlıgöze Dam Lake in Sivas, Turkey. Ecologia 5(1): 1-7.

Dunn, G. (2018). The impact of the Boko Haram insurgency in Northeast Nigeria on childhood wasting: a double-difference study. Conflict and health 12(1): 1-12. DOI: 10.1186/s13031-018-0136-2

Edith-Etakah, B. T., Shapi, M., Penaye, J., Mimba, M. E., NguemheFils, S. C., Nadasan, D. S., Davies, T.C., Jordaan, M. A. (2017). Background concentrations of potentially harmful elements in soils of the Kette- Batouri region, Eastern Cameroon. Research Journal of Environmental Toxicology 11(1): 40-54. DOI: 10.3923/rjet.2017.40.54.

Emmanuelar, I. (2015). Insurgency and humanitarian crises in Northern Nigeria: The case of Boko Haram. African Journal of Political Science and International Relations 9(7): 284-296.

Garba, H., Shinggu, D.Y., Bwatanglang, I.B., Magili, T.S. (2018). The Role of 2, 2-Dichlorovinyl Dimethyl Phosphate and the Dynamics of Heavy Metals Absorption/Translocation in Plants: Emphasis on Sorrel and Spinach. International Journal of Current Research in Biosciences and Plant Biology 5(6): 1-10.

Gębka, K., Bełdowski, J., Bełdowska, M. (2016). The impact of military activities on the concentration of mercury in soils of military training grounds and marine sediments. Environmental Science and Pollution Research 23(22): 23103-23113.

Grant, C. A., and Sheppard, S. C. 2008. Fertilizer impacts on cadmium availability in agricultural soils and crops. Human and Ecological Risk Assessment 14(2): 210-228.

Guettaf, M., Maoui, A., Ihdene, Z. (2017). Assessment of water quality: a case study of the Seybouse River (North East of Algeria). Applied Water Science 7(1): 295-307.

Hakanson, L. (1980). Ecological risk index for aquatic pollution control. A sedimentological approach. Water Research 14: 975-1001.

Heiderscheidt, J. A. (2018). The Impact of World War one on the Forests and Soils of Europe. Ursidae: The Undergraduate Research Journal at the University of Northern Colorado 7(3): 1-17.

https://www.theguardian.com/environment/2014/nov/06/whats-the-environmental-impact-of- modern-war (access 25/03/2020).

Iliyasu, D., Lawan, A., Ibrahim, Y., Omonike, O. S., Muktar, A. (2015). Repercussion of Insurgence Activities of Boko Haram on Management of Livestock and Production in Northeastern Part of Nigeria. Journal of Animal Production Advances 5(3): 624-628.

Knobloch, T., Bełdowski, J., Böttcher, C., Söderström, M., Rühl, N. P., Sternheim, J. (2013). Chemical munitions dumped in the Baltic Sea. Report of the ad hoc expert group to update and review the existing information on dumped chemical munitions in the Baltic Sea (HELCOM MUNI). Baltic Sea environment proceeding (BSEP) 142: 1-128.

Kokorīte, I., Kļaviņš, M., Šīre, J., Purmalis, O., Zučika, A. (2008). Soil pollution with trace elements in territories of military grounds in Latvia. In Proceedings of the Latvian Academy of Sciences. Section B. Natural, Exact, and Applied Sciences 62(1-2): 27-33.

Levonmäki, M., Hartikainen, H., Kairesalo, T. (2006). Effect of organic amendment and plant roots on the solubility and mobilization of lead in soils at a shooting range. Journal of environmental quality 35(4): 1026-1031.

Lewis, J., Sjöström, J., Skyllberg, U., Hägglund, L. (2010). Distribution, chemical speciation, and mobility of lead and antimony originating from small arms ammunition in a coarse-grained unsaturated surface sand. Journal of environmental quality 39(3): 863-870.

Magili, T.S and Bwatanglang, I.B. (2018). Bioaccumulation Trend Analysis and Hierarchal Presentation Based on Decision Tree. International Journal of Green and Herbal Chemistry 7(4): 401-418.

Meerschman, E., Cockx, L., Islam, M. M., Meeuws, F., Van Meirvenne, M. (2011). Geostatistical assessment of the impact of World War I on the spatial occurrence of soil heavy metals. Ambio 40(4): 417-424.

Nwakaudu, M. 2012. Boko Haram and National Development. http://www.vanguardngr.com. (accessed on 25/03/2020)

OCHA (2017a). (United Nations Office for the Coordination of Humanitarian Affairs), Nigeria.Humanitarian Response Plan 2017a, December 2016.

OCHA (2017b). (United Nation Office for the Coordination of Humanitarian Affairs), Nigeria.Humanitarian Needs Overview, November 2016

Olasoji, S. O., Oyewole, N. O., Abiola, B., Edokpayi, J. N. (2019). Water quality assessment of surface and groundwater sources using a water quality index method: A case study of a peri-urban town in southwest, Nigeria. Environments 6(2): 23.

Pesce, S. F. and Wunderlin, D. A. (2000). Use of water quality indices to verify the impact of Córdoba City (Argentina) on Suquía River. Water research 34(11): 2915-2926.

Reuveny, R., Mihalache-O'Keef, A. S., Li, Q. (2010). The effect of warfare on the environment. Journal of Peace Research 47(6): 749-761.

Semu, E. and Singh, B. R. (1995). Accumulation of heavy metals in soils and plants after long-term use of fertilizers and fungicides in Tanzania. Fertilizer research., 44(3): 241-248.

Şen, F. and Aksoy, A. (2015). Chemical and Physical Quality Criteria of Bulakbaşı Stream in Turkey and Usage of Drinking, Fisheries, and Irrigation. Journal of Chemistry., 2015: 1-8. doi.org/10.1155/2015/72508.

Şener, Ş., Davraz, A., Karagüzel, R. (2013). Evaluating the anthropogenic and geologic impacts on water quality of the Eğirdir Lake, Turkey. Environmental earth sciences 70(6): 2527-2544.

Şener, Ş., Şener, E., Davraz, A. (2017). Evaluation of water quality using water quality index (WQI) method and GIS in Aksu River (SW-Turkey). Science of the Total Environment 584: 131-144.

Shtangeeva, I. V. (1995). Behaviour of chemical elements in plants and soils. Chemistry and Ecology 11(2): 85-95.

Shuaibu, S. S., Salleh, M. A., Shehu, A. Y. (2015). The impact of Boko Haram insurgency on Nigerian national security. International Journal of Academic Research in Business and Social Sciences 5(6): 254-266.

Sims, N.C., England, J.R., Newnham, G.J., Alexander, S., Green, C., Minelli, S., Held, A. (2019). Developing good practice guidance for estimating land degradation in the context of the United Nations sustainable development goals. Environmental Science and Policy 92: 349–355.

Sun, Z. and Chen, J. (2018). Risk Assessment of Potentially Toxic Elements (PTEs) Pollution at a Rural Industrial Wasteland in an Abandoned Metallurgy Factory in North China. International journal of environmental research and public health 15(1): 85. doi: 10.3390/ijerph15010085.

Tebbutt, T. H. Y. (1998). Principles of Water Quality Control, 5th edition, chapter 2, Butterworth-Heinemann Elsevier, Oxford, UK.

Turekian, K.K. and Wedepohl, K.H. (1961). Distribution of the elements in some major units of the earth's crust. Geological Society of American Bullutin 72: 175-192.

Tyagi, S., Sharma, B., Singh, P., Dobhal, R. (2013). Water quality assessment in terms of water quality index. American Journal of water resources 1(3): 34-38.

Ukpabi, C. F., Akubugwo, E. I., Agbafor, K. N., Lebe, N. A., Nwaulari, N. J., Nneka, E. D. (2012). Appraisal of heavy metal contents in commercial inorganic fertilizers blended and marketed in Nigeria. American Journal of Chemistry 2(4): 228-233.

Varol, S. and Davraz, A. (2015). Evaluation of the groundwater quality with WQI (Water Quality Index) and multivariate analysis: a case study of the Tefenni plain (Burdur/Turkey). Environmental Earth Sciences 73(4): 1725-1744.

Wei, B. and Yang, L. (2010). A review of heavy metal contaminations in urban soils, urban road dusts and agricultural soils from China. Micro chemical Journal 94: 99–107.

WHO, (2004). Guideline for Drinking Water Quality. 3rd Edition Vol. 1 Recommendation, Geneva, 515.

WHO/FAO. (2011). Joint FAO/WHO food standards programme codex committee on contaminants in foods. Working document for information and use in discussions related to contaminants and toxins in the Gsctff. Fifth Session. Hague, The Netherlands; pp. 90.

JJEES

JJEES (2021) 12 (1): 72-80
ISS`N 1995-6681

Jordan Journal of Earth and Environmental Sciences

A GIS-EIP Model for a Mechanic Industrial Zone Site Selection in Al-Mafraq City, Jordan

Abdulla Al-Rawabdeh[1,2*], Khaled Hazaymeh[2,3*], Sara Nusiar[4], Rana Shdaifat[4], Mu'ayyad Al Hseinat[5]

[1]Yarmouk University, Department of Earth and Environmental Sciences, Jordan.
[2]Yarmouk University Laboratory of Applied Geoinformatics, Jordan.
[3]Yarmouk University, Department of Geography, Faculty of Arts, Yarmouk University, Jordan.
[4]Jordan University of Science and Technology, College of Architecture and Design, Department of City Planning and Design, Jordan.
[5]The University of Jordan, School of Science, Department of Geology, Jordan.

Received 18 July 2020; Accepted 19 September 2020

Abstract

Due to the lack of adequate infrastructure and management, the current busy mechanic industrial zone (MIZ) in the Mafraq City, Jordan is causing several negative effects on its surroundings, including a daily traffic congestion; visual-, air-, and noise pollution; and land-value degradation. The objective of the study presented in this paper is to integrate eco-industrial park principles (EIPs) into multi-criteria decision-making (MCDM) and geographic information systems (GIS) for the selection a new MIZ site in Mafraq. A GIS-EIP model was first developed by analyzing the different variables involved, which included the terrain slope suitability; proximity to transportation, utility networks, health centers, and schools; protected sites; stream networks; urban areas; and vacant land. The proposed GIS-EIP model was carried out in the following four steps: (i) identifying the potential areas for the new MIZ site based on specific EIP criteria, (ii) determining the weight and score values for each criterion, (iii) integrating the criteria using a map integration procedure, and (iv) evaluating suitable locations for the new MIZ site. A suitability map was created thereafter, based on five categories (equally suitable, slightly suitable, strongly suitable, very strongly suitable, and extremely suitable). Then, concentrating on the last three suitability categories only, twenty land parcels were identified as the best alternative sites. These identified parcels, which span an area greater than 0.7km^2 within a square of 1km and are located within vacant land, were determined to be the best fit to the EIP principles applied in this study. These results can be used by Mafraq's decision-makers to select the best place to relocate its busy MIZ and thereby reduce its current traffic congestion and environmental problems.

Keywords: MCDM; Delphi; Index overlay, Suitability analysis, GIS, Eco-industrial parks.

1. Introduction

The concept of eco-industrial park (EIP) emerged in the 1990s (Lowe, 2006). The most common definition of EIP, which has been cited by several international organizations working in this field, was introduced by Lowe (1998) as: a dedicated area for industrial use at a suitable site that ensures sustainability through the integration of social, economic, and environmental quality aspects into its siting, planning, management and operations. These EIP principles are of great value for reducing the long- and short-term impacts of industrial zones by considering the ecological and social aspects of their chosen sites. Several past studies adopted the EIP concept in a geospatial dimension to ensure the environmental sustainability and industrial ecology of an industrial zone (Shi et al., 2010; Tudor et al., 2007; Dohel, 2016). This geospatial dimension has added a new perspective to landscape ecology by providing definitive ways to identify suitable sites for industrial zones (Conticelli and Tondelli, 2014).

According to the United Nations Industrial Development Organization (UNIDO), selecting a location for an industrial zone is among the most critical steps in its development process. This selection strongly influences the demand, supply, cost, environment, and socioeconomic aspects, which in-turn can influence the overall success of the industrial zone; and this decision therefore should be made in the context of broader spatial and non-spatial geographical considerations, within which several alternative sites can be considered. The principal steps for planning an industrial zone include: (i) pre-feasibility studies, (ii) pre-identification of a shortlist of suitable sites, (iii) detailed feasibility analysis of the selected site, and (iv) financial structuring and management (UNIDO, 2016).

Furthermore, the selected site should be convenient to meet the daily needs of citizens in the immediate residential neighborhoods and the wholesaling stakeholders and distributors (Steiner et al., 2000). In this context, a detailed framework should be carefully established to ensure the sustainable development and environmental management of the industrial zone. This framework should incorporate all possible factors that could impact the optimal location,

Corresponding author email: abd_rawabdeh@yu.edu.jo

including social, environmental, human, economical, and morphological factors (Al-Shalabi et al., 2006; Bagdanavičiūtė and Valiūnas, 2013; Patil and Jamgade, 2019). The mismanagement of industrial sites could negatively impact the surrounding environment and reduce the quality of life for its surrounding neighborhoods (Arabsheibani et al., 2016). One of the most appropriate techniques for establishing such a framework is introducing multi-criteria decision-making (MCDM) within a geographic information systems (GIS) environment into the process. This technique has the capability to combine different types of spatial and non-spatial datasets to produce reliable solutions with less time and effort (Patil and Jamgade, 2019). By using MCDM-GIS, it is possible to successfully implement the EIP concept for industrial site selection (Banar et al., 2014), which could include a variety of key factors that can work with various categories in a GIS environment and could support decision-makers in solving the geospatial issues related to the area of interest (Kumar and Shaikh, 2013). It also can help decision-makers in their evaluation of the priorities of a specific location based on a set of preferences, criteria, and indicators (Johar, 2013).

In this study, a GIS-MCDM-based EIP approach was developed to select the optimal site for the potential relocation of the mechanic industrial zone (MIZ) in Mafraq City in the northeastern part of the Hashemite Kingdom of Jordan. Although MCDM has been used in several studies for site selection, combining it with EIP concepts, to the best of the authors' knowledge, has not been fully applied in Jordan. The proposed approach incorporates the concepts of sustainable and economic spatial planning by identifying two major goals: (i) the sustainable (environmental) variables including stream networks and valleys, health facilities, and topography and (ii) the economic variables, which include transportation and railway networks (the Hejaz railway, which operates passenger trains from Amman to Damascus in Syria and also operates freight trains on its tracks); protected sites; urban areas; and land vacancy. A newly-selected optimal MIZ site should strive to improve the level of services and accessibility to the area, protect the environment, and reduce pollution and traffic congestion in the city while having the least impacts on people, infrastructure, traffic, health facilities, heritage sites, and future urban development and expansion.

2. Study Area

Mafraq City is located in northeastern Jordan and covers a total area of 26km2; and its total population is about 216,900, which includes approximately 162,697 refugees (DOS, 2020; UNHCR, 2020). A rapidly growing city, Mafraq is suffering from a lack of urban planning and policies, which is contributing to problems that are lowering the quality of life, such as traffic congestion, accidents, pollution, land degradation, and the high demands on infrastructure (Sqour et al., 2016). The major economic activities of the area include agriculture, livestock herding, general services, and industry, which include the MIZ. The current location of the MIZ contains several types of activities, such as gas stations, mechanic shops, vehicle detailing shops, small-scale plastic recycling factories, and water-purifying manufactories. The wastes produced in the MIZ include oil, iron, plastic, cardboard, caoutchouc, metal liquids, and other materials. The MIZ is one of the major challenges faced by the local authorities and citizens in Mafraq. It spans an area of 0.27km2, and is surrounded by two major heavily-utilized highways and many facilities, including a new city center, the Mafraq gynecology hospital, Al al-Bayt University, the King Abdulla suburb, and many other residential areas within less than 500m from the MIZ site (Figure 1). This location has created severe traffic congestion and pollution in the area, examples are shown in Figure 2. Its land value is very high which could be invested in other high added-value commercial investments.

The study area is covered mainly by basaltic rocks, which belong to the Harrat Ash Shaam Basaltic Super Group of Neogene-Quaternary age. The Abed Olivine Phyric Basalt (Pliocene) lies unconformably above the Umm Rijam Chert Limestone Formation. Its Thickness is 20m and the distribution of this formation is in the northeast and eastern parts of the study area. The Pleistocene to recent deposits covers most of the basaltic rocks due to the high erosional rate. These deposits are composed of Plateau Gravels (Pleistocene-Recent) consists of heterogeneous mixture of gravels with different size, from 1cm to 1m. Two types of soil are mainly present. The red soil, "Terra rosa", is the Mediterranean Sea soil found in the southwest of the study area. the desert soils, yellow mostly, are a mixture aeolian sands located northeast, east, and southeast of Mafraq City (Smadi, 1997).

It would be important to mention here that the soil type could affect the selection of the location of a MIZ site, however, the soil in the entirety of the study area is considered to be the same type, so it has an equal spatial importance weight throughout the study area and therefore it would not affect the selection of the proposed MIZ sites.

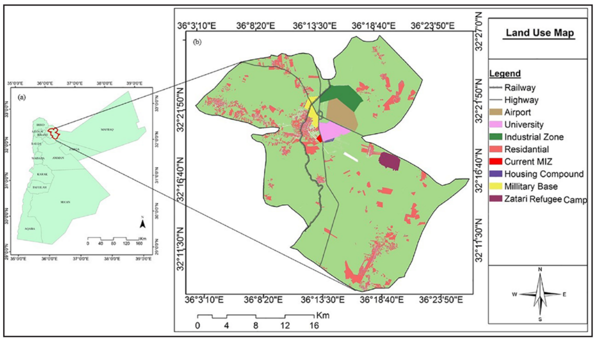

Figure 1. (a) Map of Jordan, (b) land use map of the city of Mafraq. Red polygon shows the current location of mechanic industrial zone (MIZ) dispersed throughout the city surrounded by several facilities and residential areas.

Figure 2. (a-c) are examples of plastic, cardboard, caoutchouc, metal, and oil spill pollution found in the mechanic industrial zone (MIZ); (d) illustrates the proximity of the hospital to the MIZ, which is in the upper left corner of the image.

3. Materials and Methods

A schematic diagram of the proposed GIS-EIP approach for selecting a new location for the MIZ is shown in Figure 3. The approach consists of three main steps: (i) data collection and preparation, (ii) developing the GIS-EIP model, and (iii) evaluating the new MIZ potential sites.

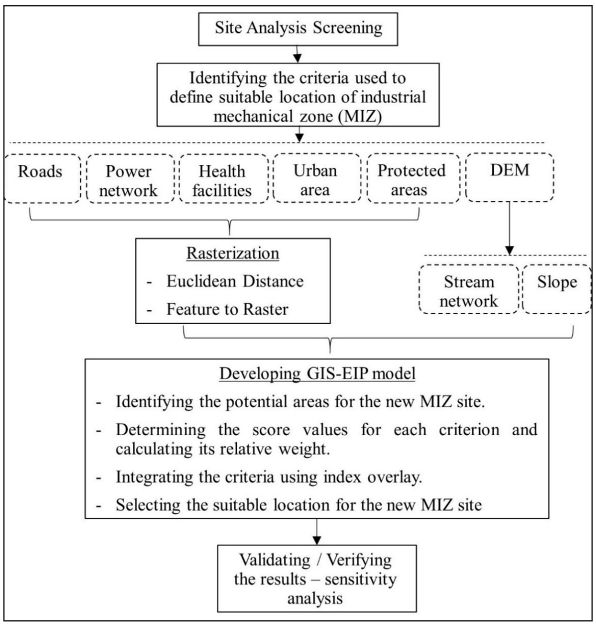

Figure 3. Schematic diagram of the proposed GIS-EIP model for selecting a new MIZ location in Mafraq city, Jordan.

3.1. Data Collection and Preparation

An intensive review of the literature and the different related sectors (i.e., ecology, environment, planning, local authority, stakeholders, and local citizens) was performed to determine the best practices' criteria. Three categories of major criteria were identified: (i) accessibility, (ii) availability, and (iii) ecological criteria, which are listed in Table 1.

The first category includes sub-criteria for the local transportation network, railways, highways, and power networks. Information about these sub-criteria were collected from open street maps and local authorities in the form of hard-copy maps and then georeferenced to the Jordan Transfers Mercator (JTM) coordinate system. The power network information was obtained from local authorities, and was added to the geodatabase. The second category contained the land parcels and information about their ownership, area, and vacancy. The built-up and protected areas, including military-owned parcels were stored with their attributes in the land parcels' database. These land use types were considered as protected lands for the MIZ site selection.. The third category (ecological criteria) included the stream network and slope values of the terrain. Both were extracted from the ALOS PALSAR digital elevation model (DEM) at 12.5m spatial resolution using the spatial analysis tools within the GIS environment. The stream network is very important as the MIZ could impose groundwater pollution and flood risk. Currently, the existing MIZ is not served with a sewage system infrastructure; and all the liquid and sewage waste produced are drained into nearby valleys and streams causing pollution to groundwater storage in the area and affecting water quality (Al-Mefleh et al., 2019). It is worth noting here that the study area has an arid climate that tends to have short but intensive rainfall during the winter season; and the area may receive water flows from the mountainous area of Al-Arab Mountain in southern Syria during different times of the year (Al-Olemat, 2019).

Table 1. Description of the major criteria and sub-criteria used to define suitable location of the MIZ) in Mafraq city.

Major criteria	sub-criteria	Data Source	Description
Accessibility	Transportation, and Power network	Open street map, 2019 and local authorities	The new MIZ site should be accessible by transportation and power networks to reduce the infrastructure cost. Condition: less than 5km from the networks.
	Health facilities	Digitized from Google Earth pro, 2019	The new MIZ site should be as far as possible from the city's health facilities, especially the central hospital, for health issues.
Availability	Land parcels	Ministry of Local Administration, 2019	The potential site should be at a distance of more than 2km from the current urban boundary, taking into consideration future urban sprawl and to reduce the potential pollution impacts on citizens.
	Urban area		
	Land vacancy		All vacant land is given priority in the selection to reduce the cost of compensating owners and restructuring.
	Protected areas		These areas include the land parcels of the military base and airport, Al al-Bait University, and Zatari Refugee Camp.
Ecologic criteria	Stream network and Slope	Derived from ALOS PALSAR DEM (Alaska Satellite Facility, 2019)	To decrease the chance of pollution affecting groundwater tables, by discarded oils, paints, and other chemical poisons draining into the streams (Gratzfeld, 2003).

3.2. Developing the GIS-EIP Model

The proposed GIS-EIP model was carried out in four steps: (i) identifying the potential areas for the new MIZ site based on specific EIP criteria; (ii) determining the weight and the score values for each criterion; (iii) integrating the criteria using a map integration procedure; and (iv) evaluating potentially suitable sites for the new MIZ site. According to the proposed GIS-EIP model, the new MIZ location must meet the following criteria: (i) It should be within the ecosystem capacity; (ii) establish an interconnected system to reduce waste and water consumption; (iii) use an intelligent grid system for the exchange of waste, energy and recycling, thus, increasing the environmental capacity; (iv) adopt and use environment-friendly systems and methods to match the natural perspective of the area; and, (v) have an area greater than 0.7km^2 as shown in Table 2. The design of the selected area should be divided into four main workspaces which include an industrial area, waste management, green corridors, and urban services.

3.2.1. Identifying the Potential Locations for the New MIZ Site

To identify potential locations for the new MIZ site, several spatial masks were applied to exclude all the non-suitable regions based on the specific EIP criteria. In the first step, the existing built-up areas, Al al-Bait University and the military base, were masked out. Then, the regions within the buffer zones that were less than 0.5km from protected areas, 2km from residential areas, and 0.5km from valleys and stream network were eliminated; and the areas greater than 5km from transportation and power transmission lines and terrain that had a slope greater than 15 degrees also were excluded. Conditional if/else functions (Con; Equation (1)) were applied to exclude these regions due to several environmental, technical, safety/security, social, and economic constraints.

Con (restriction_masks,2,0, ((R)+(P) +(H) +(U) +(Pr) +(PA) + (SN)+(S) ...(1)

where R = Road network, P = Power network, H = Health centers, U = Urban area, Pr = Protected areas, SN = Stream network, S = Slope, and V = vacant. Con is a geospatial tool that performs a conditional if/else evaluation on each of the input raster variables. The value 2 represents restricted areas, and 0 represents areas that have a zero score in the evaluation of criteria layers. In Equation (1), the condition function returns areas that are not equal to 2 or 0 in the restriction masks layer, and then the other criteria inputs were combined as potential areas for the next step of suitability analysis.

Table 2. The proposed design of the new MIZ site in Mafraq city according to EIP concepts.

Type of use	Sub-use	Area	
		m^2	%
Industrial use	Gasoline	455,000	65
	Mechanical		
	Large trucks		
	Vehicle paint workshops		
	Factories		
	Water filtering		
Waste management	Oils waste	49,000	7
	Iron waste		
	Plastic waste		
	Vehicle board waste		
	Caoutchouc		
	Metal		
	Liquid material		
Green corridors	Outer green barrier	91,000	13
	Natural draining path		
	Internal green barriers		
Urban services	Service facilities	105,000	15
	Pavements		
	Logistic support		
	Parking lots and transportation		
Total area		700,000	100

3.2.2. Determining the Score Values for each Criterion and Calculating its Relative Weight

The potential areas identified in the first step were tested for their suitability as the new MIZ site. An expert knowledge-based approach (the Delphi method) was used to determine the score values, which then were used to calculate the relative weights of each criterion using Equation (2). A pairwise comparison matrix designed based on the Saaty (1994) scale of preferences (Table 3) was designed and distributed to the experts, from which the analytical hierarchy process (AHP) measures were calculated. Note that the score values for each criterion defined the spatial proportional importance of a tested location compared to the other locations within a single criterion, while the relative weight values defined the proportional importance of a specific criterion compared to the other criteria (Hazaymeh et al., 2018). For the purpose of this study, the odd score values in Table 3 were used to define the spatial proportional importance of any location. The even score values were ignored as they represented transferring strata in the scale levels. Locations/criteria were deemed more suitable when they had higher scores/weight values depending on their relative importance when computing the final suitability map (Chen et al., 2010). Then, the consistency index (CI) and the consistency ratio (CR) were calculated using Equations (3) and (4), respectively, to measure the inconsistency associated with the pairwise comparison matrix. As a rule of thumb, when the CR value was less than or equal to 10%, then the pairwise matrix was considered consistent, and the relative weight values could be used for further suitability analysis.

$$W_i = \frac{\sum V_{ij}/S_j}{n} \quad (2)$$

$$CI = \frac{\lambda_{max} - P}{P - 1} \quad (3)$$

$$CR = \frac{CI}{RI} \quad (4)$$

where, is the relative weight for criterion (i), is the value of criterion (i) in column (j) in the pairwise matrix, is the sum of column (j), and n is the number of criteria. is the largest eigenvalue that can be obtained once its associated eigenvector is identified (this value is obtained from applying and calculating the AHP matrix.); P is the number of columns of the pairwise matrix. RI is the random inconsistency index as defined in Table (4).

Table 3. Saaty scale of performance used for generating the pairwise comparison matrix of AHP in this study.

Description	Score Value
equally suitable	1
slightly more suitable	3
strongly suitable	5
very strongly suitable	7
extremely suitable	9
intermediate values	2, 4, 6, 8

Table 4. Random inconsistency indices (RI) used for calculating the consistency ratio associated with the AHP pairwise comparison matrix.

n criteria	1	2	3	4	5	6	7	8	9	10
RI	0	0	0.58	0.9	1.12	1.24	1.32	1.41	1.45	1.49

3.2.3. Integrating the Criteria Using the Index Overlay Method

All the input maps were converted into raster format to allow for map integration. The raster format is a grid commonly used to represent spatial continuous surfaces with varying values, and is considered a simple and flexible spatial data structure to perform map overlay and integration (Reddy, 2018). To accomplish this, the Euclidean distance function was used to generate arbitrary distance classes from each feature in the input layers, which included transportation, railway, power network, health facilities, stream network, and land parcel layers. The feature to raster function was used to convert the land parcel layers to raster format based on their attributes. These raster layers were then numerically standardized (reclassified) according to the score values obtained from the previous step (Section 3.2.2). Table 5 summarizes the score values of the standardization process. Finally, the suitability of each pixel (location) in the output suitability map for locating the new MIZ site was calculated using the index overlay method as in Equation (5). Note that the value of each pixel in the output suitability map represents the cumulative importance of the integrated scored pixel in the input maps which could be represented in more than two gradual classes of importance (Kamali et al., 2017; Rikalovic et al., 2014; Moghaddam et al., 2014).

$$Z_{ij} = \frac{\sum_{k=1}^{n} w_k * (C_{ij})_k}{\sum_{k=1}^{n} w_k}$$

where; Z_{ij} is the suitability index score value of pixel ($_{ij}$) in the final output map; $(C_{ij})_k$ is the corresponding score value of pixel $_{(ij)}$ in the criterion $_{(k)}$ of the input scored map; W_k is the weight value of criterion $_{(k)}$; (n) is the number of input criteria.

Table 5. Score values and their respective cut-off threshold proximities (intervals) used in the standardization process for each input layer in the index overlay method.

	Input Layers							
	Cut-off threshold distance values in meters							
Score value	Transport-ation	Utilities network	Health centers and schools	Urban area	Protected areas	Stream network	Slope°	Vacant land
9	100-200	100-200	>5000	>5000	>10000	>1000	< 5	9
7	200-400	200-400	4000-5000	4000-5000	7000-10000	700-1000	5-7	
5	400-700	400-700	3000-4000	3000-4000	4000-7000	400-700	7-10	
3	700-1000	700-1000	2000-3000	2000-3000	2000-4000	200-400	10-13	
1	>1000	>1000	1000-2000	1000-2000	1000-2000	100-200	13-15	
0	<100m	<100m	<1000m	<1000m	<1000	<100m	>15	

4. Results and Discussion

4.1. The Potential Regions for MIZ Sites

The potential areas for allocating the new MIZ site are shown in Figure 4. The conditional geospatial masks integrated the final outputs of the non-restricted proximities and were regained as a result of utilizing a conditional if/else function [Con; Equation (2)]. The potential map shows that approximately 5.4km^2 of the study area was identified as a potential site for relocating the MIZ, representing approximately 55.2% of the study area. These areas, thus, were used for performing further suitability analysis procedures.

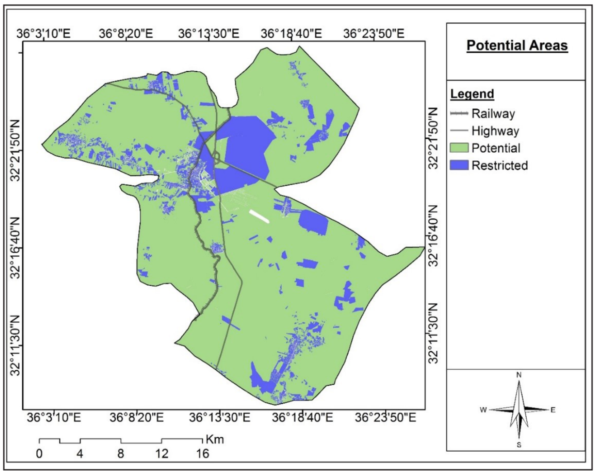

Figure 4. Potential regions for MIZ sites in Mafraq city; the unsuitable regions show the restricted areas according to the geospatial masks in equation (2).

4.2. The Score Values for each Criterion and its Relative Weight

The Delphi method showed that all the sub-criteria could influence the selection of the MIZ site in the study area. Table 6 shows the relevant weights for each sub-criterion as calculated in the AHP matrix. It shows that the distance to the transportation network, utilities network, and vacant land variables were found to be the highest influence criteria with relative weights of 23%, 19%, and 17%, respectively. The distance to health centers, urban areas, and stream network variables had moderate relative importance with weights of 10 %, 10%, and 9 %, respectively. Distance to protected areas and slope were found to have less influence on the MIZ site selection with relative weights as low as 7 % and 5 %, respectively. UNIDO (2016) and Kamali et al. (2015; 2017) also considered transportation and utilities networks as the most suitable criteria. The consistency ratio (Cr) was found to be 8%, indicating consistent relative weights and an acceptable pairwise matrix (Table 7). Note that if the Cr values were less than the acceptable threshold (10%), the relative weights were considered valid for further suitability analysis.

Table 6. The relative weight values for each sub-criterion for selecting the new MIZ site as calculated by the AHP matrix.

Sub-criterion	Weight (%)
Transportation	23
Utilities network	19
Health centers and schools	10
Urban area	10
Protected areas	7
Stream network	9
Slope	5
Vacant land	17
Total	100

Table 7. Pairwise matrix of the eight criteria for the MIZ site selection. Values in the crossed cells represent the Saaty scale of performance for the comparison pair in row i and column j as defined in Table (3) or its replication.

Criteria	R	P	H	U	Pr	SN	S	V
R	1.00	5.00	7.00	3.00	5.00	5.00	3.00	0.14
U	0.20	1.00	7.00	5.00	3.00	3.00	3.00	0.20
H	0.14	0.14	1.00	1.00	0.33	0.33	0.33	0.11
U	0.33	0.20	1.00	1.00	1.00	0.33	0.20	0.11
Pr	0.20	0.33	3.00	1.00	1.00	0.20	0.20	0.11
SN	0.20	0.33	3.00	3.00	5.00	1.00	1.00	0.11
S	0.33	0.33	3.00	5.00	5.00	1.00	1.00	0.14
V	7.00	5.00	9.00	9.00	9.00	9.00	7.00	1.00

** R = Road network, P = Power network, H = Health centers, U = Urban area, Pr = Protected areas, SN = Stream network, S = Slope, and V = vacant land.*

The suitability analysis was accomplished by aggregating the eight layers shown in Figure 5 and utilizing the map algebra function within the geospatial model. A map was generated showing the suitable locations for the new MIZ site as shown in Figure 6. It was classified into five categories (i) equally suitable: (ii) slightly more suitable, (iii) strongly suitable, (iv) very strongly suitable, and (v) extremely suitable. The classification of the cumulative score values from the index overlay method was performed using equal interval thresholds in which the extremely suitable areas collected score values of 634-750, very strongly suitable was 515-633, strongly suitable was 398-514, slightly more suitable was 278-397, and equally suitable was 41-158. The extremely and very strongly suitable areas were found to be close to the highway and were accessible to transportation and utility networks; and as a result of their accessibility to transportation and utility networks, they were given the highest weight value among the other sub-criteria. Meanwhile, there were locations identified that were away from urban areas, hospitals, schools, and protected areas which could contribute more to the conservation and sustainable use of the environment in the city.

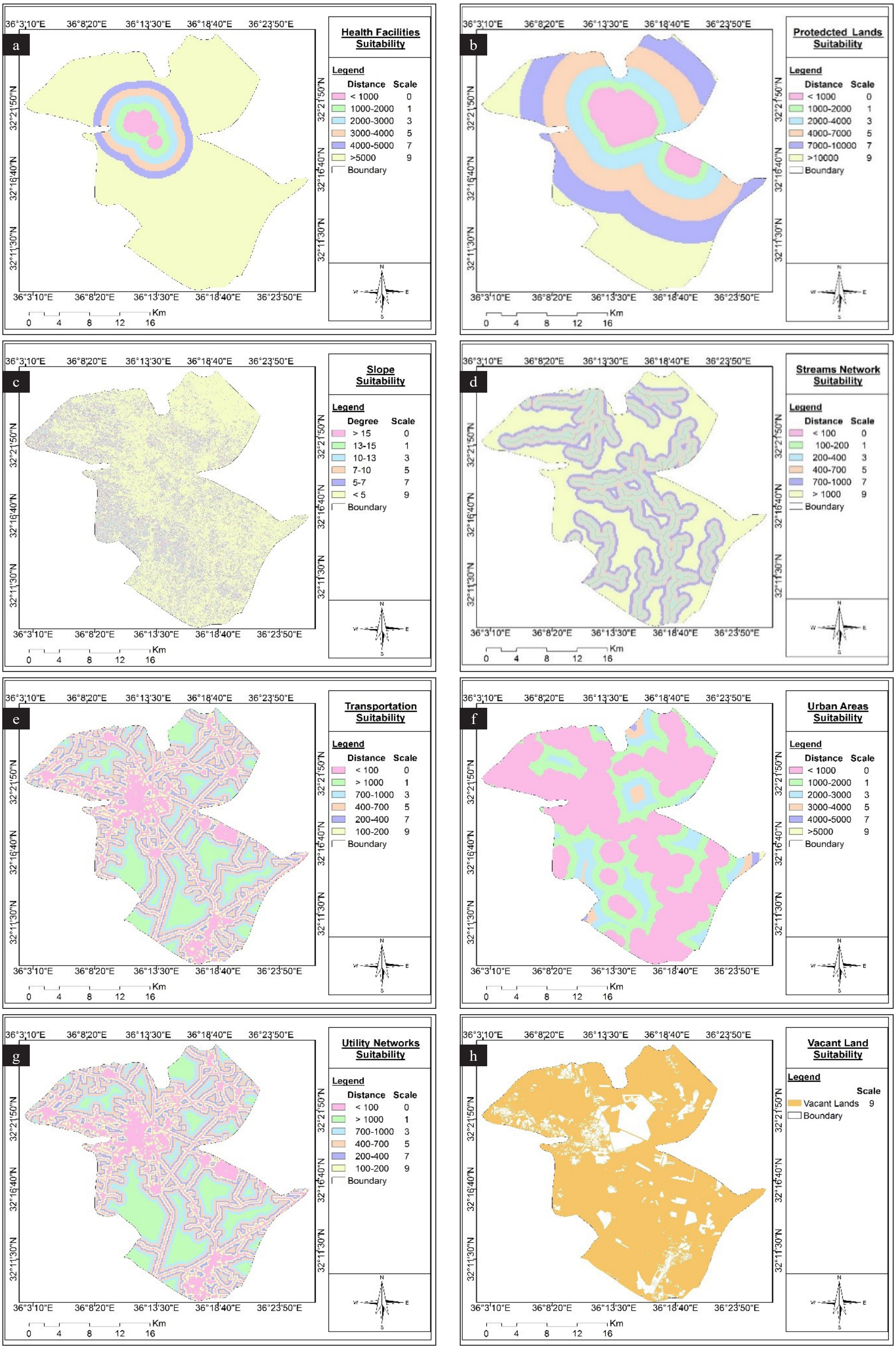

Figure 5. Suitable areas for allocating the new MIZ site in the study area according to the evaluation of each sub-criterion. (a) health facilities suitability, (b) protected lands suitability, (c) slope suitability, (d) stream network, (e) transportation suitability, (f) urban areas suitability, (g) utility network suitability, (h) vacant land suitability.

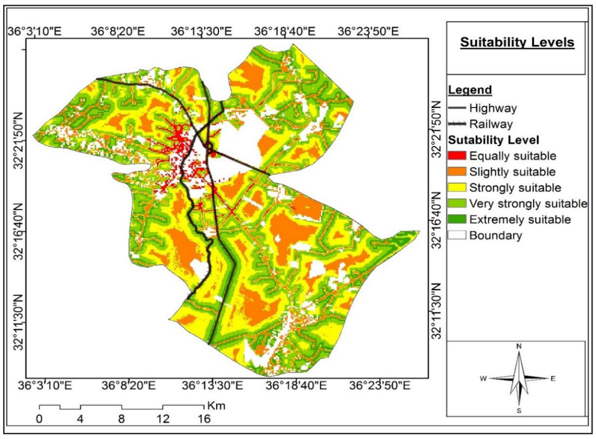

Figure 6. The spatial distribution map of suitable areas for allocating a MIZ site in the study area as a function of the weighted index overlay of the eight suitability maps of the sub-criteria.

Among the strongly suitable categories (levels 5, 7, and 9), the parcels that had (i) an area greater than 0.7km^2, (ii) a regular-shaped geometry (within a square of 1km^2), and (iii) within the vacant lands were subsequently identified as the set of optimal locations (best alternatives) for establishing the new MIZ site. As a result, 20 land parcels were identified as shown in Figure 7. Among these, parcels 1-9 were identified as preferred over the other parcels and, therefore, were designated as the optimal choices for establishing the new MIZ. These parcels offered easy access to the transportation network to the Amman-Zarqa highway that links Mafraq with these two major cities and could positively contribute to the acceleration of MIZ development. Also, the geometric shapes of these parcels were compatible with the structuring plan of the MIZ site according to the EIP principles. Parcels 13-16 were the next most appropriate as they were much closer to each other than the other alternatives, which could support potential future growth of the MIZ site, but they were not as close to the transportation network as parcels 1-9. Also note that further revision may be necessary in terms of land values and assessing the cost for possible future expansion.

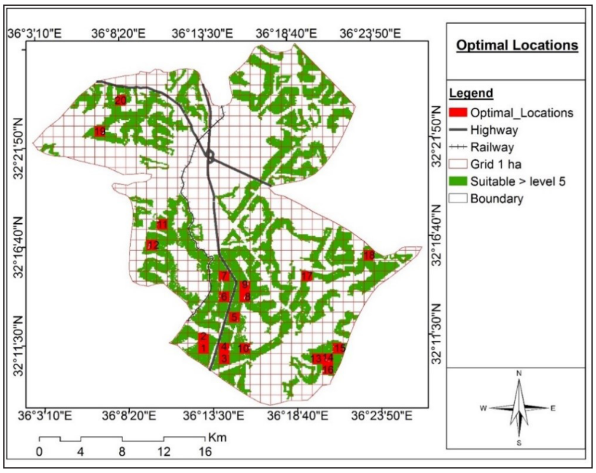

Figure 7. Map of the 20 selected optimal parcels for allocating a new MIZ site in Mafraq.

5. Conclusions

The emergence of the Eco-Industrial Park (EIP) concept has come as a much-needed solution to the growing population in global cities in terms of people and industries. The concept seeks to ensure sustainability by integrating environmental, economic, and social aspects in the planning of busy-cities. One such city is Al- Mafraq in Jordan, which is plagued by a busy mechanic industrial zone (MIZ). The city has faced several challenges due to inadequate infrastructure to accommodate people, machines, and industries. The resultant effects have been traffic congestion, land value degradation, and extreme pollution, which reduces visibility. From the study, it is evident that the implementation of Eco-Industrial Park (EIP) principles will come as a welcome addition to the city that is suffocating from its own population and industries. The implementation of EIP would involve a selection of a part of the city to be designed as the eco-industrial park, which can sustain multiple activities. The site is selected through multi-criteria decision-making (MCDM) through the involvement of strategic stakeholders of the city, including the government, residents, and industry owners. The EIP professionals would also use geographic information systems (GIS) to establish the site's viability for the industrial park. The aspects that will be considered will include accessibility, the possibility of developing recreational institutions, the terrain, and utility networks. A suitability analysis conducted in Al- Mafraq city, shows that several viable areas in the city can accommodate an Eco-Industrial Park (EIP). These conclusions have been made based on the study results, which took into consideration the requirements for the site of EIP. However, more studies need to be conducted to firmly establish the perfect part of the city that can be an EIP site. The site has to attain high suitability scores in the geological model.

Acknowledgments

The authors acknowledge Mafraq Municipality for supporting this research by providing GIS data of the study area.

References

Al-Mefleh, N.K., Al Ayyash, S.M., Bani Khaled, F.A. (2019). Water management problems and solutions in a residential community of Al-Mafraq city, Jordan. Water Supply 19(5): 1371-1380.

Al-Olemat, H. (2019). The governor instructions for stakholders to inspect valleys and streams.Retrieved 18 May 2019 http://factjo.com/news.aspx?Id=50940&fbclid=IwAR0WU3CNT9vc2SsN841__MnJcGiZ7n0Ziuq7lDW5BsdUh5Jjil3PjLA4-zQ.

Al-Shalabi, M.A., Mansor, S.B., Ahmed, N.B., Shiriff, R. (2006). GIS based multicriteria approaches to housing site suitability assessment. In XXIII FIG congress, shaping the change, Munich, Germany, October (pp. 8-13).

Arabsheibani, R., Kanani Sadat, Y., Abedini, A. (2016). Land suitability assessment for locating industrial parks: a hybrid multi criteria decision-making approach using Geographical Information System. Geographical Research 54(4): 446-460.

Bagdanavičiūtė, I. and Valiūnas, J. (2013). GIS-based land suitability analysis integrating multi-criteria evaluation for the allocation of potential pollution sources. Environmental Earth Sciences 68(6): 1797-1812.

Banar, M., Tulger, G., özkan, A. (2014). Plant site selection for recycling plants of waste electrical and electronic equipment in turkey by using multi criteria decision making methods. Environmental engineering and management journal 13(1): 163-172.

Chen, Y., Yu, J., Khan, S. (2010). Spatial sensitivity analysis of multi-criteria weights in GIS-based land suitability evaluation. Environmental modelling and software 25(12): 1582- 1591.

Conticelli, E. and Tondelli, S., (2014). Eco-industrial parks and sustainable spatial planning: a possible contradiction?. Administrative Sciences 4(3): 331-349.

Dohel, I. (2016). Eco-industrial park: creating shared prosperity and safeguarding the environment. Retrieved from https://www.unido.org/news/eco-industrial-parks- creating-shared-prosperity-and-safeguarding-environment.

Gratzfeld, J. (2003). Extractive industries in arid and semi-arid zones: environmental planning and management: IUCN Gland and Cambridge 2003.

Hazaymeh, K., Zeitoun, M., Al-Rawabdeh, A., Al-Sababhah, N. (2018). A Regional Scale Photovoltaic Site Selection Based On Geospatial Techniques. Jordan Journal of Earth and Environmental Sciences 9(1): 47-56.

Johar, A. (2013). Land suitability analysis for industrial development using GIS. Journal of Geomatics 7: 101-106.

Kamali, M., Alesheikh, S., Alavi Borazjani, A., Jahanshahi, A., Khodaparast, Z. Khalaj, M. (2017). Delphi-AHP and weighted index overlay-GIS approaches for industrial site selection case study: large extractive industrial units in Iran. Journal of Settlements and Spatial Planning 8(2): 99-105.

Kamali, M., Hosseinnia Kani, S.M., Asghar, A. (2015). Application of Delphi-AHP approach for criteria prioritization of large extractive industrial units site selection.
International Management Conference 26th June 2015 (p. 238).

Kumar, M. and Shaikh, V.R. (2013). Site suitability analysis for urban development using GIS based multicriteria evaluation technique. Journal of the Indian Society of Remote Sensing 41(2)P: 417-424.

Lowe, E. (2006). Industrial ecology—an organizing framework for environmental management. Environmental Quality Management 3(1): 73-85. DOI: 10.1002/tqem.3310030108.

Lowe, E.A., S.R. Moran, Holmes., D.B. (1998). Eco-Industrial Parks – A Handbook for Local Development Teams. Oakland, USA: Indigo Development, RPP International.

Moghaddam, M.K., Samadzadegan, F., Noorollahi, Y., Sharifi, M.A., Itoi, R. (2014). Spatial analysis and multi-criteria decision making for regional-scale geothermal favorability map. Geothermics 50: 189-201.

Open StreetMap., 2019. Retrieved 11 June 2019. https://www.openstreetmap.org/#map=13/32.3303/36.1957.

Patil, S. and Jamgade, M. (2019). Site Suitability Analysis for Urban Development Using GIS Base Multicriteria Evaluation Technique in Navi Mumbai, Maharashtra, India. International Journal of Advanced Research in Engineering and Technology 10(1): 55-69.

Reddy, G. P. O. (2018). Spatial data management, analysis, and modelling in GIS: principles and applications. In Reddy, G. P. O. and Singh, S. K. (Eds.), Geospatial technologies in land resources mapping, monitoring and management. Geotechnologies and the environment 21: 127–142. Cham: Springer. https://doi.org/10.1007/978-3-319-78711-4_7.

Rikalovic, A., Cosic, I., Lazarevic, D. (2014). GIS based multi-criteria analysis for industrial site selection. Procedia engineering 69(12): 1054-1063.

Saaty, T.L. (1994). How to make a decision: the analytic hierarchy process. Interfaces 24(6): 19-43.

Shi, H., Chertow, M., Song, Y. (2010). Developing country experience with eco-industrial parks: a case study of the Tianjin Economic-Technological Development Area in China. Journal of Cleaner Production 18(3): 191-199.

Smadi, A. (1997) Geological Map of Al-Mafraq, Map Sheet No. 3254-IV. The Hashemite Kingdom of Jordan, Natural Resources Authority, Amman.

Sqour, S., Rjoub, A., Tarrad, M. (2016). Development and Trends of Urban Growth in Mafraq City, Jordan. Architecture Research 2016: 116-122. doi:10.5923/j.arch.20160605.02.

Department of Statistics., 2020. Jordan Statistical Yearbook 2017(Vol. 68). Retrieved from http://dosweb.dos.gov.jo/DataBank/Population_Estimares/PopulationEstimatesbyLocalit y.pdf.

Steiner, F., McSherry, L., Cohen, J. (2000). Land suitability analysis for the upper Gila River watershed. Landscape and urban planning 50(4): 199-214.

Tudor, T., Adam, E., Bates, M. (2007). Drivers and limitations for the successful development and functioning of EIPs (eco-industrial parks): A literature review. Ecological Economics 61(2-3): 199-207.

UNHCR, Syria Regional Refugee Response., 2020. Jordan Statistical Yearbook 2017(Vol. 68).

UNHCR. Retrieved 11 June 2019. https://data2.unhcr.org/en/situations/syria/location/36.

UNIDO, FAO, UNDP, Italian Development Cooperation and Ethiopian Ministries of Industry, Agriculture, and Finance and Economic Cooperation, Feasibility Studies for Four Pilot Integrated Agro-Industrial Parks, as summarized in UNIDO, Integrated Agro-Industrial Parks in Ethiopia, CPC Ethiopia (2016).

JJEES

JJEES (2021) 12 (1): 81-91
ISSN 1995-6681

Jordan Journal of Earth and Environmental Sciences

Determination of Flash Floods Hazards and Risks for Irbid Governorates Using Hydrological and Hydraulic Modelling

Naheel Al Azzam and Mustafa Al Kuisi

The University of Jordan, School of Science, Department of Geology, Amman, Jordan.

Received 15 July 2020; Accepted 28 September 2020

Abstract

Irbid city has suffered from several flash floods over the past few years, which caused several damages to the infrastructure and to people's lives. In this study, an approach based on the integration of Geographic Information System, Watershed Modeling System, Hydrological Modeling System, and River Analysis System has been used to construct hydrologic, hydraulic, and floodplain models to detect the areas with the high risk of flooding. The Digital Elevation Model from Shuttle Radar Topographic Mission was used in WMS to delineate drainage networks and sub-catchments' characteristics. The hydrological modeling was carried out using rainfall data from fifteen meteorological stations obtained over thirty-eight years. The SCS curve numbers for the subcatchments were obtained for normal conditions according to the land use data and the soil types of the study area, and were calculated to be 85.7, 88.1, 83.6, 79.9, and 82.4, respectively. The peak flood discharge was calculated over 2, 10, 25, 50, 100 and 1000-Year return periods. The hydraulic modeling carried out by the HEC-RAS model is based on the hydrographs resulting from the hydrological modeling, and steady-flow simulations were performed for the return periods of 2, 10, 25, 50, 100, and 1000-Years. Different scenarios for the maximum water surface profiles were constructed for each return period for the twenty main channels in the study area. The results showed that the volume of the flooded water will exceed the wadi banks for the 100- and 1000-Year rainfall return periods and flood inundation will occur.

Keywords: Irbid, Jordan, Hydrological, Hydraulic, modeling, Flash Floods, HEC-RAS

1. Introduction

Natural hazards are events capable of causing significant damage to the natural and built environment. Flood is probably the most damaging, common, and frequent natural hazard in the world. In Dry lands such as Jordan, flash floods caused by storms of high intensity and short duration are common and are associated with heavy rainstorms which could be considered as the most frequent widespread and disastrous natural hazard in Jordan in the last decade (Youssef and Hegab, 2019). Recently, flash-flood problems in Jordan have largely increased due to different factors such as the continuous changing in land use/land cover due to inadequate enforcement laws, urbanization activities' expansion in flash-flood prone areas, low-quality constructions, and the increasing of the urbanization density. It is expected that; flood damages will increase over the years due to the previous different factors mentioned in addition to the effects of global climate change (Ibitoye, 2020). Therefore, it is necessary to define a methodology to predict flash floods in any region and predict the best method to protect the urban areas against inundations. The most common method to determine flash floods occurrence and the relationships between rainfall and runoff data is the River Analysis System (HEC-RAS) modeling (Derdour et al., 2017). Nowadays, flood hazard assessments have been improved due to the use of Geographic Information System (GIS) in integration with hydrological and hydraulic modeling. The GIS environment has the capability to extract the hydrological parameters, indispensable and morphometric characteristics from a high-resolution Digital Elevation Models (DEM), including catchments delineation, catchment shape, flow directions, slopes, longest path, and stream orders (Derdour and Bouanani, 2019). Moreover, it is necessary to make an assessment of flood-affected areas resulting from extreme precipitation and change in land use which can be helpful for a better understanding of the flood events (Derdour and Bouanani, 2019).

Non-accurate determination of rainfall and the hydrologic data and statistics are among the difficulties of estimating flood properties in basins, especially in arid regions such as Jordan. Recently, it is a routine approach to use models to simulate rainfall–runoff, to access flood properties, including time to-peak discharge. Therefore, the calibration and assessment of models are inevitable and necessary tasks. WMS is a conceptual model, which consists of different methods, including TR-55 (Technical Release 55), TR-20, SCS, and HEC-HMS (Hoseini et al., 2017).

Few studies in Jordan have dealt with flash floods using hydrologic and hydraulic modeling. Abu Islaih et al. (2020) conducted a comprehensive study and analysis of the main reasons which caused the flash flood in the Zarqa Ma'in area on October 25th, 2018. They calculated the runoff values for Zarqa Ma'in catchment area using the Soil Conservation Services (SCS) method, the hydrological modeling in Watershed Modeling System (WMS 11), and Geographic

Corresponding author email: geo2004.azzam@gmail.com

Information System (ArcGIS 10.7). Farhan and Anbar (2016) conducted a study to assess the flash flood in Wadi Yutum watershed, southern Jordan. The assessment was conducted using remote sensing and the Geographical Information System (GIS) techniques combined with geomorphic and geological field data to test the probability of the risk of flooding spatially. Al-Weshah and El-Khoury (1999) described a flood analysis model developed and calibrated for the Petra catchment, using this model, flood volumes and flows have been estimated for storm events of different return periods.

Other studies integrated the hydrological and hydraulic models with GIS to predict the flood prone areas in arid regions. Abu El-Magd et al. (2020) used a multi-criteria process combined with the Geographical Information System (GIS) and remotely sensed data to produce a flash flood susceptibility map in Awlad Toq-Sherq, Southeast Sohag, Egypt. Niyazi et al. (2020) assessed runoff and reservoir capacity of the Jazan Basin in different return periods of rainfall events based on integrations between Watershed Modeling System (WMS) and the Hydrological Modeling System (HEC-HMS) in addition to the Geographic Information System (GIS). Abu-Abdullah et al. (2020) created a flood risk management program for Wadi Baysh Dam in Jizan Region, Saudi Arabia by integrating hydrologic and hydraulic models. Derdour and Bouanani (2019) used HEC-RAS and HEC-HMS in combination with the Watershed Modeling System (WMS) and the Geographic Information System (GIS) for rainfall runoff modeling and evaluating flood plain inundation maps in Ain Sefra city, SW of Algeria. Marko et al. (2019) used the GIS, WMS and HEC-RAS programs for hydraulic simulation, to present a two-dimensional flood inundation modelling in urbanized areas in Wadi Qows, Jeddah City, Saudi Arabia. Echogdali et al. (2018) compared the results of two methods used for delineating the extent of flooding in El Maleh Basin, Morocco. The first method was based on the integration of WMS and HEC-RAS. The second method is the Flood Hazard Index (FHI) method. El Alfy (2016) integrated the Geographic Information System (GIS), remote sensing, and rainfall–runoff modeling, to assess the impact of urbanization on flash floods in the arid southwest of Saudi Arabia. Sadrolashrafi et al. (2008) integrated GIS and WMS with commercial standard hydrological and hydraulic models, including HEC-1, HEC-RAS to modulate flooding in the Dez River Basin in Iran.

Irbid city, similar to other cities in Jordan, has suffered from several flash floods over the last few years. On 26-04-2018, the Civil Defense Forces rescued 1,000 factory workers who were surrounded by water. Moreover, in Ramtha city, several houses raided by floodwaters were evacuated, while several electricity poles fell to the ground (WFP, 2019). These flash floods, have caused several damages to the infrastructures and lives. Property damage may include houses, rooms, vehicles, and other property that came in contact with flood waters, in addition, homes that were flooded can be susceptible to harmful molds. Vehicles that were submerged usually have irreparable water damage to the engine and other critical components. Therefore, reliable predictions are one of the key challenges for successful flash flood management in any catchment area (Pregnolato, 2017).

Two years ago, Jordan faced two waves of flash floods that took the lives of twenty-one people; most of which were children, near the Dead Sea. In addition, at least twelve people were killed after a heavy rainfall that triggered flash flooding in other several areas of the country, including Madaba region and Petra city, in addition, to the evacuation of nearly 4,000 tourists from the ancient city of Petra. These two accidents have raised flags for immediate actions and more focus on flash floods as a serious concern in Jordan (WFP, 2019).

2. Methods

2.1 Location and Climateq

Irbid city is located in the northern part of Jordan in Irbid governorate (Figure 1). Irbid city is one of the major cities in Jordan and the second most populated area in Jordan; 19% of Jordan's population live in Irbid governorate (DOS, 2018). Irbid governorate is approximately 1572 km^2 in size, and includes nine districts. According to the department of Statistics in Jordan, 83% of the Irbid population live in urban areas.

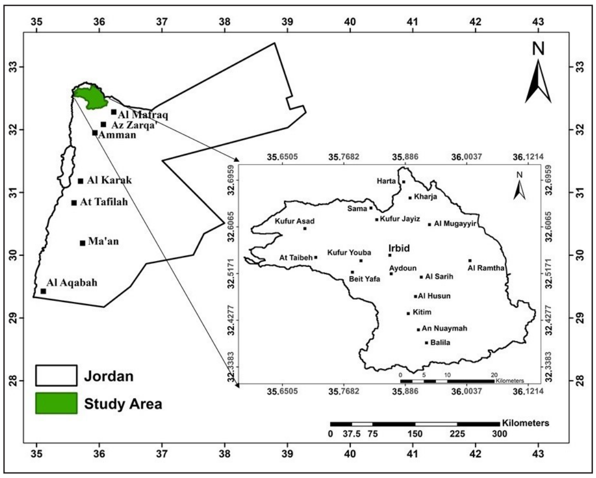

Figure 1. Location of the study area.

There are seventeen hospitals, sixteen universities and colleges, and 927 schools (DOS, 2020). Between 2015 and 2019, the total population of Irbid governorate had increased from 1.77 million inhabitants occupying around 356 thousand households to 1.92 million inhabitants occupying around 400 thousand households (DOS, 2020). The city of Irbid faced a large demographic growth and changes over the years, which involved the arrival of Palestinians, Iraqis, Syrians, economic migrants from Egypt, Asia, and elsewhere (UNHCR, 2018). In addition, many Jordanians moved there to receive education at the universities of Irbid gevernorate. The city has witnessed a significant increase in urban sprawl on agricultural areas in recent years due to the growth in population following the refugee movement from the neighboring countries of Syria and Iraq. The rates of urban expansion for Irbid governorate during the period (2003–2015) showed that the annual rates of municipal land transformation into urban area were around 1% of the municipalities' lands; 12% of Irbid lands were changed into urban area by 2015. The annual rate of land transformed into urban areas was around 1% during this period; this rate of urban expansion takes place mainly on agricultural lands. The annual loss of Irbid's agricultural lands is about 2% (Al-Kofahi et al., 2018).

The climate of Irbid region is classified as semi-arid, with cold, rainy winters and dry, warm summers extending from May until October. The mean annual temperature is around 24 °C in the summer season, and about 8 °C during winter (Abdulla and Al-Qadami, 2019). The average annual precipitation ranges between 488 mm over the highlands to the west and southwest of Irbid, and 156 mm to the East (near Mafraq). The potential evaporation ranges from 2000 mm/year in the northwest, to 2400 mm/year in the southwest of the catchment (Hyarat, 2016).

The study area is about 1170 Km^2 which covers 74.5% of Irbid governorate. This area resulted from the watershed delineation of the Digital Elevation Model (DEM) using the WMS software package V.11. Figure (2) shows the DEM with 12.5m resolution from Shuttle Radar Topographic Mission (SRTM) dataset. The elevations in the watersheds of the study area range from around 267 m below sea level (bsl) in the western parts to 1194 m above sea level (asl) on the southwestern highlands near Ajlun area. As the slopes vary between 0-43°, the plain surfaces with slopes less than 4° occupy the eastern parts and cover more than 50% of the area. The land surfaces with slopes greater than 20^o are found in the mountainous regions in the North (next to Hartha and Kharja) and to the West of the study area; they are mainly oriented North and Northwest as shown in Figure (3).

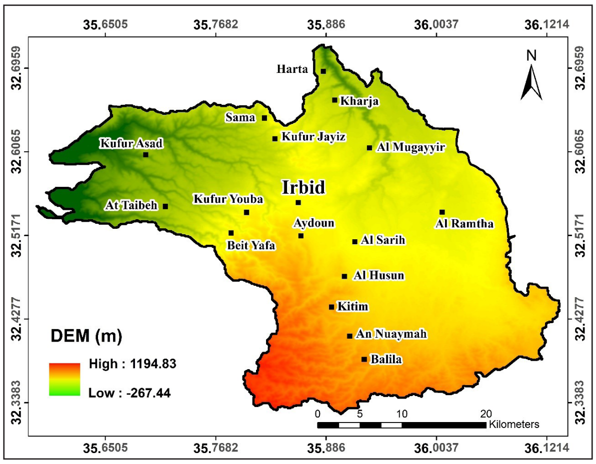

Figure 2. Digital Elevation Model of the study area.

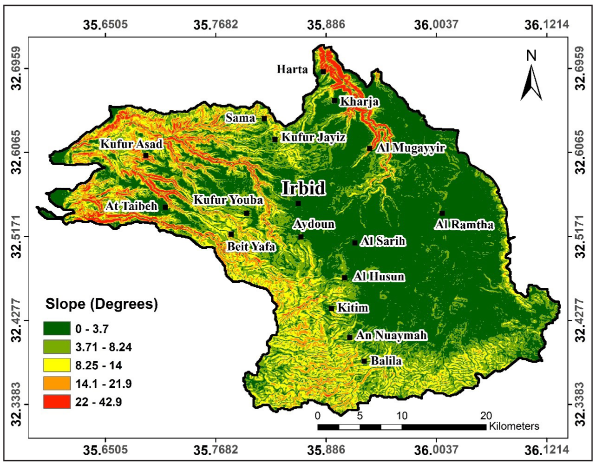

Figure 3. Slope map of study area.

2.2 Land Use Land Cover Cover and Soil

A land use land cover map of the study area was prepared on the basis of a google earth map of 2019, and was reclassified as shown in Figure (4). Most of the land is field crops covering 26.1% of the study area, forests cover 9.4%, tree crops cover 16%, the urban fabrics cover 24.3%, the pastures cover 17%, bare rocks cover 3.6%, bare soil covers 3.5%, and the remaining 0.1% area is water bodies (Wadi Al-Arab dam). The urban areas with high population densities are mainly located in the middle and northeastern parts of the study area, while the remaining parts of the study area are charecterized by a low population density.

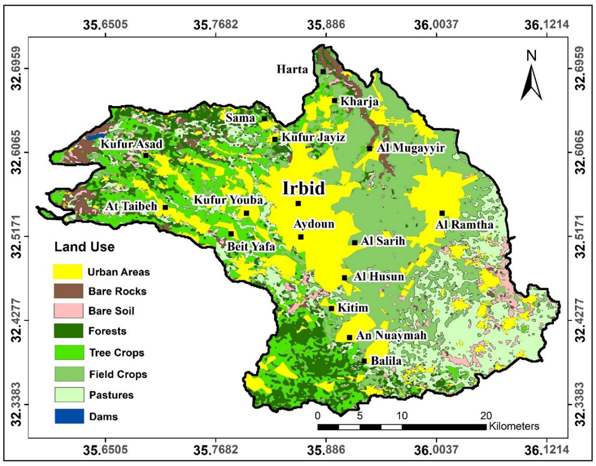

Figure 4. Land use map of the study area based on a google earth map of 2019.

The soil map of the investigated area was prepared after a detailed study of the soil profiles created by the Ministry of Agriculture for the study area. According to the classification of soils from the Ministry of Agriculture in Jordan there are seventeen nomenclature soil types (HTS and SSLRC, 1993). However, the Ministry of Agriculture in Jordan have created and produced three levels of soil maps. The soil map for the study area was taken from level 1. According to level 1 soil map, there are eight soil types present in the study rea. Moreover, these soil types were reclassified according to their texture in order to be used for the SCS curve number method (Figure 5). After that, each type of soil was assigned to its hydrological soil group created by US Soil Conservation Service (SCS) depending on permeability and infiltration and the resulting four groups are A, B, C, and D (SCS, 1986). The final soil map according to the Hydrological Soil Groups (HSG) is shown in Figure (6).

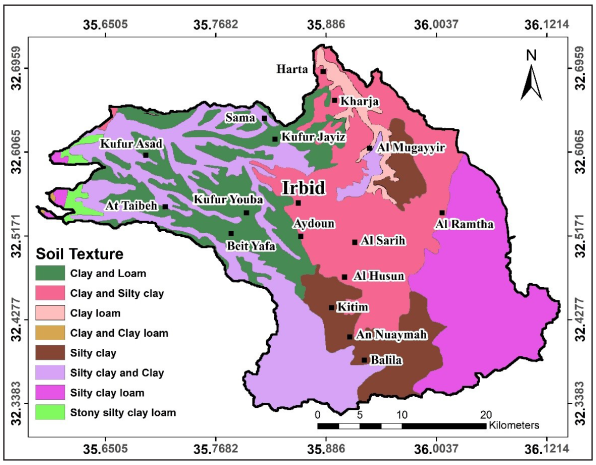

Figure 5. Soil textures map of the study area.

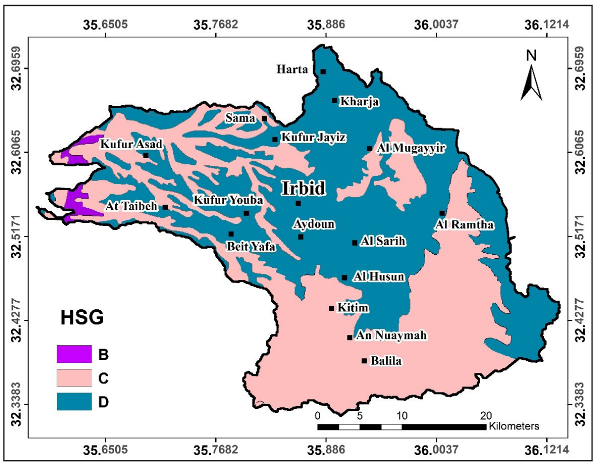

Figure 6. Hydrological soil map of the study area.

2.3 Geological and Hydrogeological Setting

A sequence of more than 1000m of sedimentary rocks is well-exposed in the study area ranging in age from Upper Cretaceous to Recent. This sequence is subdivided into many geological formations, as described in the detailed geological maps (1: 50,000) produced by the Geological Mapping Division in NRA. According to geological maps (Irbid 3155(II) and as Shuna Ash Shamaliyya 3155(III)) in 1:50,000 scale acquired from Natural resources authority, the study area is mainly dominated by sedimentary rocks of Late Cretaceous (Turonian) to Quaternary (Pleistocene). The sedimentary rocks are comprised mainly of limestone, chalky marl, chert, bituminous marl, phosphate, and Quaternary terrace, and river bed deposits. The later sediments are mainly composed of sand, silt, clay, debris of chalky marl and basalt of Quaternary to Neogene in age (Moh'd, 2000) as shown in Figure (7).

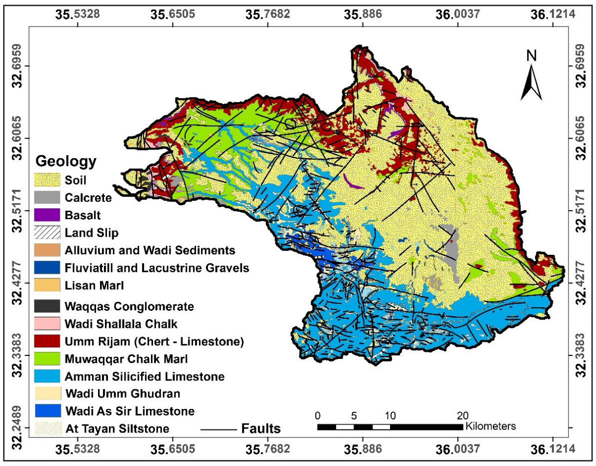

Figure 7. Geologic map of the study area (modified after Moh'd, 2000).

The study area is bounded to the west by the Jordan valley, a segment of the major rift structure recognizable from east Africa to South Turkey where a sinistral movement took place during the last 27 MA, with a proven horizontal movement slightly exceeding 100 km (Abed, 2000 and Moh'd, 2000). Regional dips are a few degrees towards the north, northeast, and northwest; high westerly dips accompanying the north-south step faulting associated with the rift formation are well-expressed in the western parts of the study area especially the Miocene Waqqas Conglomerate Group.

From a hydrogeological point of view, the main aquifer systems in the study area are: Wadi Shallala/Umm Rijam (B5/B4) and Amman/Wadi Es Sir Formations (B2/A7). These two aquifers are of excellent potential and are characterized by many wells for drinking and agricultural purposes.

3. Methodology

This study presents the application of Geographic Information Systems (GIS), Hydrologic and Hydraulic Models (WMS, HEC-HMS) to construct a hydrological model due to potential flash- flood hazards and to understand the relationship between rainfall depth and flood hazards at different return periods. The proposed methodology is listed through the next steps:

1- Catchment delineation, stream networks, and their characteristics by DEM processing, using ArcGIS and WMS modeling.

2- Finding out the CNs and the Intensity Duration Frequency (IDF) curves to be used in calculating the peak discharge.

3- Modeling rainfall/runoff relation, using HEC-HMS modeling in WMS, and extracting the unit hydrographs for different return periods (2, 10, 25, 50, 100, and 1000-Years).

4- Creating triangulated irregular network TIN for the study area using WMS.

5- Extracting cross-sections from the TIN in WMS.

6- Creating a conceptual model such as the river reaches, the stream centerline, the main channel banks, the cross-section lines, and the material zones which are called channel geometry using WMS.

7- Importing the results to be used as input data in hydraulic model HEC-RAS.

8- Defining the network schematic on HEC-RAS using Manning's roughness coefficients (n).

9- Applying a steady flow data which consists of peak discharge information, the reaches of boundary conditions, and flow regimes to compute the water surface elevation along the channel geometry.

10- Creating flood elevation maps with different return periods.

The conceptual framework for the methods used is explicitly defined in Figure (8).

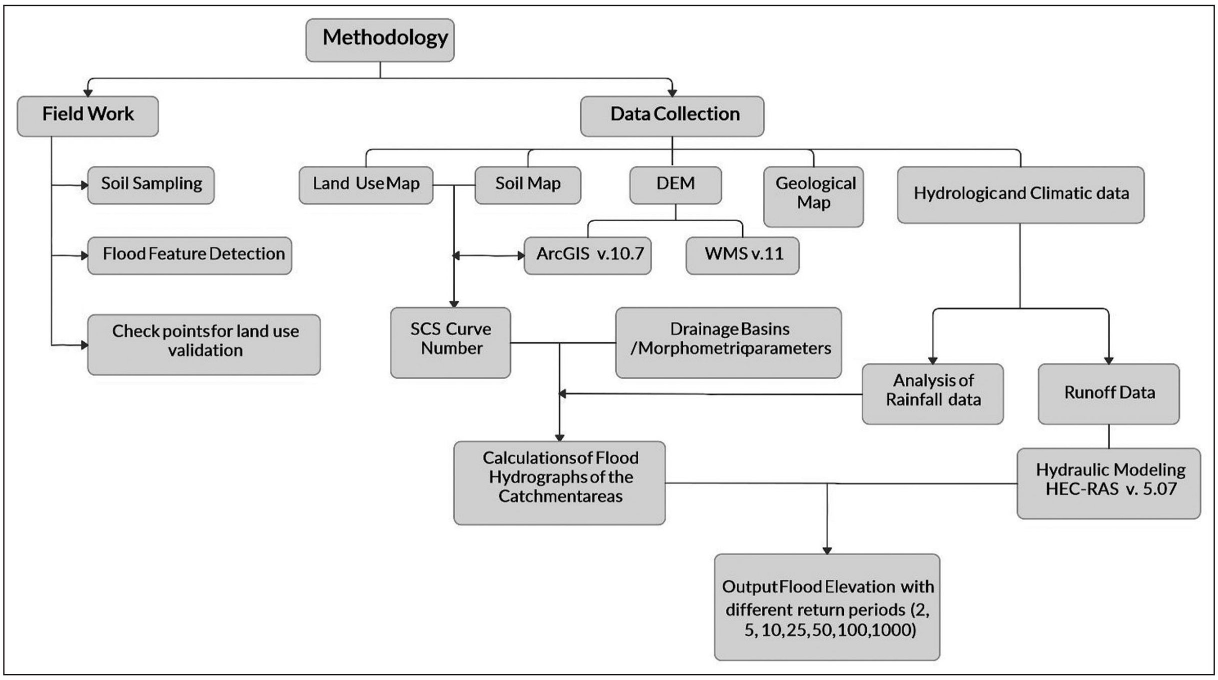

Figure 8. Schematic working flow of the used methodology.

4. Results

4.1 Catchment Delineation and Their Characteristics

To generate rainfall-runoff models, comprehensive information of the study area is required, including the topographic map to delineate drainage networks, catchment boundaries, flow paths, slopes and reach lengths, the WMS software was used to extract these parameters. The study area has been divided into five sub-catchments (B1, B2, B3, B4, and B5) as shown in Figure (9). The morphometric parameters of the sub catchments are shown in Table (1).

Table 1. Morphometric characteristics of the sub-catchments.

Sub-Catchment	Sub-Catchment Area Km^2	Maximum Flow Distance (m)	Sub-Catchment Slope (m/m)	Maximum Flow Slope (m/m)
B1	448.62	66644.32	0.0923	0.0164
B2	351.49	52641.71	0.0500	0.0172
B3	276.26	41969.26	0.1415	0.0261
B4	29.52	14130.75	0.1503	0.0450
B5	64.03	37052.09	0.1788	0.0346

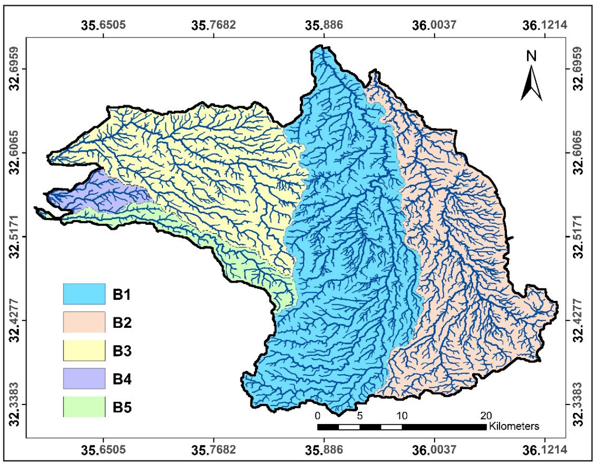

Figure 9. Sub Catchments of the study area.

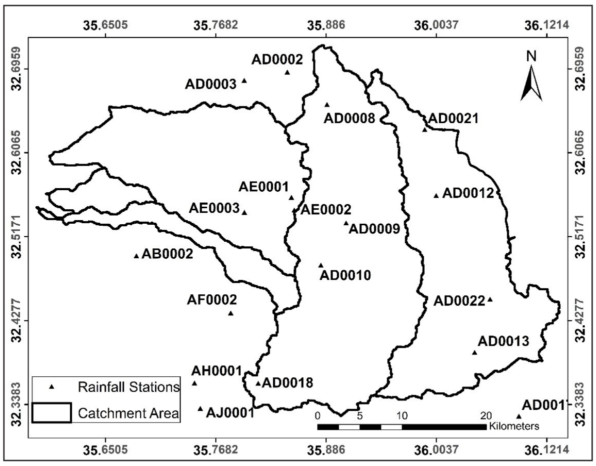

Figure 10. Rainfall Stations within and surrounding the study area.

4.2 Rainfall Frequency Analysis

The daily rainfall data for seventeen rainfall stations located inside and outside the study area were obtained from the database of the Ministry of Water and Irrigation (MWI). The location of rainfall stations is shown in Figure (10).

The daily rainfall data extends from 1980 to 2017, where the long-term average was calculated for each rainfall station. However, only fifteen rainfall gauge stations were selected to study and to be compared the climatic indication from meteorological parameters. During the past two decades, there was an increasing trend in the rainfall amounts from east (ie: Hosha 156 mm/yr) to north west (Kufur Youba 457mm/yr) and south west (Rihaba 489mm/yr) for the study area. The highest average annual rainfall was registered at Rihaba Station (488.91 mm), whereas the lowest was recorded at Hosha Station (156 mm). In Hosha Station, there was a gradual decrease in the amount of precipitation over the last three decades, however there was an increasing trend in precipitation during the last ten years. Its maximum rainfall recorded was in 2013 with the amount of (327) mm. Moreover, in Kufur Youba Station, the trend of the rainfall data indicates a decrease in annual precipitation during the last three decades and its maximum rainfall recorded was 773 mm in 1992. In Rihaba Station, there is a gradual increase in the rainfall during the period (1982-1992) with a maximum rainfall of 1092.5 mm recorded in 1992. After that, during the last twenty-five years, there was a decrease in precipitation amounts. It is not surprising to see that precipitation was declining during that period as a result of climate change impacts which were very pronounced by the increasing desertification and the potential of sand and dust storms (SDS) in the region (Atashi et al., 2020).

The 3, 5, 7, 9, 11-year moving averages were calculated for each station. The eleven-year moving average mostly behaved as the long-term average line as shown in Figure (11).

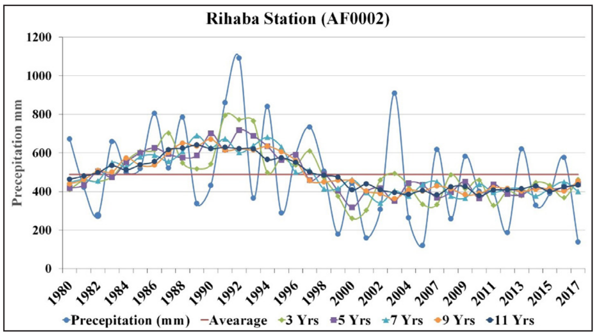

Figure 11. Moving averages calculated for Rihaba Station rainfall data.

The areal distribution of rainfall over the catchment areas was calculated by using the annual average rainfall for all rainfall stations and was illustrated by Isohyetal and Theissen polygon methods as shown in Figure (12 a and b). The WMS v.11 software has used the theissen polygon to calculate the maximum flood discharge in this study by taking the gauge weights.

It is clear that the rainfall records in the middle and west regions of the study area show high amounts of precipitation, while in the eastern parts there is a decreasing trend in the amount of precipitation (Figure 12 a). However, in the last ten years in the dry regions east of the study area, precipitation amounts show an increasing trend. This high precipitation rates can be attributed to the consequences of climate change and the thunder storms characterized by high precipitation intensities with short periods.

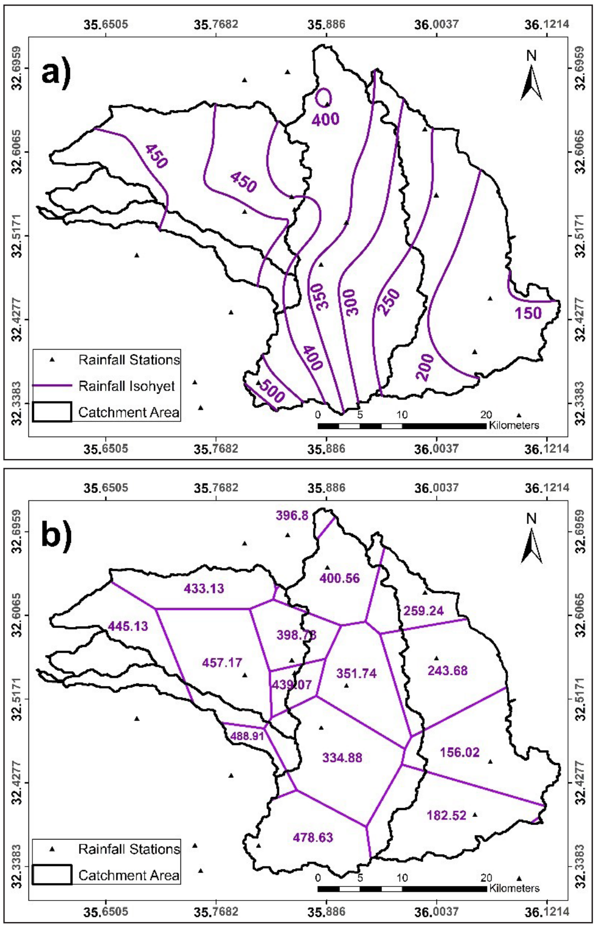

Figure 12. (a) Isohyetal and (b) Theissen polygon maps.

The rainfall Intensity-Duration-Frequency (IDF) curves show a graphical presentation of the possibility that certain rainfall intensity, duration, and return period will occur with similar characteristics. The IDF Curve is a graphical representation of the probability that a rainfall with a specific intensity and duration will occur within a given period of time. It is used to determine the frequency of a given precipitation in terms of its intensity and duration (Dupont and Allen, 1999). The daily rainfall depth and maximum records of rainfall stations are available over thirty-eight years for the seventeen gauge stations inside and outside the five sub-catchment area. Therefore, IDF curves were constructed using data from all stations and covering the period of 1980-2017. The IDF computations and IDF-curves were prepared for all rainfall stations; however, Irbid School Station was taken as an example and is illustrated in Table (2) and Figure (13).

Table 2. Rainfall Intensity (mm/min), Duration and Frequency at Irbid School Station.

Return Period	Duration (min)									
	5	10	20	30	60	120	180	360	720	1440
2	93.52	58.92	37.12	28.33	17.84	11.24	8.58	5.40	3.40	2.14
5	136.72	86.15	54.26	41.41	26.09	16.43	12.54	7.90	4.98	3.14
10	165.33	104.17	65.62	50.08	31.55	19.87	15.17	9.55	6.02	3.79
25	201.47	126.94	79.96	61.02	38.44	24.22	18.48	11.64	7.33	4.62
50	228.28	143.84	90.60	69.14	43.56	27.44	20.94	13.19	8.31	5.24
100	254.90	160.61	101.17	77.21	48.64	30.64	23.38	14.73	9.28	5.85
1000	342.84	216.02	136.07	103.84	65.42	41.21	31.45	19.81	12.48	7.86

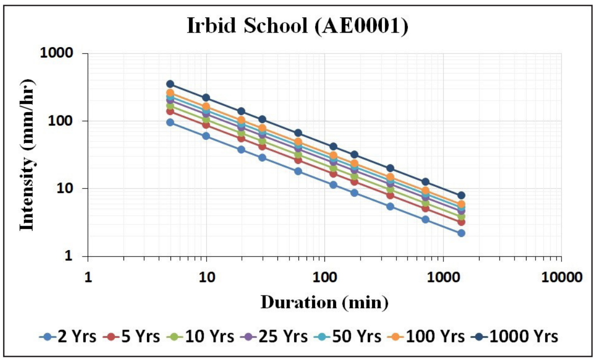

Figure 13. IDF Curve for Irbid School Station (Authours calculations).

4.3 Rainfall-Runoff Model Approach

The SCS curve number method is the most commonly used and efficient rainfall-runoff method for estimating the amount of runoff generated from rainfall data in any area. The method can be used to find average annual runoff values. The curve number is based on the area's hydrologic soil group, land use, and other factors affecting runoff and retention in a watershed and its values. The Curve Number (CN) is a dimensionless number defined as $0 \leq CN \leq 100$. For impervious and water surface CN=100, for natural surface $CN \leq 100$. The curve numbers for the five sub-catchments B1, B2, B3, B4, and B5 were calculated to be 85.7, 88.1, 83.6, 79.9, and 82.4, respectively. It is worth mentioning that when the precipitation storm/event is less than the computed initial abstraction (Ia), no runoff exists.

The standard SCS curve number method (SCS, 1986) is based on the following relationship between rainfall depth (p) and runoff depth (Q):

$$\boldsymbol{Q = (p - 0.2S)^2 (p + 0.8S)} \quad \text{.......................... (1)}$$

Where:

Q = the runoff depth (mm)

P = the precipitation depth in the same unit of the runoff (mm)

Ia = the initial abstraction (mm) =0.2S

S = the total losses of the rainfall depending on soil type (mm) and it can be found by the following equation:

$$\boldsymbol{S = \left(\frac{25400}{CN}\right) - 254} \quad \text{....................................... (2)}$$

The results of the computations of rainfall runoff relations discussed in the methodology are presented in Figure (14), which shows the annual runoff data for thirty-eight years (1980-2017) representing one of the main stations in the area, Irbid School Rainfall Station where the average runoff is equal to 65.62 mm/year.

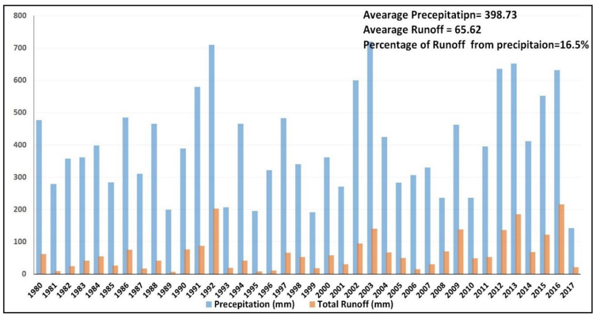

Figure 14. Annual precipitation and runoff, runoff percentage from Irbid School Station.

4.4 Unit Hydrograph

The unit hydrograph approach is used in this study to determine the peak discharge and its magnitude values. Results obtained by applying these applications are acceptable for hydrological simulation purposes. The unit hydrograph represents the catchment response to collect a unit rainfall excess of D-hour duration to produce the direct runoff hydrograph. By using the necessary basin parameters for running the hydraulic model, the peak flood discharge was estimated using HEC-HMS, SCS methods. The UH is multiplied by the effective rainfall out of the design storms at different return periods in order to produce the runoff hydrographs. The peak flood discharge was calculated by considering 2, 5, 10, 25, 50, 100, and 1000-Years return periods. Figure (15 a, b, c, d) shows results for sub-catchment B1 obtained using a fore method for different return periods. Figure (16) shows the peak flood discharge calculated considering the 2, 5, 10, 25, 50, 100 and 1000-Year return periods in different durations over twenty-four hours in sub-catchment B1.

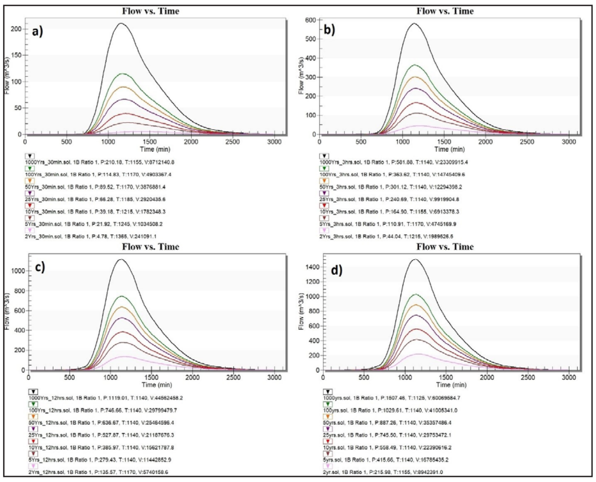

Figure 15. Unit hydrographs show the peak flood discharge estimated using HEC-HMS, SCS methods in sub-catchment B1 for different return periods in: a) 30 min. b) 3 hrs. c) 12 hrs and d) 24 hrs.

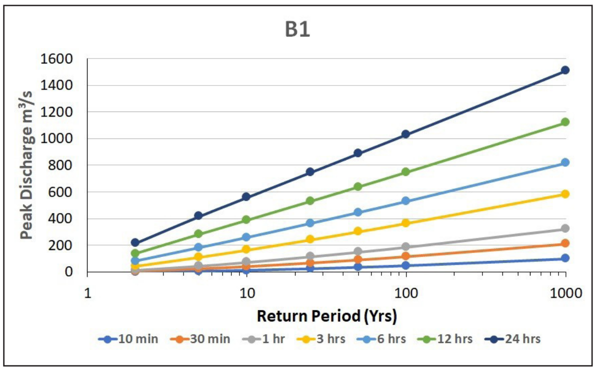

Figure 16. The peak discharge (m^3/s) in different durations and return periods in B1.

4.5 Hydraulic Modeling Results

The hydraulic model (HEC-RAS) requires information about channel and floodplain geometry and Manning's roughness values. In this study, the input data for HEC-RAS were prepared using WMS and HEC-HMS. HEC-RAS represented the structure of the channel networks by a series of interconnected reaches. Three main geometry data required for HEC-RAS, consists of stream center line, main channel banks, and cross section cut lines. Twenty main channels divided into sixty reaches with well-defined junctions were extracted from the DEM in urban areas in the study area. Cross sections were constructed manually perpendicular to the flow lines of channels as shown in Figure (17). The twenty channels' networks and cross-sectional profiles were exported from WMS into HEC-RAS. The HEC-RAS model was run with detailed channel networks. It computes the depths based on the peak discharge computed by HEC-HMS at the determined cross sections and conducts interpolations along the reaches (Derdour and Bouanani, 2019).

The peak discharge data for each catchment was calculated with HEC-HMS, and were used as an input to the HEC-RAS for modelling water depths along the flood path. Data from all return periods, were imported and calculated by WMS. In HEC-RAS, the flood path is defined through about 1000 cross-sections extracted from the TIN of the study area. The initial model has on average 1 profile every 500 m. To have an even finer space step, cross profiles were created by interpolation of the extracted profiles, and a profile was added as soon as the distance between two profiles exceeded 200 m, so the flood path is defined through 40-45 cross-sections in each channel.

To make this study valuable for researchers, one example was taken for flood inundation plains, named Irbid A Channel, which represents an urban area upstream downtown zone located to the east of Irbid city (between Bushra and Hawwara). The cross-sections width ranges between 500 and 600 m for the main channel. Roughness coefficients (Manning n-values) were assigned to each cross-section in WMS, HEC-RAS. Coefficients were assigned using aerial photographs of the wadis, verified or adjusted by field observations and were almost determined based on the field visits. The USGS Guide for selecting Manning Roughness coefficients (Manning's n) for natural and flood plain was used in the study area. Roughness coefficients (Manning's n) used in the study area were 0.03 for river area, 0.10 for agriculture area, 0.08 for the urbanized area, and 0.04 for bare soil. In addition, the normal depth was the channel segment slope, and the flow regime in HEC-RAS is set to be mixed (Arcement and Schneider, 1989; Echogdali et al., 2018). The upstream and the downstream boundaries condition is set as a normal depth. After fulfilling all the input data and boundary conditions in HEC-RAS, the simulation was done as a steady-state analysis.

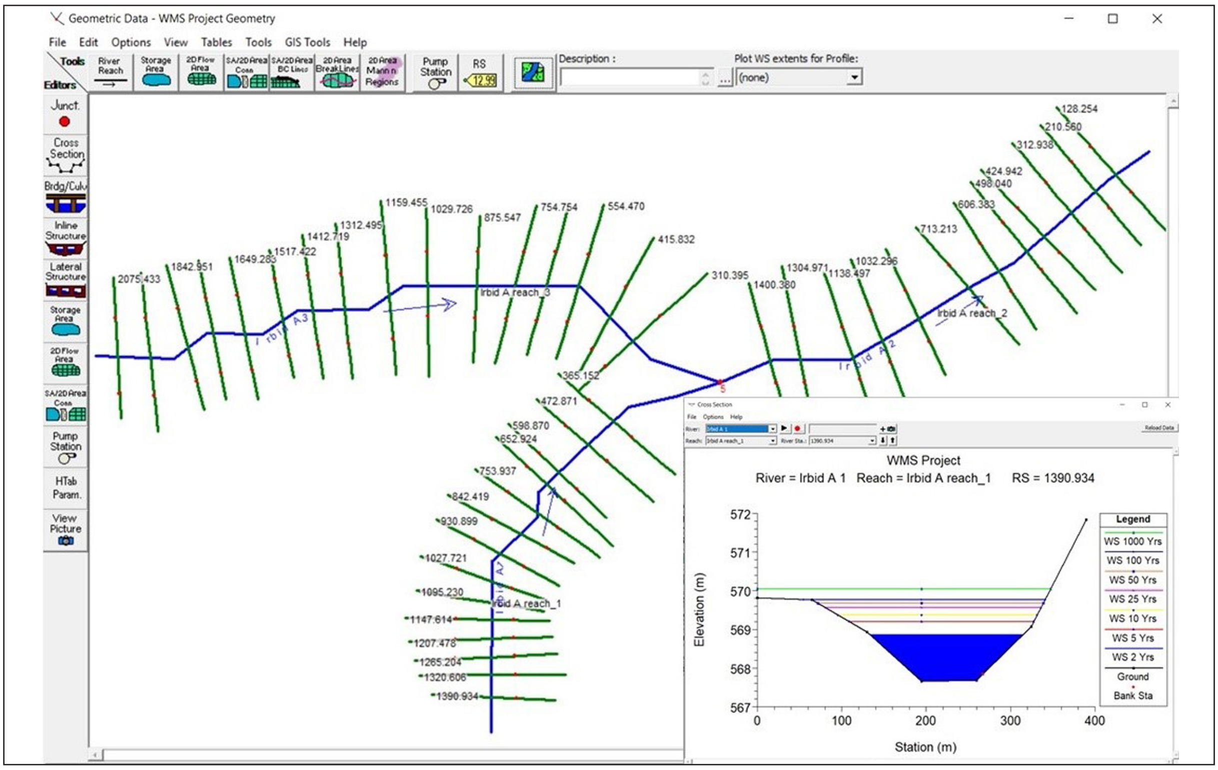

Figure 17. One of the channels and perpendicular cross sections in Irbid city (Irbid A channel).

Based on the hydrographs resulting from the rainfall runoff model, steady-flow simulations were performed for the return periods of 2, 10, 25, 50, 100, and 1000-Years. The peak discharge calculated by HEC-HMS was entered into HEC-RAS; the results were imported and prepared by WMS for all return periods. HEC-RAS interpolate the results of water-surface elevation data and delineate the flood inundation, as shown in Figures (18 and 19). This calculation revealed that the region most affected by the flood is both upstream and downtown areas that is marked by low altitudes. The water depth in this area exceeds 2.43 m downstream for a two-Year flood and maximum depth of 3.3 m for 1000-Year flood. Moreover, the width of the flooded areas reached during the 100-Year flood and 1000-Year flood was 400 m and the 430 m, respectively. It is clear that the volume of the flooded water will exceed the wadi bank for the 100- and 1000-Year rainfall return period and flood inundation will occur.

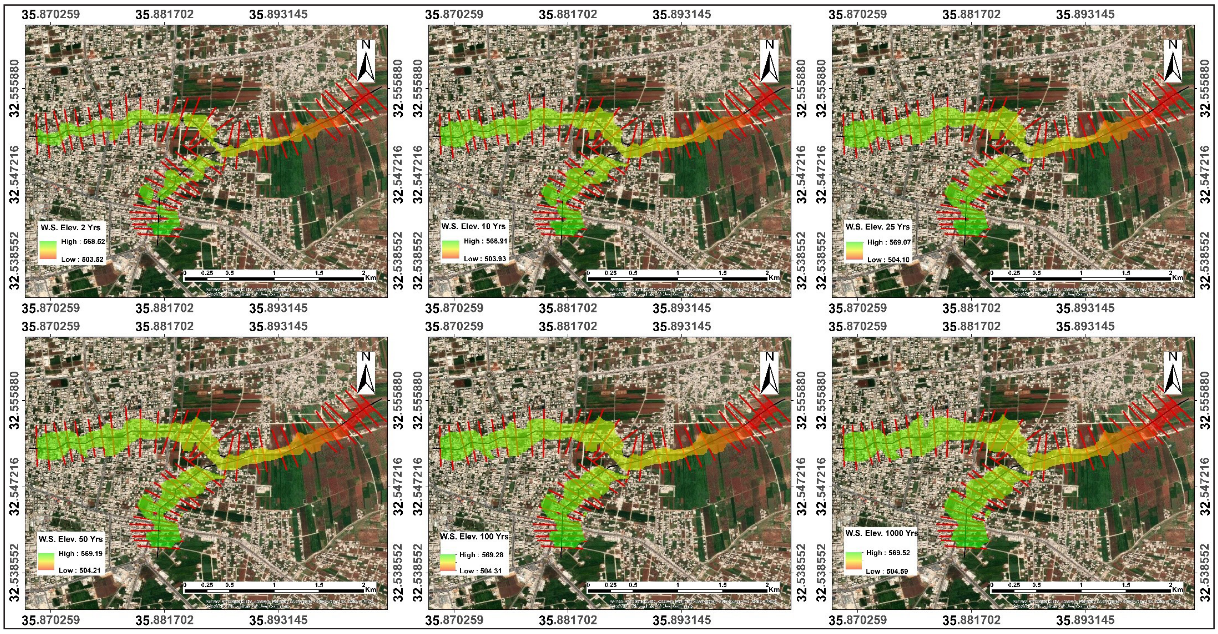

Figure 18. Flood inundation map, surface water elevation for Irbid (A) channel (return period 2, 10, 25, 50, 100, and 1000-Years).

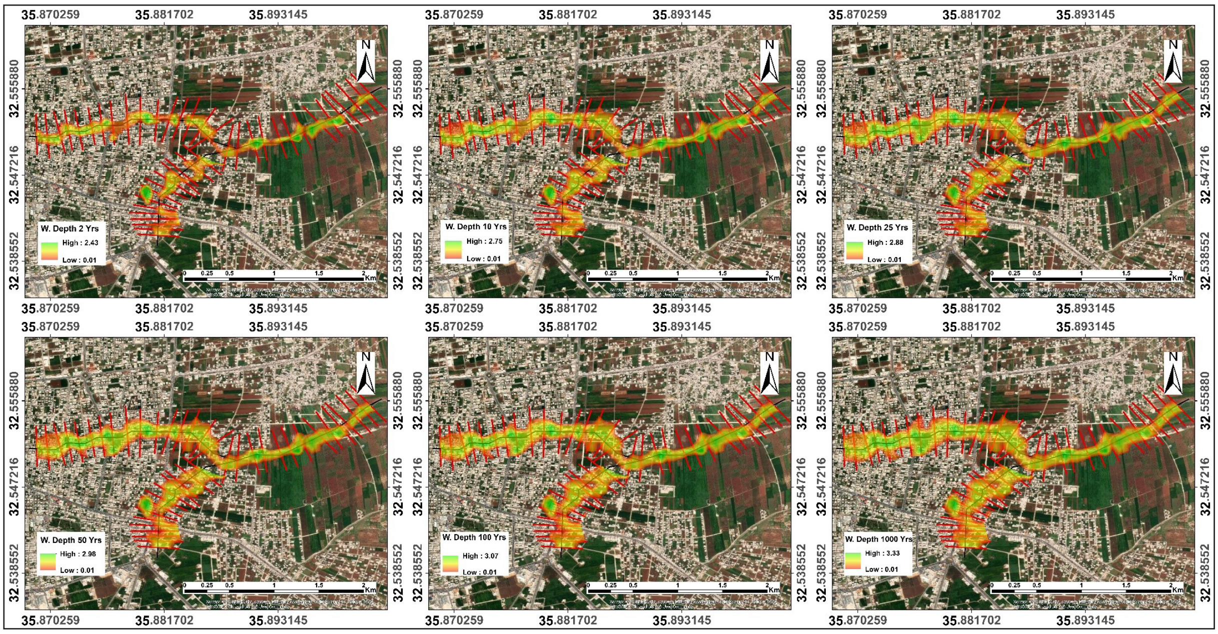

Figure 19. Flood inundation map, water depth for Irbid (A) channel (return period 2, 10, 25, 50, 100, and 1000-Years).

5. Discussions

The findings of flood depth assessment as indicated in Figure 19 revealed a significant increase in inundated areas in the study area. An increase of 2.4m (2-Yr) and 3.3m (1000-Yr) was detected in the area with flood depths greater than 0.9 m. As a result of the climate change impacts characterized by the intensification of rainfall, the inundated areas will increase. Heavy and extreme rainfall represented by an exceedance of the average rainfall level can result in flooding. Irbid area is characterizing by flat area morphology with low slopes, a high population density, and intensive urban growth. In fact, heavy or persistent rains in the catchment area or the upper regions of the drainage system can lead to an excess of water in the wadis and can create floods downstream. In addition, the growth of inundated areas will lead to an increase in the risk of the exposed built-up areas to flood. The increase in built-up areas will lead to an enhanced exposure of assets to flood water. The hydrologic modeling shows that flooding caused by more frequent rainfall events (with a smaller return periods and durations) is exacerbated more by urbanization than by large storm events. This can be seen more clearly in the southern and middle of the watershed, which might experience an increase in the discharge caused by the 2, 5, 10-year storms if fully urbanized. Urbanization, in general, will increase the peak discharge, the runoff volume, and the extent of the flooded area within a catchment. For urban areas, this means that more streets and built areas will be flooded and inundated as shown in Figure 20.

Figure 20. Inundated street in Irbid (A) channel area.

The impact will also depend on the terrain. For steep areas, the flooding will last for a shorter duration, but water velocities will be high. This can cause the vehicles on the streets to be swept away and may cause destruction due to the force of the water. Stagnant water on gentle slopes (Figure 21) also poses other threats, including water contamination. These findings are supported by several studies demonstrating that the increasing urban activities in flood plain areas will increase peak discharge, decrease the time to peak, and increase runoff volume (Almousaw et al., 2020; Mancini et al., 2020).

Figure 21. Stagnant water in Irbid (A) channel area.

6. Conclusions

The study area is subdivided into five sub-catchments B1, B2, B3, B4, and B5 with the areas of 448.6, 351.5, 276.3, 29.5, and 64 Km^2, respectively. The study presents a systematic approach to identify flash floods and their future risks based on the spatial extent of inundations in Irbid city.

The SCS curve numbers were obtained for normal conditions according to the LULC and the soil types of the study area; they were calculated to 85.7, 88.1, 83.6, 79.9, and 82.4. The peak flood discharge was calculated considering 2, 5, 10, 25, 50, 100 and 1000-Year return periods. The peak discharges at the sub catchments were calculated showing that the minimum discharge is 66.27 m^3/s at the sub catchment B4, 164.68 m^3/s at B5, 319.23 m^3/s at B2, 746.66 m^3/s at B1, and the maximum is 765.29 m^3/s at B3 for a (100-Year) return period.

The hydraulic modeling carried out by the HEC-RAS model based on the hydrographs resulting from the hydrological modeling steady-flow simulations was performed for the return periods of 2, 10, 25, 50, 100, and 1000-Years. Different scenarios for the maximum water surface profiles were predicted for each return period for twenty main channels in the study area. It is proven that the area will suffer from flood hazards and infrastructure damages.

Acknowledgments

The authors extend their thanks to the Ministry of Water and Irrigation, Jordan for providing the hydrological dataset. The authors are highly indebted to Prof. Dr. Mohammad Mubarak for his efforts in reading and evaluating the manuscript. Our thanks also go to or Dr. Maha Al-Zu'bi for her valuable comments, suggestions and for reading the manuscript. Sincere thanks also go to Tala Al Kuisi for proof-reading and valuable suggestions.

References

Abed, A. (2000) Geology of Jordan (In Arabic). Dar Wae'l publication 550p. Amman, Jordan.

Abdulla, F. A., and Al-Qadami, A. (2019). "Structural Characteristics of in Jordan." In Patterns and Mechanisms of Climate, Paleoclimate and Paleoenvironmental Changes from Low-latitude Regions. In: Zhang, Z., Khelifi, N., Mezghani, A., Heggy, E. (Eds.), GAJG 2018. Advances in Science, Technology and Innovation. 103–105. Cham: Springer. https://doi:10.1007/978-3-030-01599-2_24.

Abu-Abdullah, M. M., Youssef, A. M., Maerz, N. H., Abu-AlFadail, E., Al-Harbi, H. M., Al-Saadi, N. S. (2020). A Flood Risk Management Program of Wadi Baysh Dam on the Downstream Area: An Integration of Hydrologic and Hydraulic Models, Jizan Region, KSA. Sustainability 12(3): 1-24. https://doi:10.3390/su12031069.

Abu El-Magd, S. A., Amer, R. A., Embaby, A. (2020). Multi-criteria decision-making for the analysis of flash floods: A case study of Awlad Toq-Sherq, Southeast Sohag, Egypt. Journal of African Earth Sciences 162: 103709. https://doi: 10.1016/j.jafrearsci.2019.103709.

Abu Islaih, A., Yaghan R., Al Kuisi M., Al-Bilbisi, H. (2020). Impact of Climate Change on Flash Floods Using Hydrological Modelling And Gis: Case Study Zarqa Ma'in Area. International Journal of Applied and Natural Sciences 9(5): 29–52.

Al-Kofahi, S., Hammouri, N., Sawalhah, M., Al-Hammouri, A. Aukour F. (2018). Assessment of the urban sprawl on agriculture lands of two major municipalities in Jordan using supervised classification techniques. Arabian Journal of Geosciences 11: 45. https://doi.org/10.1007/s12517-018-3398-5.

Almousawi, D., Almedeij, J., Alsumaiei, A.A. (2020). Impact of urbanization on desert flash flood generation. Arabian Journal Geosciences 13, 441. https://doi.org/10.1007/s12517-020-05446-z.

Al-Weshah, R. A. and El-Khoury, F. (1999). Flood Analysis and Mitigation for Petra Area in Jordan. Journal of Water Resources Planning and Management 125(3): 170–177. https://doi:10.1061/(asce)0733- 496(1999)125:3(170).

Atashi, N., Rahimi, D., Al Kuisi, M., Jiries, A., Vuollekoski, H., Kulmala, M., Vesala, T., Hussein, T. (2020). Modeling Long-Term Temporal Variation of Dew Formation in Jordan and Its Link to Climate Change. Water 12(8): 2186. https://doi:10.3390/w12082186.

Arcement, G. J. and Schneider, V. R. 1989. Guide for Selecting Manning's Roughness Coefficients for Natural Channels and Flood Plains (U.S. Geological Survey Water Supply Paper 2339). U.S. Geological Survey.

Brunner, G. and CEIWR-HEC (Hydrologic Engineering Center) (2016). River Analysis System HEC-RAS user's Manual, Version 5.0, U.S. Army Corps of Engineers Hydrologic Engineering Center, Davis, CA.

Department of Statistics(DOS) (2018) Jordan In Figures. http://dosweb.dos.gov.jo/ar/products/jordan-in-figure2018/. Accessed 9 June 2020.

Department of Statistics (DOS) (2020). http://dosweb.dos.gov.jo/ar/population/population-2/ . Accessed 9 June 2020.

Derdour A. and Bouanani A. (2019). Coupling HEC-RAS and HEC-HMS in rainfall–runoff modeling and evaluating floodplain inundation maps in arid environments: case study of Ain Sefra city, Ksour Mountain. SW of Algeria. Environmental Earth Sciences. 78(19):586. https://doi.org/10.1007/s12665-019-8604-6.

Derdour, A., Bouanani A., Baba-Hamed, K. (2017). Hydrological modeling in semi-arid region using HEC-HMS model. Case study in Ain Sefra watershed, Ksour Mountains (SW, Algeria). Journal of Fundamental and Applied Sciences 92: 1027–1049. https://doi.org/10.4314/jfas.v9i2.27.

Dupont, B. S. and Allen, D. L. (1999). Revision of the Rainfall Intensity Duration Curves for the Commonwealth of Kentucky. Kentucky Transportation Center Research Report. 292.https://uknowledge.uky.edu/ktc_researchreports/292.

Echogdali, F.Z., Boutaleb, S., Elmouden, A., Ouchchen, M. (2018). Assessing Flood Hazard at River Basin Scale: Comparison between HECRASWMS and Flood Hazard Index (FHI) Methods Applied to El Maleh Basin, Morocco. Journal of Water Resource and Protection 10: 957-977. https://doi.org/10.4236/jwarp.2018.109056.

El Alfy, M. (2016). Assessing the impact of arid area urbanization on flash floods using GIS, remote sensing, and HEC-HMS rainfall–runoff modeling. Hydrology Research 47(6): 1142–1160. https://doi:10.2166/nh.2016.133.

Farhan, Y. and Anabr, A. (2016). Flash Flood Risk Estimation of Wadi Yutum (Southern Jordan) Watershed Using GIS Based Morphometric Analysis and Remote Sensing Techniques: Open Journal of Modern Hydrology 6: 79-100.

Hyarat, T. (2016). Disaster Management, Flood Hazard and Risk Assessment: Case Study Wadi Al Arab Basin, M.S. thesis, The University of Jordan.

Hoseini, Y., Azari, A., Pilpayeh, A. (2017). Flood modeling using WMS model for determining peak flood discharge in southwest Iran case study: Simili basin in Khuzestan Province. Applied Water Science 7: 3355–3363. https://DOI 10.1007/s13201-016-0482-4.

Hunting Technical Services, Soil Survey and Land Research Centre (HTS and SSLRC) 1993. The Soils of Jordan. Ministry of Agriculture, National Soil Map and Land Use Project, Level 1: Reconnaissance Soil Survey (Scale 1: 250,000), 3 Volumes, Amman.

Ibitoye, M.O., Komolafe, A.A., Adegboyega, A.S., Adebola, A. O., Oladeji, O. D. (2020). Analysis of vulnerable urban properties within river Ala floodplain in Akure, Southwestern Nigeria. Spatial Information Research 28: 431–445. https://doi.org/10.1007/s41324-019-00298-6.

Mancini, C.P., Lollai, S., Volpi, E., Fiori, A. (2020). Flood Modeling and Groundwater Flooding in Urbanized Reclamation Areas: The Case of Rome (Italy). Water 12(7): 2030. https://doi.org/10.3390/w12072030

Marko, K., Elfeki, A., Alamri, N., Chaabani, A. (2019). Two Dimensional Flood Inundation Modelling in Urban Areas Using WMS, HEC-RAS and GIS (Case Study in Jeddah City, Saudi Arabia). Advances in Science, Technology and Innovation 265–267. Published in: Advances in Remote Sensing and Geo Informatics Applications.

Ministry of Water and Irrigation (MWI), (2018). Daily Rainfall Data, Open files.

Moh'd, B. (2000). The geology of Irbid and Ash Shuna Ash Shamaliyya (Waqqas) map sheet no. 3154-II and 3154-III. Natural Resources Authority, Geol. Mapping Division, Bull. 46.

Niyazi, B. A., Masoud, M. H., Ahmed, M., Basahi, J. M., Rashed, M. A. (2020). Runoff assessment and modeling in arid regions by integration of watershed and hydrologic models with GIS techniques. Journal of African Earth Sciences 172. 103966. https://doi:10.1016/j.jafrearsci.2020.103966.

Pregnolato M., Ford A., Wilkinson S., Dawson, R. (2017) The impact of flooding on road transport: A depth-disruption function. Transportation Research Part D 55 (2017): 67–81.

Sadrolashrafi, S.S., Samadi, A., Rodzi, M.A., Thamer, A.M. (2008). Flood Modeling using WMS Software: A Case Study of the Dez River Basin, Iran. In: Altinakar, M.S., Kokpinar, M.A., Darama, Y., Yegen, E.B., Harm A. (Eds.), River Flow. Kubaba Congress Department and Travel Services, Turkey.

SCS U (1986). Urban hydrology for small watersheds, technical release no. 55 (TR-55). US Department of Agriculture, US Government Printing Office, Washington, DC.

UNHCR, (2018). Cash in hand- Urban refugees, the right to work, and UNHCR's advocacy

activities. Available at: https://reliefweb.int/report/egypt/cash-hand-urban-refugees-right-work and-unhcrs-dvocacy-activities.

World Food Programme (WFP) (2019) Flood Hazard Map Integrated Context Analysis Jordan July 2019.

Youssef, A. and Hegab, M. (2019). Flood-Hazard Assessment Modeling Using Multicriteria Analysis and GIS: A Case Study—Ras Gharib Area, Egypt. Spatial Modeling in GIS and R for Earth and Environmental Sciences 2019: 229-257. https://doi.org/10.1016/B978-0-12-815226-3.00010-7.

JJEES

JJEES (2021) 12 (1): 92-98
ISS`N 1995-6681

Jordan Journal of Earth and Environmental Sciences

A Review and Evaluation of K. H. Karim and M. Al-Bidry's 2020 Study "Zagros Metamorphic Core Complex: Example from Bulfat Mountain, Qala Diza Area, Kurdistan Region, Northeast Iraq" (Jordan Journal of Earth and Environmental Sciences, 11 (2): 113-125).

Sarmad Ali [1,2]*, Yousif Mohammad[3], Nabaz Aziz[3], Ahmed Aqrawi[4], Fadhil Lawa[3], Rafid Aziz[5], Mohsin Ghazal[5], Mohammed Sofy[4], Irfan Yara[3], Imad Abdulzahra[6]

[1]Department of Applied Geology, College of Science, Kirkuk University, Kirkuk, Iraq.
[2]School of Earth, Atmospheric and Life Sciences, University of Wollongong, NSW 2522, Australia.
[3]Department of Geology, University of Sulaimani, Sulaimani, Kurdistan Region, Iraq.
[4]Department of Geology, University of Salahaddin, Erbil, Iraq.
[5]Department of Geology, College of Science, Mosul University, Mosul, Iraq.
[6]Geological Survey, P.O. Box; 986, Alwiya, Baghdad, Iraq.

Received 20 July, 2020; Accepted 29 September 2020

Abstract

The attention of the present authors is drawn to what looks like odd or even erroneous evidence presented by a paper recently published by Karim and Al-Bidry (2020), focusing on the Zagros Metamorphic Core Complex and providing an example from Bulfat Mountain, Qala Diza area, Kurdistan Region, northeast Iraq. For instance, the ophiolite at Mawat is of the Cretaceous age (105 ±5 Ma; Mohammad and Qaradaghi (2016), the plagiogranites are also of the Cretaceous age, but are slightly younger (92.6 ±1.2 Ma - Mohammad and Qaradaghi (2016), 96.0 ±2.0 Ma - Ismael et al. (2017) and the Hasanbag ophiolite is 106-92 Ma (Ali et al., 2012). On the other hand, 40Ar–^{39}Ar dates on the magmatic feldspar separates from the Walash and Naopurdan volcanic rocks indicate an Eocene–Oligocene age (43.01 ± 0.15 to 24.31 ± 0.60 Ma; Ali, 2012; Ali et al., 2013).

Many studies of the Zagros region have been undertaken on structure, origin of the ophiolites and the related igneous rocks, as well as on the geodynamic evolution (Ghazal, 1980; Alavi, 1980, 1994, 2004, 2007; Agard et al., 2005; Ali, 2012, Ali et al., 2012, 2013, 2014, 2017, 2019; Ali,2017; Aswad et al., 2011, 2013; Aziz et al., 2011; Mohammad et al., 2014; Mohammad and Qaradaghi, 2016; Mohammad and Cornell, 2017; Ali, 2017; Lawa, 2018). Therefore, the following points will be addressed:

(1) Possible Metamorphic Core Complex.

(2) Absence of volcanic rocks in the "Bulfat Complex" and absence of dykes and bosses.

(3) The origins of the sedimentary rocks in the "Bulfat Complex" that were originally transported to the Bulfat area from the Urumeh-Dokhtar Magmatic (basaltic) Arc (UDMA) by turbidity currents during Paleocene-Early Eocene.

(4) the paleogeographic and tectonic model of the deposition of mafic and felsic volcaniclastic sandstones (and other sediments) by turbidity currents sourced mainly from the Urumieh-Dokhtar Magmatic Arc and transported to the Iraqi side of the Sanandaj-Sirjan Zone (SSZ) in the Bulfat and Mawat areas.

Keywords: Bulfat, Igneous Complex, Bulfat Mountain, Zagros Suture Zone, Walash-Naopurdan Groups, Kurdistan region, Iraq.

(1) Possible Metamorphic Core Complex

Karim and Al-Bidry (2020) avoid including any geological background or data on the regional geology of the studied area. This is an important part in any study to show readers some established knowledge about the studied area. Plentiful information about the geological background can be found in papers by Pshdari (1983), Aziz (1986, 2008), Buda (1993), Aswad et al. (2013, 2016), Ali (2017) and Karo et al. (2018). Unfortunately, the idea of a possible Metamorphic Core Complex (MCC) presented by Karim and Al-Badry (2020) is based on work of Ring (2014), Coney (1980), Lister and Davis (1989) and Huet et al. (2011). For example, the section on "MCC is defined by Lister and Davis (1989) as a crust structure which resulted from major continental extension, when the middle and lower continental crust is dragged out from beneath the fracturing, extending the upper crust. Deformed rocks in the footwall are uplifted through a progression of different metamorphic and deformational environments, producing a characteristic sequence of (overprinted) meso- and microstructures," an idea taken entirely from the abstract by Lister and Davis

Corresponding author email: sarmad@uokirkuk.edu.iq

(1989) even without any paraphrasing.

A basic feature of metamorphic core complexes are the exposures of deep crustal rocks exhumed in association with a largely magmatic extension. Metamorphic core complexes are exciting examples of large-scale continental extension, usually juxtaposing metamorphic lower crust against upper crustal rocks (Coney, 1980). Detachment faulting is associated with large-scale extensional tectonics. Detachment faults often have very large displacements and juxtapose unmetamorphosed hanging walls against medium to high-grade metamorphic footwalls forming the metamorphic core complexes (Singleton, 2013). It is not necessary for all metamorphic core complexes to contain only metamorphosed sedimentary rocks. Many metamorphic core complexes consist of plutonic rocks in addition to the metamorphosed sedimentary rocks. The best example is the Shuswap Complex in Canada, which is the largest and longest recognized metamorphic core complex and is considered a typical example (Coney 1980; for more information see Reesor, 1965, 1970; Reesor and Moore, 1971; Simony et al., 1980; Banks, 1980; Davis, 1983; Lister and Davis, 1989). Therefore, on the basis of the new evidence in sections 2, 3, and 4, the authors of the present work completely reject a new Metamorphic Core Complex tectonic model for the Bulfat igneous complex.

(2) Absence of Volcanic Rocks in the "Bulfat Complex" and Absence of Dykes and Bosses.

The present work argues that most of the observations in Karim and Al-Bidr (2020) do not support the idea that volcanic rocks, dykes, and bosses are absent in the Bulfat Igneous Complex as mentioned in the introduction. Most of their field photographs and petrographic thin section descriptions leave doubts about their mineral and texture identifications since they are not accompanied by illustrations. Therefore, this work provides data on some of the volcanic and dyke thin sections as well as field photographs taken from publications on the Bulfat Igneous Complex. The publication discussed here is a good example of duly documented misidentifications (see figures 1, 2, 3; for more see Aswad and Pshdari, 1984; Aziz, 1986; Aqrawi and Sofy, 2007; Aswad et al., 2013; Ali, 2017; Karo et al., 2018; Zrary, 2019).

Below are a few examples of misidentifications with some revised identifications:

a. Karim and Al-Bidry (2020) state that the pyroxenite facies is a regional metamorphic one. This is quite incorrect as facies refers to the set of predictable mineral assemblages and the P-T conditions they represent. The three common types of facies series are: High P/T facies series: (zeolite) – (prehnite-pumpellyite) – blueschist - eclogite; Medium P/T series: (zeolite) – (prehnite-pumpellyite) – greenschist – amphibolite – (granulite); Low P/T series: (zeolite) – (prehnite-pumpellyite) – albite-epidote hornfels – hornblende hornfels – (pyroxene hornfels) – (sanidinite). It is clear from the above-mentioned information that the pyroxenite facies is related to the Low P/T series, and it is formed in high geothermal orogenic settings or contact metamorphism (Winter, 2001).

b. Karim and Al-Bidry (2020) state that during a traverse from the southern boundary to the core of the "Bulfat Complex," the signature of gradation is clear; woefully this is supported by only two thin-section photomicrographs which do not validate their claim about the boundary conditions of the Bulfat Igneous Complex. Instead, they should have supported their observed gradation with field photographs of rock units.

c. Karim and Al-Bidry's (2020) reinterpretation of previously published figures is completely wrong as they do not give the exact location of the thin-sections. It seems they never examined those thin-sections under a microscope; instead they should produce new thin-sections to support their interpretations.

d. Karim and Al-Bidry's (2020) interpretation of Figures 7 and 16 is completely wrong, as they consider fresh typical gabbro to be mafic granulite, and for the first time in the literature they claim irregular intergranular hornblende as a cement matrix, which has never been mentioned even in principle petrographic books. Karim and Al-Bidry (2020) state that no contact metamorphism was seen in the field, yet Figure 10b in the Karim and Al-Bidry (2020) shows hornfels. Hornfelsic rocks are the product of contact metamorphism (Aswad and Pshdari, 1984). This means their postulated channel in Figure 10b is actually an igneous intrusion that metamorphosed the country rocks. In addition, Figures 7a, 7b, 16, and 17a in Karim and Al-Bidry (2020) clearly show typically igneous textures and not a sandstone or conglomerate protolith. Moreover, Figure 7a is definitely igneous amphibole and this was documented by Ali (2015) using electron microprobe mineral analyses (for more information see Ali, 2012; Ali et. al., 2013; Ali, 2015).

e. A sign of misleading is obvious in Figure 9, as they criticize other unnamed authors who consider this view to be a mafic igneous rock.

Figure 1. Typical felsic dyke intruded into an older gabbroic rock unit of the Bulfat Igneous Complex northwest of Hero.

Karim and Al-Bidry (2020) state that "the Walash-Naopurdan Series occurs around the Bulfat and Mawat Complexes (at least, to the south, southwest and southeast) apparently below the Red Bed Series, and consists (as previously indicated) of a mixture of volcanic rocks, sedimentary rocks, and carbonate sediments. But the present study inferred that the series does not contain volcanic rocks; instead, it consists of volcaniclastic sandstone, shale and greywacke (Figure 17) that was derived mainly from the volcanic (basaltic arc) source areas. These sediments can produce the gabbro or diorite-like rocks after metamorphism and crystallization". The present authors completely disagree with these three unusual results. First, in all Iraqi geological databases the Walash-Naopurdan Groups represent the lower allochthon, which is thrust over the Red Bed Series in all parts of the Iraqi Zagros Thrust Zone. Secondly, the igneous rocks in the Walash-Naopurdan Groups are genuine igneous rocks in terms of texture, mineralogy, and field occurrence, which is documented in all previously published papers about the Walash-Naopurdan Groups (for more information see Aziz, 1986, Aziz, 1993; Aziz et al., 1993a; Aziz et al., 1993b; Ali, 2002; Aziz and Ali, 2005; Ali, 2012; Ali et al., 2013, 2014, 2017, 2019; Aswad et al., 2013). Thirdly, one asks if it is possible for sediments to produce the gabbro or diorite-like rocks after metamorphism and recrystallization? It is impossible to generate ultrabasic or basic rocks from clastic sediments by metamorphism. In studying metamorphic rocks, the first thing to be considered is their protolith and thermodynamics. The metamorphic products depend on the prevailing temperature, the type of pressure whether it is directed (deviatoric stress) or confined pressure (non-directed pressure), and the protolith rocks (Winter, 2001). Additionally, a geochemical and petrological study of twelve closely-spaced rock samples from the Bulfat Igneous Complex at Wadi Rashid, which consists of gabbro and granitic composite intrusions, show that the gabbro or diorite-like rocks preserve igneous textures with domains of ferromagnesian igneous minerals showing minimal replacement by secondary tremolitic green amphibole and chlorite (Aswad et al., 2013). Another example from Bulfat Igneous Complex is the Shaki-Rash gabbro which contains olivine, plagioclase and clinopyroxene, with lesser orthopyroxene, biotite, brown hornblende and alkali feldspar (Figure 2) which is intruded by Eocene arc-related magmatic rocks (Ali, 2017). From all the above-mentioned evidence, it is clear that Karim and Al-Bidry (2020) failed to distinguish between the different kinds of igneous rocks, serpentinite and other sedimentary rocks in the field (Figure 3).

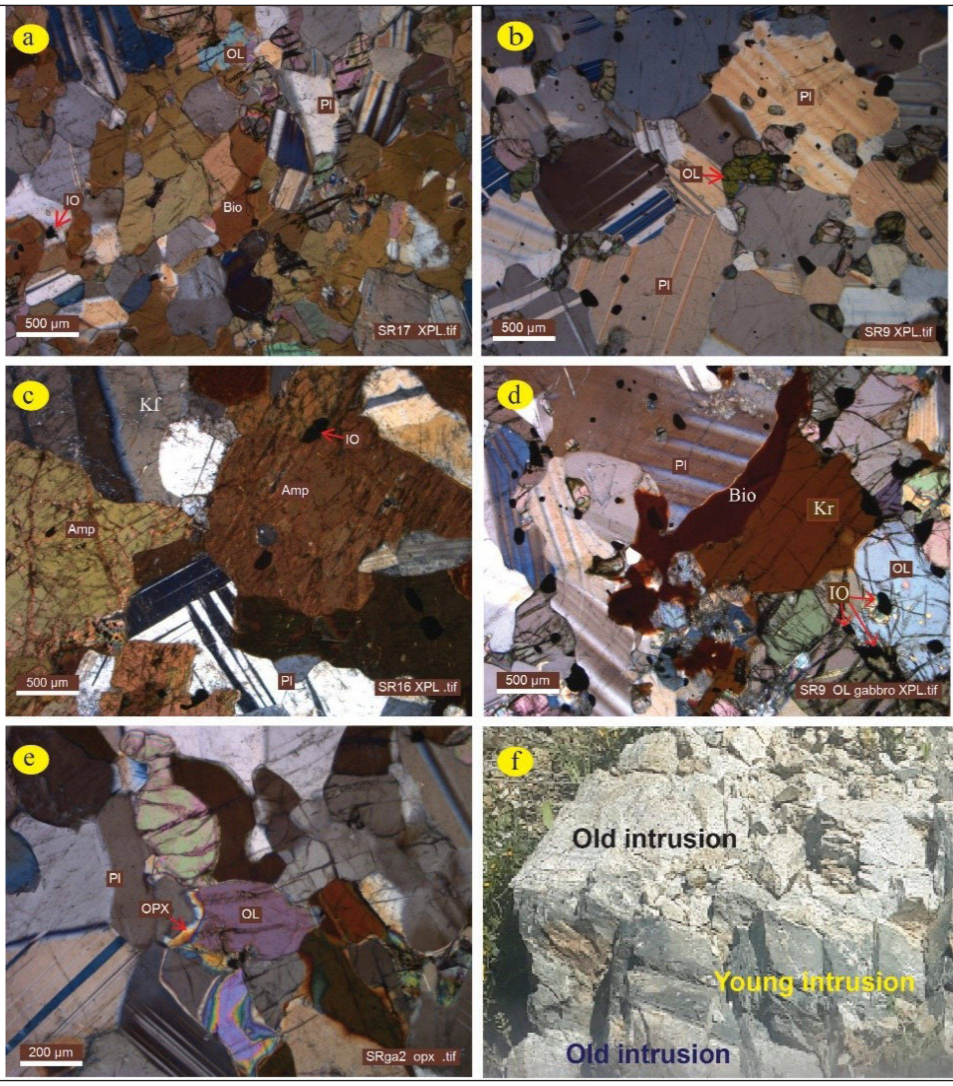

Figure 2. Photomicrographs of Shaki-Rash gabbro rocks showing typical igneous minerals and textures (for more details see Ali, 2017).

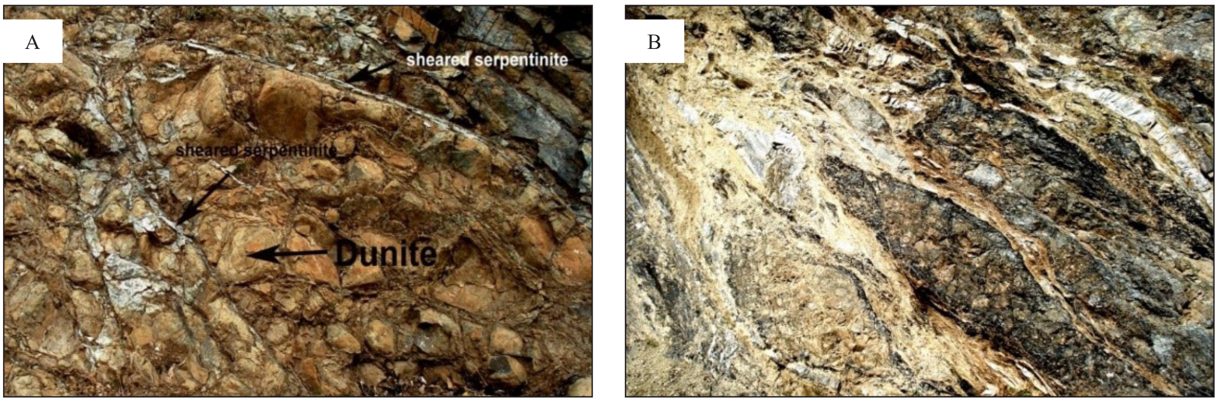

Figure 3. Field photograph of sheared serpentinite (A), and massive serpentinite (B) in the Pauza area of the Bulfat Igneous Complex (after Aziz, 2008).

(3) The origins of the rocks in the "Bulfat Complex" are sediments that were originally transported to the Bulfat area from the Urumeh-Dokhtar Magmatic (basaltic) Arc by turbidity currents during Paleocene -Early Eocene.

The Iraq (Kurdish) section of the Zagros Suture Zone is marked by numerous allochthons of Neotethyan ophiolitic and volcanic arc assemblages that were obducted onto the Arabian margin (Ali et al., 2012, 2013, 2014, 2017, 2019). New geochronological data, including SHRIMP U-Pb zircon, combined with whole rock geochemistry, indicate that both Cretaceous (~96 Ma) and Cenozoic (~40 Ma) assemblages are present (Ali et al., 2019). An increase of $^{40}Ar/^{39}Ar$ mineral and U–Pb zircon geochronology has revealed two important periods of arc magmatism: in the Cretaceous (Albian–Cenomanian) and the Paleogene (Eocene–Oligocene; Aswad et al., 2011, 2013; Ali et al., 2013, 2016, 2019). Aswad et al. (2016) discovered unrelated but essentially coeval Paleogene arc magmatism in two separate allochthons which points to the complex tectonic episodes in the final stages of Neotethys consumption. It is well-known that ophiolites are of an oceanic crust protolith, composed dominantly of basic rocks. No one has ever, even in international works, suggested the protolith of ophiolites to be arenites, greywacke or pyroclastic rocks. Karim and Al-Bidry (2020) are claiming that the source of sediment in the "Bulfat Complex" was derived from the Urumieh-Dokhtar Magmatic Arc and was transported 90 km by turbidity currents to a basin of deposition in the Qaladiza and Bulfat area (as a part of the SSZ) during the Paleocene-Eocene. This is a completely incorrect statement as the rocks in the SSZ are much older than the Cenozoic Urumieh-Dokhtar Magmatic Arc (Figure 4; for more information see Chiu et al., 2013). From this point, it is very clear that the Karim and Al-Bidry have no sufficient knowledge of the tectonic evolution of the Zagros Orogenic Belt. Moreover, their perplexing model shows that the SSZ is represented by a gigantic fan of about 115 km extending from Penjween to Bulfat fed by a submarine channel without any hydraulic sorting of the sediments and no record of a submarine canyon along the entire Zagros.

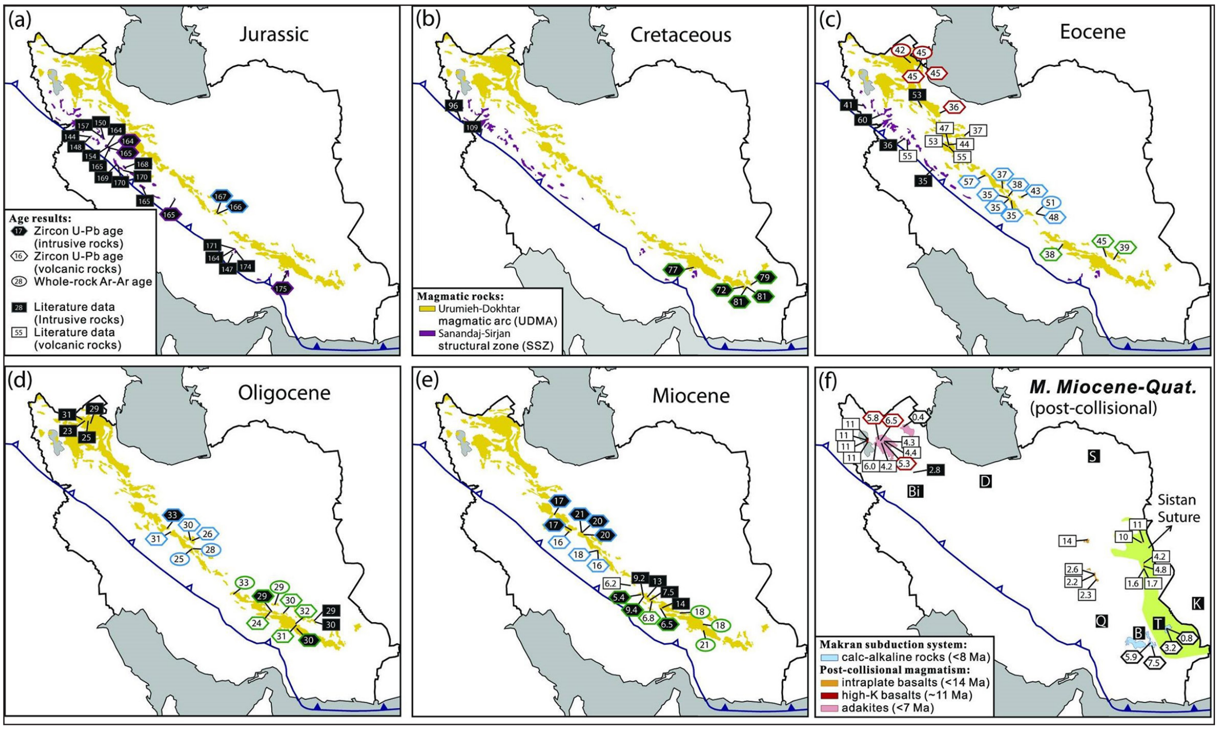

Figure 4. Magmatic distribution in the UDMA and SSZ plotted in age spans from Jurassic to Quaternary along Zagros Orogenic Belt (after Chi et al., 2013), clearly indicate that the younger UDMA cannot be a sediment source of older SSZ rocks.

(4) Paleogeographic and tectonic model of the deposition of mafic and felsic volcaniclastic sandstones (and other sediments) by turbidity currents sourced mainly from the Urumieh-Dokhtar Magmatic Arc and transported to the Iraqi part of the Sanandij-Sirjan Zone (Bulfat and Mawat areas).

The new tectonic model of a "Metamorphic Core Complex" proposed by Karim and Al-Bidry (2020) for the Bulfat Igneous Complex depended mostly on literature reviews (e.g. Ring, 2014; Coney, 1980; Lister and Davis, 1989; Huet et al., 2011) and on field photos, using twenty thin sections for such a large area. However, the model cannot be accepted on the basis of a similarity of some of the features between Bulfat and those mentioned in the above literature reviews without doing a detailed structural study of the Bulfat area. Karim and Al-Bidry (2020) state that 'the Bulfat MCC is associated with extension and normal faulting both locally and regionally. On a local scale, many normal faults can be seen which occurred after metamorphism (during uplifting).'' They use no references to support their tectonic model hypothesis; in fact there is no structural study or any publication done on the Bulfat Igneous complex preceding this study. Therefore, the authors of the current work completely reject the new Metamorphic Core Complex tectonic model for the Bulfat Igneous Complex.

It is important to mention that the Urumieh-Dokhtar Magmatic Arc lies several hundred kilometers from the Bulfat area, and it is separated from Bulfat Igneous Complex by the Sanandaj-Sirjan Zone igneous and metamorphic complex. The transportation of huge deposits by rivers from the Urumieh-Dokhtar Magmatic Arc to the Bulfat area during Paleocene-Eocene has not been recorded or recognized in any geological work in Iraq and Iran for more than a century (Alavi, 1980, 2004, 2007; Pshdari, 1983; Agard et al., 2005; Jassim and Goff , 2006, Aziz et al., 2011; Aswad et al., 2011, 2013; Ali, 2017; Ali et al., 2012, 2013, 2014, 2016, 2017, 2019; Mohammad et al., 2014; Mohammad and Qaradaghi, 2016; Mohammad et al., 2016; Ali, 2017; Mohammad and Cornell, 2017; Lawa, 2018). Furthermore, there are neither erosional, nor depositional features of those rivers in Iraq or Iran. There are no incised valley deposits of those rivers, no fresh water deposits have been recorded, and no fresh water fossils. The submarine fan as part of a major foreland basin should contain fossils (fauna or flora) or other bio-markers. The proposed submarine fan model contains no mentioning of fossils as in the Neotethys basin, such as planktic foraminifera in the shale or Nummulites in the Bulfat carbonates, or any record of reworked fossils or even any trace fossils. Karim and Al-Bidry (2020) mentioned that, after erosion, these sediments were transported and deposited by turbidity currents in the Zagros Foreland basin during the Paleocene-Eocene. Actually, the rocks show no turbidite sedimentary structures, and there are no field data or laboratory indications for the presence of submarine canyon, gullies, channels, levees, and lobate surfaces. Also, there are no field or laboratory indications for any arenite deposits in channels. The lobe and levee dirty sandstone (greywackes) oppose the argument that these sediment have been transported for a very long distance from the source to the Bulfat area.

Karim and Al-Bidry (2020) mis-identified the rock types and the sedimentary structures as follows:

a. Figures 4, 5, and 6 are used as a proof of bedding or lamination; they use the terms sandstone, shale and marl. Actually there is no bedding or lamination, or any sandstone or shale. The rocks are schist and phyllite with clear schistosity and foliations. In addition, a marl should include planktonic foraminifera (like Morozvella and Subbottina spp., Lawa, 2004), nanofossils and/or palynomorphs to support the age determination and submarine fan model.

b. Figure (7) was used to indicate sorting and roundness; actually it shows angular crystals without any roundness, sphericity or porosity.

c. Figure (10a) is explained as an erosional surface below a small channel with laminations in the metamorphosed volcaniclastic sandstone. In reality, it is gabbro (Aswad et al., 2013, 2016) that was subjected to intense deformation with folding, and faulting (note two minor sets), without any erosional surface or any type of channel.

e. Figure (11b) showed the contact between Kolosh and Sinjar Formations. This boundary between the two formations had been recorded by Lawa et al. (2013) who determined the gap age between the Paleocene and Eocene, which is not mentioned by the authors.

Karim and Al-Bidry (2020) mention that the foreland basin occupied part of the Sanandaj-Sirjan Zone of Iran and the whole of Iraq, without using any reference. Again it is a big mistake, because the foreland basin simply does not cover the whole of Iraq, as mentioned by Lawa (2018). On the same page, they also state that during the Paleocene-Eocene, a thick succession of volcaniclastic sandstones and shales was deposited in the rapidly subsiding foreland basin. Stratigraphically in Iraq, they were called the "Walash-Naopurdan Series," which consists of clastic and carbonate sediments without volcanic rocks. Such a statement points (without adding references and without being studied) to the fact that they were not able to differentiate between two different tectonic thrust sheets, the Iraqi Zagros Thrust Zone contains two thrust sheets; the Upper and Lower Allochthons (see Figure 2b in Ali et al., 2019). The Upper Allochthon ophiolite bearing terrane is part of the Outer Zagros Ophiolite Belt. The Bulfat Igneous Complex is located in the Upper Allochthon ophiolite-bearing terrane, while the Walash-Naopurdan Groups are located in the Lower Allochthon, and these two allochthons represent two different tectonic domains (Ali, 2012; Ali et al., 2012; 2013; 2014; 2016; 2019; Aswad et al., 2016). Consequently, there are no original sedimentary structures and textures such as the planar bedding, laminations, cross-bedding, folding or erosional surfaces in the granular textures in Bulfat Igneous Complex. Also without any fossils (neither as flora nor as fauna, and even no trace fossils). However, The presence of quasi-sedimentary structures in igneous rocks, such as cross bedding, layering, graded bedding, and channeling are quite common in igneous intrusions such as those found in the Skeargard Massif. The origins of the rocks of the Bulfat Igneous Complex are not sediments that were originally transported to the Bulfat area from the Urumeh-Dokhtar Magmatic (basaltic) Arc by turbidity currents during the Paleocene -Early Eocene. The present authors believe that, today, the Iraqi geological Wikipedia, that has long benefited from the pioneer geological investigations, should contribute to helping fill this huge scientific gap made by some researches including Karim and Al-Bidry (2020) in supporting new modern igneous and metamorphic investigations.

Acknowledgments

The present authors thank Brian Jones from Wollongong University who carefully revised the English text.

References

Agard, P., Omrani, J., Jolivet, L., Mouthereau, F. (2005). Convergence history across Zagros (Iran): constraints from collisional and earlier deformation. International Journal of Earth Sciences 94: 401–419.

Alavi, M. (1980). Tectonostratigraphic evolution of the Zagros sides of Iran. Geology 8: 144–149.

Alavi, M. (1994). Tectonics of the Zagros orogenic belt of Iran: New data and interpretations. Tectonophysics 229: 211–238.

Alavi, M. (2004). Regional stratigraphy of the Zagros fold-thrust belt of Iran and its proforeland evolution. American Journal of Science 304:1–20.

Alavi, M. (2007). Structures of the Zagros Fold-Thrust Belt in Iran. American Journal of Science 307: 1064–95.

Ali, S.A. (2002). Petrography and Geochemistry of Walash Volcanics in Haj-Omran and Sidekan Provinces, NE Iraq, M. Sc. Thesis, Mosul University.

Ali, S.A. (2012). Geochemistry and Geochronology of Tethyan Arc Related Igneous Rocks, NE Iraq, Ph.D. Thesis, University of Wollongong.

Ali, S.A., Buckman, S., Aswad, K.J., Jones, B.G., Ismail, S.A., Nutman, A.P. (2012). Recognition of Late Cretaceous Hasanbag ophiolite-arc rocks in the Kurdistan region of the Iraqi Zagros thrust zone: a missing link in the paleogeography of the closing Neo-Tethys Ocean. Lithosphere 4: 395–410.

Ali, S.A., Buckman, S., Aswad, K.J., Jones, B.G., Ismail, S.A., Nutman, A.P. (2013). The tectonic evolution of a Neo-Tethyan (Eocene-Oligocene) island-arc (Walash and Naopurdan Groups) in the Kurdistan region of the NE Iraqi Zagros suture zone. Island Arc 22: 104–125.

Ali, S.A., Mohajjel, M., Aswad, K.J., Ismail, S.A., Buckman, S., Jones, B.G. (2014). Tectonostratigraphy and general structure of the northwestern Zagros collision zone across the Iraq-Iran border. Journal of Environment and Earth Science 4: 92–110.

Ali, S.A. (2015). Petrogenesis of metabasalt rocks in the Bulfat Complex, Kurdistan region, Iraqi Zagros Suture Zone. Kirkuk University Journal Scientific Studies (KUJSS) 10 (3): 242-258.

Ali, S.A., Ismail, S.A., Nutman, A.P., Bennett, V.C., Jones, B.G., Buckman, S. (2016). The intra oceanic Cretaceous (~108Ma) KataeRash arc fragment in the Kurdistan segment of Iraqi Zagros suture zone: implications for Neotethys evolution and closure. Lithos 260: 154-163.

Ali, S.A., Sleabi, R.S., Talabani, M.J.A., Jones, B.G. (2017). Provenance of the Walash- Naopurdan back-arc - arc clastic sequences in the Iraqi Zagros suture zone. Journal of African Earth Sciences 125: 73–87.

Ali, S.A. (2017). 39 Ma U-Pb zircon age for the Shaki-Rash gabbro in the Bulfat igneous complex, Kurdistan region, Iraqi Zagros suture zone: rifting of an intra-Neotethys Cenozoic arc. Ofioliti 42:69–80.

Ali, S.A., Allen P. Nutman, Khalid J. Aswad, Brian G. Jones. (2019). Overview of the tectonic evolution of the Iraqi Zagros thrust zone: sixty million years of Neotethyan ocean subduction, Journal of Geodynamic 129:162-177.

Aqrawi, A.M. and Sofy, M.M. (2007). Petrochemistry and Petrogenesis of Bulfat Mafic Intrusion, Qala Dizeh, Iraqi National Journal of Earth Sciences 7(1): 33-60.

Aswad, K.J, and Pshdari, M.A. (1984). Thermal metamorphism of impure carbonate xenoliths in the gabbroic rock of Bulfat complex, NE-Iraq. Journal Geological Society of Iraq17:208–235.

Aswad, K.J.A., Aziz, N.R.H., Koyi, H.A. (2011). Cr-spinel compositions in serpentinites and their implications for the petrotectonic history of the Zagros Suture Zone, Kurdistan Region, Iraq.

Geological Magazine, 148 (5-6): 802-818.

Aswad, K.J., Al-Sheraefy, R.M., Ali, S.A. (2013). Pre-collisional intrusive magmatism in the Bulfat Complex, Wadi Rashid, Qala Deza, NE Iraq: geochemical and mineralogical constraints and implications for tectonic evolution of granitoid-gabbro suites. Iraqi National Journal of Earth Sciences 13 (1): 103-137.

Aswad, K.J., Ali, S.A., Al-Sheraefy, R. M., Nutman, A. P., Buckman, S., Jones, B. G., Jourdan, F. (2016). 40A r/39A r hornblende and biotite geochronology of the Bulfat Igneous Complex, Zagros Suture Zone, NE Iraq: New insights on complexities of Paleogene arc magmatism during closure of the Neotethys Ocean, Lithos 266–267: 406-413.

Aziz, N.R. (1986) Petrochemistry, petrogenesis and tectonic setting of spilitic rocks of Walash volcano sedimentary Group in Qala Diza area, NE Iraq, M.Sc. Thesis, University of Mosul.

Aziz, N.R. (2008). Petrogenesis, Evolution, and Tectonics of the Serpentinites of the Zagros Suture Zone, Kurdistan Region, NE Ira Iraq, Ph.D. Thesis, University of Sulaimani.

Aziz, N. R., Aswad, K. J., Koyi, H. A. (2011). Contrasting settings of serpentinite bodies in the northwestern Zagros Suture Zone, Kurdistan Region, Iraq. Geological Magazine 148: 819-837. doi: 10.1017/S0016756811000409.

Aziz, R. M. (1993). The slate horizons in Walash Group, Sidekan Province, NE-Iraq; their tectonic and metamorphic history. Journal Geological Society of Iraq 26 (2): 100-122.

Aziz, R.M., Al-Hafdh, N. and Al-Ghadanfary, E. (1993a). Geochemistry and Petrogenesis of the Walash Volcanics in Draband, NE Iraq. Abhath-Al-Yarmouk pure science, and Engineering Series 2 (1): 135-155.

Aziz, R.M., Elias, E.M. and Al-Hafdh, N.M. (1993b). The Igneous and Metamorphic Metaclastics of Naopurdan group and their relation to the tectonic regime in NE-Iraq. Mu'tah Journal of Research Studies 8(4): 155-172.

Aziz, R.M. and Ali, S.A. (2005). Petrochemistry and Tectonic setting of the Naupordan Metavolcanics from Jabal Qalander, NE-Iraq. Tikrit Journal of Pure Science 10 (2):227-235.

Banks, N. G. (1980). "Geology of a zone of metamorphic core complexes in southeastern Arizona". In: Crittenden, M. D., Coney, P. J., Davis, G. H. (Eds.), Cordilleran Metamorphic Core Complexes. Boulder: Geological Society of America. Geological Society of America Memoir 153: 177-215. DOI: https://doi.org/10.1130/MEM153.

Chiu, H. Y., Chung, S. L., Zarrinkoub, M. H., Mohammadi, S. S., Khatib, M. M., Iizuka, Y. (2013). Zircon U–Pb age constraints from Iran on the magmatic evolution related to Neotethyan subduction and Zagros orogeny. Lithos 162: 70-87.

Coney, P. J. (1980). Cordilleran metamorphic core complexes: An overview. In: Crittenden, M. D., Coney, P. J., Davis, G. H. (Eds.), Cordilleran metamorphic core complexes. Boulder: Geological Society of America. Geological Society of America Memoir 153: 7–31.

Davis, G. H. (1983). Shear-zone model for the origin of metamorphic core complexes. Geology, 11: 342–347.

Ghazal M. M. (1980). Petrology and Geochemistry of the Basic Rocks occurring around Hero (Kala-Dizeh), Northeast Iraq, M.Sc. Thesis, Mosul University.

Huet, B., Le Pourhiet, L., Labrousse, L., Burov, E., Jolivet, L. (2011). Post-orogenic extension and metamorphic core complexes in a heterogeneous crust: the role of crustal layering inherited from collision. Application to the Cyclades (Aegean domain). Geophysical Journal International

184 (2): 611–625. DOI: 10.1111/j.1365-246X.2010.04849.x.

Ismail, S.A., Ali, S.A., Nutman, A.P., Bennett, V.C., Jones, B.G. (2017). The Pushtashan juvenile suprasubduction zone assemblage of Kurdistan (northeastern Iraq): a Cretaceous (Cenomanian) Neo-Tethys missing link. Geoscience Frontiers 8:1073–1087.

Jassim, S.Z., and Goff, J.C. (Eds.). (2006). Geology of Iraq. Dolin, Prague and Moravian Museum, Brno.

Kamal H. Karim and Mayssaa Al-Bidry. (2020). Zagros Metamorphic Core Complex: Example from Bulfat Mountain, Qala Diza Area, Kurdistan Region, Northeast Iraq. Jordan Journal of Earth and Environmental Sciences 11 (2): 113-125.

Karo, N.M., Oberhänsli, R., Aqrawi, A.M., Elias, E. M., Aswad, K. J., Sudo, M. (2018). New 40Ar/39Ar age constraints on cooling and unroofing history of the metamorphic host rocks (and igneous intrusion associates) from the Bulfat Complex (Bulfat area), NE-Iraq. Arabian Journal of Geosciences 11, 234 (2018). https://doi.org/10.1007/s12517-018-3571-x.

Lawa, F.A. (2004). Sequence stratigraphic analysis of the Middle Paleocene-Middle Eocene in the Sulaimani District (Kurdistan Region), Ph.D. Thesis, University of Sulaimani.

Lawa, F.A, Koyi, H., Ibrahim, A. (2013). Tectono-stratigraphic evolution of the NW segment of the Zagros fold-thrust Belt, Kurdistan, NE Iraq. Journal of Petroelum Geology 36(1):75–96.

Lawa, F.A, (2018). Late Campanian–Maastrichtian sequence stratigraphy from Kurdistan foreland basin, NE/Iraq. Journal of Petroleum Exploration and Production Technology 8: 713–732.

Lister, G.S. and Davis, G.A. (1989). The origin of metamorphic core complexes and detachment faults formed during Tertiary continental extension in the northern Colorado River region, U.S.A. Journal of Structural Geology 11: 65 - 94.

Mohammad, Y.O., and Cornell, D.H. (2017). U-Pb zircon geochronology of the Daraban leucogranite, Mawat ophiolite, Northeastern Iraq: a record of the subduction to collision history for the Arabia-Eurasia plates. Island Arc 26: e12188.

Mohammad, Y.O., and Qaradaghi, J.H. (2016). Geochronological and mineral chemical constraints on the age and formation conditions of the leucogranite in the Mawat ophiolite, Northeastern of Iraq: insight to sync-subduction zone granite. Arabian Journal Geosciences 9: 608.

Mohammad, Y.O., Cornell, D.H., Qaradaghi, J.H., Mohammad, F. O. (2014) .Geochemistry and Ar-Ar muscovite ages of the Daraban Leucogranite, Mawat Ophiolite, northeastern Iraq: implications for Arabia-Eurasia continental collision. Asian Journal Earth Sciences 86:151–165.

Mohammad, Y., Kareem, H., Anma, R. (2016). The Kuradawe Granitic Pegmatite from the Mawat Ophiolite, Northeastern Iraq: Anatomy, Mineralogy, Geochemistry, and Petrogenesis. The Canadian Mineralogist 54: 989–1019.

Pshdari, M. (1983). Mineralogy and geochemistry of contact rocks occurring around Hero and Asnawa, N E - I r a q, M.Sc. Thesis, Mosul University.

Reesor, J. E. (1970). Some aspects of structural evolution and regional setting in part of the Shuswap metamorphic complex. Geological Association of Canada Special Paper 6: 73-86.

Reesor, 1. E., Moore. I. M. Jr. (1971). Petrology and structure of Thor-Odin gneiss dome, Shuswap metamorphic complex. Geological Survey of Canada bulletin 195: 147

Reesor, J. E. (1965). Structural evolution and plutonism in Valhalla gneiss complex, British Columbia. Geol. Geological Survey of Canada bulletin 29: 128

Ring. U. (2014). Metamorphic Core Complexes, Encyclopedia of Marine Geosciences Springer Science DOI 10.1007/978-94-007-6644-0_104-4.

Simony, P. S., Ghent, E. D., Craw, D., Mitchell, W., Robbins, D. B. (1980). Structural and metamorphic evolution of northeast flank of Shuswap complex, southern Canoe River area, British Columbia. In: Crittenden, M. D., Coney, P. J., Davis, G. H. (Eds.), Cordilleran Metamorphic Core Complexes. Geological Society of America Memoir 153: 445–461.

Singleton, J. S., 2013. Development of extension-parallel corrugations in the Buckskin- Rawhide metamorphic core complex, west-central Arizona, Geological Society of America Bulletin 125:453–472.

Winter, J. D. (2001). An Introduction to Igneous and Metamorphic Petrology. Prentice Hall, New Jersey.

Zrary, M. M. S. (2019). Petrogenesis and geochemistry of gabbro and granitoid plutonic rocks on Bulfat Complex at ShakhaRash Mountain, Qala- Diza, NE-Iraq, Ph.D. Thesis, University of Mosul.

المملكة الأردنية الهاشمية　　صندوق دعم البحث العلمي　　الجامعة الهاشمية

المجلة الأردنية
لعلوم الأرض والبيئة

JJEES

مجلة علمية عالمية محكمة

المجلد (١٢) العدد (١)

http:// jjees.hu.edu.jo/

ISSN 1995-6681

المجلة الأردنية لعلوم الأرض والبيئة

مجلة علمية عالمية محكمة

المجلة الأردنية لعلوم الأرض والبيئة: مجلة علمية عالمية محكمة ومفهرسة ومصنفة، تصدر عن عمادة البحث العلمي في الجامعة الهاشمية وبدعم من صندوق البحث العلمي - وزارة التعليم العالي والبحث العلمي، الأردن.

ترسل البحوث إلكترونيا إلى البريد الإلكتروني التالي:

رئيس تحرير المجلة الأردنية لعلوم الأرض والبيئة

jjees@hu.edu.jo

لمزيد من المعلومات والأعداد السابقة يرجى زيارة موقع المجلة على شبكة الانترنت على الرابط التالي:

www.jjees.hu.edu.jo

المملكة الأردنية الهاشمية صندوق دعم البحث العلمي الجامعة الهاشمية

JJEES

المجلة الأردنية لعلوم الأرض والبيئة

المجلد (١٢) العدد (١)

مجلة علمية عالمية محكمة تصدر بدعم من صندوق دعم البحث العلمي

ISSN 1995-6681 jjees.hu.edu.jo آذار ٢٠٢١